SELECTED STUDIES ON ALKALINE ADDITIVES

SULFUR DIOXIDE CONTROL

U. S. ENVIRONMENTAL PROTECTION AGENCY

SELECTED STUDIES ON ALKALINE ADDITIVES FOR SULFUR DIOXIDE CONTROL

by

R. H. Borgwardt, D. C. Drehmel,
T. A. Kittleman, D. R. Mayfield,
and J. S. Bowen

ENVIRONMENTAL PROTECTION AGENCY
National Environmental Research Center
Research Triangle Park, North Carolina
December 1971

The APTD (Air Pollution Technical Data) series of reports is issued by the Office of Air Programs, Environmental Protection Agency, to report technical data of interest to a limited number of readers. Copies of APTD reports are available free of charge to Federal employees, current contractors and grantees, and nonprofit organizations - as supplies permit - from the Office of Technical Information and Publications, Environmental Protection Agency, Research Triangle Park, North Carolina 27711 or from the National Technical Information Services, 5285 Port Royal Road, Springfield, Virginia 22151.

Office of Air Programs Publication No. APTD-0737

TABLE OF CONTENTS

TABLE OF FIGURES

LIST OF TABLES

A. SUMMARY

Concentrated on limestone-sulfur dioxide (SO_2) reactions, alkaline additives research has defined the kinetics and capacity as well as the effects of overburning. The kinetics of SO_2 sorption by limestone calcines has been determined with a high temperature differential bed gas solids contactor. It has been shown that for small particles the reaction is first order and chemical rate controlled with activation energies in the range of 8.1 to 18.1 k cal/g. mole. In general, reaction occurs initially throughout the particle volume and the internal diffusion resistances become limiting only after conversion of at least 20% calcium oxide. The reaction rate was weakly dependent on particle size and strongly depressed by sulfate loading. For average particle diameters less than 500 microns, the rate was essentially independent of particle size. The effect of increasing conversion on rate is explained as an exponential relationship between the frequency factor and sulfate loading.

Experiments on a wide range of carbonate rocks using the differential reactor confirm the importance of chemical reaction rate controlling for SO_2 sorption. Furthermore, the strong influence of physical properties on limestone reactivity has been delineated. Small pores and large surface areas lead to high reaction rates while large pores lead to high capacity.

Pores smaller than 0.1 micron plug rapidly with reaction products and are apparently responsible for shell formation on certain stones. The results confirm the exponential decay of reaction rate during the chemical reaction-controlled phase, which generally extends from 50 to 90 percent conversion of CaO in 95 micron particles at 980°C. Stones of varying geological type yield calcines of distinctly different physical structures which show correspondingly large differences in both rate of reaction and total capacity for SO_2 sorption.

The loss of reactivity due to overburning has been studied using an oil fired boiler belonging to the Florida Power Corporation (in St. Petersburg). During these field tests, samples of lime were collected from the flue gas at various points in the boiler and analyzed to determine the degree of calcination, extent of sulfation, and changes in physical properties related to chemical reactivity. The boiler samples were found to be considerably less reactive with SO_2 than stone calcined in the laboratory. The low porosity and high density of the injected lime indicates that overburning is at least partly responsible for the low boiler desulfurization achieved when additives are injected with fuel.

The effects of overburning for calcination temperatures ranging from 1700 to 3200°F were determined by measuring more than a dozen chemical and physical properties of these calcines. While

density increased, other reactivities (e.g., SO_2 sorption, CO_2 sorption, extent of slaking), pore volume, and surface area decreased markedly with calcination temperature. Loss of reactivity is as high as 80% for sorption of SO_2 from flue gas in 120 seconds when the calcination temperature is raised from 1700°F to 2600°F. Moreover, a strong intercorrelation was noted between SO_2 reactivities, surface area and pore volume. This supports the conclusions that (1) reactivity is a function of surface area and pore volume and (2) loss of reactivity (or dead-burning) is attributable to growth of CaO crystals which decreases the surface area and pore volume. The best test for determining the loss of reactivity of partially sulfated lime involves measuring the weight gain of hydrated samples.

Eighty-six carbonate rock samples were tested in a fixed-bed reactor to determine their capacity to react with flue gas containing sulfur dioxide. Although most of the work was performed with the carbonate and the oxide at standard test conditions, supplementary tests were made on hydrates, oxides and carbonates over a wide range of reaction temperatures and calcination conditions. At 980°C the average sulfur loading of the carbonate feed was practically equivalent to the loading for the precalcined samples. Differences among the samples were only slightly related to chemical composition; porosity, as measured by mercury pore volume, best explained variations in capacities of the samples. Chalks and oolitic samples were

the most efficient absorbents, and magnesite and Iceland spar, the least efficient of the stones tested.

In addition to limestone as a material for sorbing SO_2, other materials have also been considered. Interest had been shown in kiln dust from Portland cement manufacturing as a SO_2 sorbent. Tests conducted with kiln dust samples exposed to flue gas in a differential reactor and an aqueous batch scrubber indicated that kiln dust has absorptivity and reactivity comparable to limestone, but no better. Metal oxides such as cupric oxide have also been suggested as potential SO_2 sorbents. Thermogravimetric analysis (TGA) of a sample of cupric oxide exposed to pure SO_2 had a maximum weight gain of 48 weight percent at 738°C. However, at the temperature of interest (315°C) the cupric oxide had only a 2-3 percent weight gain. Finally, the reactivity of char with sulfur oxides within the Westvaco sorption-regeneration scheme has been studied. At the time ten percent of the feed SO_2 concentration broke through the bed of char, loading on the char was 15.8 wt. percent SO_2. Loaded SO_2 in the form of H_2SO_4 was regenerable with H_2S to form sulfur.

B. GENERAL INTRODUCTION

Limestone processes for controlling sulfur oxides, especially the dry limestone injection process, have long been of great interest because of their simplicity and low cost. The Division of Process Control Engineering at an early date selected the dry limestone injection process for development and large scale demonstration of optimum performance on a power boiler unit of the 150 MW class. This is in accord with a report of the National Academy of Engineering[26]*, which recommended the development of throw-away processes for SO_2 control on the highest priority basis. In support of this goal, the activities of the Process Research Section have been directed toward specific problem areas relating to the limestone processes, with major emphasis over the past two and one-half years on acquiring information on the dry injection process which will be required to apply the process on a wide scale. Little was known about the mechanism and rate of reaction between limestone and sulfur oxides, nor had the differences between limestones been related to their potential reactivity. That this information was vital for optimization of the process can easily be seen. The limestone injected into a power boiler must calcine (evolve CO_2 to become lime) and react with most of the sulfur oxides present - all within two seconds or less. If the limestone is injected

---

* Refers to bibliography listed under G. REFERENCES.

too close to the fireball, the lime produced will be dead-burned and become unreactive. If the limestone is injected higher or farther from the fireball, the residence time for the lime particles in the zone of the boiler favoring reaction with sulfur oxides will be seriously reduced. Hence, an understanding of the kinetics of lime-SO_2 reactions and the characteristics of dead-burning were necessary. In addition, data on the capacity of limestones was of interest to evaluate the maximum potential of limestones to absorb sulfur oxides, and to identify those unsuitable for injection due to markedly low capacity.

From the general objectives of defining the capacity and kinetics of limestone-SO_2 reactions as well as determining the nature of overburning, there evolved five discrete investigations:

1. Kinetics of the Reactions of SO_2 with Calcined Limestone
2. Physical Properties of Carbonate Rocks Related to SO_2 Reactivity
3. A Field Study of the Role of Overburning
4. Methods for Testing the Degree of Overburning of Calcined Limestones
5. Capacity of Limestones for Sorption of SO_2

The first of these was undertaken to determine the mechanism and rate of reaction of limestones after calcination under standardized conditions. Effects of reaction temperature,

particle size, and extent of reaction on the reaction rate were investigated. The second study characterized ten diverse types of naturally occurring carbonate rocks for their SO_2 reactivity. It was the goal of this study to identify those physical or petrographic properties (such as pore size, surface area and crystal structure) which contribute to greatest SO_2 reactivity, and to identify those types of limestones which perform most effectively as sorbents for sulfur dioxide.

For the field study of overburning, limestone was injected with the fuel in an oil-fired furnace. In so doing, the limestone was given the maximum solids residence time and high temperatures for fast calcination and fast reaction. If SO_2 removal efficiency were to be poor, it would be the result of calcination at excessively high temperatures leading to dead-burning. Other laboratory tests were made to confirm overburning of the limestones. To develop a test for dead-burning in the presence of fly ash as well as partial sulfation, which could be used to quantify the influence of the effect of dead-burning in full scale evaluation of the process, a fourth study was initiated. Not only was a dead-burning test desired, but the nature of dead-burning itself in terms of physical and chemical property changes needed to be defined.

The last of the above listed investigations was responsible for determining the ability of a large number of limestones to achieve a high absorption efficiency. Thus, a comprehensive limestone inventory was established and a ranking within this inventory as to SO_2 reaction capacity was identified so that selective recommendation of limestones would be possible.

Other materials besides limestone have been studied as sorbents for controlling sulfur oxides. Among them are kiln dust, copper oxides, and char. In general, these investigations were designed to test the feasibility of proposed processes and were not intended to be in depth experimental programs. Brief discussions of the results may be found in the appendices. The kiln dust tests are discussed in Appendix D; the copper oxide study, in Appendix E, and the char, in Appendix F.

C. DISCUSSION OF PROJECTS

In this section are given individual detailed discussions of each of five project areas which have been investigated during the past two and one-half years (July 1968 to December 1970) by the Process Research Section. The intent of each of these projects as discussed fully in the general introduction was to delineate some aspect of limestone reactivity with respect to SO_2 sorption. Each of the five parts of this section identifies its own objectives and conclusions as well as the details of the experimental procedure and results. General conclusions drawn from the whole of the experimental effort may be found in the section immediately following.

1. Kinetics of the Reaction of SO_2 with Calcined Limestone

a. Introduction

Processes in which limestone and dolomite are used to desulfurize flue gas are being intensively investigated under the sponsorship of the Air Pollution Control Office. Such processes include the dry injection of pulverized stone into boiler furnaces, the wet scrubbing of flue gases and combinations of dry injection and wet scrubbing, and the use of fluidized bed contactors, fluid bed combustion, and thin fixed beds. An understanding of the chemical reactions associated with these processes is desirable to obtain most efficient performance when such process is applied.

It is generally assumed that limestone absorbs SO_2 by a mechanism involving two consecutive steps - dissociation of the calcium carbonate, followed by reaction of CaO with sulfur dioxide. It is expected that the rate of the second step will be important in any of the proposed pollution control processes, and especially in the dry injection process[28]. Several investigators[14, 29] have determined the saturation capacities of a large number of naturally occurring limestones and dolomites under various conditions of reaction with SO_2. Other studies under way will define the rate of reaction of uncalcined limestones in the disperse phase[8]. The purpose of the investigation reported here was to determine the rate of reaction of limestones after calcination under standardized conditions.

b. Experimental

Bench scale experiments were carried out to measure the rates of reaction for several selected limestone calcines when exposed to a fly ash-free flue gas of controlled composition. Table 1-1 shows the chemical composition and primary physical characteristics of the calcined stones used in this work. Complete geological descriptions of the stones are given in a separate report[15]. Calcination was carried out in 180 g. batches in an Inconel kiln 12.5 cm. long and 8 cm. in diameter, rotated at 1 r.p.m. It was heated to 980°C. in an electric furnace and then charged with 10/28 mesh stone. The kiln was maintained at 980°C. and purged with air for 2 hours to remove CO_2 during calcination. Conversion to the oxide was complete under these conditions (CO_2 < 0.5%). The calcined stone was cooled, crushed, and screened into size ranges of 12/16, 42/65, and 150/170 mesh (Tyler). The calcined samples were stored in airtight containers until used.

The rate of reaction with SO_2 was determined in a differential reactor (Figure 1-1) constructed of Inconel alloy. In this type of reactor the thin layer of solid and high gas flow prevent gas-phase concentration gradients around the reacting solid. The gases, preheated in an outer annular section, pass downward through the inner reactor tube about 73 cm. long and 3.42 cm. in inside diameter. The sample is supported on a 30-mesh Inconel screen in a removable carrier. The carrier

Table 1-1. Properties of Calcines

Stone	LOI %[a]	%CaO	%MgO	%Fe_2O_3	%SiO_2	Bulk density,[b] g./cc.	Porosity,[b] cc./cc.
1337	47.4	55	43	0.33	0.92	1.41	0.58
1351	42.4	54	28.5	7.0	8.2	1.59	0.56
1343	42.8	94	0.8	0.66	2.98	1.88	0.45
1360	43.8	81	13.0	1.25	3.65	1.51	0.56

[a] Weight loss on calcination at 980°C.

[b] 150/170 mesh particle size.

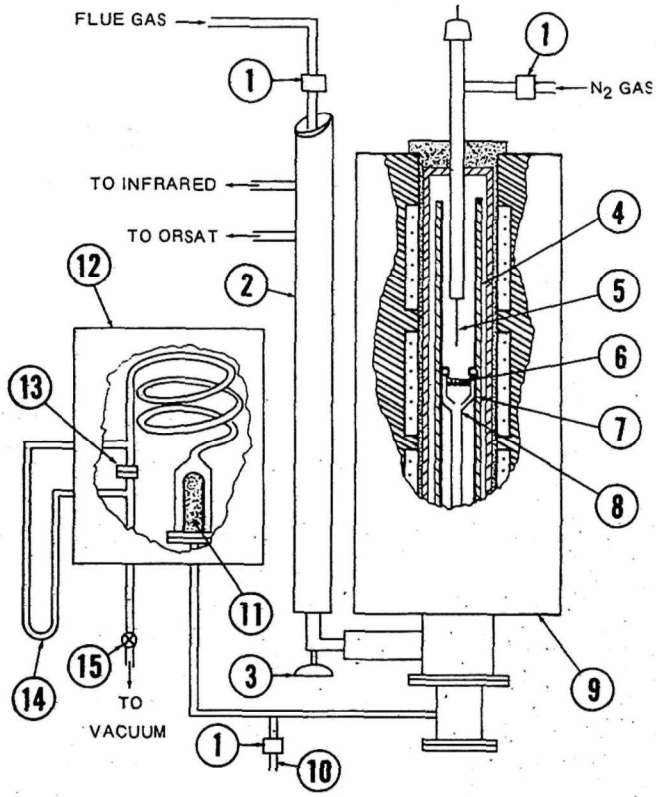

Figure 1-1. Differential Reactor

1. Teflon solenoid valve 2. Heating tapes 3. Thermometer 4. Preheat section 5. Thermocouple 6. Sample 7. Reactor tube 8. Sample carrier 9. Heating furnace 10. N_2 Purge exhaust 11. Alundum filter 12. Constant-temperature oven 13. Orifice 14. Manometer 15. Flow control valve

is sealed against a flange in the center of the reactor tube so that the entire gas flow passes through the solid during exposure.

In this investigation a sample consisted of 30 mg. of calcined stone, distributed uniformly over the 2.65 cm. diameter screen. For small particle sizes a disk of woven refractory fabric was placed on the screen and a 1 cm. thickness of refractory (fused quartz) gauze was placed on the fabric. The lime particles were dispersed into the gauze.

The mass flow rate of gas through the screen was maintained constant at 0.075 g./(sq. cm.)(sec.), which at 870°C. corresponds to a superficial velocity of 240 cm. per sec. A high gas velocity reduced gas film resistance to a negligible value, so that mass transfer to the particle surface did not affect rate measurements. The gas fed to the reactor was a flue gas generated by combustion of fuel oil containing carbon disulfide. The composition of the flue gas was 10.5% CO_2, 3.4% O_2, 9.9% H_2O, 0.27% SO_2, 0.003% SO_3, and 75.9% N_2 by volume. The sulfur dioxide concentration was monitored continuously with an infrared analyzer after removal of the water vapor from the sample stream.

The reactor was mounted in an electric furnace containing three heating sections. The center section was energized

by a proportional controller acting on a thermocouple located 3.4 cm. above the screen supporting the lime sample. The other two sections were equipped with variable transformers set by thermocouples in the top and bottom of the reactor tube to maintain a uniform temperature over the full length of the reactor and preheater assembly. The thermocouples were calibrated in situ against a multiple shielded, high-velocity thermocouple. A multipoint recorder continuously monitored reactor temperatures.

Before a run was started, the carrier and sample were allowed to heat up for 5 minutes to the reactor temperature. The time of exposure of the solid to the gas stream was controlled by solenoid valves that started the gas flow at the beginning of the run and purged the reactor with nitrogen at the end of the run. The sample was removed from the carrier after exposure (along with the refractory gauze, if used) and analyzed for sulfate. The exposed sample was dissolved in water by soaking with ion exchange resin, filtered, and the filtrate titrated in 80% isopropyl alcohol with barium perchlorate using thorin indicator.

c. Discussion of Results

The chemical reaction between limestone and sulfur dioxide at high temperature in the presence of excess oxygen is:

$$CaO + SO_2 + 1/2\ O_2 \rightleftharpoons CaSO_4 \qquad (1)$$

Equilibrium data for the reaction have been summarized by researchers at Battelle Memorial Institute[34]. The reaction proceeds to the right at temperatures up to 1230°C. at partial pressures of SO_2 corresponding to flue gas concentrations of about 3000 p.p.m. Equilibrium would also permit the MgO component of dolomite to react at temperatures below 840°C., and it has been reported to participate in the reaction with SO_2 in the presence of iron oxide impurities[35]. More recent investigations[4] have shown that SO_2 reacts only slightly with MgO at 430° to 700°C. in a fluidized bed, reaction occurring preferentially with calcium even when Fe_2O_3 content is as high as 7%. Calcined magnesite ($MgCO_3$) and calcined brucite [$Mg(OH)_2$] were shown to have low capacities for sorption of sulfur dioxide. Dolomites injected into a pilot furnace[2] have been examined by X-ray diffraction analyses, but showed no $MgSO_4$ as a reaction product, although small amounts were detectable by DTA methods. No distinction is made in this study between CaO and MgO, although the data support the conclusion that only CaO has a significant reaction rate under the conditions investigated.

When reaction 1 takes place in flue gas containing high concentrations of carbon dioxide, equilibrium also favors a competing reaction[34] below 770°C.:

$$CaO + CO_2 \rightleftharpoons CaCO_3 \qquad (2)$$

Typical experimental results for the sorption of SO_2 are shown in Figure 1-2; the mg. of SO_3 found in 150/170-mesh particles

Figure 1-2

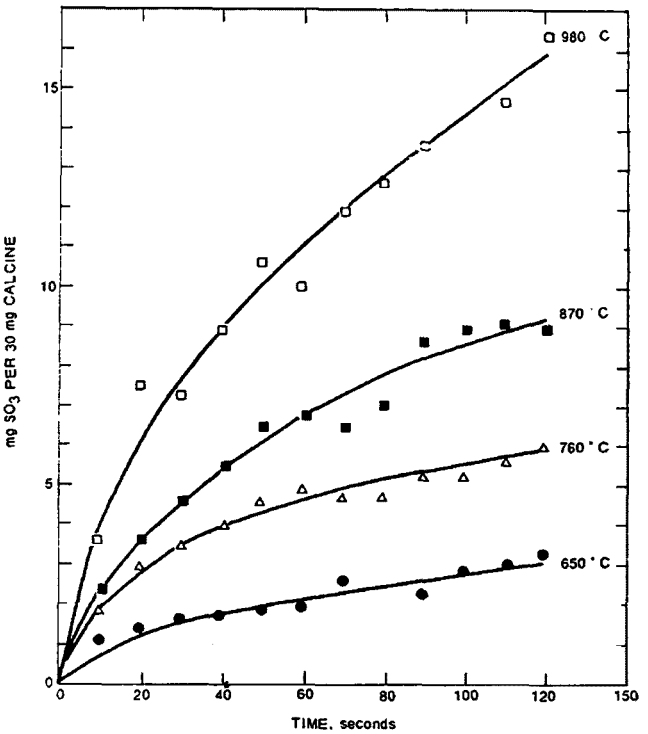

Sorption of sulfur dioxide by dolomite 1351 at various reactor temperatures

SO_2 concentration = 3000 p.p.m. (dry basis), particle size = 150/170 mesh

Figure 1-3

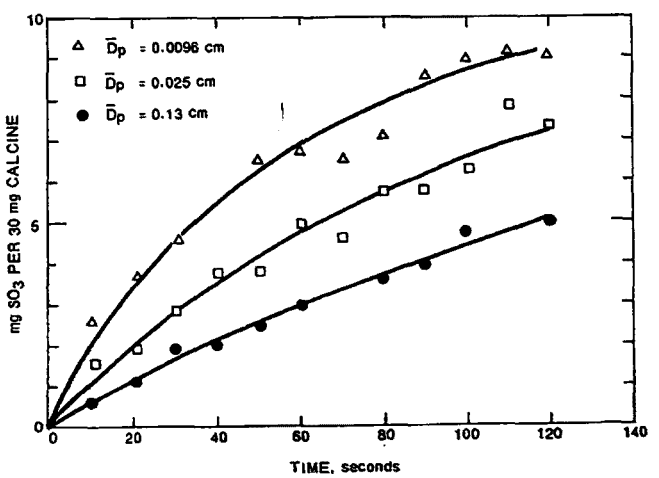

Sorption of sulfur dioxide by different particle sizes of dolomite 1351

SO_2 concentration = 3000 p.p.m. (dry basis), temperature = 870° C.

($\bar{D}_p$ = 0.0096 cm.) after reaction is plotted against exposure time at various reaction temperatures. Figure 1-3 shows a similar plot for different particle sizes at a reaction temperature of 870°C. Total conversion of the CaO in this dolomite would correspond to an ordinate value of 23.2 mg. These figures illustrate the strong sensitivity of the reaction to temperature and the surprisingly low sensitivity to particle size, which were characteristic of all the stones examined.

The rate of sorption was measured as the tangent to the smooth curve drawn through the data and is defined as:

$$r = \frac{1}{W} \frac{dn'}{dt} \tag{3}$$

where W is the grams of calcined stone exposed in the reactor, and n' is the gram moles of SO_3 in the stone at time t. (Note: Nomenclature is summarized under Subsection e. at the end of this section).

The data were correlated according to the rate expression for chemical reaction in a porous solid[31]:

$$-\frac{dn}{dt} = k_v V C^m \eta \tag{4}$$

since dn'/dt = -dn/dt

$$\frac{1}{W} \frac{dn'}{dt} = \frac{\eta}{\rho} k_v C^m \tag{5}$$

The effect of SO_2 concentration, C, on the rate of sorption is shown in Figure 1-4. The SO_2 concentration was varied between

Figure 1-4

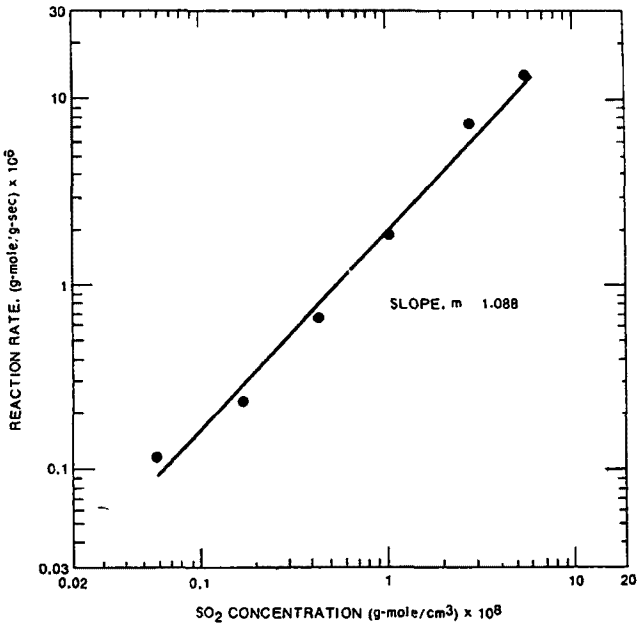

Log *r vs.* log *C* to estimate *m*

Dolomite 1337, 12/16 mesh particle size, 870° C.

Figure 1-5

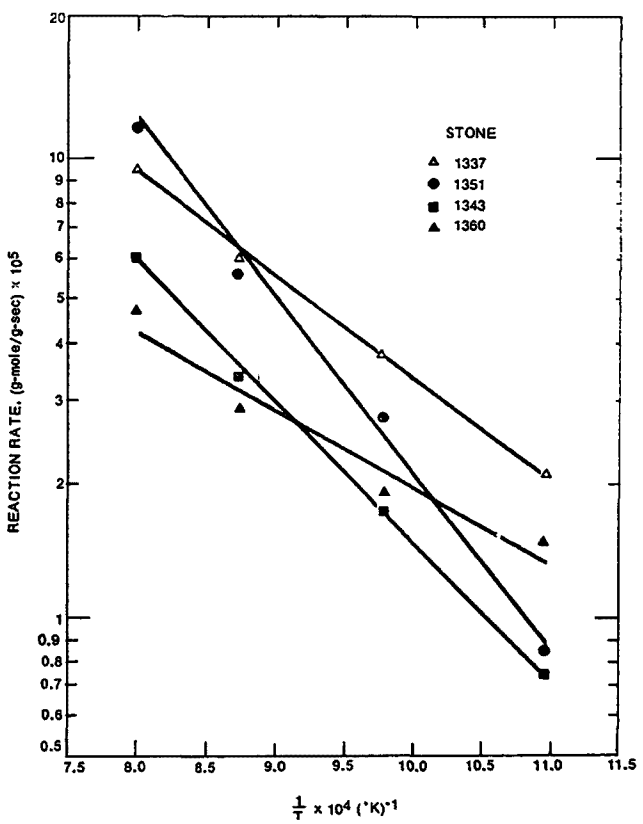

Arrhenius plots for the reaction of sulfur dioxide with four limestones

58 and 6000 p.p.m. by changing the carbon disulfide content of the fuel oil burned in the furnace. The rate was measured at a conversion of 10.5% of the CaO in 12/16-mesh stone reacted at 870°C. The line fitted to these data by the method of least mean squares has a slope of 1.008 or $m \simeq 1$, indicating that the reaction is first order with respect to the concentration of SO_2 in the gas phase. For the remainder of the experimental work, which is reported below, the SO_2 concentration was fixed at 3000 p.p.m. (dry basis) or 2.9×10^{-8} g. moles/cc. (wet basis, 870°C., 1 atm.).

The rate constant k_v is a function of temperature and also some function of n'/W, the sulfate loading; it decreases as the reaction progresses and the solid reactant is consumed. The temperature dependency was correlated by the Arrhenius equation:

$$k_v = Ae^{-E/RT} \qquad (6)$$

An Arrhenius plot for each of the four calcined stones is shown in Figure 1-5 for reactions with SO_2 at temperatures between 650° and 980°C. The rates were measured at a sulfate loading of 1×10^{-3} g. mole/g. of 150/170-mesh particle size sample. This loading corresponds to approximately 10% conversion of the CaO. The data show a linear correlation between log r and 1/T, as specified by Equations 5 and 6. The apparent activation energy determined from the slope of these plots was distinctly different for each stone, ranging from 8.1 to 18.1 k cal/g. mole.

When rates were measured at higher CaO conversions - up to 20% - the plots shifted toward the abscissa, but remained parallel to the lines shown in Figure 1-5, thus indicating no significant change in the activation energy.

The high sensitivity of the rate to temperature suggests chemical reaction to be the predominant rate-controlling resistance during the initial period of SO_2 sorption by small particles. The apparent activation energy for sorption, controlled solely by bulk diffusion, would be only 3.4 k cal./g. mole. A summary of the empirical kinetic parameters estimated for the four stones is given in Table 1-2.

The data in Figure 1-5 further indicate that reduction in rate of reaction with SO_2 as a result of competition with CO_2 was not important at 650°C. At 540°C., however, there was evidence that reaction 2 was significant and the Arrhenius plots could not be extrapolated to that temperature. The plots also failed when the reaction temperature was raised from 980° to 1100°C., sorption rates decreasing at the higher temperature. Subsequent experiments in which the calcine was heated for 10 minutes at 1100°C. and then reacted at 870°C. showed the same difference in rate when compared to a sample which was not exposed to the high temperature. It was concluded that the loss of reactivity was due to the changes in porosity and bulk density which occur when lime is "hard-burned"[7].

Table 1-2. Kinetic Parameters[a] for Sorption by Calcined Limestones

Stone	Activation energy, E, cal./g. mole	Reaction rate constant, k_v, sec.$^{-1}$	Frequency factor, A, sec.$^{-1}$
1337	10,000	4.8×10^3	2.4×10^5
1351	18,100	7.2×10^3	9.0×10^6
1343	14,200	4.0×10^3	1.1×10^6
1360	8,100	2.3×10^3	5.5×10^4

[a] Evaluated at sulfate loading of 1×10^{-3} g. moles/g., 150/170 mesh particle size; 980°C.

To ensure that gas film diffusion was not influencing the rate measurements, a supplementary experiment was made with a 0.95-cm. diameter sample carrier which permitted exposure of the solid at high gas velocity. Samples of dolomite 1337 ($\bar{D}_p$ = 0.13 cm.) were exposed for 2 minutes at 980°C. The amount of sulfate found in the stone was only 5.3% greater at 2400 cm./sec. gas velocity than found at 225 cm./sec. The negligible effect of gas velocity verified that the rate of sorption was not limited by mass transfer to the solid surface.

The effect of particle size on reaction rate is shown in Figure 1-6, in which the value of r at a sulfate loading of 2×10^{-3} g. mole/g. is plotted against the inverse of particle diameter. If the particles are assumed to be spherical, the total exterior surface of a given mass of stone (specific surface) would increase with $1/\bar{D}_p$ when the particle size is reduced. If the reaction were occurring only at the outer surface, the plot shown in Figure 1-6 would be expected to be a straight line through the origin. It is clear that the rate was not proportional to specific surface and for fine particles was essentially independent of it. The results suggest that some reaction takes place within the interior structure of the solid and that the relative importance of the internal reaction becomes greater as the particle size decreases. These observations are similar to the effects associated with highly porous catalysts and are consistent with the fact that the pore space in calcined limestones usually accounts for 50%

Figure 1-6

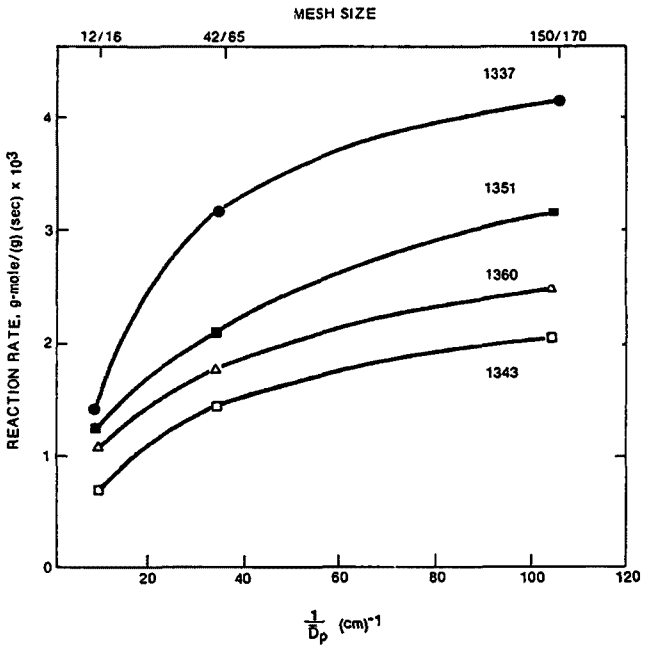

Reaction rate vs. $1/\bar{D}_p$

Sulfate loading = 2 × 10–³ g. moles/g.

Figure 1-7

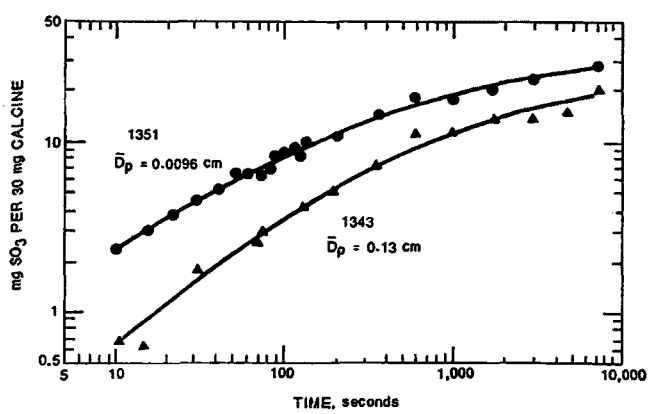

Sorption of sulfur dioxide by calcined limestones

or more of the total volume of the particles. The porosities (or fraction of particle volume that is pore space) for the four calcined stones are given in Table 1-1.

Figure 1-7 shows the conversion versus time response for different particle sizes of stones 1351 and 1343 over long periods of exposure at 870°C. An analysis of the response according to the method of Shen and Smith[32] was made to test for intraparticle diffusion. This model is based on diffusion through the product crust as the rate limiting mechanism and a nonporous solid reactant in which reaction occurs only at the interface of the unreacted core. The data from this investigation could not be correlated by the shell diffusion model given by Shen and Smith's Equation 31. Figure 1-6 shows that the model for shell diffusion, which predicts that the rate of sorption at a given sulfate loading will increase with $1/\bar{D}_p^2$, is clearly inconsistent with data on particle size versus reaction rate.

The data could be correlated empirically by a plot of log r against sulfate loading, n'/W, as shown in Figure 1-8. The data were linear for all particle sizes of each of the four stones examined at the reaction temperature of 870°C. The observed response can be interpreted in terms of a change in the frequency factor, A, of Equation 5. The frequency factor, which relates the reaction rate to the number of molecular

Figure 1-8

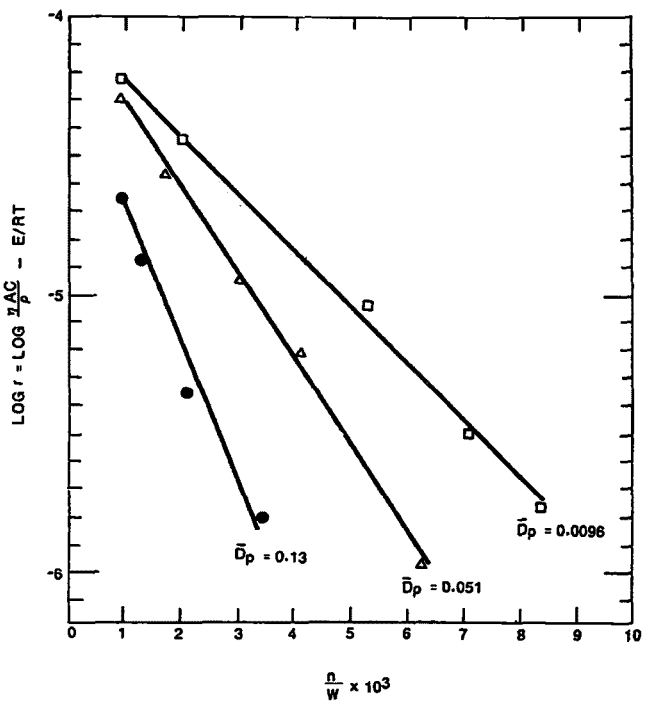

Relation of reaction rate and sulfate loading for dolomite

1337

collisions occurring per unit volume per unit time, is dependent upon the amount of SO_2 and the amount of unreacted CaO present (as well as other factors such as surface effects and probability of reaction of the molecules). As the reaction progresses and CaO is consumed, the frequency factor will be expected to decrease in some manner related to the amount of sulfate formed. If r_o and A_o are the rate and frequency factor at zero sulfate loading, then, from Equations 3, 5, and 6,

$$r_o = \frac{\eta A_o C}{\rho} e^{-E/RT} \tag{7}$$

designating the slope of the straight line fitted to the data in Figure 1-8 as β, the equation for the rate of reaction can be written as a function of sulfate loading:

$$\log \frac{\eta AC}{\rho} - \frac{E}{RT} = -\beta \frac{n'}{W} + \log r_o \tag{8}$$

Equations 7 and 8 reduce to

$$A = A_o e^{-\beta n'/W} \tag{9}$$

The observed relationship between rate and sulfate loading thus indicates an exponential decrease in the frequency factor. The data of Figure 1-8 show that coefficient β is a function of particle size, the rate of reaction of large particles being more sensitive to sulfate loading than small particles. Estimates of the effectiveness factor, obtained by extrapolation of the straight lines of Figure 1-8 to zero sulfation, indicate

$\eta \simeq 1$ for particles smaller than 0.05 cm. as shown by the approximately equal intercept of the two lines on the ordinate. The lower intercept for $\bar{D}_p = 0.13$ cm. indicates $\eta < 1$, implying the presence of pore diffusion resistance of significant magnitude for the larger size particles.

The results of this study show that the rate of sorption of SO_2 by calcined limestones is dependent to a very large extent upon the kinetics of the chemical reaction, particularly at small particle sizes, and that the rate of reaction predominates as the overall rate-controlling resistance for conversion of at least the first 20% of the CaO.

d. Conclusions

Differential reactor techniques were used to measure the rate of reaction of sulfur dioxide with four natural specimens of limestone, after calcination at standardized conditions. The rates were measured as a function of SO_2 concentration, particle size, and CaO conversion between 540° and 1100°C. A first-order chemical reaction was the predominant resistance limiting the rate of sorption of SO_2 by small particles. The activation energy was dependent upon the type of stone, and ranged between 8.1 and 18.1 k cal./g. mole. The rate was essentially independent of particle size for $\bar{D}_p < 0.05$ cm. Reaction occurs initially throughout the particle volume under the isothermal reaction

conditions studied and the internal diffusion resistances become limiting only after conversion of at least 20% CaO. The reaction rate decreased rapidly with increasing conversion, explained by an exponential relationship between the frequency factor and the sulfate loading.

e. Nomenclature

A = frequency factor, $sec.^{-1}(g.\ moles/cc.)^{m-1}$

A_o = frequency factor at zero solid conversion, $sec.^{-1}(g.\ moles/cc.)^{m-1}$

C = gas phase concentration of sulfur dioxide, g. moles/cc.

$\bar{D}_p$ = mean particle diameter, cm.

E = activation energy, cal./g. mole

k_v = reaction rate constant per unit volume of solid, $sec.^{-1}(g.\ moles/cc.)^{m-1}$

m = order of reaction with respect to sulfur dioxide

dn/dt = rate of change of SO_2 in the gas phase, g. moles/sec.

n' = sulfate in solid as SO_3, g. moles

R = gas constant, 1.987 (cal./g. mole°K.)

r = rate of formation of SO_3 in solid, g. moles/(g. sec.)

r_o = rate at zero solid conversion, g. moles/(g. sec.)

V = volume of solid, including intraparticle pores, cc.

W = weight of solid sample, g.

T = temperature, °K.

t = time, sec.

β = empirical correlation coefficient defined by Equation 9

η = effectiveness factor, ratio of reaction rate to the rate that would be obtained if entire volume of particle participated equally in reaction

ρ = bulk (particle) density of solid, g./cc.

2. Properties of Carbonate Rocks Related to SO_2 Reactivity

a. Introduction

This report summarizes an experimental study of the SO_2 sorption characteristics of ten diverse types of carbonate rocks (limestones, dolomites, magnesites, etc.). Specimens representative of a broad spectrum of naturally occurring stones were selected for detailed petrographic, mineralogical and chemical examinations under Contract CPA 22-69-65 with the Illinois State Geological Survey (ISGS). It is the goal of that contract to establish criteria, based on petrographic and mineralogical properties, for selecting carbonate rocks of greatest potential for the desulfurization of stack gases. Tests conducted by APCO, to evaluate the isothermal rates of reaction of calcines prepared from these stones are reported here. The rate of reaction of the raw stone under non-isothermal conditions will be determined by Battelle Memorial Institute under Contract PH 86-67-115 using a dispersed phase reactor.

A brief description of the rock types selected for this study is shown in Table 2-1. This was taken from the ISGS Quarterly Report, dated December 4, 1969. Two additional stones were also tested which are not included in that report: Stone No. 2129 (ISGS Type 11), a Michigan marl, which is an unconsolidated form of $CaCO_3$, and Stone No. 1336 (ISGS Type 10), which is a

Table 2-1

Stone Identification and Description

Type 1. Calcite, variety Iceland spar, transparent, colorless and optically near perfect; cleavage rhombs up to 1 inch.

Type 2. Calcite, very coarse calcite spar, translucent milky in color due to abundance of crystalline imperfections; cleavage rhombs up to 1 inch.

Type 3. Calcite limestone, with few scattered fine-grained dolomite rhombs; coarse unequant granular and porous; consists of recrystallized crinoid fragments and a few finely recrystallized bryozoans. Gray.

Type 4. Calcitic limestone, very fine, equant granular, and dense; light brownish gray.

Type 5. High purity dolomite, medium-grained, granular and porous; gray reef type of dolomite.

Type 6. 81 percent dolomite, contains clay and fine quartz silt impurities; medium-grained, granular and microporous; buff color, non reef type of dolomite.

Type 7. Magnesite, high purity, very fine, equant granular and microporous; near white.

Type 8. Aragonite sand, contains traces of magnesium calcite; consists of oolitic and concentrically banded fossiliferous sand-sized particles. The particles have a banded structure and consist mostly of fibers of aragonite.

Type 9. Calcitic dolomite (70% dolomite, 18% calcite) with limonite along grain boundaries and a few scattered particles of chert; fine-grained, moderately equigranular, and microporous; mixture of brown and gray colored stone.

marble. These two stones were tested because of the unusually high reactivity found for the marl in pilot scale coal-fired furnace tests conducted by Babcock & Wilcox (Contract PH 86-67-127) and the contrastingly low reactivity found for the marble in similar tests. Chemical compositions of all stones are reproduced in Table 2-2.

b. Experimental

The reactivity of the eleven types of limestone was measured and correlated by the methods outlined in the previous section (C 1 b.) and in the paper, "Kinetics of the Reaction of SO_2 with Calcined Limestone"[5]. Calcines prepared in a small rotary kiln (2 hours at 980°C.) were crushed and screened into 3 particle size ranges: 12/16 mesh ($\bar{D}_p$ = 0.13 cm.), 42/65 mesh ($\bar{D}_p$ = 0.025 cm.) and 150/170 mesh ($\bar{D}_p$ = 0.0096 cm.). Thirty-milligram samples of the calcines were exposed for varying lengths of time to flue gas containing 3000 p.p.m. SO_2, dry basis (2.63×10^{-8} g. mole/cm.^{3}, wet basis, 980°C.). Using the smallest particle size, reaction rates were determined at reactor temperatures of 650°C. (1200°F), 760°C. (1400°F), and 870°C. (1800°F). The rates were evaluated and compared at a sulfate loading of 2.5 mg. SO_3/30 mg. calcine (10^{-3} g. mole/g.). The sorption curves and Arrhenius plots for these data are given in Appendix A.

Table 2-2

Chemical Analyses in Weight Percent

ISGS Stone Type	1	2	3	4	5	6	7	8	9	10	11
APCO Stone No.	2201	2202	2203	2204	2205	2206	2207	2208	1701[f]	1336	2129
Mineralogical Type	Iceland spar	calcite spar	calcite	calcite	dolomite	dolomite	magnesite	aragonite	calcitic dolomite	marble	marl
SiO_2	ND	ND	ND	1.53	0.03	11.8	0.47	0.19	5.88	0.85	3.63
TiO_2	ND	ND	ND	ND	ND	0.02	ND	ND	0.15	-	0.05
Al_2O_3	ND	0.01	ND	0.01	0.02	1.77	0.08	0.27	0.69	0.20	0.95
Fe_2O_3	ND	0.19[c]	0.20[c]	0.31[c]	0.34[c]	0.13	ND	ND	2.82	0.15	ND
FeO	.13	-	-	-	-	0.41	0.07	0.01	1.75	-	-
MnO	ND	0.06	0.10	0.09	0.02	0.02	ND	ND	0.21	-	0.01
MgO	ND	ND	1.86	0.00	21.40	17.4	44.2	ND	15.33	1.4	ND
CaO	55.3	55.5	53.4	54.8	30.30	26.5	2.93	55.2	30.82	53.7	46.6
Na_2O	0.03	0.07	0.08	0.06	0.10	0.06	0.03	0.29	0.28	-	0.14
K_2O	0.02	0.02	0.02	0.04	0.03	0.90	0.03	0.03	0.22	-	0.18
P_2O_5	trace[b]	-	-	-	-	0.02	trace	0.01	0.10	-	0.67
CO_2	43.95	43.35	43.75	43.35	47.30	40.27	50.96	42.10	40.68	43.4	37.18
SO_3	0.01	0.17	0.20	0.15	0.13	0.03	0.01	0.37	0.42	-	0.50
SrO	0.14	0.002	0.009	0.019	0.019	0.04	0.01	0.10	0.04	-	-
Cl	ND	0.04	0.03	ND	0.09	trace	ND	0.24	ND	-	-
C (organic)	-	-	-	-	-	-	-	-	-	-	5.60
H_2O (100°C)	-	-	-	-	-	-	-	-	-	-	4.04
Ign. Loss	43.49	43.15	43.67	43.15	47.24	40.46[d]	51.56[e]	43.33	41.85	43.4	47.06

[a] ND - not detected: Limits of detection for SiO_2, 0.03; TiO_2 and MnO, 0.01; Al_2O_3, 0.05; Fe_2O_3, 0.01; MgO, 0.10; Cl, 0.02.

[b] Trace of P_2O_5 is approximately 0.005%.

[c] Percentage of total iron expressed as Fe_2O_3.

[d] Includes 0.30% H_2O+.

[e] Includes 0.61% H_2O+.

[f] Stone No. 1701 came from the same source as Stone No. 1351, studied by various investigators.

Previous data were correlated by the expression

$$\frac{1}{W}\frac{dn'}{dt} = \frac{k_v}{\rho_p} C_{so_2} \eta \qquad (1)$$

Because of inaccuracies involved in measuring particle densities, ρ_p, of finely divided calcines, the rate data are correlated in this report on the basis of total surface area, S_g, which is more easily and accurately determined. Since $k_v = k_s \rho_p S_g$,

$$\frac{1}{W}\frac{dn'}{dt} = k_s S_g C_{so_2} \eta \qquad (2)$$

where k_s is the reaction rate constant per unit surface with units of cm./sec. Values of S_g were obtained from B.E.T. measurements and are expressed in $cm.^2/gm$. Equation (2) is the simplified model used for data correlation in this report.

The effectiveness factor is used here to represent the degree to which reaction occurs within the internal structure of the solid. The maximum value of $\eta = 1$ indicates that reaction occurs equally throughout the internal pore structure. Low effectiveness factors, $\eta << 1$ are associated with strong pore diffusion resistances and indicate that internal structure does not participate in the reaction, i.e., that reaction takes place primarily on the outside surface of individual particles. By analogy with catalytic reactions, η would be expected to be a function of particle size, and the ratio of reaction rate/pore diffusion

rate (and hence, pore size). All other factors being equal, η decreases with (1) increasing particle size, (2) increasing temperature or reaction rate and (3) small pore size.

Three different particle sizes of each calcine were exposed at 980°C. for periods of 5 seconds to 2 hours to obtain additional parameters which have not been measured previously. These include effectiveness factors, η; reaction rates at zero sulfation, r_o; the β coefficient (sensitivity of SO_2 sorption rate to sulfate loading); and total CaO utilization. The estimation of these parameters is based on plots of log reaction rate versus sulfate loading, which have been shown to give a linear correlation over a wide range of solid conversions[1].

Total CaO utilization was determined for each particle size by exposure for 2 hours at 980°C.

Samples of calcines were submitted to International Minerals and Chemical Company for complete physical characterization (pore size distribution, pore volume and B.E.T. surface) and these data are summarized in the discussion of results. Calcines were also submitted to Illinois State Geological Survey for study by scanning electorn microscope.

c. Results

Large differences were found in SO_2 sorption rates for the calcines prepared from the various types of limestone examined in this study. Figure 2-1 compares the reactivities of 150/170 mesh particles at 980°C. In general, the marble and spars showed the lowest rates of sorption, whereas the dolomites and marl showed the highest.

The kinetic parameters for the reaction are summarized in Table 2-3. The activation energies, determined from the Arrhenius plots given in Appendix A, fall within the range previously reported for the reaction of calcined stone with SO_2, and again showed distinct differences between stones. The lowest activation energies were found for Iceland spar (Type 1), and an impure dolomite (Type 6). The Iceland spar showed other clear effects of strong diffusional resistance. The high impurity content of the dolomite may account for its kinetic behavior.

Particle size had a marked effect on sorption rate for nearly all stones at 980°C. Figure 2-2 illustrates typical sorption curves for three different particle sizes of one calcine. Rate measurements obtained from such plots were correlated in the manner shown in Figure 2-3. Extrapolation of the rate data to zero sulfation permitted the initial rate, r_o, to be evaluated independent of the effects of sulfation. The reaction rate

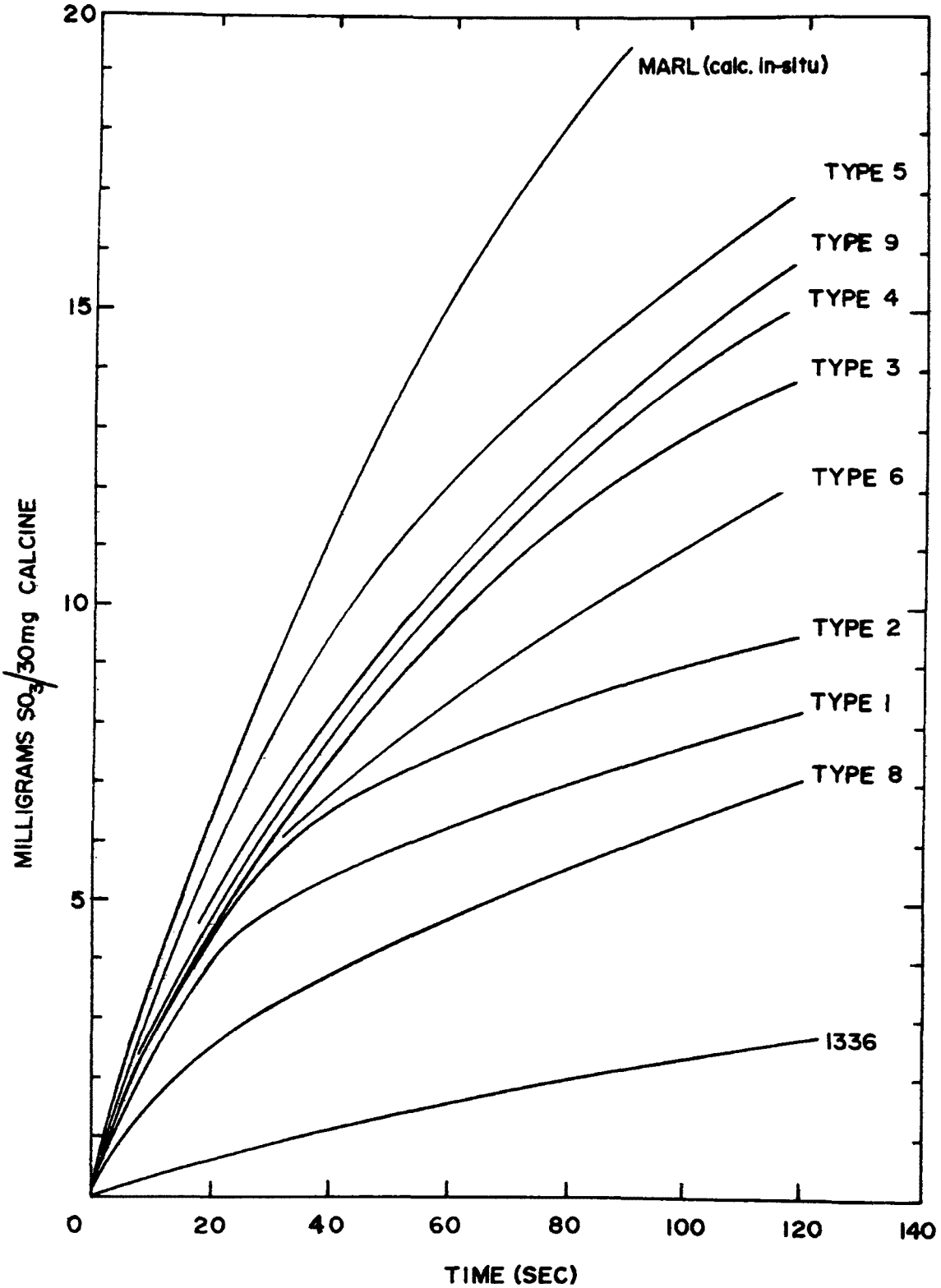

Figure 2-1.

Comparison of Reactivity of Calcines with SO_2 at 980°C.

Particle size = 150/170 mesh.

Table 2-3. Kinetic Parameters for SO_2 Sorption by Calcines (150/170 mesh particles, 980°C.)

ISGS Stone Type	APCO Stone No.	Activation Energy, E, cal./g. mole	Reaction rate constant, k_s, cm./sec.	Frequency factor, A_o, cm./sec.
1	2201	9,500	0.186	8.50
2	2202	26,500	0.737	3.18×10^4
3	2203	15,500	0.228	1.19×10^2
4	2204	12,500	0.219	31.2
5	2205	19,500	0.186	4.84×10^2
6	2206	9,200	0.068	2.78
8	2208	14,400	0.152	47.3
9	1701	18,100	0.147	2.20×10^2
11	2129	-	0.16	-

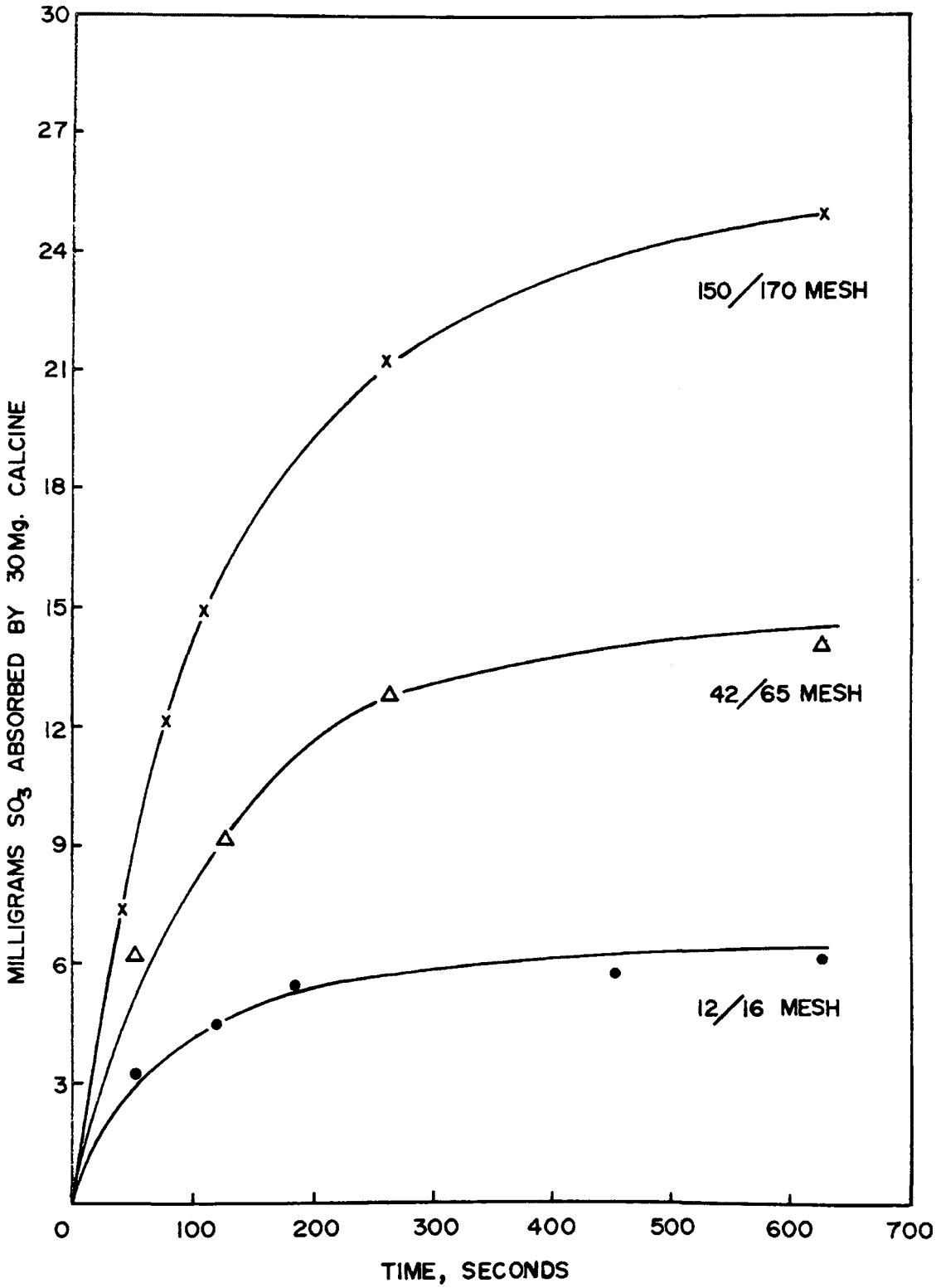

Figure 2-2.

Sorption of SO_2 by Different Particle Sizes of Type 4 Calcine at 980°C.

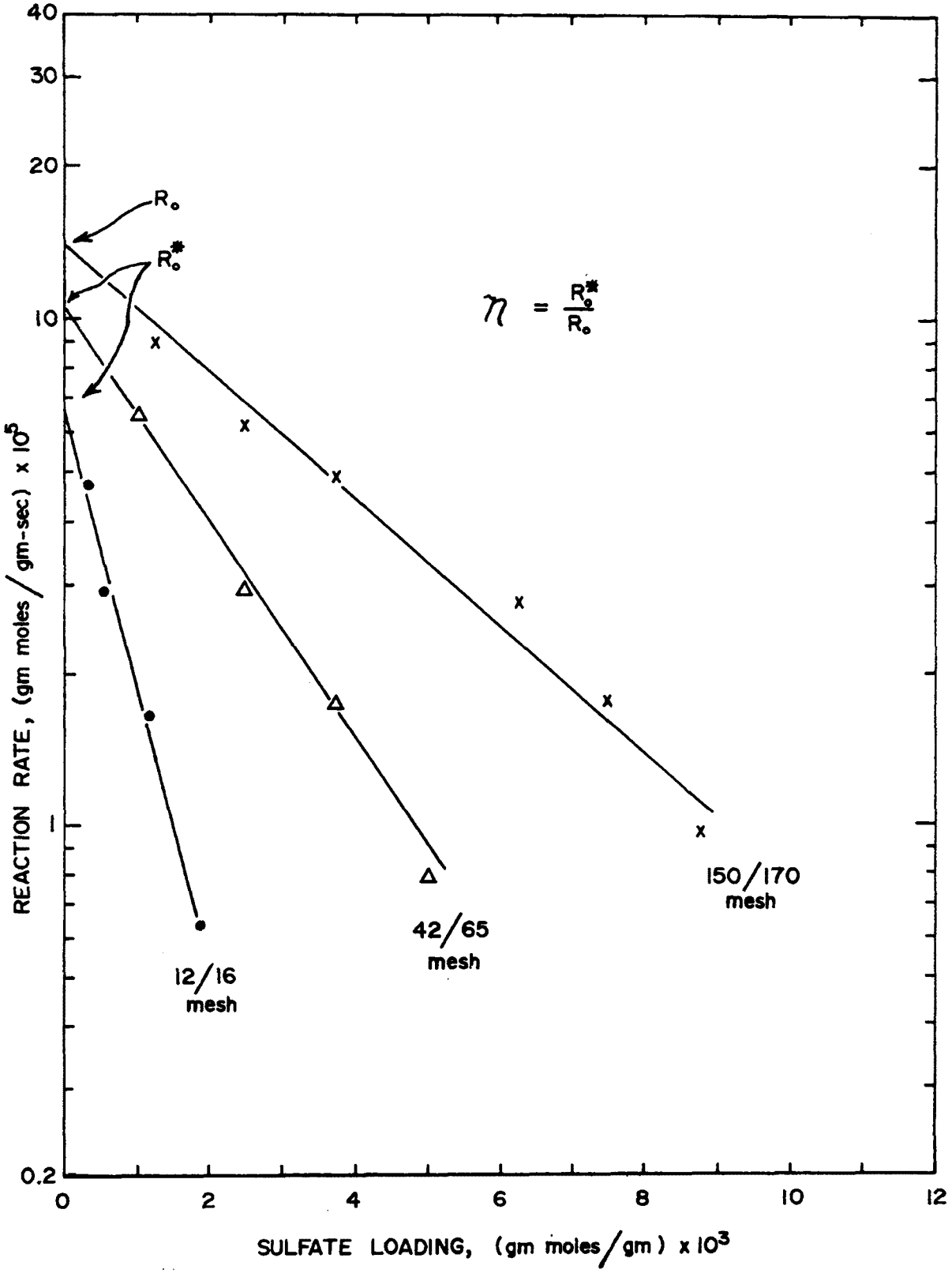

Figure 2-3.

Estimation of Initial Rate, r_o, and Effectiveness Factor, η, for the Sorption of SO_2 by Type 4 Calcine,

constants given in Table 2-3 were computed from r_o for the 150/170 mesh particles, based on the surface area of the unreacted calcine. The effectiveness factors given in Table 2-4 were estimated as the ratio of r_o for the particle size in question to the value of r_o for 150/170 mesh particles. This assumes $\eta \simeq 1$ for the smallest particle size. This assumption appears to be well justified by the experimental evidence for all stones except the Iceland spar (Type 1) and the marble (Type 10), as will be discussed later.

The empirical relationship shown in Figure 2-3, which was previously reported to correlate reactivity at 870°C., was found in this study to be also valid at 980°C. Effectiveness factors, however, which had been evaluated at $\eta \simeq 1$ for particles of 42/65 mesh at 870°C., were lower at the higher temperature used in this evaluation. At 980°C. the value of η was generally in the range of 0.7 for 42/65 mesh and about 0.3 for 12/16 mesh particles. Log r versus sulfate loading was linear for small particles to at least 50% CaO conversion at 980°C.; for two stones, marl (Type 11) and aragonite (Type 8) results were linear over the full range of conversion.

The capacities of Iceland spar (Type 1) and marble (Type 10) were especially sensitive to particle size, utilization increasing by a factor of 2 when particle size was reduced from 12/16 mesh to 42/65 mesh, and increasing again by a factor of 3 when particle size was reduced further from 42/65 to 150/170 mesh.

Table 2-4. Parameters for SO_2 Sorption by Calcines as a Function of Particle Size (980°C.)

Stone Type	Particle size, mesh	Initial rate, r_o, gm.moles/gm.sec.(x 10^4)	Effectiveness factor, η	Coefficient β, (x 10^{-2})	Total Capacity[a]	Total CaO Utilization[b]
	12/16	0.0090	< 0.0018	25.4	2.6	6.2
1	42/65	1.04	< 0.21	30.4	6.0	13.6
	150/170	5.00		13.4	18	43
	12/16	0.274	0.17	12.3	17	40
2	42/65	1.41	0.85	10.5	18	43
	150/170	1.61		7.75	21	50
	12/16	0.673	0.62	6.62	20	49
3	42/65	0.849	0.79	3.83	25	61
	150/170	1.08		2.77	33	80
	12/16	0.649	0.47	12.5	6.8	16
4	42/65	1.02	0.74	4.80	18	43
	150/170	1.39		2.89	33	80

Stone type	Particle size, mesh	Initial rate, r_o, g.moles/g.sec.(x 10^4)	Effectiveness factor, η	Coefficient β, (x 10^{-2})	Total capacity[a]	Total CaO utilization[b]
	12/16	0.610	0.32	17.9	9.0	37
5	42/65	0.935	0.49	3.93	22	90
	150/170	1.91		3.03	22	90
	12/16	0.195	0.27	4.58	19	100
6	42/65	0.457	0.63	3.00	19	100
	150/170	0.728		1.92	19	100
7	150/170	--	--	--	1.3	50
8	42/65	0.316	1	2.38	36	86
	150/170	0.316		2.38	39	93
	12/16	0.894	1	2.14	35	100
Marl	42/65	0.894	1	2.14	35	100
	150/170	0.894		2.14	35	100
	12/16				2.0	4.9
1336	42/65				4.8	11.7
	150/170	0.50			14.3	35

[a] Milligrams SO_3 absorbed by 30 mg. calcine, 2 hr. exposure.

[b] Percent conversion of CaO to sulfate, 2 hr. exposure.

Type 7, a magnesite, showed no SO_2 sorption beyond that attributable to CaO impurities for any reaction temperature from 540°C. to 980°C. To ensure that poor performance was not a result of dead-burning at the 980°C. calcination temperature, additional tests were made in which the raw stone was calcined in-situ at reaction temperature. The maximum reactivity was found at 650°C., at which temperature 6.5 mg. of SO_3 was absorbed by 30 mg. calcine in 100 seconds. At 760°C. sorption dropped to 2.6 mg. per 100 seconds exposure. At 540°C., as at 980°C., pickup was only about 1 mg. of SO_3.

d. Discussion of Results

(1) Pore Structure

Since 50 percent or more of the total particle volume of calcined limestone consists of pore space, it would be expected that the characteristics of the internal particle structure, such as pore volume, pore diameter and surface area, would significantly influence reactivity with SO_2. This would be especially anticipated where large particles are concerned. The primary physical properties of the calcines, determined by American Instrument Company and International Minerals & Chemicals Company, are summarized in Table 2-5. These measurements show marked differences between the properties of the calcines prepared from the different types of stone. Mean pore size, for example, varied from 0.07 micron (Type 1) to 4 microns (Type 8): a factor of 60.

Table 2-5

Summary of Physical Properties of Calcines

Stone Type	Particle size, mesh	Mean pore diam.,[a] microns	Pore volume,[b] cc./g.	B.E.T. Surface, $m^2/g.$
1	12/16	0.075	0.26	9.8
	42/65		0.23	9.9
	150/170		0.26	10.2
2	12/16	2.1	0.34[c]	0.83
	42/65		0.27	0.7
	150/170		0.28	0.7
3	12/16	0.60	0.31	1.5
	42/65		0.29	1.6
	150/170		0.26	1.8
4	12/16	0.44	0.32	1.9
	42/65		0.31	2.1
	150/170		0.32	2.4
5	12/16	0.27	0.39	3.6
	42/65		0.37	3.4
	150/170		0.50	3.9
6	12/16	0.30	0.40	3.6
	42/65		0.40	3.9
	150/170		0.40	4.1
7	12/16	0.01	0.34	22.7
	42/65			29.0
	150/170			37.8
8	12/16			
	42/65	4.0	0.39[c]	0.65
	150/170		0.34	0.79
9	12/16	0.42	0.37	3.4
	42/65		0.39	3.7
	150/170		0.31	3.1
10 (marble)	12/16	0.065	0.032	0.63
11 (marl)	12/16	1.6	1.15[c]	3.5
	42/65		1.19	2.2
	150/170		1.28	3.5

[a] by mercury intrusion [b] excluding voids > 1μ [c] excluding voids > 10μ

Surface areas were also quite different, ranging from 0.6 to 10 $m.^2/g.$ for different limestones. Complete pore spectra were obtained for each calcine; however, since the distribution of pore sizes in a given calcine covered a narrow range (indicating uniform-sized pores), only the mean pore diameters listed in Table 2-5 are used in making comparisons.

For a given calcine, pore structures showed no apparent dependence on particle size. The data of Table 2-5, for example, show that the total pore volume of smaller particles was not consistently or appreciably different from that of the larger particles. Mean pore size also showed no trend with particle size. A small increase in surface area, about 0.4 $m.^2/gm.$, is evident when particles are reduced from 12/16 to 150/170 mesh. This is attributed to the new surface exposed at the points of fracture when the solid is crushed to make smaller particles.

Previous work has indicated that SO_2 sorption by small particles is controlled by chemical reaction rate. If diffusion into the internal pore structure is fast relative to the reaction rate, the entire B.E.T. surface area will participate in the reaction. Under such conditions $\eta = 1$ and, from equation (2) the rate of reaction of different calcines (compared at a given sulfate loading, temperature, and SO_2 concentration) would be expected to be directly proportional to B.E.T. surface area, S_g. The

rate curves of Figure 2-1 are reproduced in Figure 2-4 with the B.E.T. surface of each calcine (determined prior to reaction) shown in parenthesis. With three exceptions the reactivity does increase with surface as expected.

Before pursuing this analysis further, some discussion of these three exceptions, Type 6, Type 1 and Type 10, is in order. In Type 6, considerable amounts of impurities are present, the calcine containing about 23 percent inerts. These inerts, in addition to reducing the amount of CaO per unit weight of calcine, can presumably block SO_2 from access to the reactive CaO in a manner similar to $CaSO_4$, thus affecting the initial reaction rate as though the stone were partially sulfated. Furthermore, physical measurements of the raw stones (Table 2-6) show an unusually high surface area for Type 6, indicating that much of the pore structure is not attributable to CaO, but rather to the impurities. As a result of these considerations Type 6 is not further considered in this analysis.

The two other stones, Type 1 and Type 10, have no chemical impurities which could account for their low sorption rates. Examination of the data in Table 2-5 reveals that these two calcines are physically similar with regard to their small pore size. Both have mean pore diameters less than 0.1 micron. These small pores, which account for nearly all of the surface area, are apparently the cause of the slow SO_2 sorption rates.

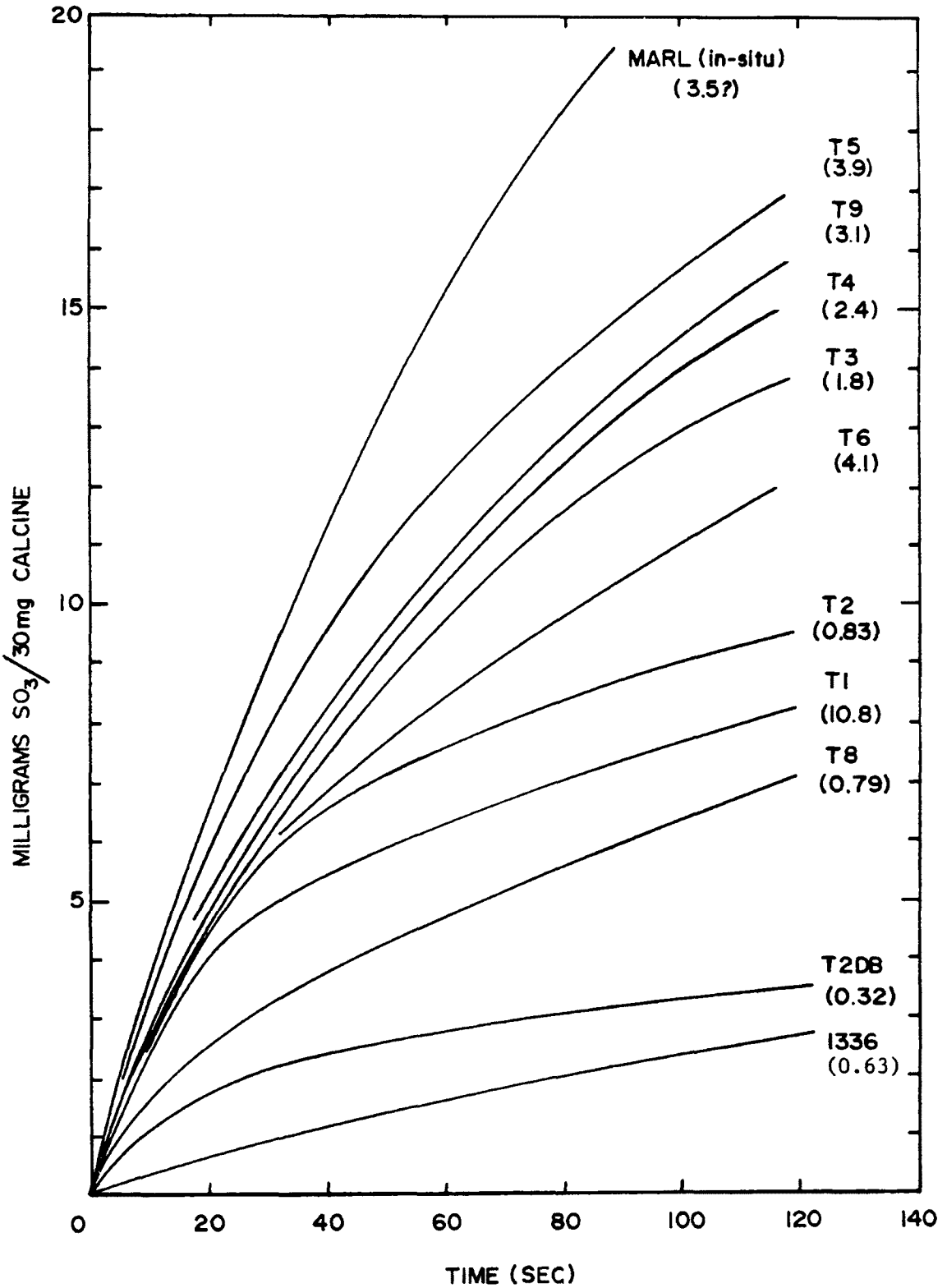

Figure 2-4.

Comparison of Reactivity with B.E.T. Surface Area (in parentheses, $m^2/gm.$)

Table 2-6

Physical Properties of Raw Limestones, 10/28 Mesh

Stone Type	Mean Pore Diam. Microns	Pore Volume, cc./gm.	B.E.T. $_2$Surface, m^2/gm.
1	40	0.040	0.19
2	35	0.019	0.17
3	5	0.041	0.32
4	2	0.041	0.46
5	20	0.016	0.18
6	0.3	0.051	2.87
7	0.15	0.054	1.54
8	0.2	0.069 (a)	3.26
10	20	0.016	0.09
11	1	0.89	4.48

(a) -42 mesh particle size, voids larger than 20 microns omitted.

Several different sources of evidence show that these small pores lead to high diffusion resistance and plug easily with reaction products. For example, the data of Table 2-5 show an unusually strong sensitivity of capacity to particle size for these two stones. In no other case were such large increases in utilization found when particle size was reduced. A test of sorption capacity with -325 mesh Stone Type 10 (D_p = < 44μ) showed that 83 percent CaO utilization can be achieved with very fine particles. This compares to 4.8 percent utilization with 12/16 mesh stone, which indicates clearly that reaction occurs with this stone only at the outside surface of the particles.

Comparison of reaction rates (at a given sulfate loading) is made for several stones in Figure 2-5. Most stones had responses characteristic of pore diffusion resistance for particles down to 150/170 mesh (pore diffusion corresponds to a straight line through the origin). Marl (Type 11) and aragonite (Type 8) showed complete absence of diffusional effects (horizontal line). Iceland spar (Type 1) and marble (Type 10), however, showed the concave-upward response which is characteristic of shell diffusion on a non-porous solid. These two stones are the only specimens of approximately 15 examined at APCO in which shell formation could be confirmed by SO_2 sorption characteristics. This result is logically attributable to quick pluggage of the small pores with reaction products. The conclusion that SO_2 sorption by Type 1 involves shell formation is in accord with

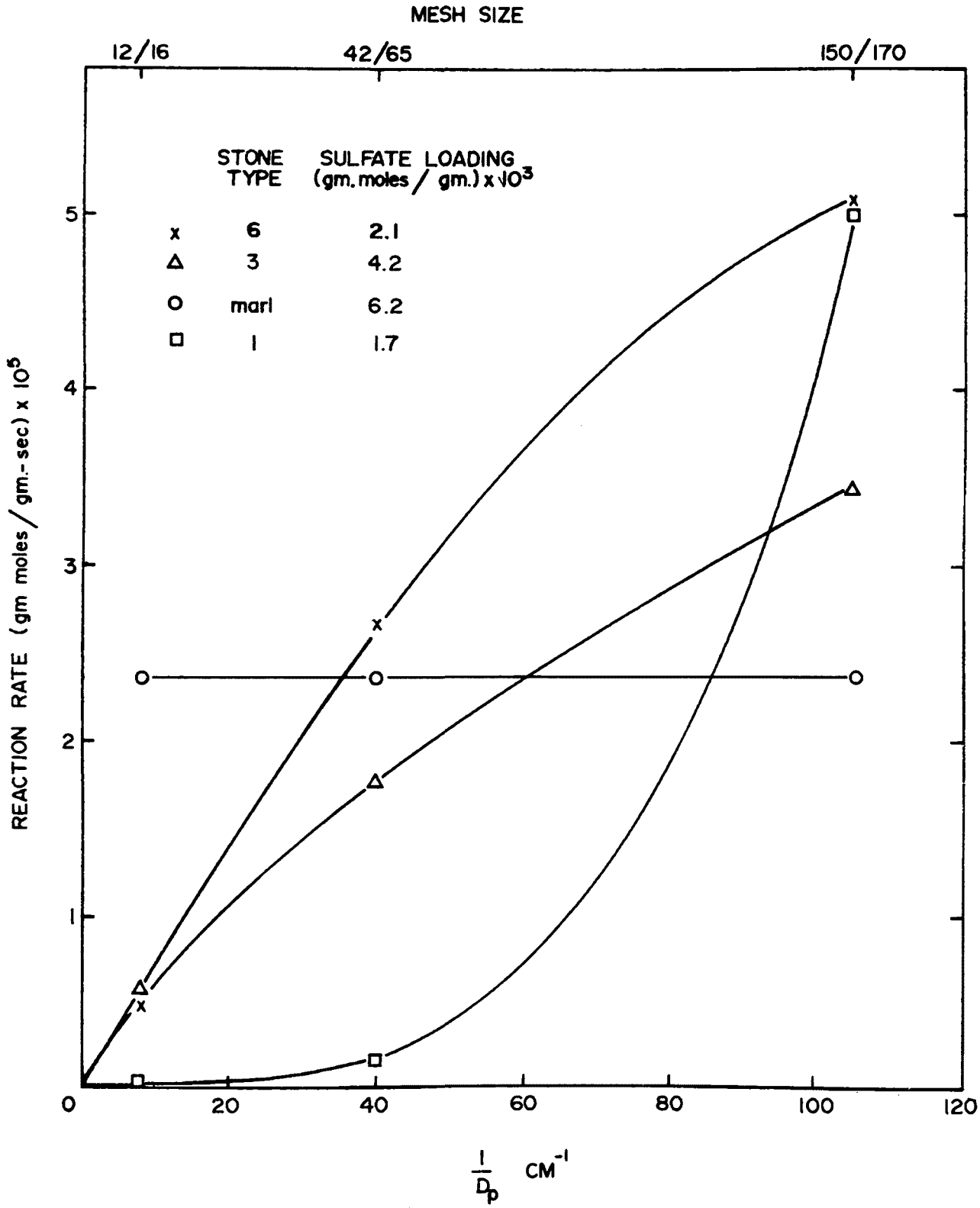

Figure 2-5.

Reaction Rate at Constant Sulfation as a Function of Particle Diameter.

the results reported by TVA for Iceland spar calcite as observed by direct microscopic examination of reacted particles (March 1968 progress report to APCO).

From the experimental evidence discussed above, it is concluded that the Iceland spar (Type 1) and marble (Type 10) are, in effect, non-porous solids. This results in the case of the marble from a combination of low porosity and small pore size. Although the Iceland spar has sufficient porosity, the mouths of the pores are of uniform small size which plug quickly with reaction product. In both cases the reaction with SO_2 is confined to the outside particle surface. It should be noted that these two stones are not typical. Mercury intrusion tests on calcines prepared from 85 different limestones generally available in the United States showed average mean pore sizes of about 0.3 micron. Calcines with mean pore sizes of 0.1 micron or less are rare, when prepared under these conditions.

Referring again to Figure 2-2, the correlation of reaction rate data with B.E.T. surface was made by comparison of rates at a sulfate loading of 7 mg. SO_3 per 30 mg. calcine. Comparison at a constant degree of sulfation is necessary to ensure that the effect of sulfation does not mask out the effect of surface area, since it has been established that rate decays exponentially with sulfation. The rates evaluated at constant sulfation are plotted against B.E.T. surface (of 150/170 mesh particles

prior to reaction) in Figure 2-6, for reaction at 980°C. Additional data which is available on other stones are also included. It is apparent from Figure 2-6 that the reaction rate does increase with B.E.T. surface area in a manner which is approximately linear. This result confirms again that chemical reaction controls the rate of sorption of SO_2 by small particles and indicates that $\eta \simeq 1$ for $D_p \bar{<} 0.01$ cm. at 980°C.

The presumption that small pores plug more rapidly than large pores (made with regard to the discussion of Type 1 and Type 10) was confirmed by an experiment in which samples of a calcine were reacted with SO_2 for varying lengths of time, and the pore spectra determined by mercury intrusion measurements on each reacted sample. Comparison of the changes in spectra showed considerable difference in the rate of decrease in pore volume for pores of different size. The volume of small pores (between 1 and 0.1μ) decreased with sulfation at a rate about 2.3 times greater than the rate of decrease in volume of pores larger than 1 micron.

Surface Diffusion, Ionic Diffusion

A short experiment was made to test for the presence of surface diffusion resistances and also to test for effects of $SO_3^=$ diffusion through the CaO lattice as possible rate-limiting steps. For this purpose, Type 2 calcine (which has large pores and therefore would be expected to show such effects most strongly)

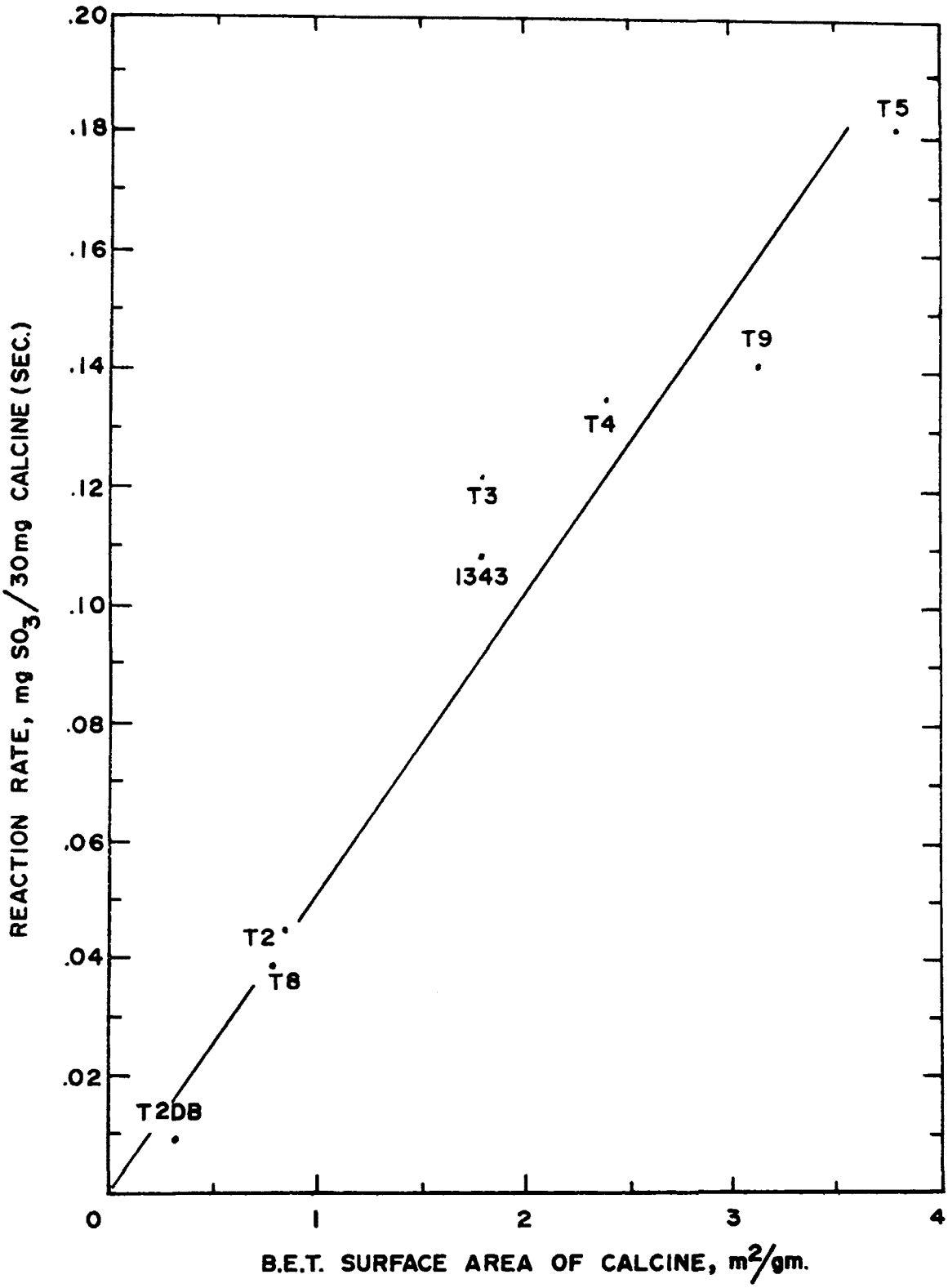

Figure 2-6.

Reaction Rate vs. Surface Area of 150/170 mesh Particles. Rates Evaluated at 980°C. and Sulfate Loading of 29.1×10^{-4} gm.moles/gm.

was exposed in the reactor to SO_2 for short periods followed by long periods of soaking at reaction temperature but without SO_2 present. For example, a sample was exposed for 35 seconds to flue gas, purged and held at 980°C. for 30 minutes and then exposed again to SO_2 for 35 seconds. The amount of sulfate in the sample was then compared to that absorbed by another sample exposed continuously for 70 seconds. The results showed no difference between the two modes of exposure, indicating that diffusion of sulfate into the solid during long periods of soaking does not increase the reactivity and therefore solid diffusion would not appear to be a significant factor. This experiment was repeated several times with different exposure times and multiples of exposures with the same result.

Calcination Temperature

Four samples of Type 2 calcite spar (10/28 mesh) were calcined in the rotary kiln for 2 hours at temperatures of 930°C. (1700°F), 980°C. (1800°F), 1040°C. (1900°F) and 1115°C. (2040°F). The physical properties of the calcines thus prepared are shown in Table 2-7. The maximum surface area was obtained at 980°C. and the surface area decreased sharply at temperatures above 980°C. The SO_2 reactivity shown in the table was determined at 980°C. with 150/170 mesh particles, by exposing five samples for 300 seconds. The average amount of SO_2 absorbed again correlated well with the B.E.T. surface area. The observed reduction in SO_2

reactivity is clearly a case of loss of surface area (due to overburning). Since this stone contains no silica impurities, chemical side reactions are obviously not responsible for loss of reactivity.

Table 2-7

Effect of Calcination Temperature on Physical Properties of Type 2 Calcite Spar, 12/16 Mesh

Calc. Temp.	Mean Pore Diam. Microns	True Density gm./cm.^{3}	Pore Vol. cc/gm.	BET Surface m^2/gm.	SO_2 Reactivity[a]
1700°F	1.5	3.46	0.35	0.65	10.7
1800°F	2.0	3.43	0.40	0.83	12.5
1900°F	2.2	3.67	0.38	0.59	10.1
2040°F	3.0	3.46	0.26	0.32	6.2

(a) mg. SO_3 absorbed by 30 mg. 150/170 mesh particles in 300 seconds at 980°C.

In-Situ Calcination

The kinetic parameters presented in Tables 2-3 and 2-4 were determined with stone calcined in a rotary kiln at 980°C. for two hours. In order to ensure that the reactivity of such samples was not altered as a result of their being cooled and stored for some time prior to reaction, a series of tests was made in which the stone was calcined in the reactor immediately preceding exposure to SO_2. This was done by placing 150/170 mesh particles of raw stone in the reactor carrier and inserting the carrier into the heated reactor at 980°C. The amount of raw stone placed in the carrier was equivalent to 30 mg. calcine

(about 52 mg. uncalcined). The sample was thus subjected to shock calcination when the carrier was inserted into the reactor. After 5 minutes flue gas was admitted to the reactor and the sample exposed for 100 seconds.

Ten such runs were made with each stone; the average SO_2 sorption is compared in Table 2-8 with the sorption found for kiln calcined stone. Although several stones showed significant changes in reactivity, depending on the mode of calcination, the relative ranking of the reactivity was generally the same as that obtained for kiln-calcined material. Several samples, Type 8, Type 10 and Type 11, were more reactive when tested in this manner, the marl (Type 11) being the most striking example. Several tests were made with marl in which the sample was left in the reactor for 2 hours after shock calcination prior to SO_2 exposure. These samples showed no loss of reactivity compared to samples heated for only 5 minutes, thus indicating that the 2 hour calcination used in preparing kiln calcines was not responsible for the loss of reactivity. Figure 2-7 compares the reactivity of marl for the two modes of calcination. No other stone showed such an extreme enhancement of reactivity when calcined in-situ.

Table 2-8

Comparison of Reactivities[(a)] of 150/170 mesh Stones at 980°C.

Stone Type	Raw Stone Calcined in-situ	Standard Deviation of 10 in-situ tests	Kiln Calcined for 2 hours at 980°C.
1	8.8	± 0.8	7.7
2	10.3	± 0.9	9.0
3	11.3	± 0.9	13.0
4	14.4	± 0.7	13.7
5	10.0	± 0.7	15.6
6	10.9	± 0.8	10.9
7	1.1	± 0.4	1.3
8	8.5	± 0.7	6.5
10	5.5	± 0.4	2.3
11	20.4	± 2.3	12.5
2061	11.8	± 0.8	-

(a) Milligrams SO_3 absorbed by 30 mg. calcine in 100 seconds.

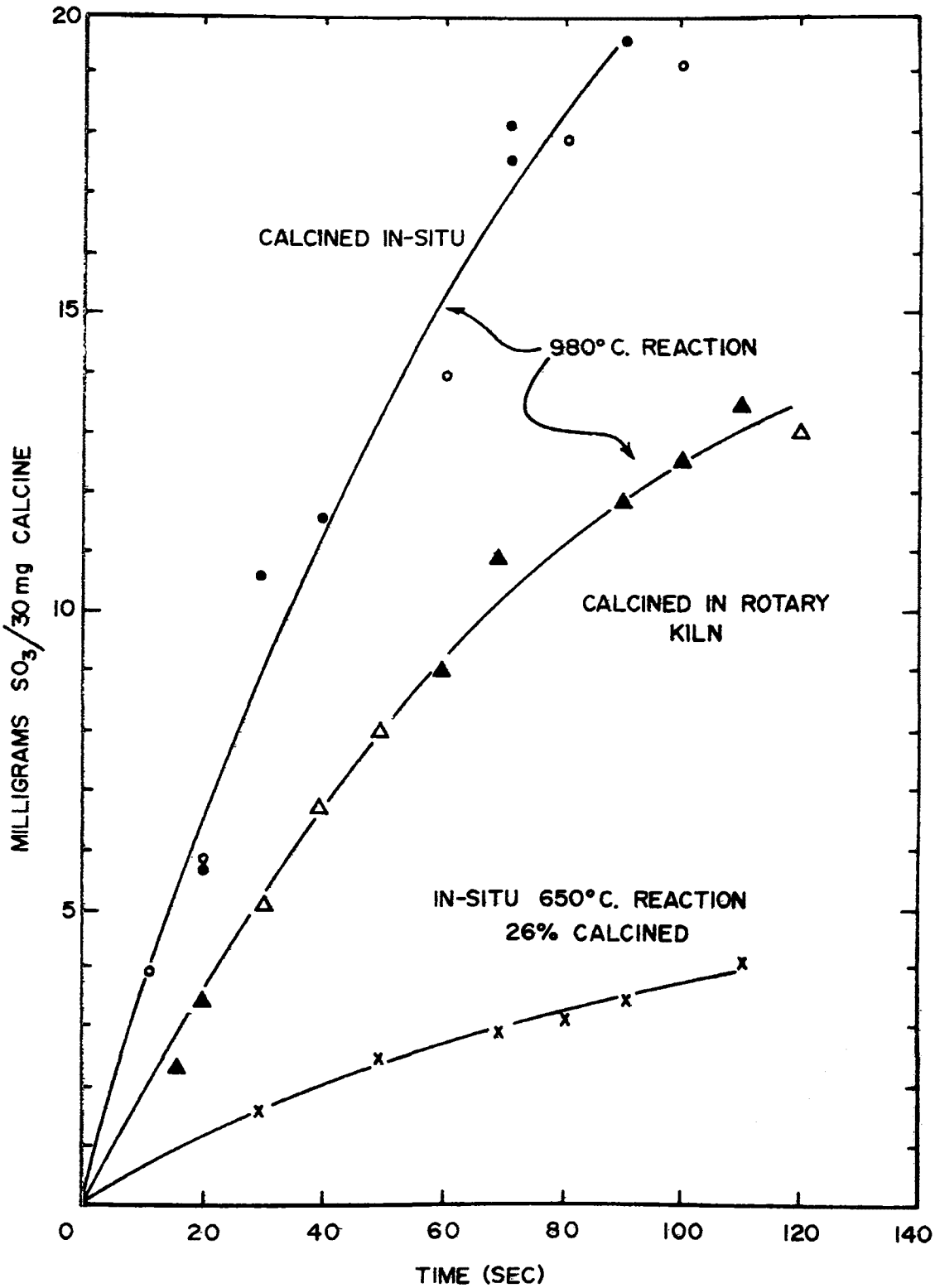

Figure 2-7.

Effect of Mode of Calcination on Reactivity of Michigan Marl.

Reaction Model

It is concluded from the above discussion that a simple model which assumes chemical reaction to be the rate-limiting resistance will adequately correlate the data for pure calcines which have pore diameters larger than 0.2 microns. The expression given by equation (2) defines the rate in terms of the initial (unsulfated) characteristics of the calcine:

$$r = \frac{1}{W} \frac{dn'}{dt} = k_s S_g C_{so_2} \eta$$

Previous data have indicated, and the present work has confirmed, that reaction rate decays exponentially as sulfation progresses. The relationship between rate and sulfate loading, n'/W, can be described empirically by:

$$r = e^{-\beta n'/W} \qquad (3)$$

This change has been interpreted in terms of a decrease in the frequency factor A_o, since

$$k_s = Ae^{-E/RT}$$

the experimental results can be expressed by:

$$A = A_o e^{-\beta n'/W}$$

An alternative interpretation of the observed relationship between rate and sulfation could be made on the basis of changes in $k_s S_g \eta$ as reaction progresses. It is known that the surface area and pore volume of the calcine/reaction-product mixture decreases as sulfate loading increases. This loss of surface,

however, is not necessarily due to changes in CaO surface, but more probably results from the reduced pore size brought about by the accumulation of reaction products on the pore walls. It may be argued that the intrinsic surface of CaO is not in fact altered at all by the presence of $CaSO_4$ product. Note that the linear relationship between rate and surface area at constant sulfate loading (shown in Figure 2-6) will not account for the exponential decay of reaction rate.

A comparison of the experimental β values also suggests that changes in the effectiveness factor, due to pore plugging, likewise will not account for the observed rate decay. The data for marl and aragonite, both of which have effectiveness factors of unity, show equivalent slopes of $\beta \sim 2.2$. These two stones have pores considerably larger than the other stones, but β values of similar magnitude. The fact that the sensitivity of rate to sulfation is similar despite the difference in pore sizes, indicates that the accumulation of products in the pores is not limiting the rate of SO_2 diffusion into the solid as long as the pores do not plug. The fact that aragonite and marl are free of pore diffusion is confirmed by the fact that particle size does not affect the rate at any degree of sulfation up to about 80 percent. It is concluded from this reasoning that the observed decay in rate of reaction does not result from pore plugging. A more likely mechanism which would more closely agree with the observed responses would be

a blockage of individual CaO sites by larger $CaSO_4$ molecules. It is concluded from these considerations that the change of rate with sulfation is best described in terms of the reaction rate constant and the preferred expression of the overall model would be in the form:

$$\frac{1}{W}\frac{dn'}{dt} = A_o\, e^{-\beta n'/W}\, e^{-E/RT}\, C_{SO_2}{}^{\eta} \qquad (4)$$

Values of A_o, β and η determined experimentally for the stones tested in this study are given in Table 2-4. This model adequately describes the sorption of SO_2 by calcines under isothermal conditions up to about 50 percent conversion of the CaO. The limits of applicability of the model, presumed to be the point at which pore plugging begins (and diffusional effects become rate limiting rather than chemical reaction), are:

Stone Type	Maximum Percent CaO Conversion to which Equation (4) applies
1	29 ($\eta < 1$)
2	50
3	48
4	50
5	62
6	63
8	77
10	19 ($\eta < 1$)
11	86

Note that the 5 purest stones (T1, T3, T4, T5 and T8) show fairly close agreement on the value of k_s. The average "intrinsic

rate constant" of these five stones has a value:

$$\bar{k}_s = 0.194 \pm 0.029 \text{ cm./sec.}$$

The effectiveness factor, η, is strongly dependent upon pore size, as would be expected. Figure 2-8 shows the relationship between the effectiveness factor (evaluated at zero sulfation) and pore size for 42/65 mesh calcines at 980°C. Pores larger than about 1μ correspond to $\eta \simeq 1$ for this particle size; when particle size was increased to 12/16 mesh, η dropped to about 0.3. Estimates based on these data using the Thiele diffusion modulus indicate that η values in the region of 1.0 should be expected for 150/170 mesh particles.

e. Conclusions

The isothermal rates of reaction of SO_2 differ widely among calcines prepared from carbonate rocks of varying geological type. Physical properties of calcines prepared from different geological types of stones also differ widely.

Many of the observed differences in SO_2 reaction rate can be logically interpreted in terms of the physical characteristics of the calcine, particularly the size of the pores.

The total SO_2-sorption capacity of the limestone calcines studied increased with pore size.

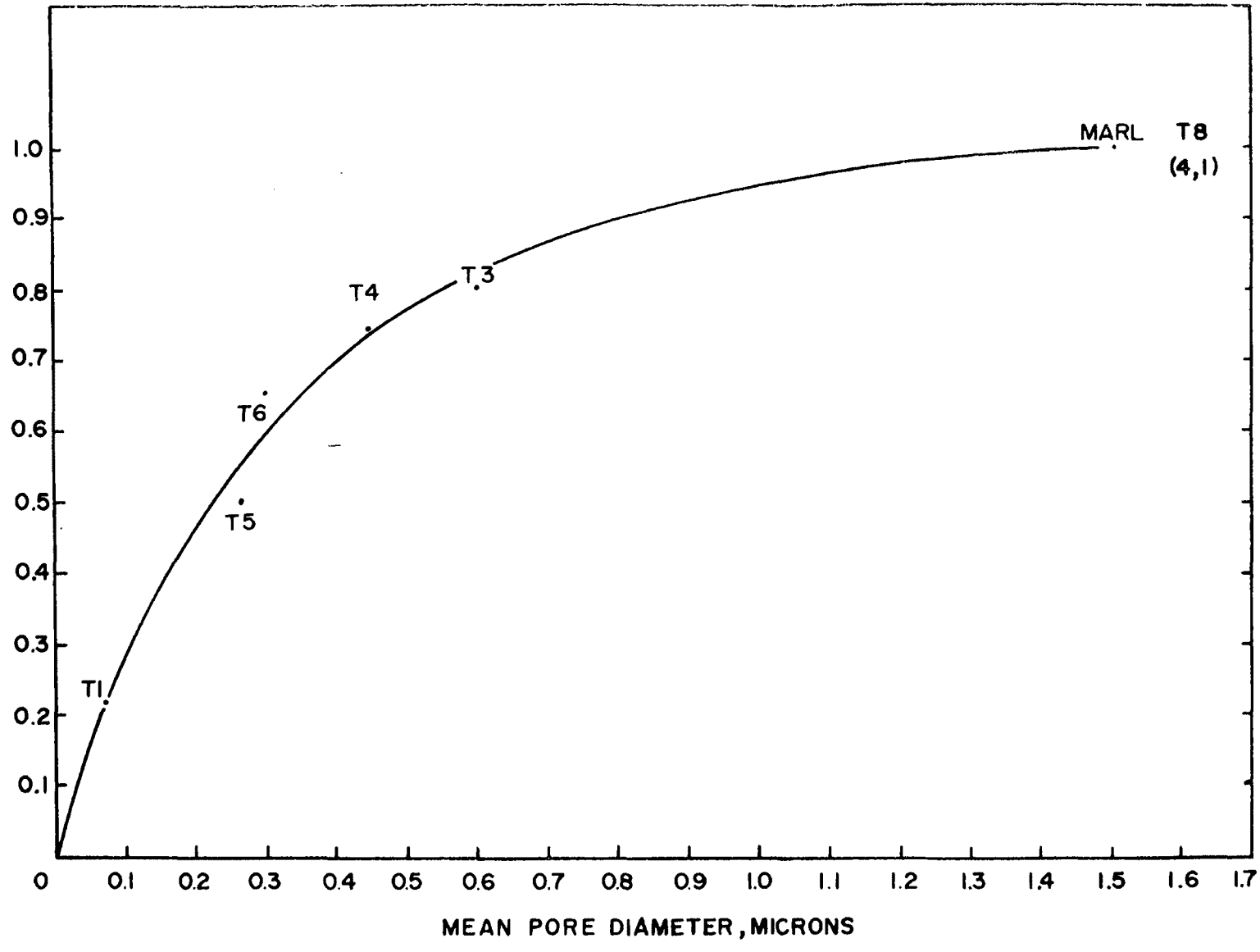
MARL T8
(4,1)
T4
T3
T6
T5
T1
1.0
0.9
0.8
0.7
0.6
0.5
0.4
0.3
0.2
0.1
0
0.1
0.2
0.3
0.4
0.5
0.6
0.7
0.8
0.9
1.0
1.1
1.2
1.3
1.4
1.5
1.6
1.7
MEAN PORE DIAMETER, MICRONS

The rate of reaction increases with decreasing pore size until a critical pore diameter of about 0.1 micron is reached. Presumably pores smaller than 0.1 micron are rapidly blocked by reaction products. These blocked pores inhibit diffusion of SO_2 into the solid interior, resulting in a lower rate. Maximum rate results when B.E.T. surface area is in the region of 3.5 $m.^2/g.$ (corresponding to pore diameters of 0.2 - 0.3μ) under isothermal reaction conditions.

Chemical reaction is the sole limiting resistance for particles smaller than 0.01 cm. at temperatures up to 980°C. when pores are larger than 0.2μ. The isothermal reaction of pure limestones with SO_2 show an intrinsic rate constant (per unit of surface) on the order of 0.2 cm./sec.

At conversions of about 50 percent the rate of sorption of SO_2 by 90μ particles of normal pore size changes from chemical reaction to a combination of chemical reaction and diffusion.

Both rate and capacity of SO_2 sorption are highly dependent upon particle size. The effect of particle size is not the same for all stones but is determined primarily by the size of the pores. Small pores lead to the highest sensitivity between the reactivity of calcines and particle size. Calcines with very large pores may show no dependence of reactivity upon particle size.

No evidence of surface diffusion or ionic diffusion could be established as a major limitation on SO_2 sorption.

The relative ranking of calcines prepared from the eleven types of stones listed in Table 2-2 was established in the following order with respect to isothermal rate of reaction with SO_2 at 980°C.: T11 (marl) > T5 > T9 > T4 > T3 > T6 > T2 > T1 > T8 > T10 (marble). In this rating marl was calcined in the reactor. T7 (magnesite) reacts only slowly with SO_2 at any temperature between 540° and 980°C., under isothermal conditions, and consequently, T7 was omitted from this rating.

f. Nomenclature

A	frequency factor, cm./sec.
A_o	frequency factor at zero solid conversion, cm./sec.
C_{SO_2}	gas phase concentration of sulfur dioxide, g. moles/cc.
$\bar{D}_p$	mean particle diameter, cm.
E	activation energy, cal./g. mole
k_s	reaction rate constant per unit surface, cm./sec.
k_v	reaction rate constant per unit volume of solid, $sec.^{-1}$ (g. moles/cc.)
dn/dt	rate of change of SO_2 in the gas phase, g. moles/sec.
n'	sulfate in solid as SO_3, g. moles
R	gas constant, 1.987 (cal./g. mole °K.)
r	rate of formation of SO_3 in solid, g. mole/g.(sec.)

r_o rate at zero solid conversion, g. moles/g. (sec.)

S_g B.E.T. surface area of calcine, $cm^2/g.$

W weight of calcine sample, g.

T temperature, °K.

t time, sec.

β empirical correlation coefficient defined by Equation 3

η effectiveness factor, ratio of reaction rate to the rate that would be obtained if the entire volume of the particle participated equally in reaction

ρ bulk density of calcine (particle density), g./cc.

3. A Field Study of the Role of Overburning of Limestone

a. Introduction

Full-scale boiler-injection tests to evaluate the dry injection process for removing sulfur dioxide (SO_2) from the flue gases of power plants were begun in late 1969. These tests called for the injection of additives into the boiler at several points downstream from the combustion zone. However, a comprehensive TVA report[33] pointed out the desirability of injection directly into the burners by mixing the additives with the fuel. This approach was reported to have several advantages over separate injection. (1) It would allow maximum residence time for the solid to mix and react with the gases. (2) It would provide optimum distribution of additive in the high-temperature zone. (3) It would reduce maintenance problems by eliminating the need for much of the injection equipment. (4) It would allow easy control of the additive-to-fuel ratio, and would automatically adjust the ratio to changes in boiler load.

The decision to inject separately during the full-scale dry injection process evaluation tests, instead of mixing with the fuel, was based on the results of several experiments in which additives fed to coal-fired furnaces with the pulverized coal produced little desulfurization. For example, Goldschmidt[13] found that dolomite hydrate removed only 8.9 percent of the SO_2 when added in stoichiometric proportion to the sulfur. Finely

pulverized dolomite injected with coal removed 12 percent of the SO_2 when fed to a pilot furnace compared to 25 percent removal when the dolomite was fed separately[2]. Limestone injected through the upper row of coal burners (2700°F), but separately from the fuel, removed only 20 percent of the SO_2 at twice stoichiometric feed rate[19]. However, the same author reported desulfurization efficiencies of 50 to 60 percent when the stone was injected at 2100°F.

It is generally believed that the low efficiency of desulfurization achieved in the high temperature injection tests was a result of the phenomenon of overburning. Overburning is the process whereby a relatively unreactive lime is produced when calcination occurs at high temperature and is known to involve both physical and chemical changes in the stone. Overburned lime can range from the qualitative extremes of hard-burned to dead-burned depending upon the severity of calcination conditions. Among the physical changes associated with overburned lime, as compared to lime calcined under moderate (or soft) conditions, are loss of porosity, increased density[7], loss of surface area, growth of crystallites, and larger mean pore diameter[23]. The extreme condition of overburning results in a lime that has lost all porosity and the bulk density of which approaches the absolute density of calcium oxide, 3.40 grams per cubic centimeter. This dead-burned lime, which is chemically inert, is produced at temperatures of 3000°F or more[7].

In addition to physical changes, chemical changes can also occur in limestone when it is overburned. These changes result from side reactions in which CaO unites with impurities in the stone to form silicates, aluminates, and ferrite, which make calcium unavailable for reaction with SO_2. These chemical changes are of particular concern where limestone injection is contemplated for coal-fired boilers[34] because of the possibility of reaction of the additives with coal ash, which is composed primarily of the oxides of silicon, iron, and aluminum.

The purpose of this field study was to determine whether additives are overburned when injected with fuel. This information is needed because no examination of the stone was made in previous tests that definitely established that the materials were hard-burned or dead-burned. Our object was to take the simplest case, in which the chemical effects of overburning would not be a factor (by using pure additive and an oil-fired furnace), and determine whether the physical properties and chemical reactivity of the lime produced during boiler calcination is significantly different from that of stone calcined under controlled conditions in the laboratory.

b. Experimental

Two separate series of injection tests were made using four different additives (two limestones and two dolomites). The test boiler was a 300,000 lb/hr., 900 psig, 900°F., Babcock &

Wilcox* type FH integral boiler, located at the Bayboro Station of the Florida Power Corporation in St. Petersburg, Florida. The boiler fired No. 6 fuel oil containing 2.3 percent sulfur at a rate of 10,000 pounds of oil per hour at an operating load of 150,000 pounds of steam per hour.

The compositions of the stone, determined spectrographically by Bituminous Coal Research, Inc., are given in Table 3-1. The possibility of tying up calcium in side reactions was minimized by using pure forms of limestone and dolomite. Because the ash content of the fuel oil was very low (0.08 percent), the reaction of the additives with ash was considered an insignificant factor. By using an oil-fired boiler, it was possible to approach the problem specifically in terms of the physical changes in the lime that might be related to its reactivity with SO_2.

During the first series of tests, the effect of boiler load on the degree of burning of additives injected with the fuel was investigated. The dry, pulverized additives were mixed with fuel oil and fed by a constant-displacement pump into the fuel line that leads to the burners. The feed rate was stoichiometrically equal to the sulfur content of the oil on the basis of the CaO and MgO content of the lime. Each additive was fed under conditions of both high boiler load (300,00 lb. steam per hour) and low boiler load (150,000 lb. steam per hour).

---

* Mention of company or product name does not constitute endorsement by the Air Pollution Control Office.

Table 3-1. COMPOSITION OF ADDITIVES, IGNITED BASIS

Component	Test series 1		Test series 2	
	Dolomite	Limestone	Dolomite	Limestone
CaO	56.0	96.0	57.0	95.0
MgO	37.0	1.0	39.0	1.9
SiO_2	4.55	1.13	1.0	2.15
Al_2O_3	0.60	0.41	0.2	0.2
Fe_2O_3	0.86	0.20	0.02	0.02
TiO_2	0.03	0.03	0.03	0.03
Na_2O	0.25	0.02	0.02	0.02
K_2O	0.1	0.1	0.1	0.1

At the boiler outlet ahead of the air preheater particulate samples were drawn by means of stainless steel probes that fed into miniature cyclones. The temperature of the cyclone was 450°F. The sample collector was purged with dry nitrogen to prevent contact of solids with the flue gas during sampling. Each run consisted of a sample period of about 4 hours.

During the second series of tests, the effects of particle size, iron content, residence time, and injection temperature on the amount of SO_2 absorbed by the additives were investigated. Stabilized dispersions of limestone and dolomite in light fuel oil were prepared by Basic Chemicals in two particles size distributions. Most of the work was done with the finer dispersion, in which 50 percent (by weight) of the particles were smaller than 2.4 microns and 10 percent larger than 5 microns. The other dispersion, which will be referred to in the following discussion as "coarse", contained particles 50 percent of which were smaller than 8 microns and 20 percent of which were larger that 30 microns. A special preparation of fine dolomite was also made containing 4 percent mill scale as an articicial source of Fe_2O_3. The additive dispersions were injected at two points: at the burners with the fuel, and downstream from the combustion zone at a temperature of 2430°F. The sampling points were located around the boiler as shown in Figure 3-1 (during separate injection tests the first sample point was used as the injection site and samples were taken at the fourth sample position only).

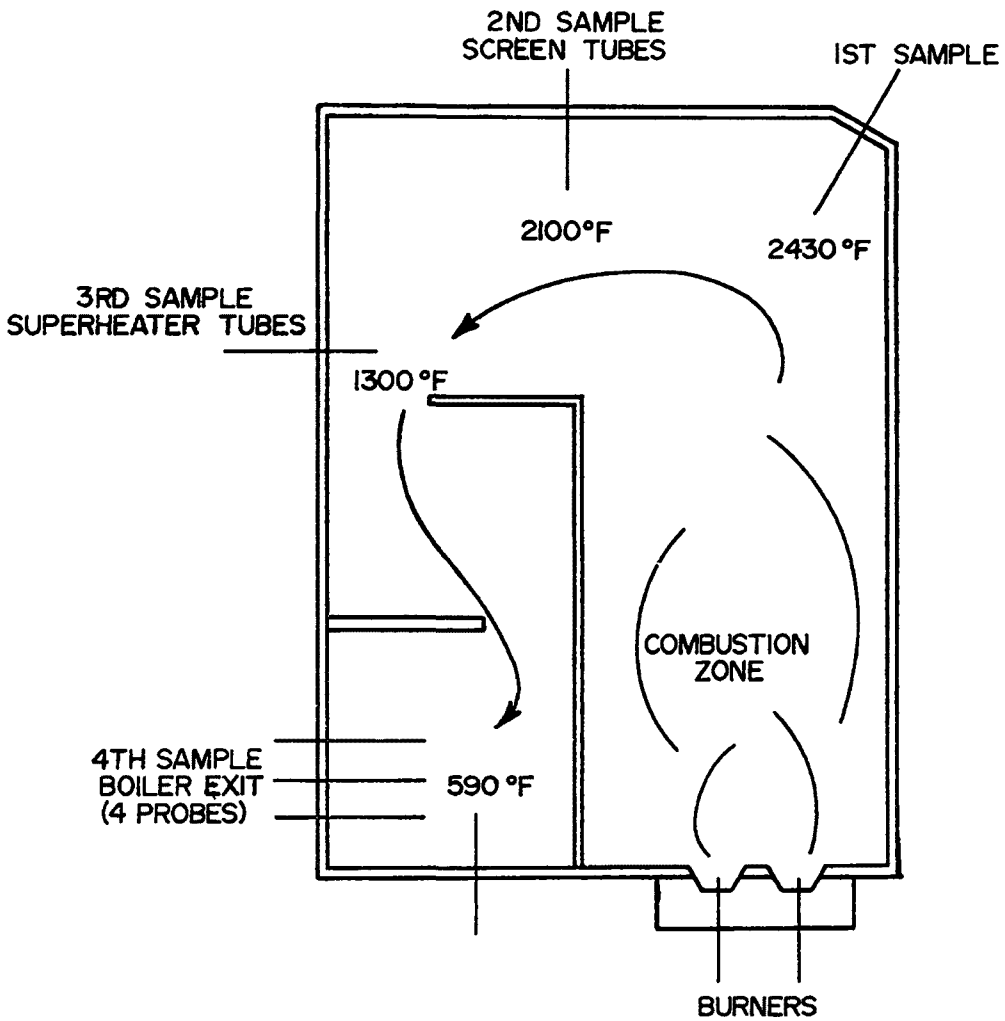

BOILER PLAN AND SAMPLE LOCATIONS, TOP VIEW

Figure 3-1.

Water-cooled sampling probes were used at the first and second positions, but otherwise the sampling equipment was the same as discussed earlier. The residence time of the particulate in the probe during sampling was less than 0.1 second.

The temperatures shown in Figure 3-1 were measured at high boiler load with a water-cooled, high-velocity thermocouple. At low load the temperatures at sample positions 1 and 2 were 2270° and 1970°F., respectively.

c. Discussion of Results

Preliminary observations based on the first series of tests showed that only a small amount of the lime had reacted with SO_2 in the boiler. Samples collected at the boiler outlet during high-load conditions contained 7 percent SO_3. The amount of sulfate found in the stone was consistently greater for samples collected at low boiler load than for samples collected at high load, but it never exceeded 14 percent utilization of the CaO and MgO. Carbonate analyses (evolution method) showed that calcination of the stone was complete when fed to the burners during either mode of boiler operation.

The chemical reactivity of the boiler samples was determined in the laboratory in two ways: as the rate of reaction with SO_2 and as the rate of hydration. The SO_2 reactivity was measured in a differential reactor[5] by exposing the samples

to flue gas containing 0.27 percent SO_2. Figure 3-2 shows the amount of sulfate formed in 30-milligram samples as a function of exposure time when reacted at 1600°F. These data are for the limestone fed during the first test series. Data for the same stone calcined under soft burn conditions (1700°F., 30 minutes) are shown for comparison. The rate of reaction, measured as the slope of the curve at a given value of sulfation, was in all cases greater for the laboratory calcine than for the limes calcined in the boiler. For the examples shown, the rate of reaction of SO_2 with the boiler-calcined limes were one-fifth the rate of reaction with the soft calcined lime when compared at a sulfation of 4 mg SO_3/30 mg calcine. On the basis of this comparison, it may be concluded that calcination in the furnace flame resulted in a lime that was considerably less reactive than stone calcined under less severe conditions.

The total SO_2-sorption capacity of stones calcined in the boiler was measured by exposing samples in the laboratory reactor for 2 hours at a temperature of 1800°F. Under these conditions 75 percent of the theoretical conversion was obtained for the dolomite samples (CaO component), and 65 percent for the limestone. These utilization values were not significantly different from those obtained with stones calcined under soft conditions. Because the primary difference was in the rate of SO_2 sorption, rather than capacity, it was concluded that the limes were hard-burned but not dead-burned.

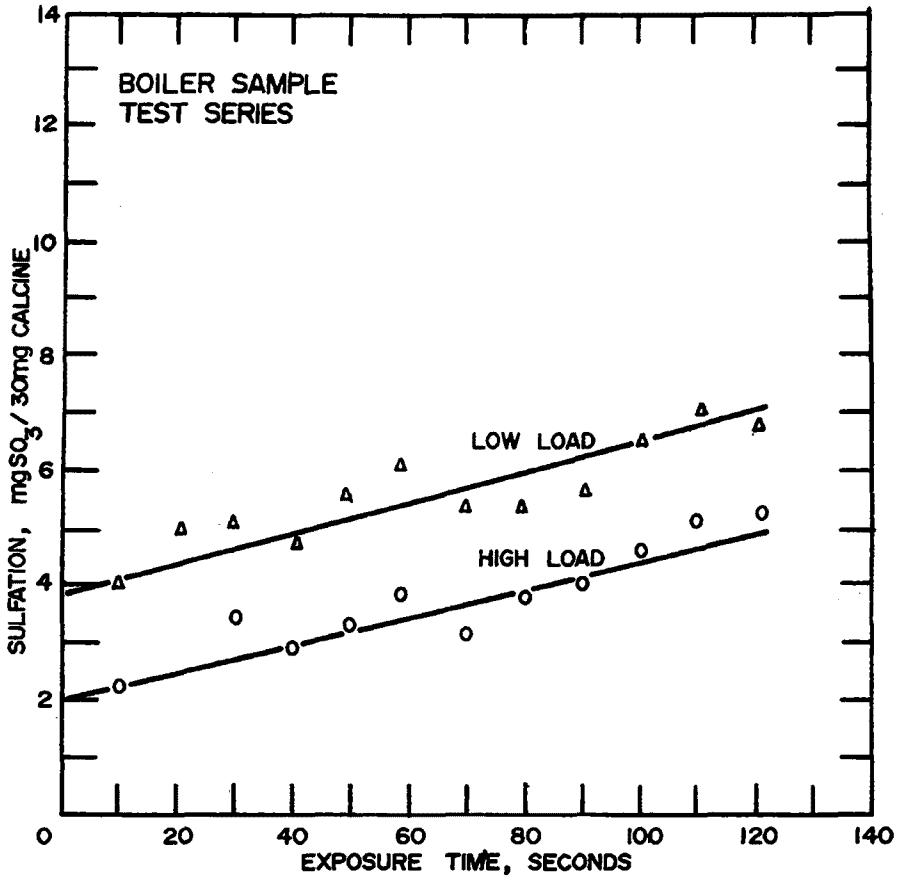

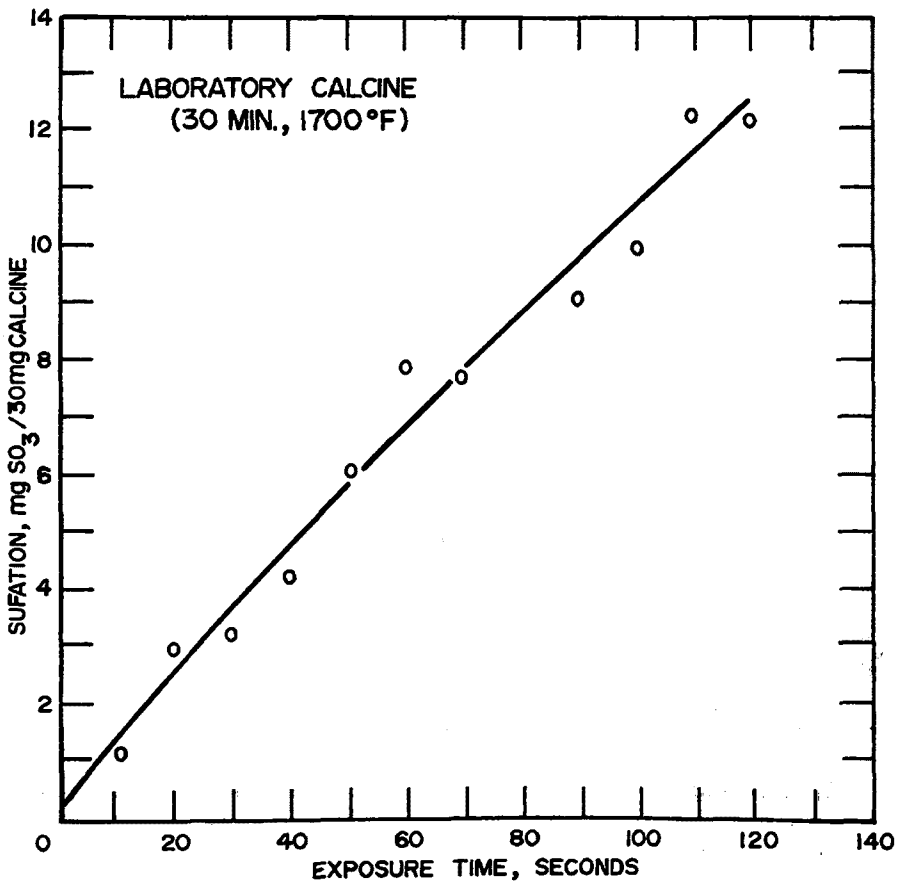

Figure 3-2. Reaction of SO_2 with Calcined Limestone at 1600°F in Flue Gas, 0.27 percent SO_2.

The rate of hydration test, a standard technique used in the lime industry for evaluating the degree of burning, was performed for four boiler samples by G. & W. H. Corson, Inc. A series of standard laboratory calcines was prepared from the raw stone at temperatures of 1800°, 2100°, 2400°, and 2700°F. The percent of hydration versus time was measured for each calcine and compared to that of the boiler samples. Figure 3-3 summarizes the results of tests with the dolomite run in the first test series. The laboratory calcines show decreasing reactivity as calcination temperature was raised, in accordance with the effects of hard-burning. The rate of hydration of the boiler limes was lower than the hardest-burned laboratory calcine prepared at 2700°F. Limestone samples showed similar results (e.g., 50 percent hydration of the boiler calcined limes required 202 minutes, compared to 21 minutes for the 2700°F. laboratory calcine and 1.2 minutes for the 1800°F. laboratory calcine). Although the accuracy of this test is confounded by the presence of sulfate, which may also influence the hydration rate, the results qualitatively confirmed that the boiler-calcined limes were overburned.

Table 3-2 is a compilation of the chemical analysis data for samples obtained from the second series of tests. Comparison of the carbonate and sulfate analyses of samples collected at sample position 1 with those of samples collected at position 4 (runs 3, 4 and 5) shows that both calcination and sulfation of the lime were completed in the furnace section before it reached

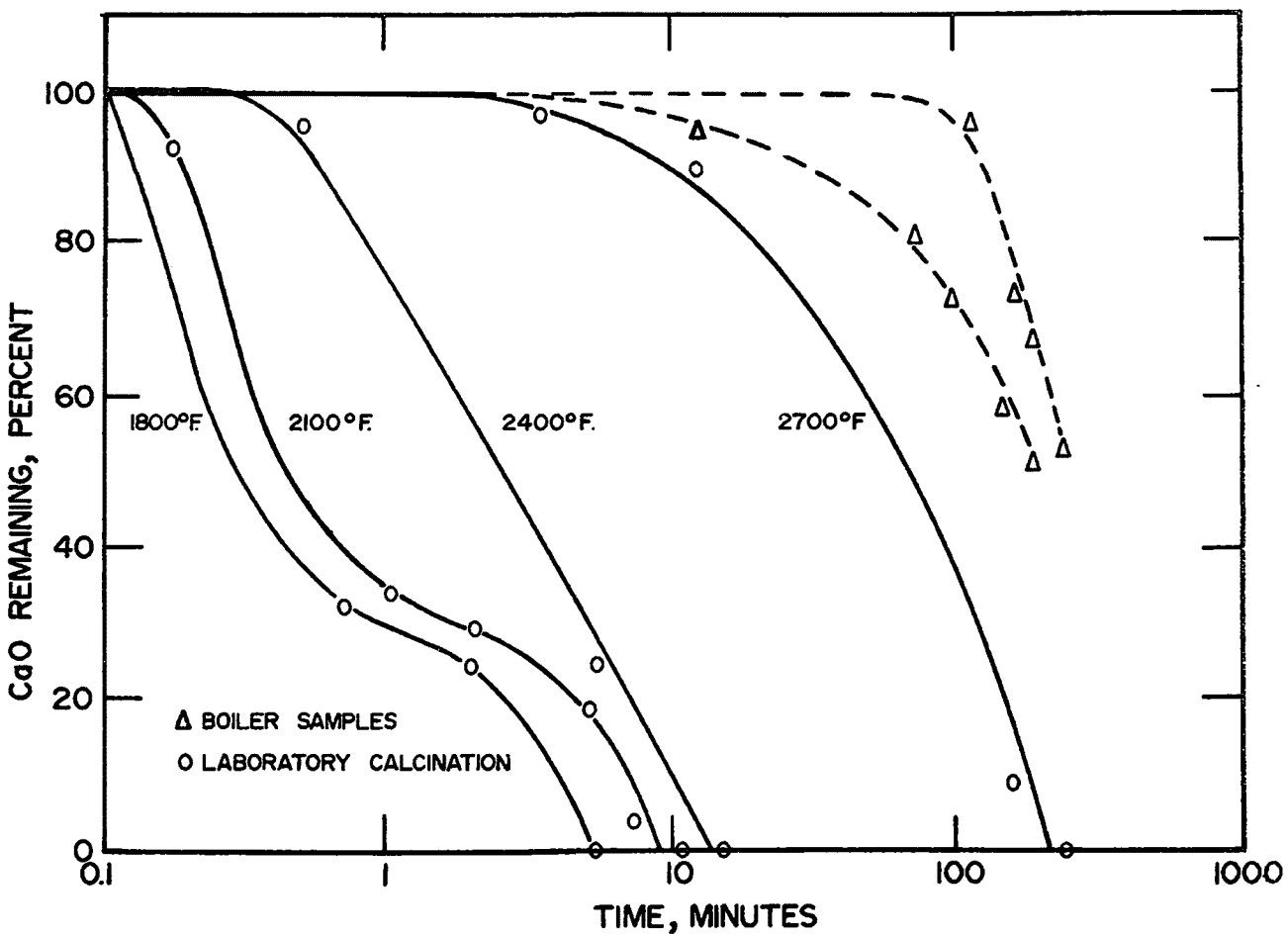

Figure 3-3. Rate of Hydration of Calcined Dolomite: Test Series 1

Table 3-2. TEST SERIES 2: SULFATE AND CARBONATE CONTENT OF BOILER SAMPLES

Run	Additive	Boiler load, 000 lbs. steam/hr	Sample position	Weight percent Sulfate As SO_3 (a)	Weight percent Carbonate As CO_2
1	Coarse dolomite	305	4	6.5	1.3
2	Fine dolomite	275	4	3.6	2.0
3	Fine dolomite	250	4	3.7	1.8
			2	3.2	0.4
			1	4.7	0.4
4	Fine dolomite	150	4	13.2	0.7
			3	13.6	1.7
			1	12.5	0.3
5	Fine limestone	250	4	4.3	1.3
			3	4.2	0.7
			2	3.8	0.04
			1	5.1	0.9
6	Coarse limestone	250	4	7.7	2.0
7	Fine limestone	150	4	13.7	2.1
8	Separate injection- Fine dolomite	250	4	13.3	10.6
9	Separate injection- Fine dolomite + Fe_2O_3	250	4	17.0	10.3
10	Separate injection- Calcined limestone	250	4	6.4	2.4

(a) Calcined basis

the first sample position, at which the temperature was 2430°F. No significant amount of SO_2 reacted with the lime while it passed through the boiler section, even though the lime was completely calcined. These facts show that the rate of calcination was not limiting SO_2 sorption, (i.e., the calcination step was completed prior to entry into the boiler, but there was no further sulfation even though the SO_2 capacity of CaO is greatest in that temperature zone). It was concluded that the deactivation occurred in the highest temperature region of the furnace. The additional residence time was not the cause of higher sulfation at low boiler load.

The coarse additives fed during runs 1 and 6 (Table 3-2) absorbed more sulfate than did the finer additives. This effect was also evident in comparing the results of series 1 and 2, greater SO_2 sorption being attained in the former case where coarser feed was used. This might be a result of less rapid calcination of the larger particles, a factor known to affect the density of lime: higher densities being associated with high rates of calcination[12].

The physical properties of boiler samples obtained from both the first and second series of tests were examined and compared to those of soft-calcined stones. Mercury porosimetry measurements on 80 limestones and dolomites calcined in the APCO laboratory show that most of the pore volume is in a range of

pore size between 1.7 and 0.1 micron. Pores in this size range typically comprise about 85 percent of the total pore volume in soft-calcined limes. Furthermore, for a given stone, the greatest mercury intrusion occurs over a narrow range of pressure, indicating that the pores are of uniform size. The mean diameter of these uniform pores can vary from stone to stone but is usually about 0.3 micron. Porosimetry measurements of the boiler samples in no case showed the large volume of pores of uniform size found in the laboratory calcines. The specific volume of pores in the range of 1 to 0.1 micron is compared in Table 3-3 for limes calcined in the boiler during test series 1 and laboratory calcines prepared from the same stones. Pores larger than 1 micron were necessarily excluded from this comparison because of the fact that interparticle voids cannot be differentiated from intraparticle pores by mercury porosimetry measurements, and the former represent most of the total void volume in the finely powdered boiler samples. The data of Table 3-3 show that the boiler samples had markedly fewer pores in the particular size range characteristic of soft calcined lime.

The bulk density and porosity of limes obtained from the second series of tests were estimated by oil sorption tests. This test gives a good indication of the total volume of intraparticle pores when the amount of oil sorbed by the interior of the particles is large compared to the amount retained on the

Table 3-3. SPECIFIC VOLUME OF PORES 1 TO 0.1 MICRON DIAMETER (BY MERCURY INTRUSION) AND DEGREE OF SULFATION OF ADDITIVES: TEST SERIES 1

	Specific pore Volume, cc/g	Sulfation, % SO_3
Dolomite		
Laboratory calcine	0.37	none
Boiler low load	0.078	16.6
Boiler high load	0.063	7.3
Limestone		
Laboratory calcine	0.31	none
Boiler low load	0.16	11.5
Boiler high load	0.15	7.1

particle surface. The powder is immersed in No. 2 fuel oil, filtered and dried on absorbent paper. The volume of oil contained in the pores is determined by multiplying the weight gain by the specific volume of the oil. Laboratory calcines prepared from the same stone were also carried through the procedure as a basis for comparison. As shown in Table 3-4, the boiler samples had high densities and low porosities. These effects are both associated with hard-burning during calcination[7]. Comparison of the high- and low-load samples showed that the greater sulfation achieved at low load could not be explained on the basis of differences in porosity. This is confirmed by the data in Figure 3-2, which shows that samples collected at different boiler loads did not have significantly different rates of reaction with SO_2. It was concluded that the degree of overburning was not related to boiler load and that improved sulfation at low load was the result of some other variable - possibly differences in oxygen content of the flue gases - associated with the higher excess air fed at low boiler load to improve heat transfer. The adverse effect of low oxygen on the desulfurization reaction has been demonstrated in pilot-scale experiments on coal-fired furnaces for both separate injection[2] and addition with the fuel[17].

Several supplementary tests were made injecting additives separately from the fuel by spraying the suspension into the

Table 3-4. PHYSICAL PROPERTIES OF BOILER SAMPLES AS DETERMINED BY OIL SORPTION: TEST SERIES 2, SAMPLE POSITION 4

	Bulk density, gm/cc	True density, gm/cc	Porosity, cc/cc
Dolomite, laboratory calcination[(a)]	1.62	3.36	0.52
Fine dolomite, run 2, high load	2.18	3.32	0.35
Fine dolomite, run 4, low load	2.24	3.37	0.34
Coarse dolomite, run 1, high load	2.05	3.30	0.39
Limestone, laboratory calcination[(a)]	1.52	3.35	0.55
Fine limestone, run 5, high load	2.07	3.27	0.37
Fine limestone, run 7, low load	2.00	3.07	0.34
Coarse limestone, run 6, high load	2.19	3.17	0.33

(a) Calcined 2 hours at 1700°F

furnace at position 1 at high boiler load. A comparison of runs 3 and 8 in Table 3-2 shows that fine dolomite absorbed 3 times as much sulfate under these conditions as when fed to the burners. This was true even though the residence time was shorter and calcination was not complete. The addition of 4 percent iron oxide to the dolomite that was injected separately improved the SO_2 sorption slightly, as shown by run 9. A test in which precalcined lime was injected separately gave poor results; only half as much SO_2 was absorbed by this material as was absorbed by uncalcined dolomite. This observation verifies the findings of others [2, 8] that no advantage is gained by precalcination before injection.

The predominant form of sulfur in the lime was sulfate whether injection was made with the fuel or separately. Measureable amounts of sulfide (averaging 0.27 percent by weight as S) were found in the 13 samples fed with the fuel. Limes from the separate injection tests contained about 0.7 percent sulfite (as SO_2) but no sulfide.

d. Conclusions

The results of these tests have shown that the dry-limestone process should not be applied by injection of the sorbent with the fuel. Instead, additives must be injected separately to

achieve most efficient utilization of the limestone. Overburning is at least partly responsible for the low efficiencies found when additives are fed to the burners. The lime produced by injection with the fuel is much less reactive with SO_2 than lime that is not calcined in the combustion zone. This loss of reactivity is associated with changes in the physical structure of the stone during calcination in the combustion zone. These physical changes are sufficient to deactivate the lime, regardless of further side reactions with impurities or ash. Additives injected into coal-fired furnaces with the fuel would therefore be expected to yield only less-satisfactory results than those reported here.

Boiler load was found to be an important variable affecting desulfurization when additives were fed with the fuel. This is apparently due to the higher excess air used during low load and is not a result of differences in flame temperature or residence time.

These field tests indicate that there is an optimum particle size as well as an optimum injection temperature. The results under the conditions of these tests show that injection temperatures somewhat higher than 2400°F. would be best for 2-micron particles.

4. Methods for Testing the Degree of Overburning of Calcined Limestones

a. Introduction

Currently, the dry injection process is being evaluated in a full scale demonstration of performance at the TVA Shawnee Steam Power Plant, Paducah, Kentucky. Optimum conditions for sulfur dioxide abatement will be determined as well as the effect on operation of the power plant and the economics of the process. Under the process evaluation planned by TVA[22, 32], carbonate rock (limestone or dolomite) is ground to 70% less than 200 mesh and is injected into the furnace above the fireball at temperatures ranging from 2400°F to 2900°F. The carbonate rock calcines (evolves CO_2) and the resultant lime reacts with the sulfur oxides in the presence of oxygen to form calcium sulfate. The calcium sulfate is removed with the fly ash in the standard dust collection systems. It has been supposed that the petrographic nature of the lime accounts for its level of chemical reactivity, and moreover, that the reactivity of the lime is dependent in part on its calcination conditions. An otherwise reactive calcitic or dolomitic lime may become unreactive due to dead-burning or overburning of the limestone. Causes of this loss of reactivity may be physical changes or side reactions with impurities in the carbonate rock or both.

As a limestone is calcined at higher temperatures, it loses reactivity as well as surface area and porosity[7]. Volumetric shrinkage as high as 52.6% has been noted[7, 23] for an oolitic stone calcined at 2450°F[7]. Loss of surface area with increased calcination temperature has been reported[21, 24, 29, 36] such as a decline from 62.9 $m^2/g.$ to 0.20 $m^2/g.$ in specific surface area for a corresponding increase from 750°C to 1300°C in calcination temperature for Iceland spar calcite[24]. Corresponding to the volumetric shrinkage there is an increase in particle or apparent density[6, 7, 9] from a low of 1.5 gm/cc for lime prepared at low temperatures up to 3.0 gm/cc for limes prepared at very high temperatures.

Changes in porosity (i.e., fraction of lime particle which is pore space) with increased calcination temperature include loss of porosity[3, 6, 7, 21, 24, 29] and increase in the mean pore diameter[24, 29]. Thus, the large pores grow at the expense of the small pores which contribute greater porosity. In conjunction with the growth of pores there is a loss of porosity attributable to the growth of large crystals by assimilating small crystals[10, 18]. As a result of increased calcination temperature, the reaction rate with sulfur dioxide or hydrochloric acid is retarded[5, 11], the CO_2 absorption is lessened[26], the slaking rate is slower[1], and the extent of sulfation declines[20, 25].

Several tests for the reactivity of calcium oxide have been widely used already. Two of these tests, the ASTM slaking rate test and the G. and W. H. Corson X-ray hydration test rely on decreased reactivity of overburned lime with water. The former test follows the reaction rate from the temperature rise during slaking in an insulating bottle. Another rate test, the coarse grain titration test, depends on titration at one-minute intervals with hydrochloric acid to construct characteristic titration curves. The titration curve for a lime calcined at high temperature will rise far more slowly than that for a lime calcined at low temperature. A fourth test proposed by Y. Ohno[27] would expose the test sample to CO_2 and judge the degree of overburning from the extent of recarbonization.

In order to determine if the limestone injection at the Shawnee Plant led to optimum calcination of the limestone, it was necessary to identify a test for lime reactivity using small samples of limes diluted with fly ash. In addition to considering the tests listed above, many other possible tests were evaluated. The procedure was to determine various chemical and physical properties of different limestones calcined at a range of temperatures. The more promising tests were then applied to samples from tests at Babcock & Wilcox and from preliminary injection runs at the Shawnee Plant.

b. Experimental

The carbonate rocks tested were two calcites and a dolomite which have been identified as Stone Nos. 2061, 2062, and 2069, respectively. An analysis of these is listed in Table 4-1. Two sets of these stones were sent to G. and W. H. Corson, Inc., Plymouth Meeting, Pa., where they were batch calcined at 1700, 2000, 2300, 2600, and 3200°F in a rotary kiln. The stones were calcined for two hours at temperature after the initial heat-up period (see Figure 4-1). The first set (Set I) was returned as calcined; the second set (Set II) was ground to minus 170 mesh at Corson's. All grinding operations were done under nitrogen and samples were shipped in cans sealed under nitrogen.

Some of the tests were performed by contractors. General Technologies Corporation was sent samples of the first set for infrared (IR) analysis. To American Instrument Corporation (AMINCO) went minus 70, plus 140 mesh (70/140) samples of the first set and 170/270 samples of the second set. Test results reported by AMINCO were surface area by the B.E.T. (Brunauer, Emmett, Teller) method and mercury penetration porosimetry data. The latter yielded information such as density, porosity, distribution of pore size, and median pore size.

The tests conducted in the APCO laboratory may be divided into two groups - chemical reactivity tests and physical property tests. The chemical reactivity experiments were as follows:

Table 4-1. Composition of Limestones

Component	Analysis, weight per cent Stone Number 2061	2062	2069
SiO_2	1.40	2.25	2.63
Al_2O_3	<0.2	<0.2	0.72
Fe_2O_3	0.27	0.31	0.70
MgO	1.77	2.42	36.0
CaO	95	94	58.0
TiO_2	0.03	0.03	0.05
Na_2O	<0.02	<0.02	0.06
K_2O	<0.1	<0.1	0.47
MnO_2	<0.03	<0.03	<0.03

Figure 4-1

TYPICAL FIRING CYCLE

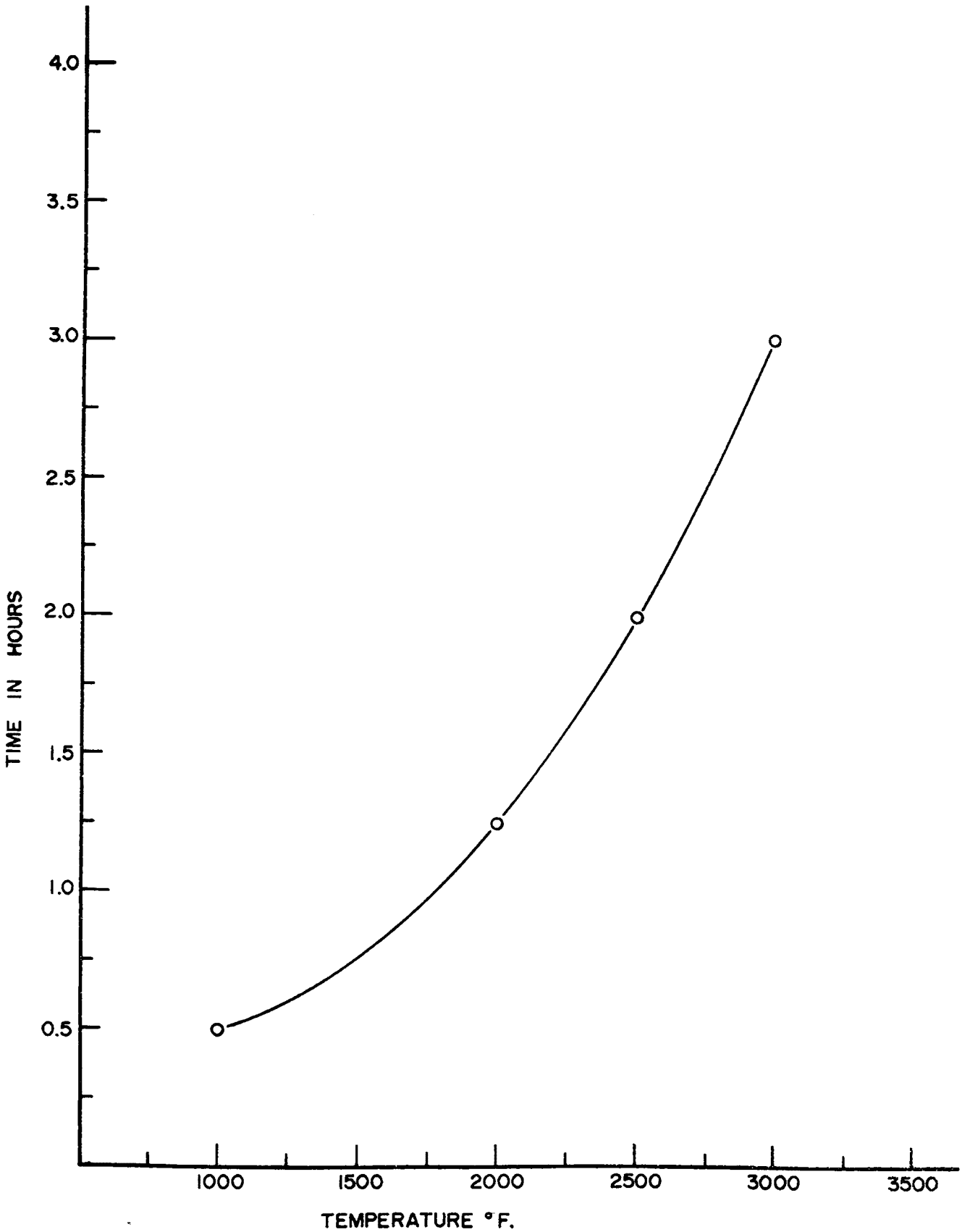

1. Absorption of sulfur dioxide from flue gas
2. Absorption of sulfur dioxide from pure SO_2
3. Absorption of carbon dioxide
4. Absorption of steam
5. Modified coarse-grain acid titration
6. Hydration-weight gain.

The physical property tests were density determinations made in one case by using an air pycnometer and in the second, by immersion in oil. A description of the procedure for these experiments is given in Appendix B.

Preliminary to the final results all proposed overburning or dead-burning tests were checked for their feasibility in the present TVA Shawnee injection test application. The most severe limitation was that the sample size could not be larger than several grams. Both the slaking rate test[17] and the coarse grain titration[15] called for sample sizes an order of magnitude larger. In the latter case, it was found that the test could be modified and still give reproducible results. Unfortunately, this was not the case for the slaking rate test which had to be eliminated for consideration in this application.

c. Discussion of Results

(1) Effect of Calcination Temperature

The results of the various physical and chemical tests show that apparent densities, median pore diameter, and average IR

band shift increased with increasing calcination temperature while all other properties decreased.

Results of the acid titration test for Stone No. 2061 are shown in Figure 4-2. All of the chemical and physical properties were significantly affected by calcination temperature; however, the most dramatic changes were in SO_2 absorption from flue gas, pure SO_2 absorption, pure CO_2 absorption, hydration-weight gain, B.E.T. surface area, and pore volume. All of these properties decrease in about the same way except for CO_2 absorption which drops abruptly at 2000°F. This behavior has been noted before by Y. Ohno[27] and has been attributed to the "shrinking, melting, and fusing of the crystals"[16], thus, obstructing carbon dioxide penetration into the lime.

Statistical analysis of the data shows that such properties as SO_2 absorption from flue gas, pure SO_2 absorption, B.E.T. surface area, and pore volume change significantly with calcination temperature but not with stone sample. Hence, the data of all three stones of a set of calcines were taken together to calculate correlation coefficients between different properties. The results shown in Table 4-2 demonstrate the high degree to which sulfur dioxide reactivities, surface area, and pore volume are intercorrelated (also refer to Figures 4-3 to 4-7 which are the crossplots for the data from Set I). This evidence supports the conclusion that loss in surface area and pore volume at higher calcination temperatures account for loss in reactivity.

Figure 4-2

ACID TITRATION OF #2061

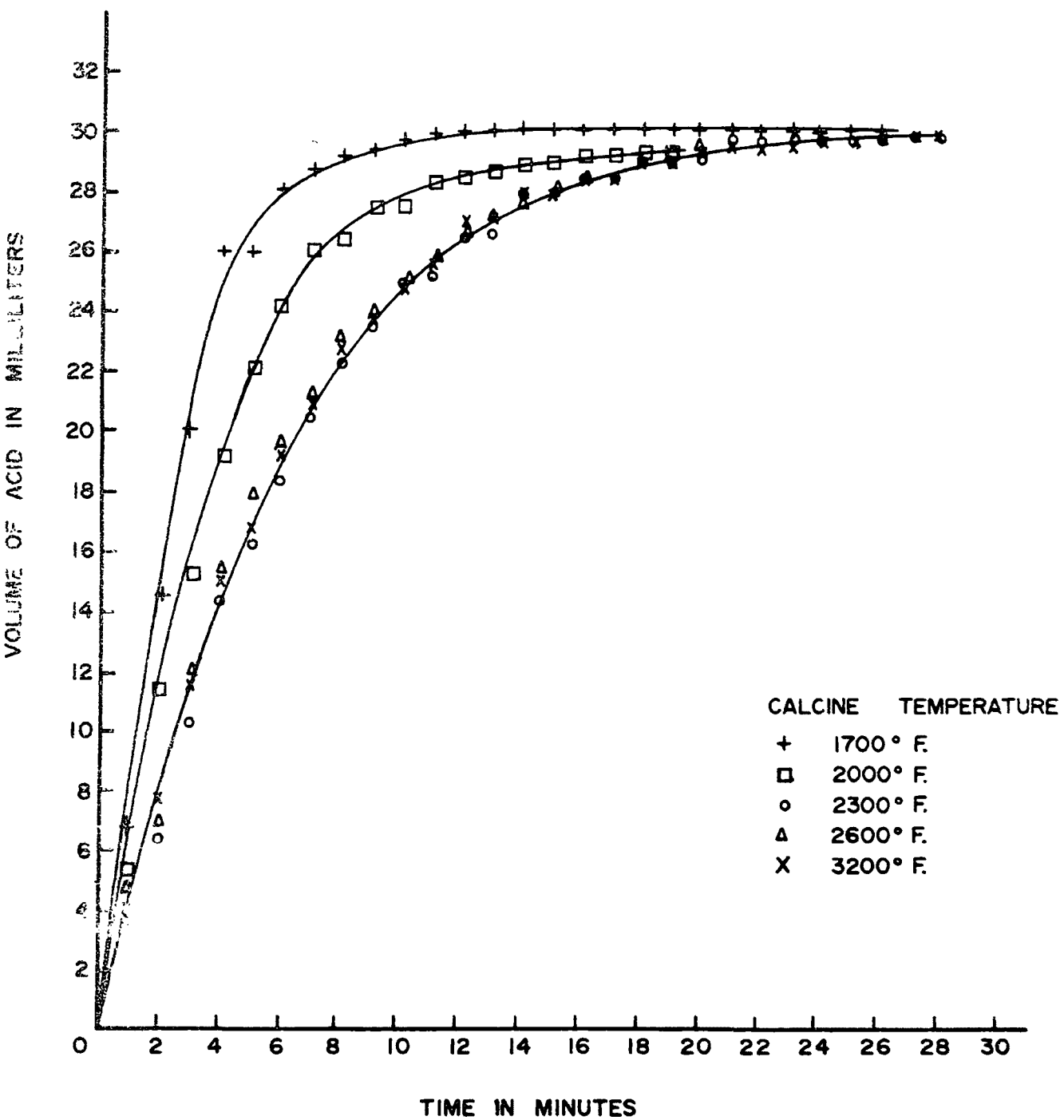

Table 4-2: Correlation Coefficients

	Pore Volume cc/g.	B.E.T. Surface Area $M^2/g.$	Pure SO_2, % gain Absorption	Flue Gas Absorption, mg./30 mg.
Flue Gas Absorption mg./30 mg.	0.894	0.908	0.980	
Pure SO_2, % gain Absorption	0.905	0.896		0.807
B.E.T. Surface Area, $M^2/g.$	0.778		0.866	0.863
Pore Volume cc/g.		0.863	0.888	0.858

Set I / Set II

Figure 4-3:

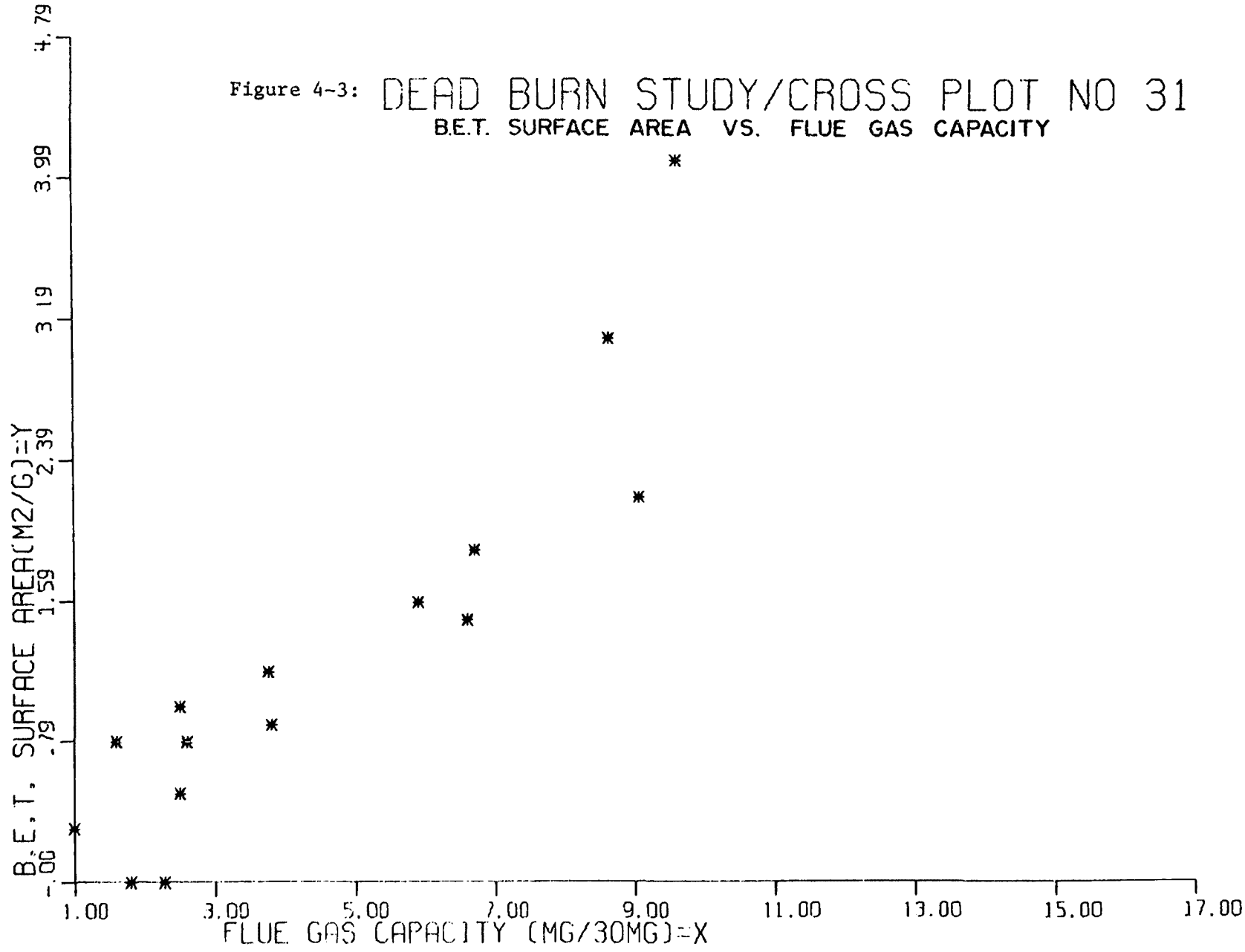
DEAD BURN STUDY/CROSS PLOT NO 31
B.E.T. SURFACE AREA VS. FLUE GAS CAPACITY
B.E.T. SURFACE AREA(M2/G)=Y
.00
.79
1.59
2.39
3.19
3.99
4.79
1.00
3.00
5.00
7.00
9.00
11.00
13.00
15.00
17.00
FLUE GAS CAPACITY (MG/30MG)=X

Figure 4-4:

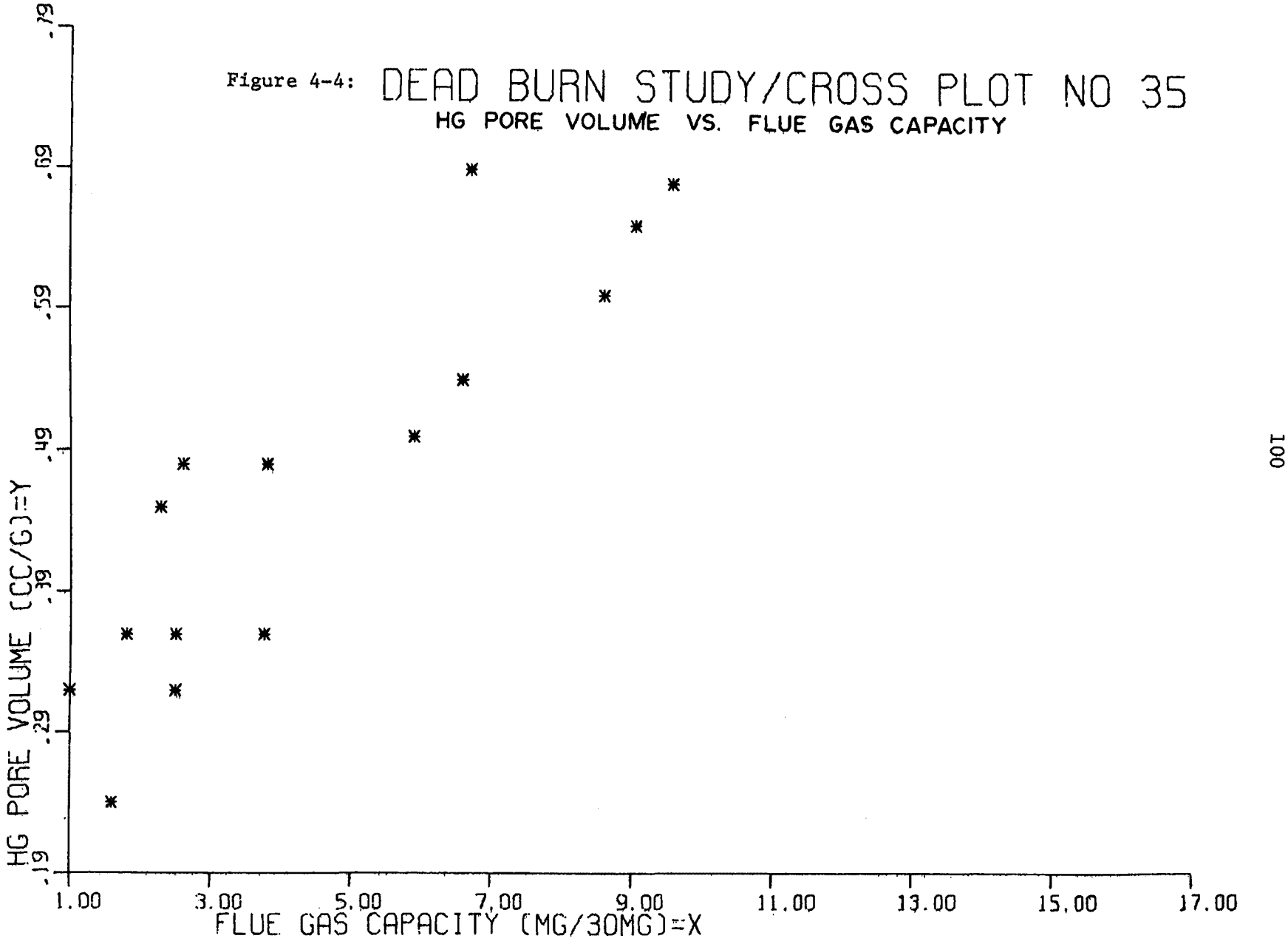
DEAD BURN STUDY/CROSS PLOT NO 35
HG PORE VOLUME VS. FLUE GAS CAPACITY
HG PORE VOLUME (CC/G)=Y
.79
.69
.59
.49
.39
.29
.19
1.00
3.00
5.00
7.00
9.00
11.00
13.00
15.00
17.00
FLUE GAS CAPACITY (MG/30MG)=X

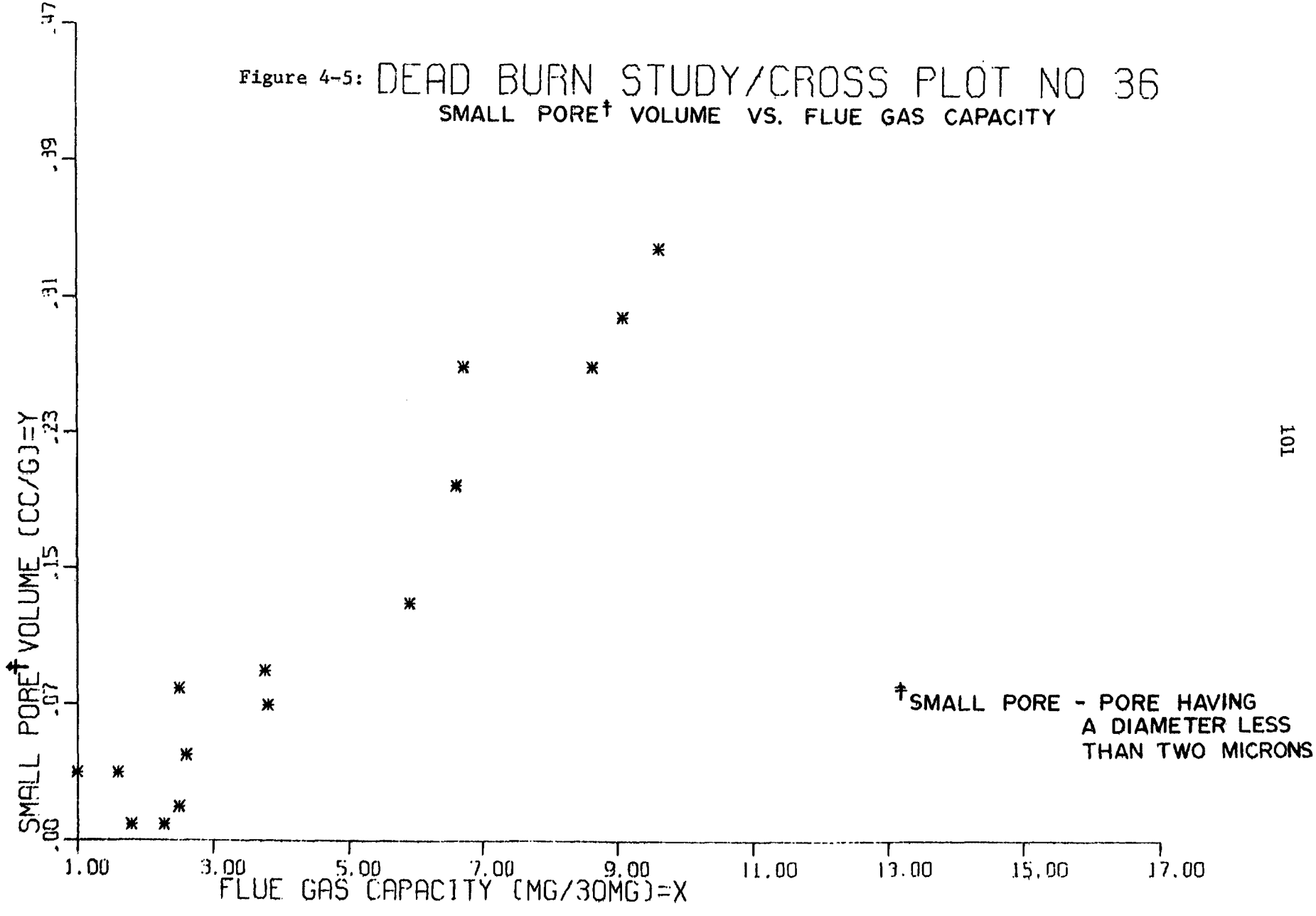
Figure 4-5: DEAD BURN STUDY/CROSS PLOT NO 36
SMALL PORE† VOLUME VS. FLUE GAS CAPACITY
SMALL PORE† VOLUME (CC/G)=Y
.00
.07
.15
.23
.31
.39
.47
1.00
3.00
5.00
7.00
9.00
11.00
13.00
15.00
17.00
FLUE GAS CAPACITY (MG/30MG)=X
†SMALL PORE - PORE HAVING A DIAMETER LESS THAN TWO MICRONS

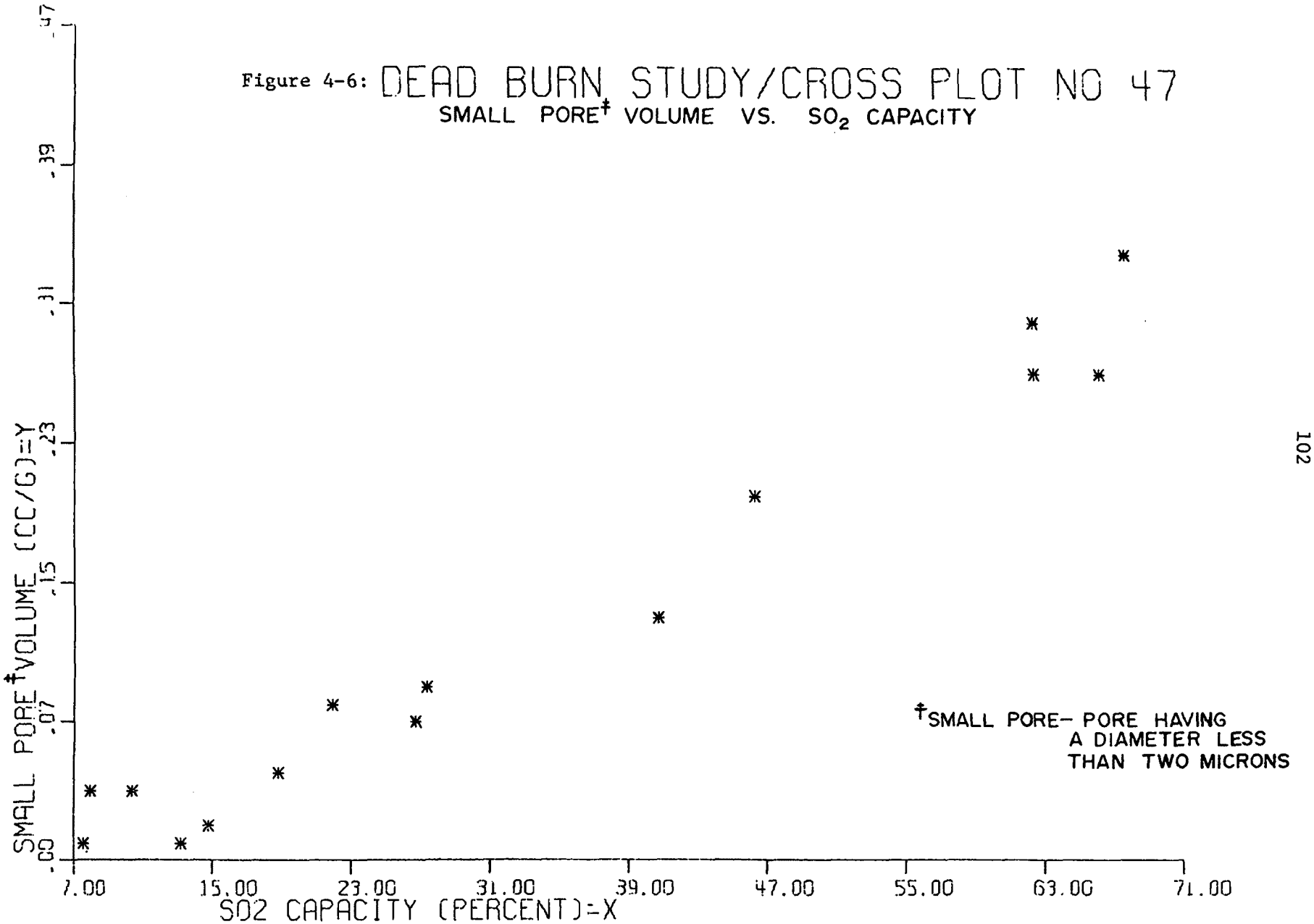
DEAD BURN STUDY/CROSS PLOT NO 47
SMALL PORE† VOLUME VS. SO2 CAPACITY
SMALL PORE† VOLUME (CC/G)=Y
.00
.07
.15
.23
.31
.39
.47
7.00
15.00
23.00
31.00
39.00
47.00
55.00
63.00
71.00
SO2 CAPACITY (PERCENT)=X
†SMALL PORE- PORE HAVING A DIAMETER LESS THAN TWO MICRONS

Figure 4-6:

Figure 4-7: DEAD BURN STUDY/CROSS PLOT NO 27

PURE SO_2 CAPACITY VS. FLUE GAS CAPACITY

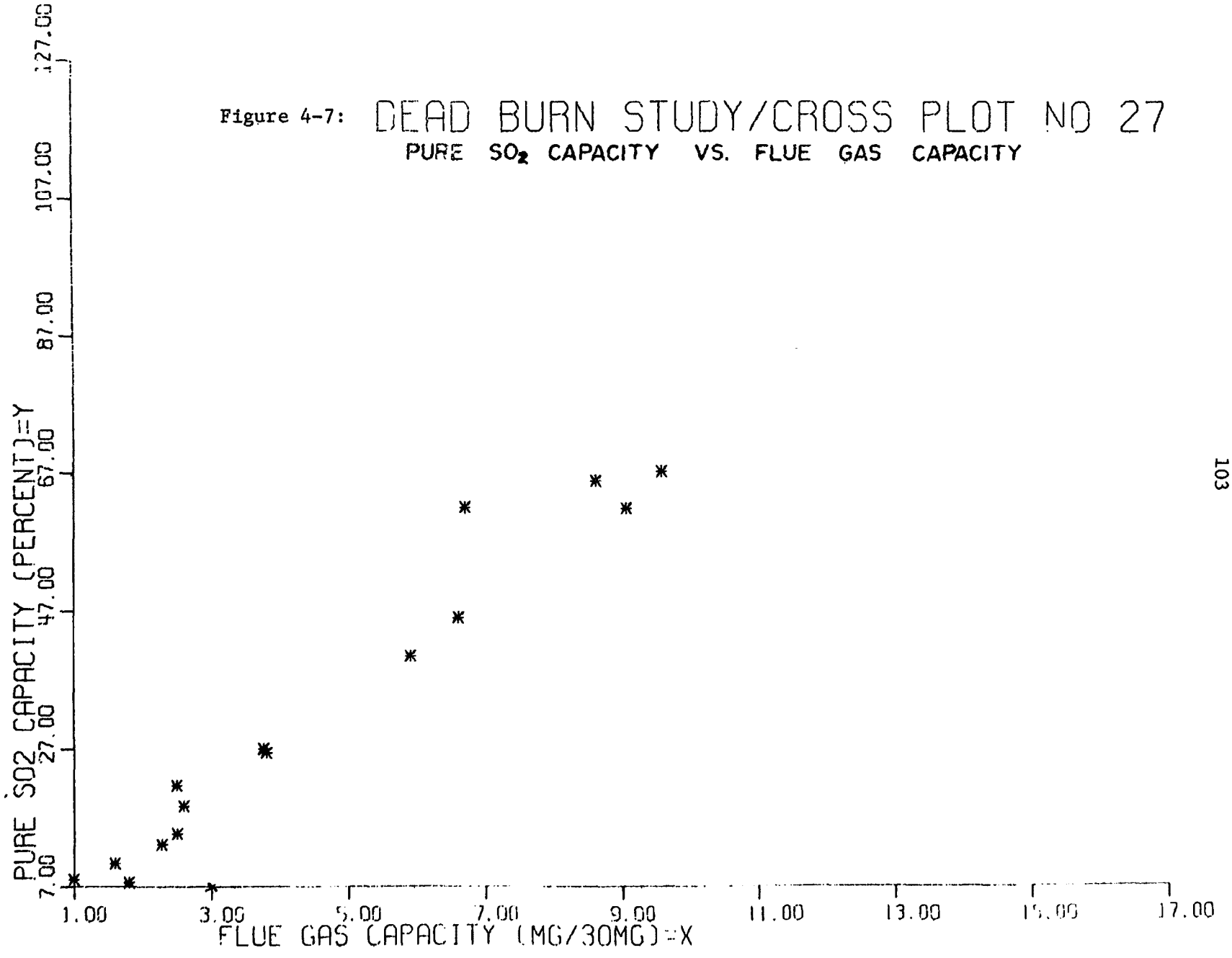

(2) Effect of Test Conditions

Upon review of the data on the effect of calcination temperature, three reactivity tests were selected for further study; they were pure CO_2 absorption and pure SO_2 absorption and hydration-weight gain. Possible parameters for the first two included reaction time, reaction temperature, gas flow rate, and particle size. The effect of particle size was studied first by finding the absorption for samples of 70/140, 140/200, 200/270, and -270 mesh ranges.

Carbon dioxide absorption was almost independent of particle size but sulfur dioxide absorption was slightly lower (less than 10 per cent) for the largest size ranges. On the other hand, carbon dioxide absorption was affected drastically by the temperature of the absorption test whereas sulfur dioxide absorption was not (see Figures 4-8 and 4-9). Both reactivity tests were independent of gas flow rate and weakly dependent on reaction time after ten minutes exposure (refer to Figures 4-10 and 4-11). Possible parameters for the hydration-weight gain test were slaking time, slaking volume, drying time, and drying temperature. Effects of the last two are not significant while the other effects are illustrated in Figure 4-12. Increasing either slaking time or slaking volume of distilled water increases the hydration-weight gain even for extremely hard-burned stones.

Figure 4-8

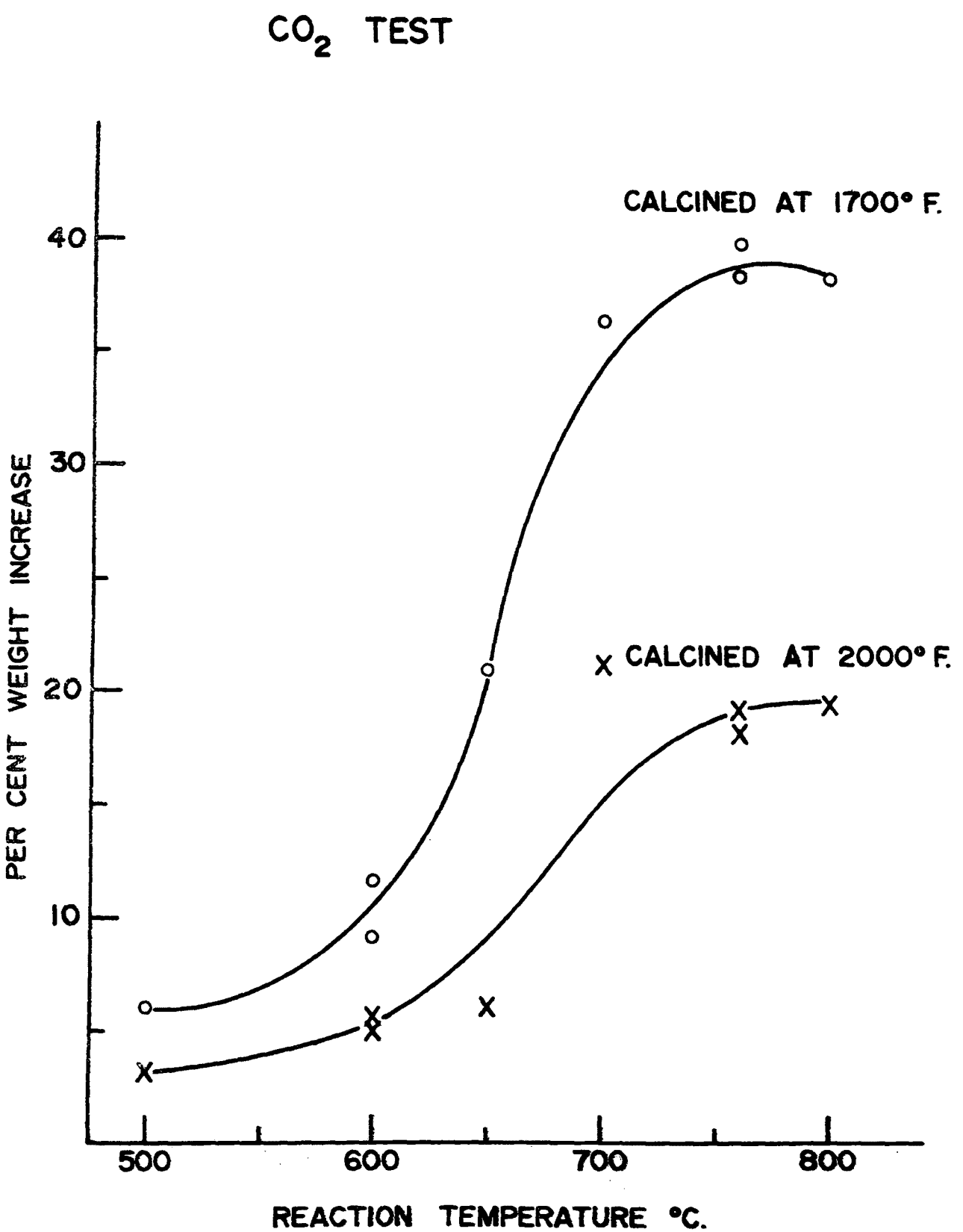
CO_2 TEST
CALCINED AT 1700° F.
CALCINED AT 2000° F.
PER CENT WEIGHT INCREASE
40
30
20
10
500
600
700
800
REACTION TEMPERATURE °C.

Figure 4-9

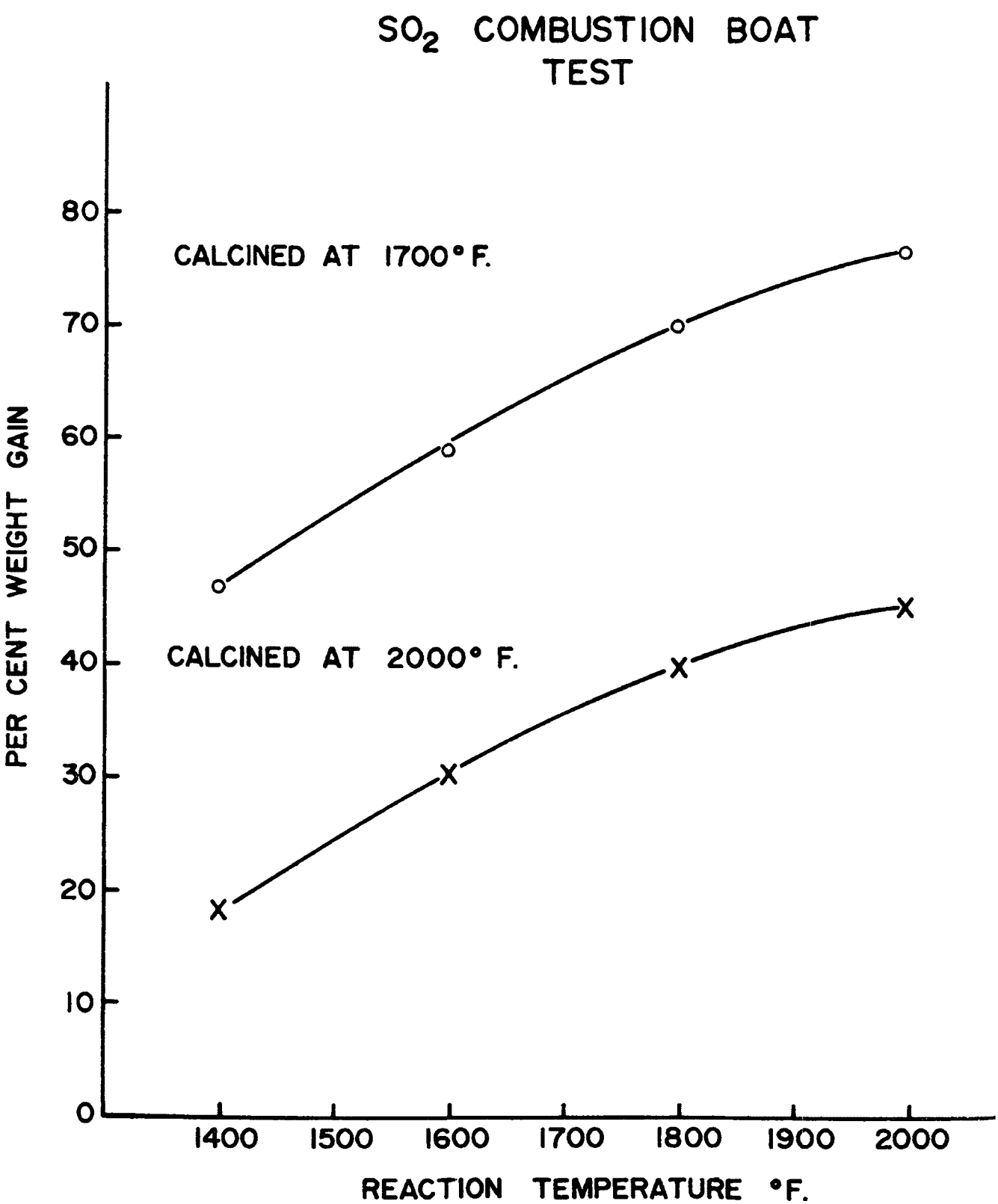
SO_2 COMBUSTION BOAT TEST
CALCINED AT 1700° F.
CALCINED AT 2000° F.
PER CENT WEIGHT GAIN
0
10
20
30
40
50
60
70
80
1400
1500
1600
1700
1800
1900
2000
REACTION TEMPERATURE °F.

Figure 4-10

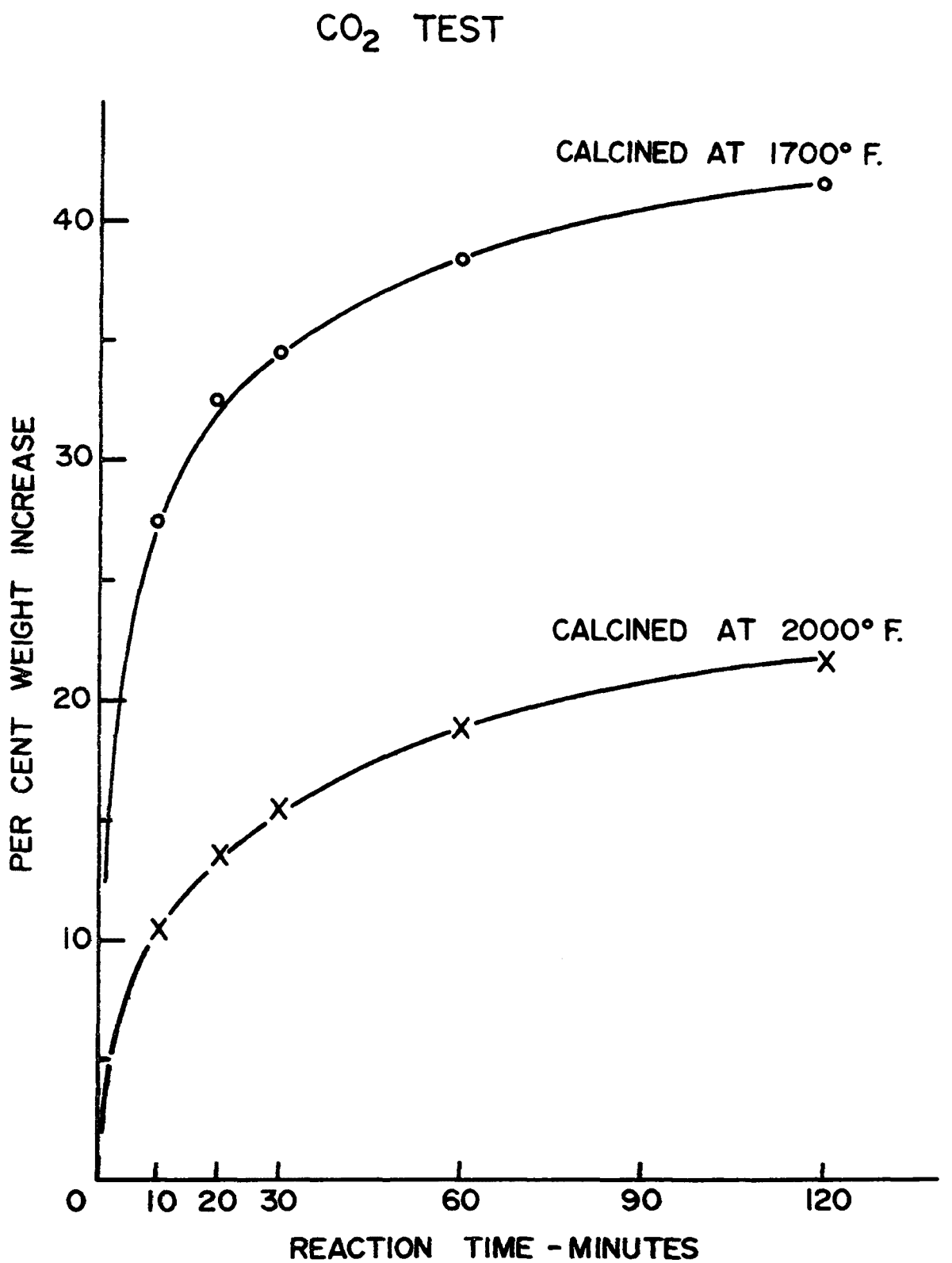
CO_2 TEST
CALCINED AT 1700° F.
CALCINED AT 2000° F.
PER CENT WEIGHT INCREASE
40
30
20
10
0
10
20
30
60
90
120
REACTION TIME - MINUTES

Figure 4-11

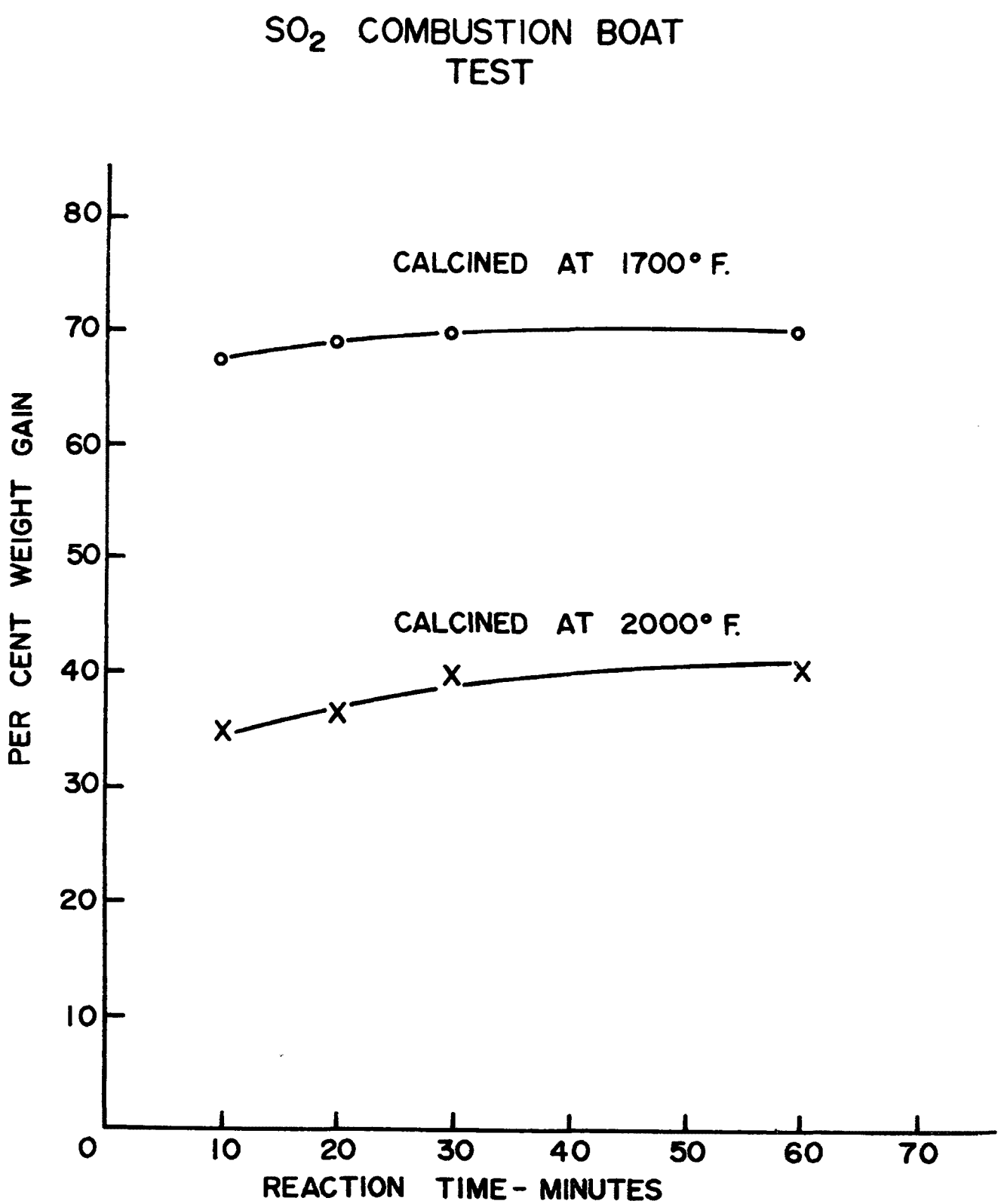
SO2 COMBUSTION BOAT TEST
CALCINED AT 1700° F.
CALCINED AT 2000° F.
PER CENT WEIGHT GAIN
80
70
60
50
40
30
20
10
0
10
20
30
40
50
60
70
REACTION TIME - MINUTES

Figure 4-12

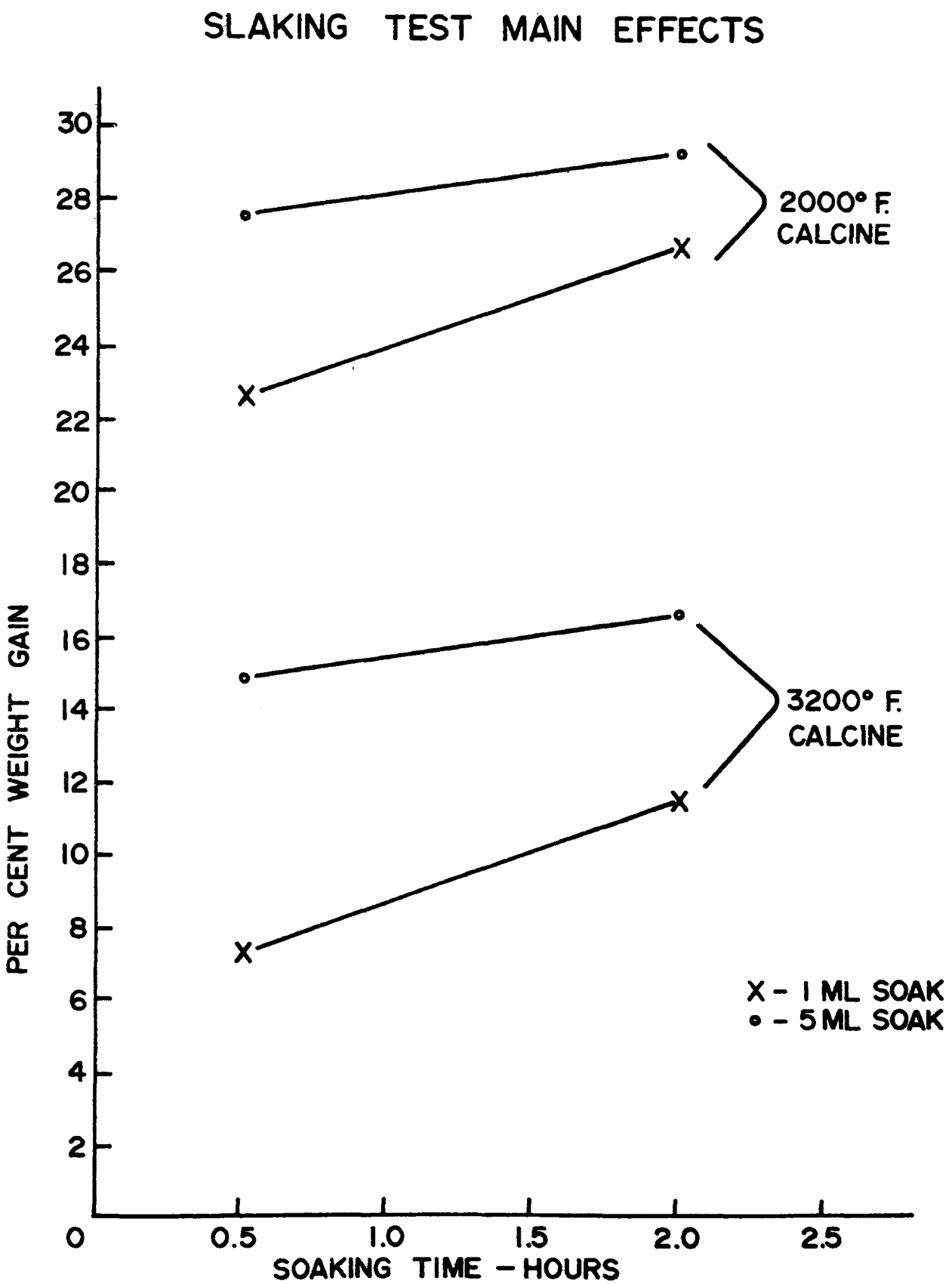
SLAKING TEST MAIN EFFECTS
PER CENT WEIGHT GAIN
30
28
26
24
22
20
18
16
14
12
10
8
6
4
2
0
0.5
1.0
1.5
2.0
2.5
SOAKING TIME – HOURS
2000° F. CALCINE
3200° F. CALCINE
X – 1 ML SOAK
• – 5 ML SOAK

(3) Effect of Partial Sulfation and Fly Ash

Besides the samples already listed above, certain samples exposed to SO_x-containing flue gases were received from Babcock and Wilcox (B&W). Under a contract to APCO, B&W injected the Stones No. 2061, No. 2062, and No. 2069 into their pilot scale coal-fired furnace. Samples of lime-fly ash mixtures from the cyclone downstream of the furnace were tested by all of the methods mentioned above. For the tests based on steam absorption and acid titration, the measured reactivity was very low or there was none at all. Results for physical property tests of these samples were difficult to interpret in comparison to results for pure limes.

To verify the exact relationship between the extent of sulfation and the degree of dead-burning measurements, the following experiment was conducted. Samples of Stone No. 2061 were exposed to either air or flue gas at 1800°F for varying lengths of time. The reactivity of the samples was determined using the CO_2 absorption test and the hydration weight gain test. The measured reactivity for samples exposed to flue gas was corrected for the calcium sulfate content, i.e., the calcium oxide content which has already reacted and is unavailable for the dead-burning test reactivity measurement. After this correction, the degree of dead-burning as measured for the samples exposed to air and for those exposed to flue gas should be the same. This is the case for the hydration weight gain test but not for the CO_2 absorption test. As shown in Figure 4-13 there is a large

Figure 4-13: COMPARISON OF MEASURED REACTIVITIES FOR SULFATED AND UNSULFATED LIMES

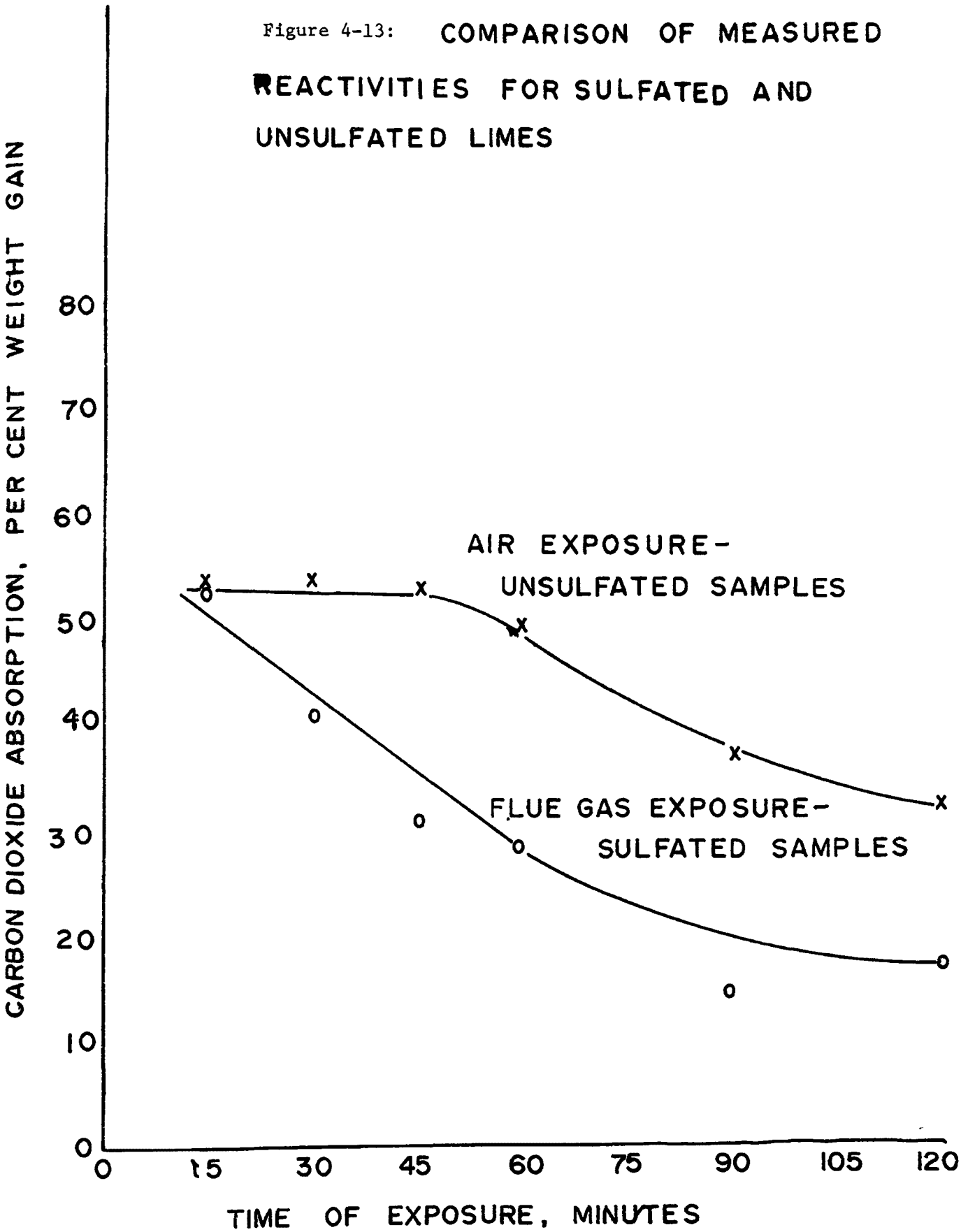

deviation between the measured reactivity for the air exposed samples and that for the flue gas exposed samples when reactivity is determined by CO_2 absorption. As shown in Figure 4-14 there is no such deviation for the hydration weight gain test; thus, this test is independent of the extent of sulfation.

d. Conclusions

Four reactivity tests - namely, flue gas absorption, SO_2 absorption, CO_2 absorption, and hydration weight gain are suitable as dead-burning tests for samples of limited size diluted with fly ash. The later three are sufficiently uncomplicated to be used as field tests. For sulfated samples, the hydration weight gain test is recommended since it is independent of the degree of sulfation. Excellent correlation between SO_2 reactivities, B.E.T. surface area, and pore volume support the conclusion that dead-burning can be accounted for by loss of surface area and pore volume.

Figure 4-14

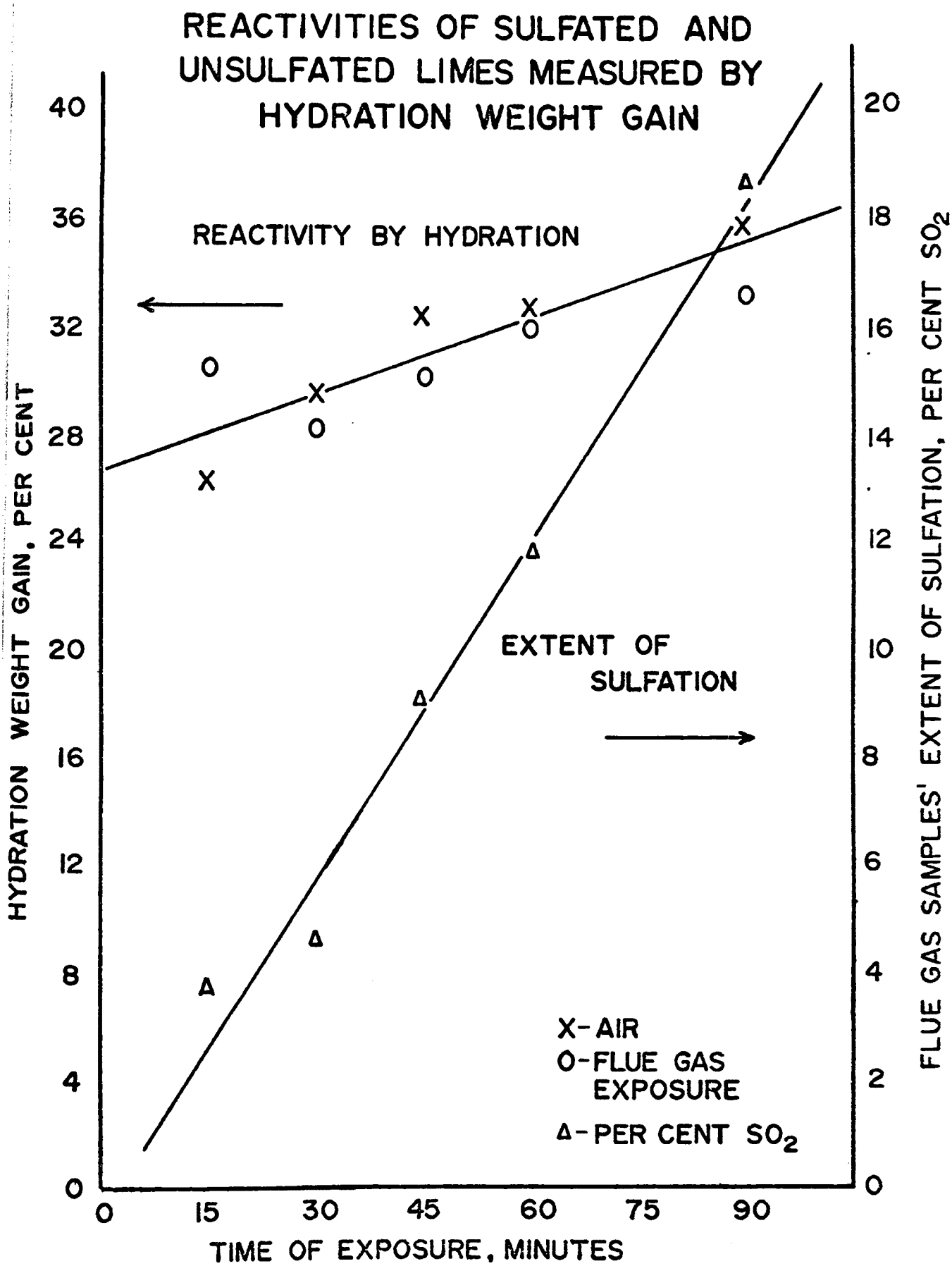
REACTIVITIES OF SULFATED AND UNSULFATED LIMES MEASURED BY HYDRATION WEIGHT GAIN
REACTIVITY BY HYDRATION
EXTENT OF SULFATION
X-AIR
O-FLUE GAS EXPOSURE
Δ-PER CENT SO2
HYDRATION WEIGHT GAIN, PER CENT
FLUE GAS SAMPLES' EXTENT OF SULFATION, PER CENT SO2
TIME OF EXPOSURE, MINUTES
0
4
8
12
16
20
24
28
32
36
40
2
6
10
14
18
15
30
45
60
75
90

5. Capacity of Limestone for Sorption of SO_2

a. Introduction

The low cost and widespread availability of naturally occurring carbonate rocks, particularly limestones*, has led to interest in their use as reactants for desulfurization of combustion gases. Potter, Harrington, and Spaite[28] have presented some of the background and engineering considerations for development of a limestone desulfurization process. In the development of the process, it became apparent that some limestones are better absorbents than others and that selective recommendation of limestones would be necessary to optimize full scale field trials in power boilers. Potter[29] has presented results of the present study which was designed to determine (1) the differences in the sulfur dioxide reaction characteristics of a large number of limestones, and (2) the physical and chemical properties responsible for these differences.

A fixed-bed reaction test was selected because of its relative simplicity. However, the fixed-bed approach is not easily suited to reaction rate studies because of the changes in conversion and SO_2 partial pressure throughout the bed. Therefore, the work has been limited to determining the ability of a sample to achieve a high absorption efficiency. In this

---

* In this report "limestone" includes all carbonate rocks containing magnesium and calcium. High purity $CaCO_3$ is termed "calcite".

report, absorption is measured as bed weight gain and is generally expressed as capacity.

Using the results of preliminary tests of ten samples[14], standard calcination and reaction conditions for comparing capacities were selected. Since the early work showed little correlation between sulfur oxide capacity and chemical composition of the limestone, in the work reported here characterization of physical properties and classification of samples was emphasized.

b. Experimental

(1) Sample Preparation and Analyses

Crushed samples of limestone were screened to obtain a -18 +20 U. S. mesh cut (mean opening size 0.92 mm). After a crushed stone was thoroughly blended, a representative sample was analyzed spectrochemically. The carbonate content of the rock was determined by dissolving a portion of the raw stone in 1N HCl.

The calcined material for the standard screening studies was prepared in a bench scale calciner consisting of an Inconel pipe rotating in a muffle furnace. A 180 g. charge was fed to the preheated kiln and held at 980°C for 4 hours. To form hydrates, hot water was slowly added to the calcined stone. After the cake was dried to constant weight at 110°C, it was

crushed and screened to obtain -18 +20 U.S. mesh hydrate pellets. Thirty-nine of the calcined stones were tested for B.E.T. surface area and mercury pore distribution. The bulk specific gravity was determined by an oil sorption test (ASTM test C-127-54) modified for use with No. 2 fuel oil.

(2) Capacity Determination

The fixed bed reactor system used to determine sulfur oxide capacity is shown in Figure 5-1. No. 2 fuel oil (C:H = 6.8 by weight) blended with controlled amounts of carbon disulfide (CS_2) was burned at 17% excess air to give a flue gas with the following average composition by volume: 10.5% CO_2, 3.4% O_2, 9.9% H_2O, 0.27% SO_2, 0.003% SO_3, and 75.9% N_2.

The 35-mm diameter Inconel reactor was preheated to the desired temperature, 980°C for the standard test condition, before the sample was dumped from the top of the reactor onto a 30 mesh screen in the center of the reactor. A 20-gram charge of calcined stone is stable at 980°C. For uncalcined and hydrated samples a weight equivalent to 20 grams of calcined stone was used. The flue gas was passed through the bed at a rate of 425 standard liters per hour for 3-1/2 hours. In an oxidizing atmosphere at 980°C the net reaction is

$$CaO_{(s)} + 1/2\ O_{2(g)} + SO_{2(g)} \rightarrow CaSO_{4(s)}$$

Figure 5-1

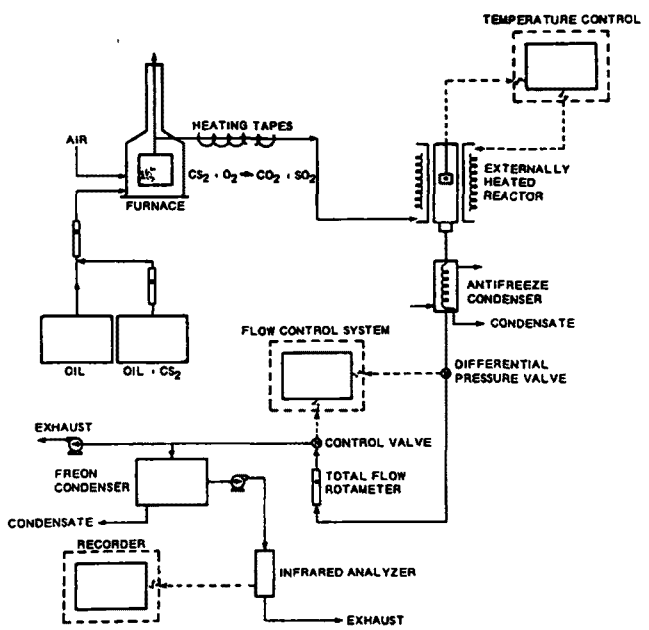

Flow diagram for fixed-bed reactor system

The SO_2 content of the effluent was monitored continuously with an infrared analyzer. At the end of the exposure period, air was admitted to the reactor to inhibit side reactions. The final weight of the bed was then determined. The sample size, flow rate, and contact time were selected so that even the most reactive stones had nearly ceased reaction. Therefore, the data give a comparison of the saturation conversions of the samples.

The bed weight gain of a 20-gram calcined sample (expressed as g. SO_3/100 g. of calcined stone) was selected as the index of sulfur oxide capacity. The bed weight gain, also referred to as "loading" or "capacity", is the weight of SO_3 removed from the flue gas. No side reactions with carbon dioxide or water were observed during the cooling and handling of the reacted sample. In order to determine the reproducibility of the test, single replicate tests were made on 22 different samples. The standard deviation was found to be 2.98 g./100 g. Since loadings varied between zero and 85 g./100 g., the test is considered to be sufficiently sensitive and precise.

c. Discussion of Results

(1) Form of Sorbent and Reaction Temperature

The carbonate, oxide, and hydroxide forms of two samples were tested at 430, 705, 980, and 1095°C. The results are given in Figure 5-2 for a high-calcium stone and a dolomite, designated A and B, respectively. This work shows the relative performance and temperature sensitivity of the different forms of the stone and also the relation between optimum capacity and capacity at 980°C, the temperature at which the bulk of the experimental work was done.

The hydrates have greater capacity than the oxides and carbonates throughout the temperature region examined. In an air pollution control process, the additional capacity of hydrates has the greatest relative advantage at low temperatures where reduced gas volumes, lower viscosity, and cheaper materials of construction might offset the cost of sorbent preparation. Below 900°C the capacity of the calcined stone is greater than that of the carbonate. Since the low temperature (400 to 800°C) loadings are substantially different from the high temperature loadings, conclusions presented here are most valid for temperatures in the region of 1000°C.

Below 1000°C the capacity of the carbonates falls off rapidly with decreasing temperature. Above 1000°C the loading generally decreased with increasing temperature. The reduced capacity at

Figure 5-2

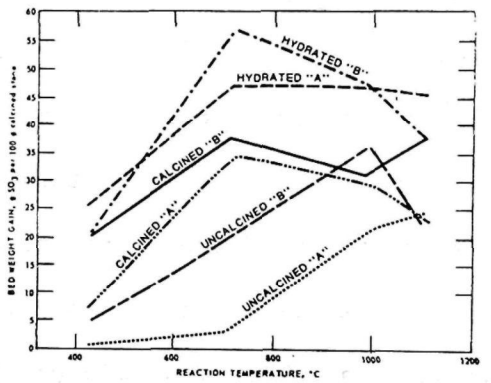

Reaction temperature and form of reactant

Figure 5-3

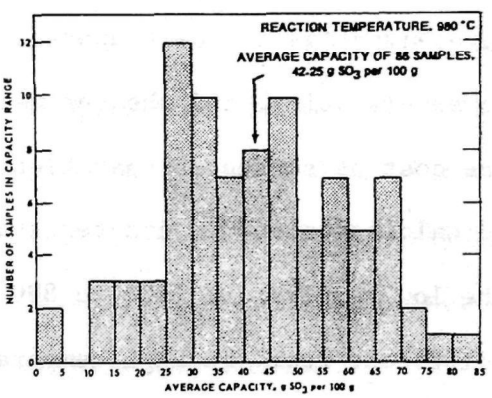

Frequency distribution of capacities of 86 stones tested

higher temperatures may result from changes in physical properties. For example, significant crystallite size growth has been reported above 1000°C[16]. Reduced capacity may also be due to thermodynamic limitations: little $CaSO_4$ formation is expected above 1230°C in combustion flue gases[34]. Disregarding these reactant considerations, there is little incentive for higher temperature desulfurization because increased gas volumes and viscosity coupled with more costly materials of construction would result in higher operating costs. The 980°C standard test temperature seems to be near the most practical temperature for a high-temperature, SO_2 control process based on the use of uncalcined limestone.

(2) Calcination

A series of fixed-bed calcinations were made at 1316°C for 16 hours to evaluate the effect of high-intensity calcination on the SO_x capacity and physical properties of calcined stones. The results are given in Table 5-1. There was in all cases a loss in surface area and an increase in the mean mercury intrusion pore size when the calcination temperature was increased from 980 to 1316°C. Loss in pore volume and surface area probably resulted from shrinkage and crystallite growth[23]. The variations in SO_3 loading that resulted from changes in calcination procedure are well explained by the volume of pores larger than 0.3μ. The minimum pore diameter measured by the mercury porosimeter is 0.017μ.

Table 5-1. EFFECT OF CALCINATION

Sample	Hg pore volume (cm^3/g)		B.E.T. surface area (m^2/g)		Mean Hg pore size (microns)		Volume of pores larger than 0.3μ (cm^3/g)		SO_x capacity (g SO_3/100 g)	
	985°C	1316°C	985°C	1316°C	985°C	1316°C	985°C	1316°C	985°C	1316°C
C	0.31	0.21	9.2	1.1	0.06	0.35	0.03	0.18	13.6	20.1
D	0.24	0.25	8.4	1.1	0.10	1.3	0.10	0.18	26.8	31.5
E	0.34	0.07	4.1	1.0	0.78	6.0	0.33	0.07	29.0	9.15
F	0.38	0.32	1.7	0.1	0.92	18.0	0.35	0.32	47.0	18.1
G	0.43	0.14	2.0	0.6	0.62	3.5	0.43	0.14	63.0	24.6

Those samples whose volume of large pores was reduced had a corresponding loss of capacity, whereas the two samples whose SO_3 loading was increased as a result of high-temperature calcination had an increased volume of pores larger than 0.3μ.

Each of the 81 samples was tested in the fixed-bed reactor in both the uncalcined and calcined conditions. The correlation coefficients* between capacities of uncalcined samples and capacities of calcined samples was +0.734. The mean loadings of uncalcined and calcined samples were 41.7 and 43.1 g. SO_3/ 100 g. of sample, respectively. These values suggest that at 980°C the relative capacity of a sample is, on the average, the same in either the uncalcined or calcined state. Analysis of variance tests on 33 combined samples and on 8 individual classes did not show statistically significant differences between uncalcined and calcined samples. Because of the equivalence of the capacities of uncalcined and calcined stones, averages of tests on uncalcined and calcined samples are used for each stone in the balance of this discussion.

---

* The correlation coefficient, r, is an index of the strength of the linear relationship between the changes of two variables. For example, $r_{xy} = 0.65$ means that 65% of the time a positive change in y is accompanied by a positive change in x.

(3) Capacity Correlations

The average SO_3 loadings of 86 samples reacted at 980°C are summarized in a frequency distribution chart (Figure 5-3). It is apparent that the capacities of various limestones for sulfur oxides differ widely. The average loading of 42.3 g./100 g. for the -18 +20 mesh particles corresponds to 30% utilization for pure CaO. However, since the average CaO content of the samples was only 65%, the actual average utilization of the CaO was 45%. Incomplete conversion of the reactant suggests diffusion limitation by the surface layer of reaction products. Electron microprobe analysis has verified the existence of such a layer[8]. However, our studies with different particle sizes suggested that the depth of penetration of sulfur is not constant. Further work is necessary to define the limiting mechanism.

The factors that best explain the wide variations in SO_3 loading at the standard test condition are summarized in Table 5-2. With the exception of ignition loss and amount soluble in HCl, the physical and chemical analyses were performed on the calcined material. Since a large number of samples was tested and analyzed, it was found that the values of the correlation coefficient did not change greatly with further increases in the number of samples considered. The absolute values of r are not as important as their relative magnitudes.

Table 5-2. CORRELATIONS BETWEEN PHYSICAL PROPERTIES AND 980°C CAPACITIES

Independent variable	Number of samples analyzed	Correlation coefficient
% CaO	59	-0.018
% MgO	59	-0.043
% Loss on Ignition	39	-0.035
% of Raw stone soluble in HCl	39	-0.202
B.E.T. surface area (m^2/g)	39	-0.246
Mean Hg pore size (micron)	39	+0.398[a]
Area of pores >0.3μ (m^2/g)	39	+0.400[a]
% Fe_2O_3	59	+0.429[b]
Bulk specific gravity	39	-0.507[b]
Volume of pores >0.3μ (cm^3/g)	39	+0.620[b]
Total Hg pore volume (cm^3/g)	39	+0.635[b]
% Oil absorption	39	+0.643[b]

[a] Significant at 95% confidence level

[b] Significant at 99% confidence level

Surprisingly, the chemical composition and carbonate content (i.e., loss on ignition and amount soluble in HCl) explain little of the variation in performance of the samples. Of the chemical components only the iron is significantly related to capacity at or above the 90% confidence level. Whether the contribution of the iron is chemical or physical is not clear at the present time.

The fact that the nitrogen adsorption surface area does not correlate with capacity indicates that pores in the angstrom size range do not significantly contribute to the fixed-bed reaction. On the other hand, a number of physical tests show that pores in the micron range account for most of the reactivity. The correlation of the mean mercury pore size indicates the relative importance of larger pores. The area of pores larger than 0.3μ was calculated by integration of mercury intrusion data[30]. A trial-and-error calculation with 12 of the samples showed that the arbitrary 0.3μ integration limit gave the best correlation with loading. Clearly, this partial surface area is more directly related to capacity than is the B.E.T. area.

Oil immersion led to significant correlations with capacity when expressed either as bulk specific gravity or as percent absorption. The total mercury pore volume was the most useful

parameter for explaining differences among samples because (1) unlike oil absorption, mercury intrusion is not limited to use on large particles and (2) correlation calculations have shown that the bulk specific gravity, oil absorption, and volume and area of larger pores are significantly related to the total mercury pore volume. Therefore, the iron content, mean mercury intrusion pore size, and the total mercury pore volume are considered to be the most fundamental variables for explaining differences in the capacities of samples. When these three variables were used in a stepwise regression analysis, the combined correlation coefficient was + 0.775.

(4) Classification of Samples

The carbonate form of limestone is the most likely feed material in an SO_2 removal process using limestone at temperatures higher than the calcination temperature. Since most of the physical properties in the preceding section were determined on precalcined material, data on eight classes of limestone are given in Table 5-3 to show the capacities of various types of carbonate rock at the standard test condition. The classes were selected to give the greatest possible variety of crystal structures, chemical compositions, and geological origins.

Iceland spar was included because this high-purity calcite is composed of very large crystallites. A magnesite was

Table 5-3. CAPACITY OF VARIOUS CLASSES OF LIMESTONE

Classification	Number of samples in class	Variance	Mean capacity[a] (g SO_3/100 g)
Iceland spar	1	2.90	17.3
Magnesite	1	0.0545	19.7
Marble	5	6.55	32.0
Calcite	7	2.14	32.7
Dolomite	7	10.32	43.8
Aragonite	3	6.45	52.1
Oolite	4	3.97	57.1
Chalk	5	6.54	66.4

[a] At 980°C

tested to determine the reactivity of $MgCO_3$. Replicate runs were made on single samples of Iceland spar and magnesite to establish their capacities under the same conditions. Hard, highly crystalline marble samples provide interesting comparisons with the soft, fine-grained chalks. The round-grained, precipitated oolitic samples represent another extreme in crystal structure. The orthorhombic aragonites were included because most limestones are rhombohedral. Calcites were defined as those having at least 95% CaO, and the dolomites were defined as samples with 40% to 44% $MgCO_3$ and 54% to 58% $CaCO_3$[7]. The results of these classifications are presented in Table 5-3 in order of increasing mean capacity.

Iceland spar is apparently an inferior form of carbonate rock for absorption of sulfur oxides. A t-test on the various classes showed that we can be 95% confident that Iceland spar has lower capacity than the average calcite. The low capacity of magnesites was also shown by the t-test. Thermodynamically MgO can react with SO_2[34], however, the rate of reaction is apparently very slow.

It was determined, with 90% confidence, that for the test conditions used the mean capacities of calcite and dolomite differ. The CaO utilization of the dolomites is about twice that of the calcites. Oolites and chalks appear to have desirable properties for reaction with sulfur oxides.

Although the five chalks had a higher mean capacity than the oolites, a t-test showed that differences between these two groups were not statistically significant.

Further refinement in the classification of samples could be achieved if mineralogical and petrographic characterizations were made. For example, crystallite sizes may be important in predicting the capacity of a stone. This idea is supported by the data in Table 5-3; the highly reactive chalks are typically fine materials, whereas Iceland spar and marble are relatively coarse materials.

d. Conclusions

1. Between 900 and 1000°C raw and precalcined samples have the same sulfur oxide absorption efficiency. At these temperatures calcined stone does not lose capacity through the changes in physical properties that accompany overcalcination at higher temperatures.

2. The wide differences in capacity are best explained by reaction in pores of the size that are measured by mercury intrusion. Chemical composition is of only secondary importance.

3. Under the chosen test conditions chalk and oolitic samples have the greatest sulfur oxide saturation

capacity. Iceland spar, magnesite, and marble are less reactive forms of limestone.

In addition to the data reported above a large amount of data has been accumulated for other limestones and dolomites. Approximately 150 limestones and dolomites have been inventoried by the Process Research Section. Data are available for most of these sorbents which include chemical compositions, physical properties (B.E.T. surface area, pore volume and distribution, etc.), and SO_2 sorption characterization (bed weight gain, CaO utilization, etc.). All such data is being compiled by the Process Research Section and will be available to interested groups.

D. GENERAL CONCLUSIONS

1. Chemical reaction is the sole limiting resistance for SO_2 sorption when particles are smaller than 100 microns at temperatures up to 980°C if pores are larger than 0.2 microns. The isothermal reaction of pure limestones with SO_2 show an intrinsic rate constant (per unit of surface) on the order of 0.2 cm/sec.

2. The rate of reaction increases with decreasing pore size until a critical pore diameter of about 0.1 micron is reached. Presumably pores smaller than 0.1 micron are rapidly blocked by reaction products. Maximum rate results when B.E.T. surface area is in the region of 3.5 m^2/g (corresponding to pore diameters of 0.2 - 0.3μ) under isothermal reaction conditions.

3. The total SO_2-sorption capacity increases with increasing pore size, Furthermore, the capacity of limestones is correlated to the area of pores greater than 0.3 microns but not to B.E.T. surface area.

4. Both rate and capacity of SO_2 sorption are highly dependent upon particle size. The effect of particle size is not the same for all stones, but is determined by the size of the pores.

Small pores lead to the highest sensitivity between the reactivity of calcines and particle size. Calcines with very large pores may show no dependence of reactivity upon particle size.

5. The relative ranking of calcines with respect to isothermal rate of reaction with SO_2 at 980°C is as follows: marl > high purity limestone > Iceland spar > aragonite > marble. Magnesite reacts only slowly with SO_2 at any temperature between 540°C and 980°C.

6. The relative ranking of limestones with respect to fixed bed capacity at 980°C with -18 +20 mesh particles is as follows: chalk > oolite > dolomite > calcite > marble > magnesite > Iceland spar.

7. Loss of reactivity because of excessively high calcination temperatures (known as dead-burning) may be attributed to the growth of CaO crystals and the subsequent loss of surface area pore volume. Since loss of surface area and loss of pore volume are similar functions of increasing calcination temperature, both reaction rate and capacity of overburned limes are lost proportionally.

8. Injection of limestone with the fuel into a boiler leads to dead-burning and poor SO_2 removal efficiency. Samples from field tests where limestone was injected with the fuel in an

oil-fired boiler demonstrated the high densities and low porosities characteristic of overburned limes.

9. Among many physical and chemical properties which are good indications of the degree of dead-burning, CO_2 weight gain, SO_2 weight gain and hydration weight gain are suitable for samples of limited size diluted with fly ash. For partially sulfated samples, the hydration weight gain test is recommended since it is independent of sulfate loading up to 20% SO_2 in the test sample.

E. APPLICATION OF RESULTS TO LIMESTONE PROCESSES

In the dry limestone injection process, sorption of SO_2 will be required of initially uncalcined limestone undergoing calcination and reaction in a nonisothermal environment. In this regard, the conditions under which the process is to be run and conditions under which experimental kinetic data of this project were collected are quite different. For instance, the kinetic data were obtained for precalcined limestone reacted under isothermal conditions. This does not mean that the data are not applicable. Polythermal reactions may be regarded as a series of isothermal reactions over short time increments provided that the rate of temperature change with time may be predicted and that there is no change in mechanism of the reaction. Rate of temperature change may be predicted with heat transfer correlations and a heat balance. While a multitude of reaction mechanisms are possible, the high injection temperature of limestone in the dry injection process would preclude the sulfite reactions and suggest the dominant reaction is direct conversion to calcium sulfate. Thus, the dominant reaction mechanism would not change.

The second difference between experimental conditions and boiler injection conditions was precalcined versus uncalcined limestone. Once again, the reaction mechanism could be significantly different

except if most of the limestone first calcines and then reacts to form the sulfate. In this case, the difference is one of calcination conditions, i.e., calcination at a low temperature for two hours versus calcination at a high temperature for a few tenths of a second. Effects of varying calcination conditions are reflected in the surface area of the calcine and, subsequently, in its reactivity.

The importance and functional relationship of the surface area to the sulfur oxide reactivity of limes has been shown in the investigations discussed above (for example, refer to conclusions Subsection e, of Section C2). It remains to describe the effect of limestone type and injection conditions on the development of surface area during calcination. To this end work at Battelle Memorial Institute has been committed using a dispersed phase reactor.

There is little doubt that dead-burning is an important phenomenon in limestone processes and in particular the dry injection process. The above studies have shown that calcination at high temperatures yields a dense lime with little surface area and little sulfur dioxide reactivity. Not only is injection of limestone with the fuel into a boiler to be avoided, but also injection should be sufficiently far from the fireball that particle temperatures never exceed 2000°F. Most tests for dead-burning

are confounded by the presence of fly ash or of partial sulfation. Although modification of procedures may be required, a simple determination of the weight gain from hydration shows the most promise as a dead-burning test for the dry injection process.

Selection of carbonate rock type for limestone processes depends on the nature of the process. For fluid bed combustion where limestone remains as a chemically active fluid bed to react completely, the proper measure of its reactivity is its capacity. Rankings of limestone and limestone types for this application are given in Table 5-3 of Section C5 and in Appendix C1. For the dry injection process, limestone may react only during very short residence times, and the proper ranking is derived from reaction rate measurements as given in Figure 2-4, Section C2.

F. RECOMMENDATIONS

1. Sulfur oxide abatement processes involving injection of limestone into a power boiler should be significantly enhanced when highly reactive types of limestones are used; especially, aragonite and marl. Testing of these materials in demonstration scale applications is recommended.

2. It has been shown that dead-burning is an important factor in the dry limestone injection process. Not only must injection of limestone with the fuel be avoided but also injection should be into a temperature zone allowing greatest residence time without overburning.

3. Two fine-grained limestone materials have shown outstanding SO_2 reactivity; specifically of the stones tested, marl with the highest rate of reaction and chalk with the largest capacity for absorption of SO_2. These materials should be studied in depth to delineate those properties contributing to high reactivity.

4. Much of the background information on limestone-SO_2 reactivity may be applicable to limestone dissolution rates in water and subsequently to limestone slurry-SO_2 reactivity. Those properties responsible for high dissolution rates of limestone in water should be identified as well as the relative dissolution rates of characteristic limestone types.

5. Limestone may well be an efficient sorbent for sulfur emissions found in reducing conditions. The kinetics of limestone - hydrogen sulfide reactions should be determined besides screening limestone types for reactivity.

G. REFERENCES

1. ASTM Standard C110-67

2. Attig, R. C., "Dispersed-Phase Additive Tests for SO_2 Control", Interim Report LR:68:4078-01:9 by Babcock and Wilcox Co. for contract PH 86-67-127 (Dec. 10, 1968)

3. Azbe, V. J., "Fundamental Mechanics of Calcination, Hydration", Lime Manufacture May 1939

4. Bertrand, R. R. et al, "Fluid Bed Studies of the Limestone Based Flue Gas Desulfurization Process", Progress Reports 9 and 10 by Esso Research and Engineering Co., for contract PH 86-67-130 (1968)

5. Borgwardt, R. H., Environmental Science and Technology, 4 (1) 59 (1970)

6. Borgwardt, R. H. et al, "The Dry Limestone Process for SO_2 Control: A Field Study of the Role of Overburning", APCA, New York, N. Y. (June 22-26, 1969)

7. Boynton, R. S., "Chemistry and Technology of Lime and Limestones", Wilev, New York 1966

8. Coutant, R. W. et al, "Investigation of the Reactivity of Limestone and Dolomite for Capturing SO_2 from Flue Gas", Reports by Battelle Memorial Institute for contract PH 86-67-115 (Aug. 30, 1968 and Feb. 12, 1969)

9. Cunningham, W. A., I and EC, 43 (3) 635-8

10. Eades, J. L. et al, "Scanning Electron Microscope Study of Development and Distribution of Pore Spaces in Calcium Oxide", 2nd Annual SEM Symp., IITRI (April 1969)

11. Eckhard, S., Z. Analyt Chem, 209:156 (1965)

12. Fischer, H. C., J. Amer. Ceramic Soc., 38:7, 245-51 (1955)

13. Goldschmidt, K., VDI Berichte, 6:21, 84 (1968)

14. Harrington, R. E. et al, Am. Ind. Hyg. Assoc. J., 29, 52-8 (1968)

15. Harvey, R. D., Environmental Geology Notes, 21, Illinois State Geological Survey (1968)

16. Hatfield, J. D. et al, Monthly Report for contract TVA-29232A (October 1968)

17. Haynes, W., "Pilot Injection Studies at the Bureau of Mines", report presented at PHS Limestone Conference (Dec. 4-8, 1967)

18. Hedin, R., "Structural Processes in the Dissociation of Calcium Carbonate", National Lime Assoc., Azbe Award #2 (1961)

19. Ishihara, Y., "Removal of SO_2 from Flue Gases by Lime Injection Method", report of Central Research Institute of Electric Power Industry, Komae, Kaitatama, Tokyo, Japan presented at PHS Limestone Conference (Dec. 4-8, 1967)

20. Kim, Y. K., "Sulfation of Limestone Calcines", PHS Symp., Cincinnati, Ohio (Feb. 5-6, 1969)

21. Lougher, E. H., "Identification of Test Methods for Determining the Degree of Burning of Limestones", Final Report (Nov. 13, 1968)

22. Ludwig, J. H. et al, Chem. Engr. Progress, 63 (6), 82-4 (1967)

23. Mayer, R. P. et al, "Physical Characterization of Limestone and Lime", National Lime Association, Washington, D. C. (1964)

24. McClellan, G. H. et al, "Scanning Electron Microscope Study of the Textural Evolution of Limestone Calcines", ASTM

25. Mullins, R. C. et al, "Effects of Calcination Conditions on the Properties of Lime", ASTM

26. National Research Council (National Academy of Engineering), "Abatement of Sulfur Oxide Emissions from Stationary Combustion Sources", 1970

27. Ohno, Y., Gypsum and Lime, 28, 22-28 (1957)

28. Potter, A. E. et al, Air Engineering, 22-6, (April 1968)

29. Potter, A. E., Ceramic Bulletin, Am. Ceramic Soc., 48 (9), 855-8 (1969)

30. Rootare, H. M. et al, J. Phys. Chem., 71, 2733 (1967)

31. Satterfield, C. N. and Sherwood, T. K., "The Role of Diffusion in Catalysis", Addison-Wesley, Reading, Mass. (1963)

32. Shen, J. and Smith, J. M., Ind. Eng. Chem. Fundam., 4, 293-301 (1965)

33. Tennessee Valley Authority, "Sulfur Oxide Removal from Power Plant Stack Gas Conceptual Design and Cost Study" (1968)

34. Ward, J. O. et al, "Fundamental Study of the Fixation of Lime and Magnesia", Report by Battelle Memorial Institute for Contract PH 86-66-108 (June 30, 1966)

35. Wicker, K., Mitt. Ver. Grosskesselbes, 83, 74-82 (1963)

36. Wuhner, J., "On the Reactivity of Lime from Different Kiln Systems", National Lime Association, Azbe Award #5 (1965)

APPENDIX A

Kinetic Data of Carbonate Rock Types

KINETIC DATA OF CARBONATE ROCK TYPES

The graphs appearing in this appendix present the kinetic data obtained in differential reactor test runs in accord with the discussions of Section C2 of the report. The carbonate rock types indicated on the graphs are identified in Table 2-1 of Section C2.

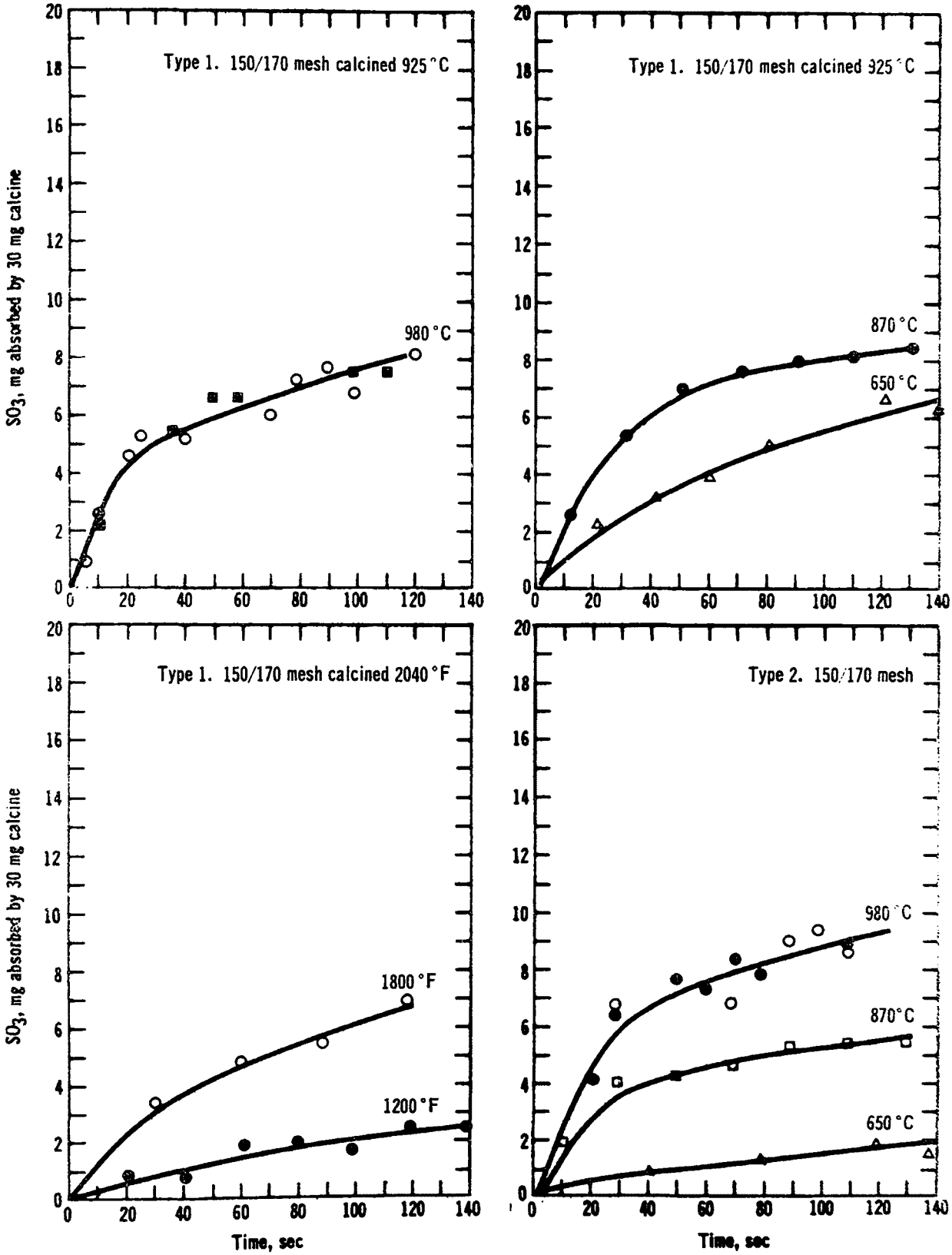
Type 1. 150/170 mesh calcined 925 °C
980 °C
Type 1. 150/170 mesh calcined 925 °C
870 °C
650 °C
Type 1. 150/170 mesh calcined 2040 °F
1800 °F
1200 °F
Type 2. 150/170 mesh
980 °C
870 °C
650 °C
SO3, mg absorbed by 30 mg calcine
Time, sec

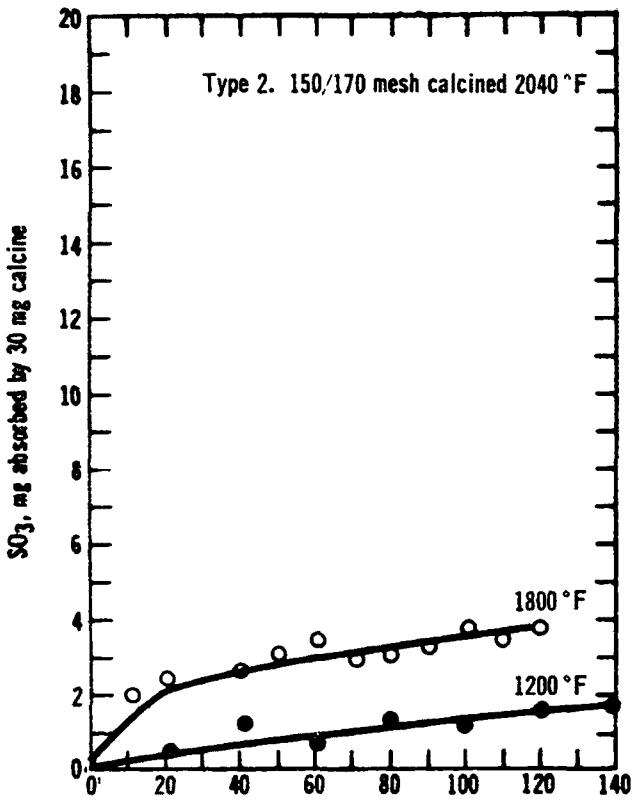
Type 2. 150/170 mesh calcined 2040 °F
1800 °F
1200 °F
SO_3, mg absorbed by 30 mg calcine

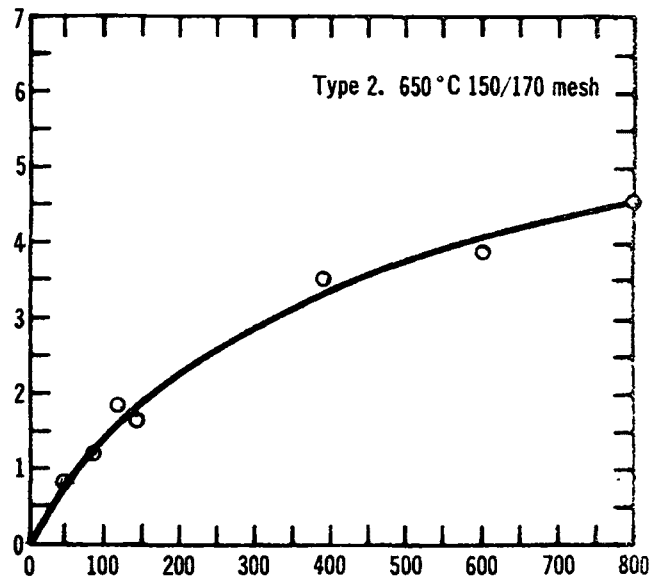
Type 2. 650 °C 150/170 mesh

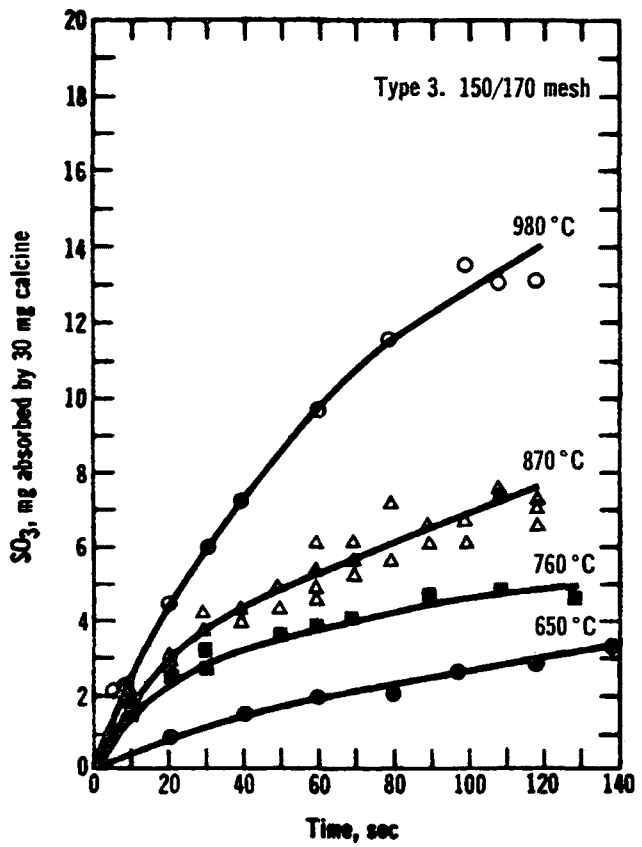
Type 3. 150/170 mesh
980 °C
870 °C
760 °C
650 °C
SO_3, mg absorbed by 30 mg calcine
Time, sec

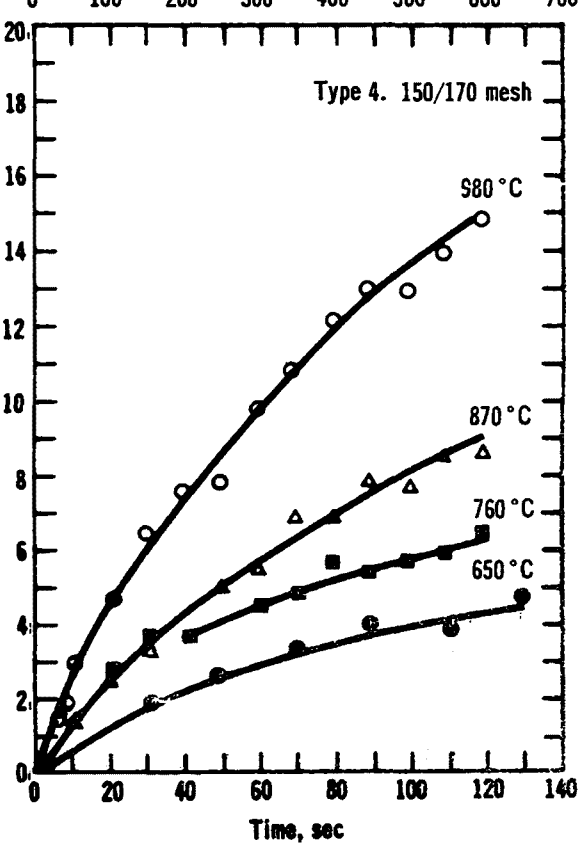
Type 4. 150/170 mesh
980 °C
870 °C
760 °C
650 °C
Time, sec

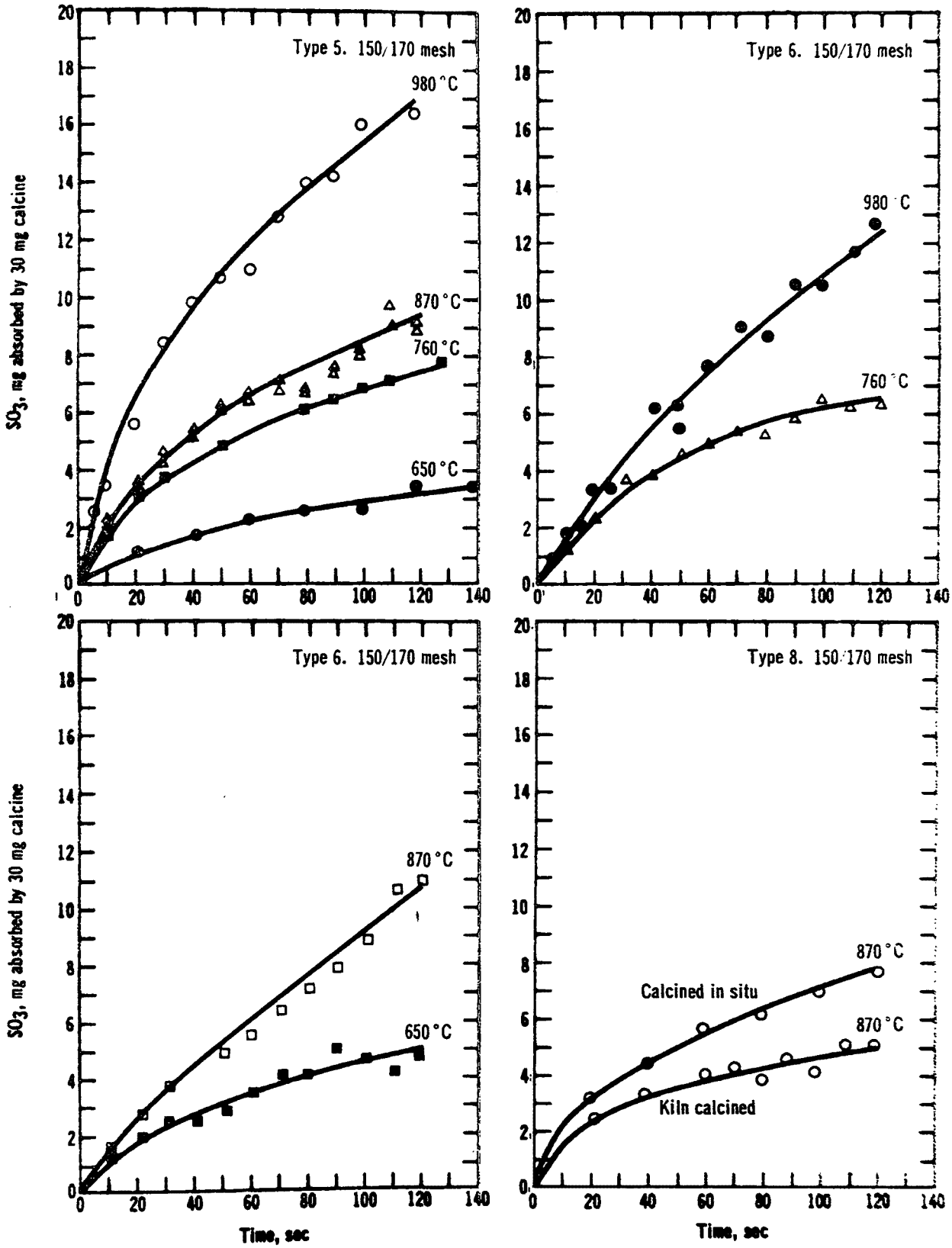
Type 5. 150/170 mesh
980 °C
870 °C
760 °C
650 °C
Type 6. 150/170 mesh
980 °C
760 °C
Type 6. 150/170 mesh
870 °C
650 °C
Type 8. 150/170 mesh
870 °C
Calcined in situ
870 °C
Kiln calcined
SO3, mg absorbed by 30 mg calcine
Time, sec

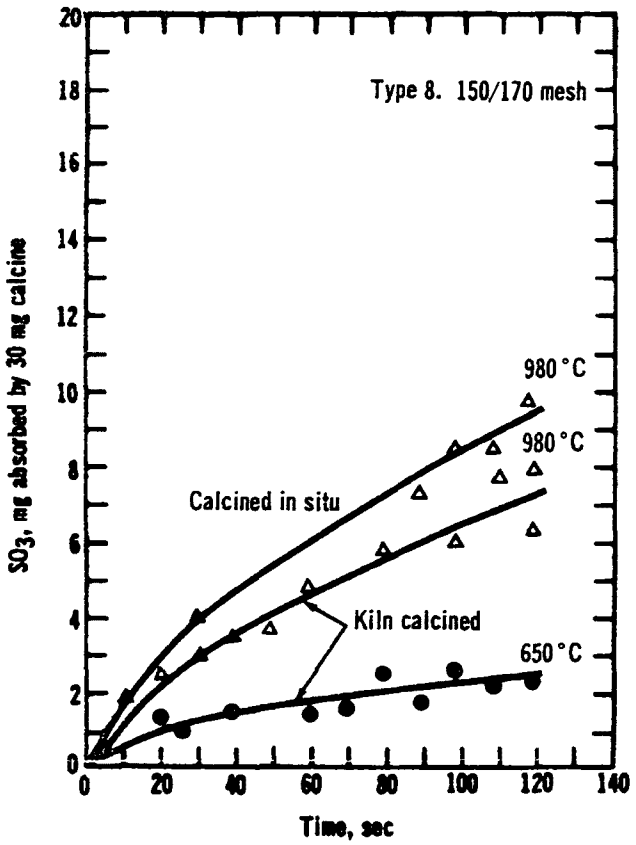
Type 8. 150/170 mesh
980 °C
980 °C
Calcined in situ
Kiln calcined
650 °C
SO_3, mg absorbed by 30 mg calcine
Time, sec

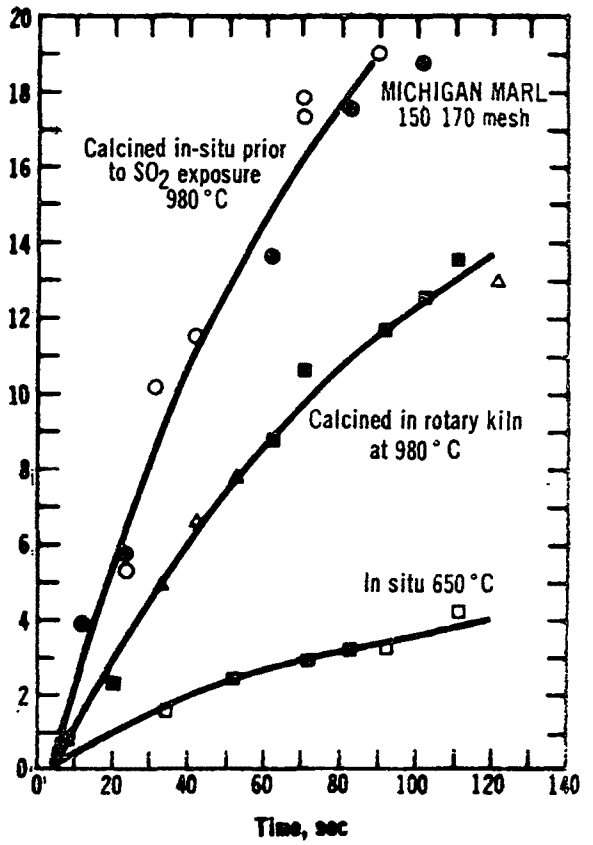
MICHIGAN MARL
150 170 mesh
Calcined in-situ prior to SO_2 exposure 980 °C
Calcined in rotary kiln at 980 ° C
In situ 650 °C
Time, sec

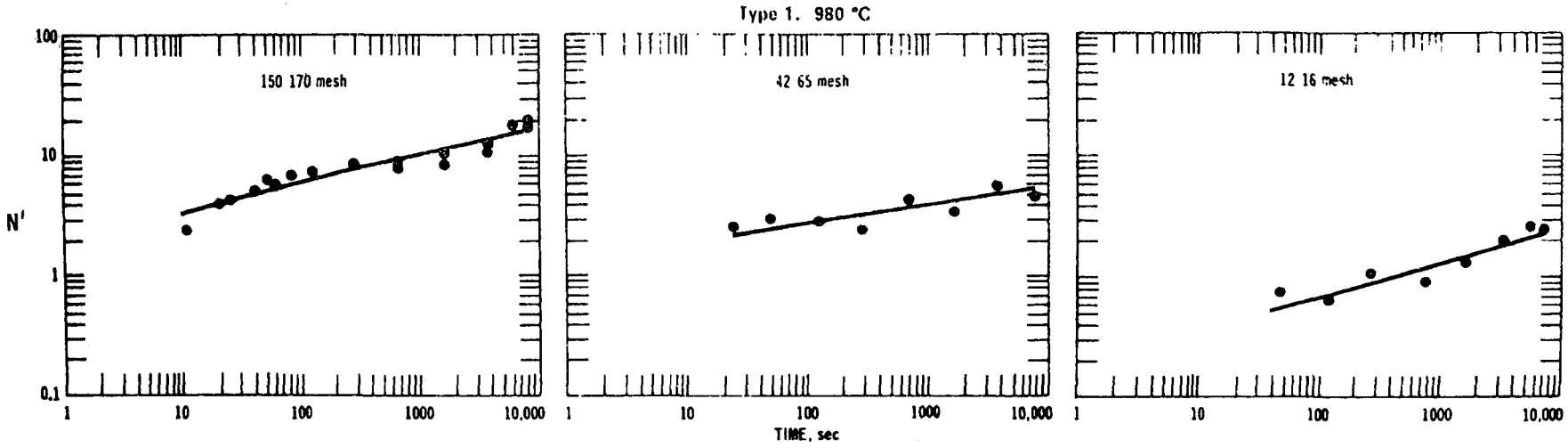

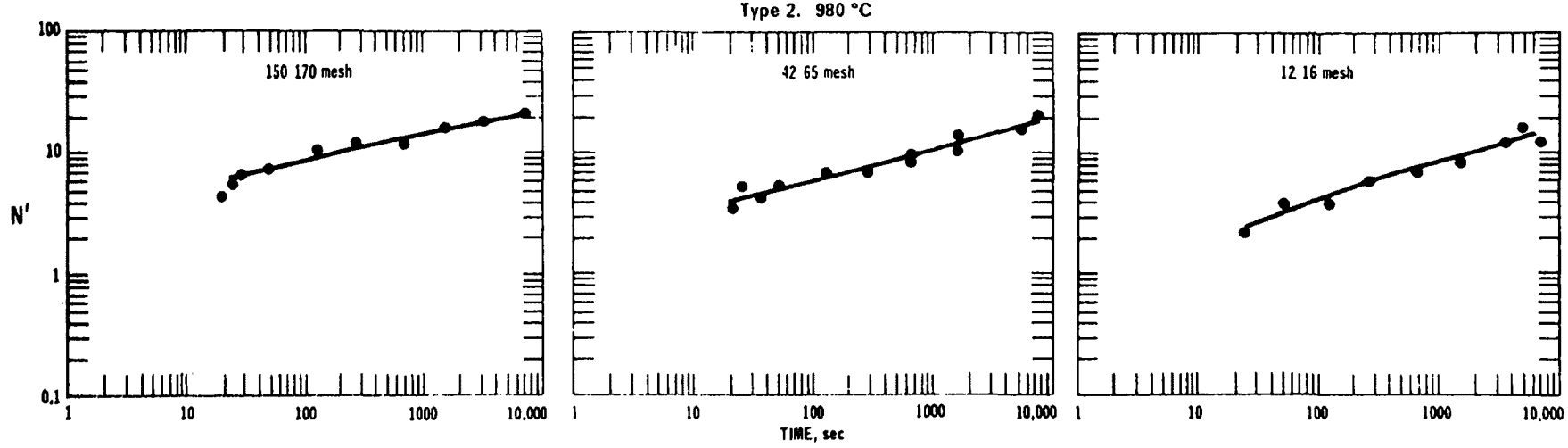

N' = mg. SO_3 absorbed by 30 mg. calcine

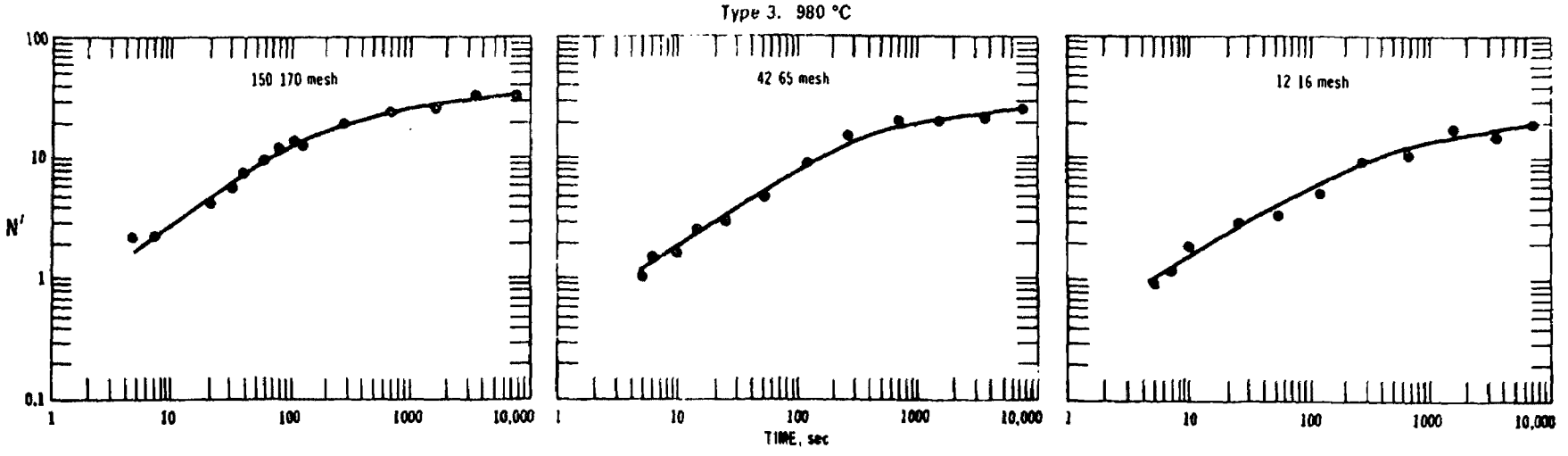

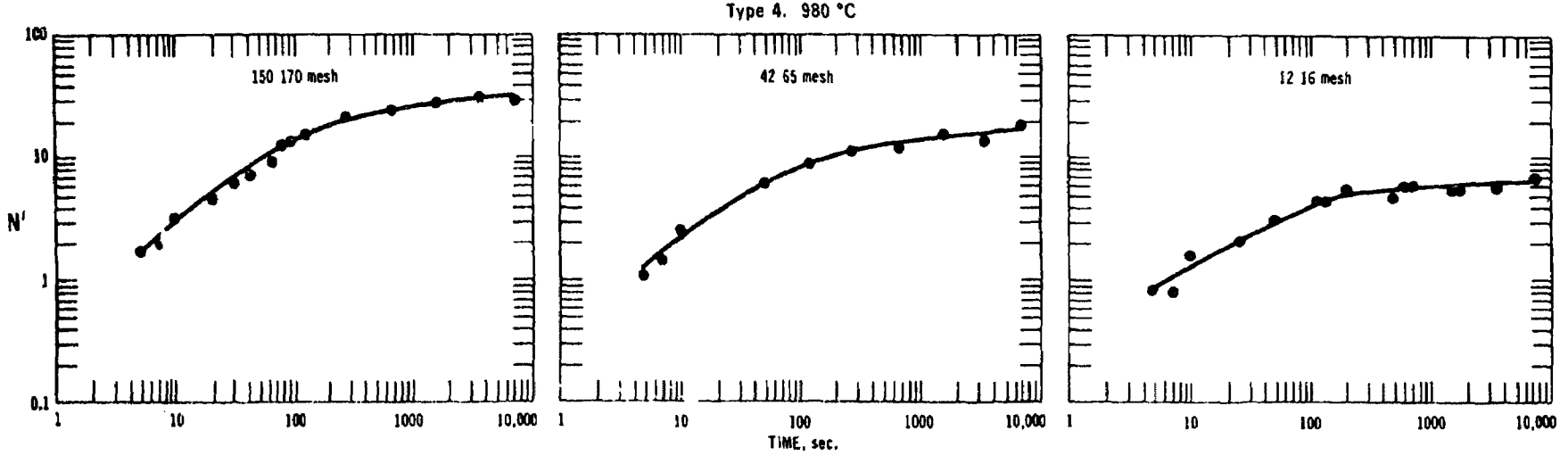

N' = mg. SO_3 absorbed by 30 mg. calcine

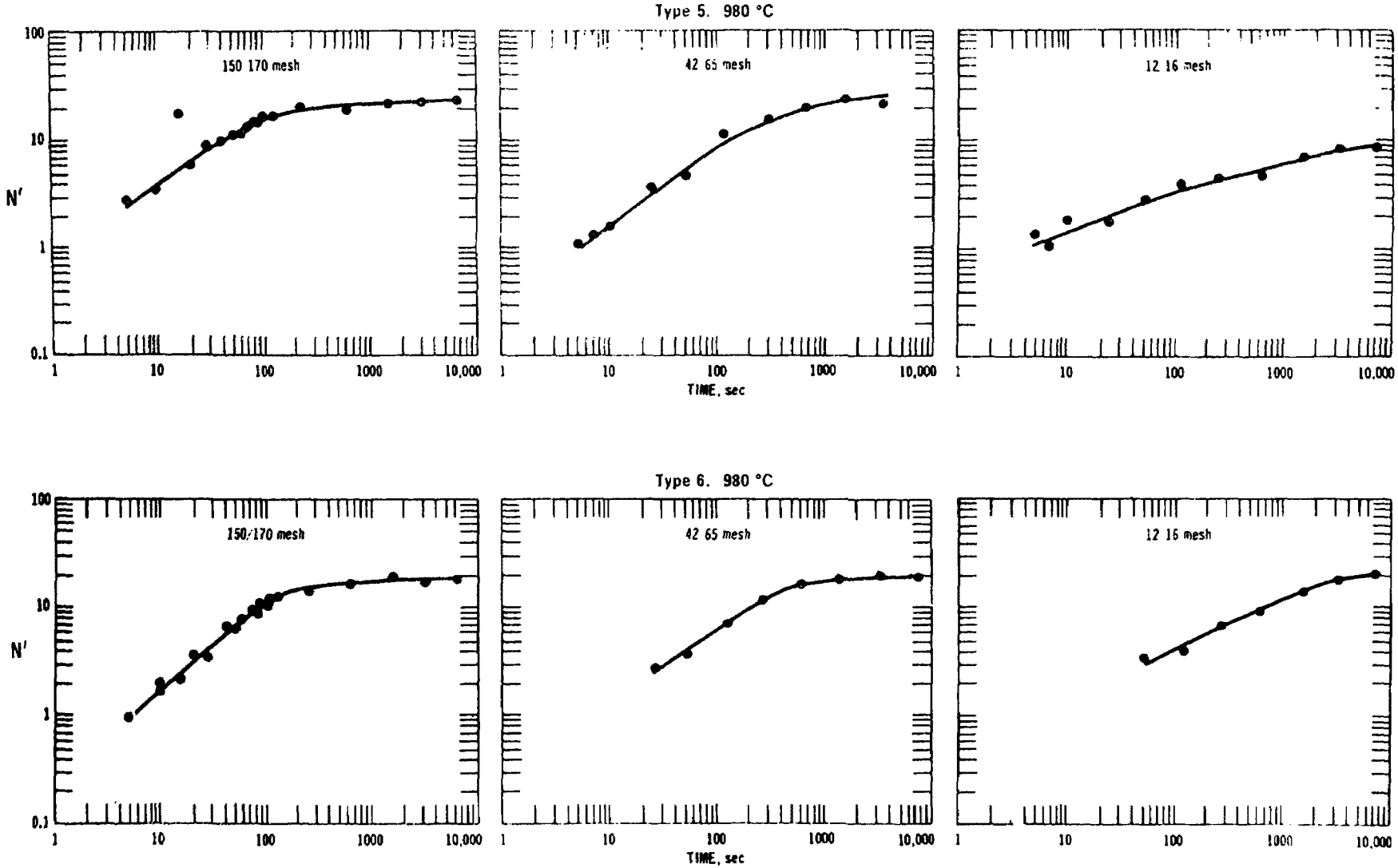

N' = mg. SO_3 absorbed by 30 mg. calcine

Type 8. 980 °C

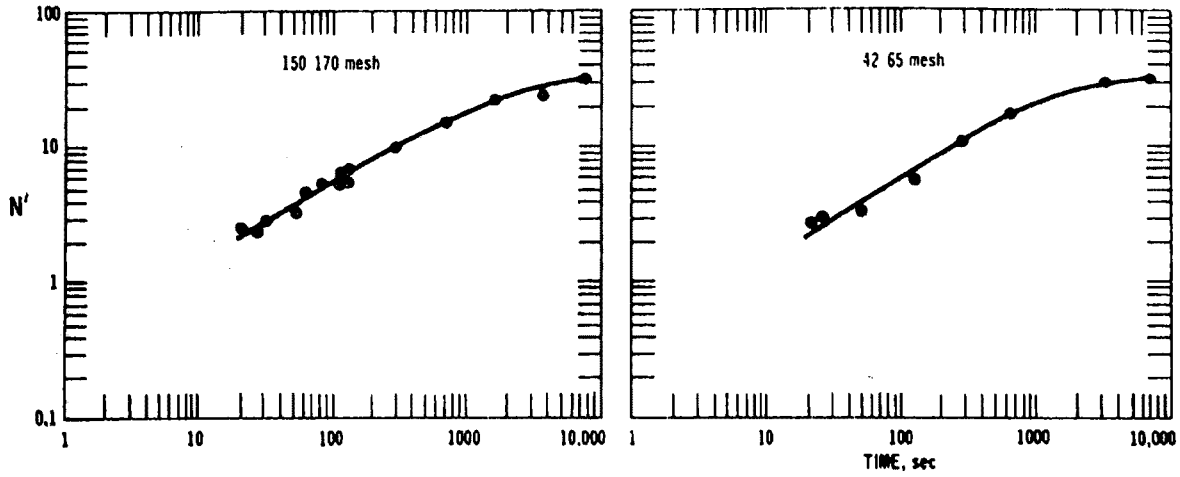

MICHIGAN MARL 980 °C

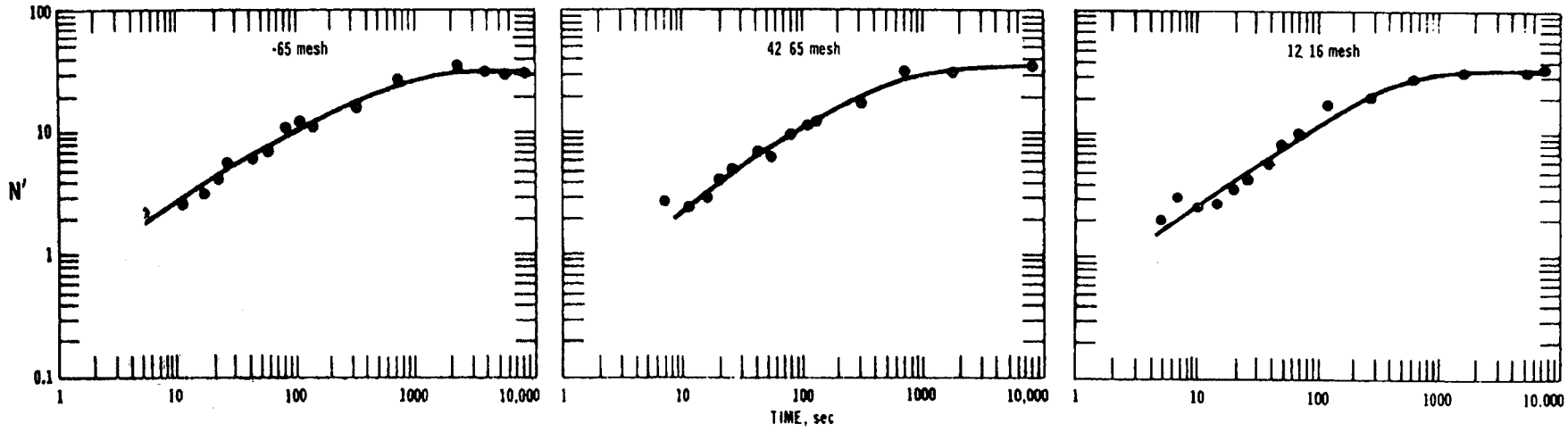

N' = mg. SO_3 absorbed by 30 mg. calcine

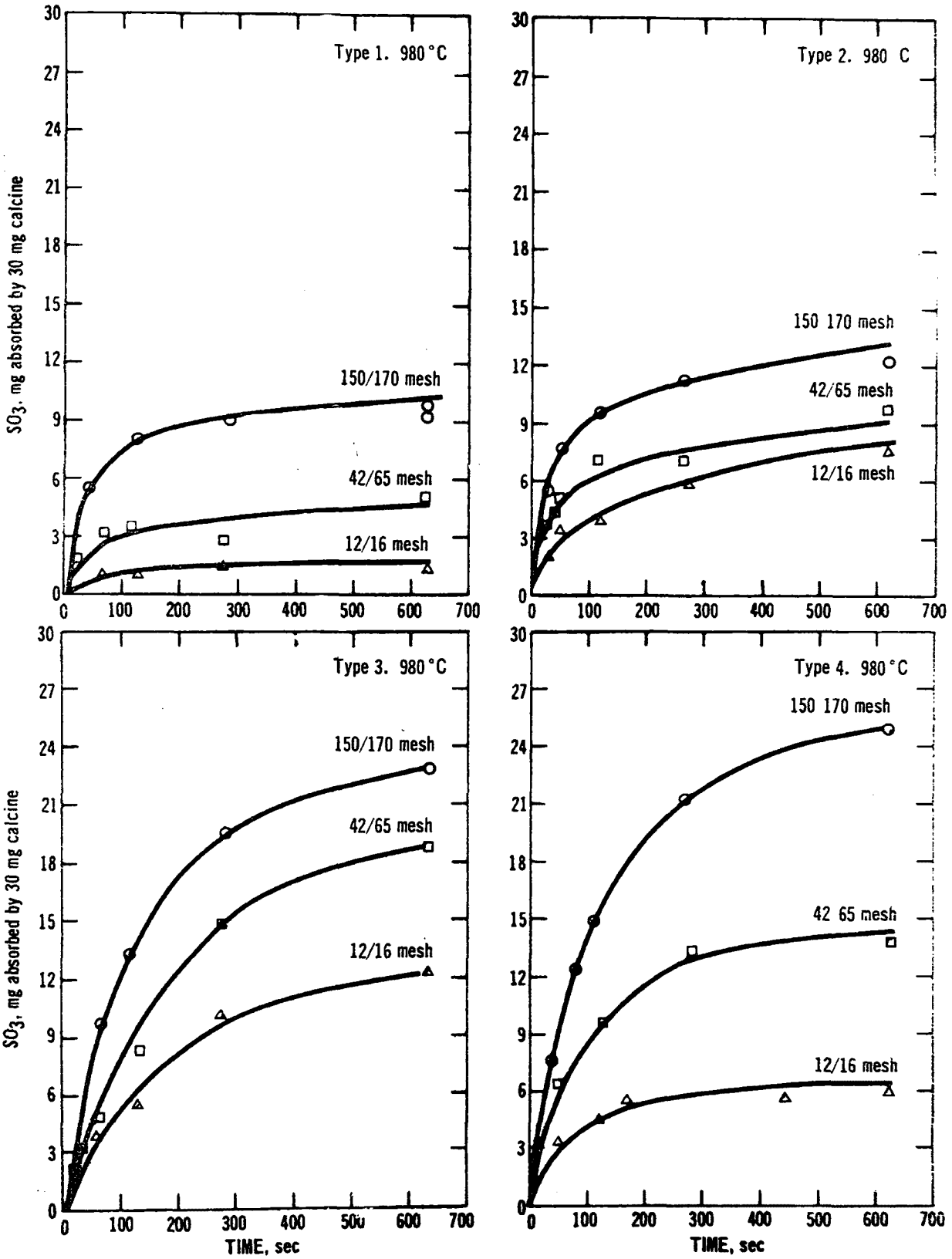
Type 1. 980 °C
150/170 mesh
42/65 mesh
12/16 mesh
Type 2. 980 C
150 170 mesh
42/65 mesh
12/16 mesh
Type 3. 980 °C
150/170 mesh
42/65 mesh
12/16 mesh
Type 4. 980 °C
150 170 mesh
42 65 mesh
12/16 mesh
SO3, mg absorbed by 30 mg calcine
TIME, sec

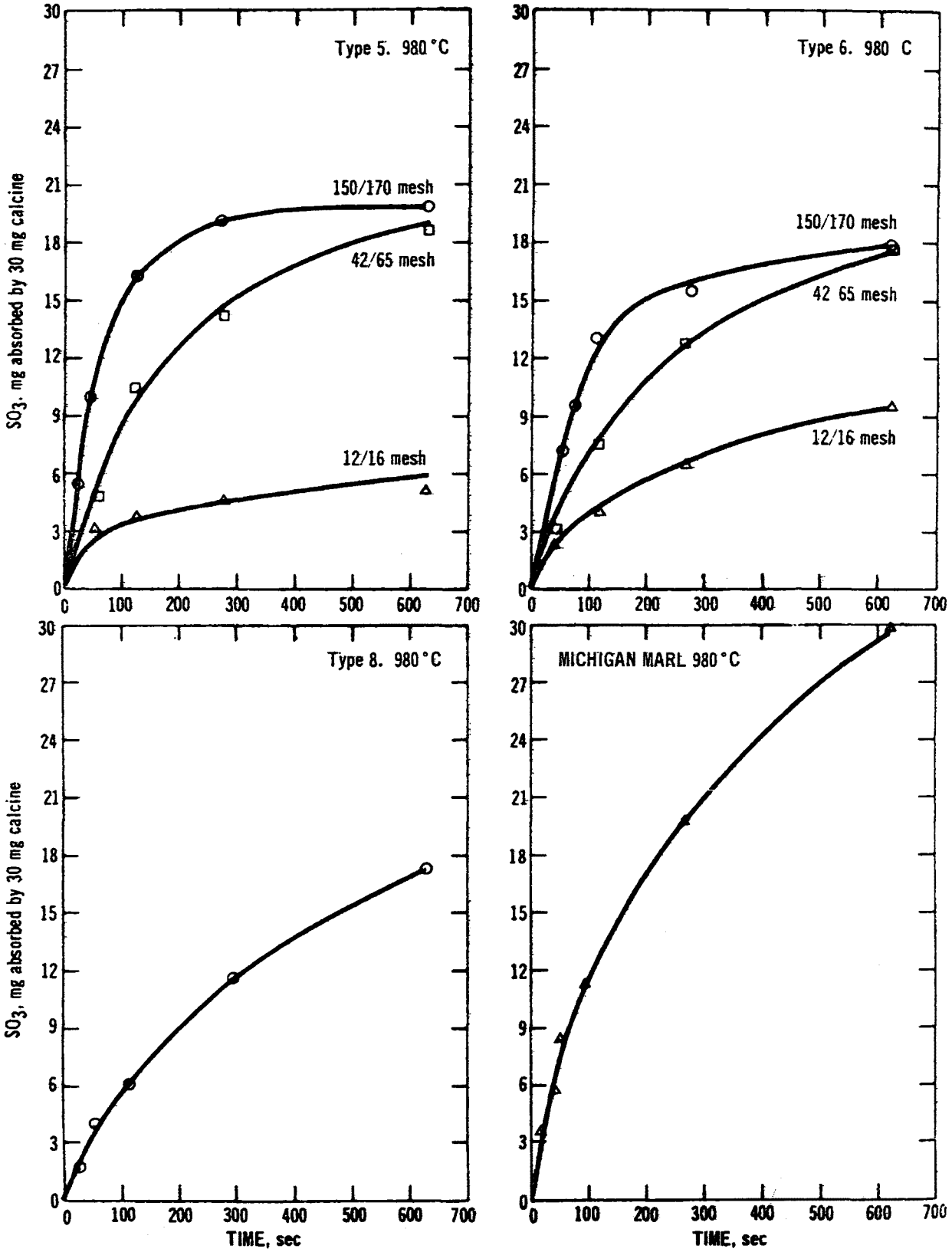
Type 5. 980 °C
150/170 mesh
42/65 mesh
12/16 mesh
Type 6. 980 C
150/170 mesh
42 65 mesh
12/16 mesh
Type 8. 980 °C
MICHIGAN MARL 980 °C
SO3, mg absorbed by 30 mg calcine
TIME, sec

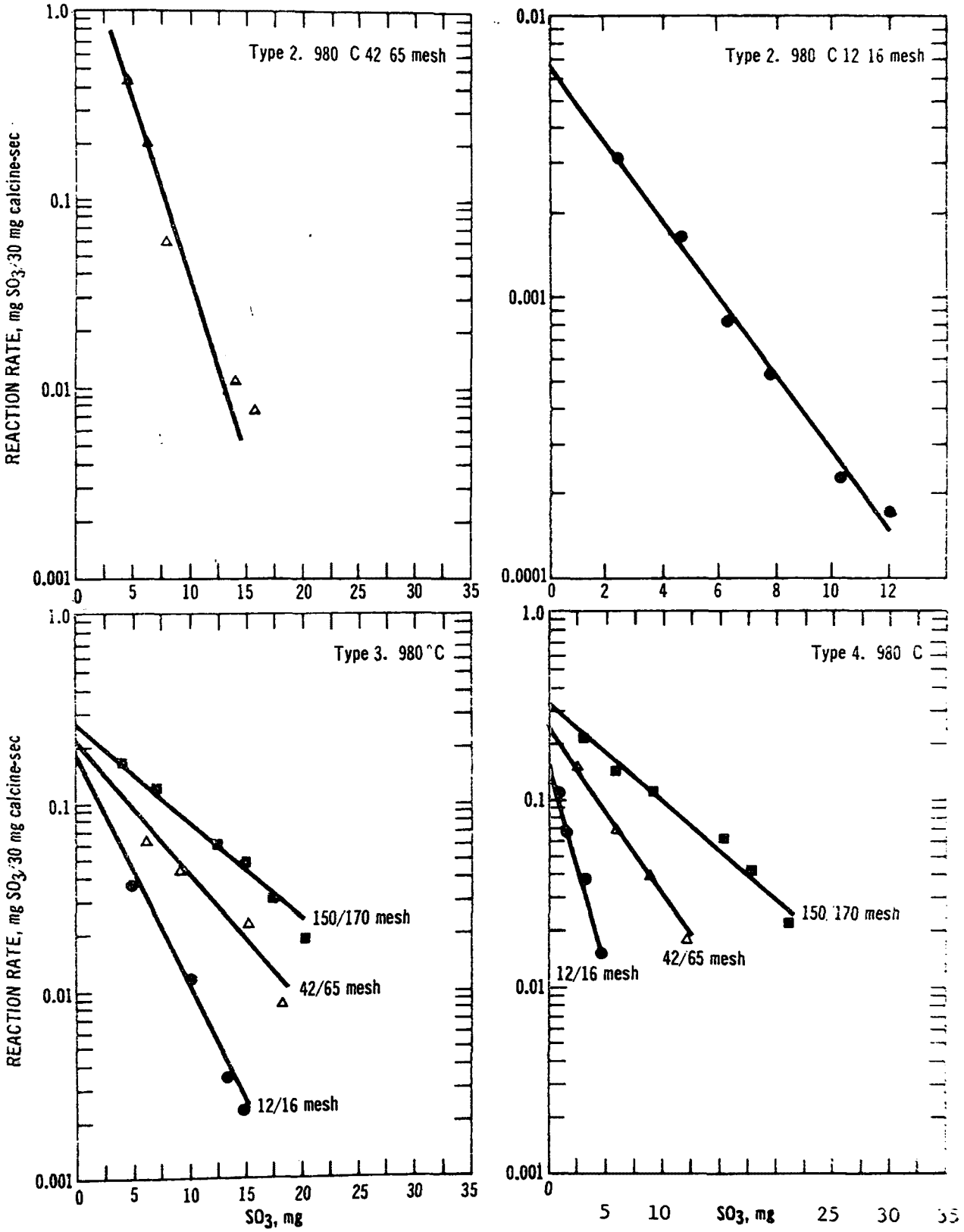
Type 2. 980 C 42 65 mesh
Type 2. 980 C 12 16 mesh
Type 3. 980 °C
Type 4. 980 C
150/170 mesh
42/65 mesh
12/16 mesh
REACTION RATE, mg SO3/30 mg calcine-sec
SO3, mg

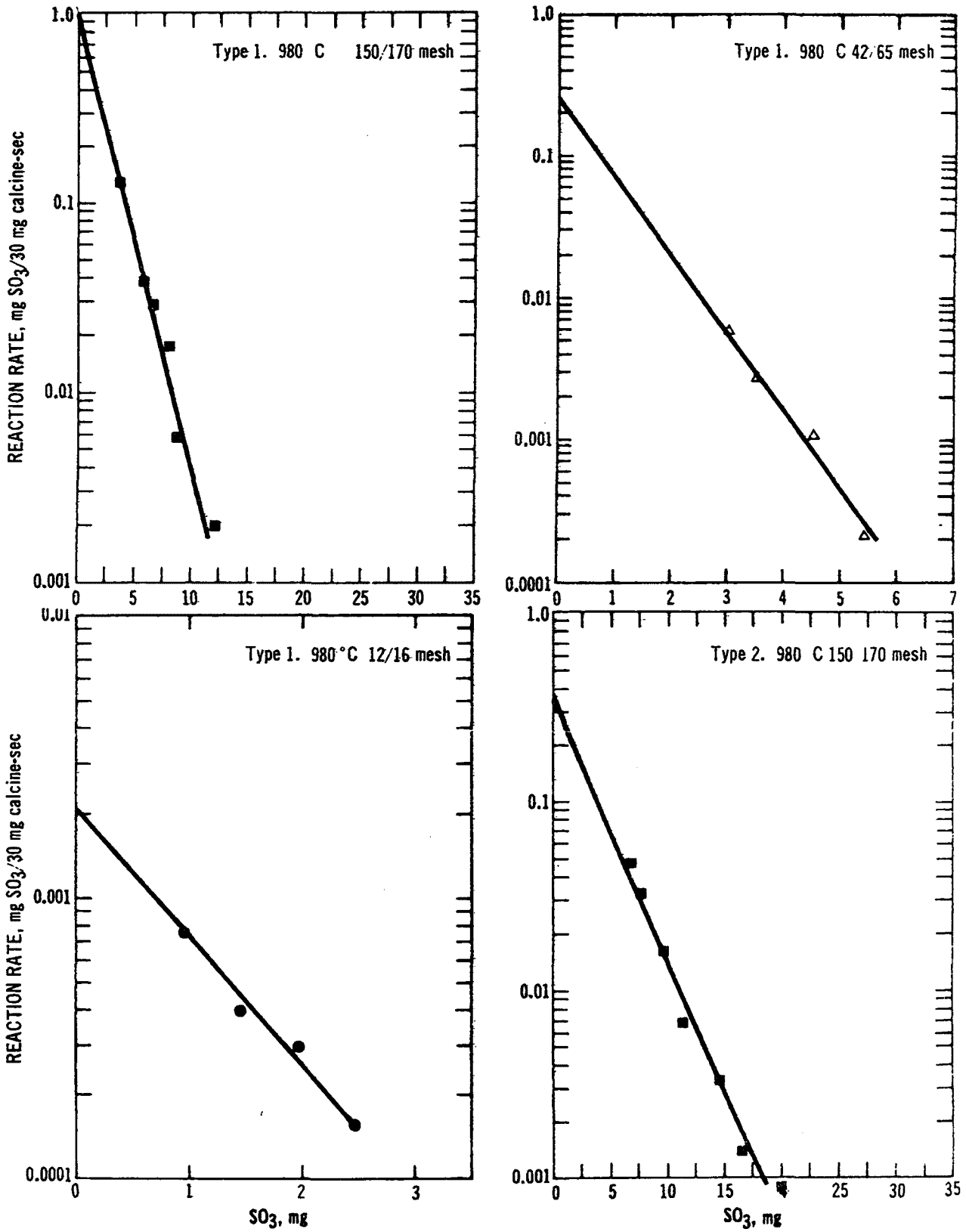
Type 1. 980 C 150/170 mesh
Type 1. 980 C 42/65 mesh
Type 1. 980 °C 12/16 mesh
Type 2. 980 C 150 170 mesh
REACTION RATE, mg SO3/30 mg calcine-sec
SO3, mg

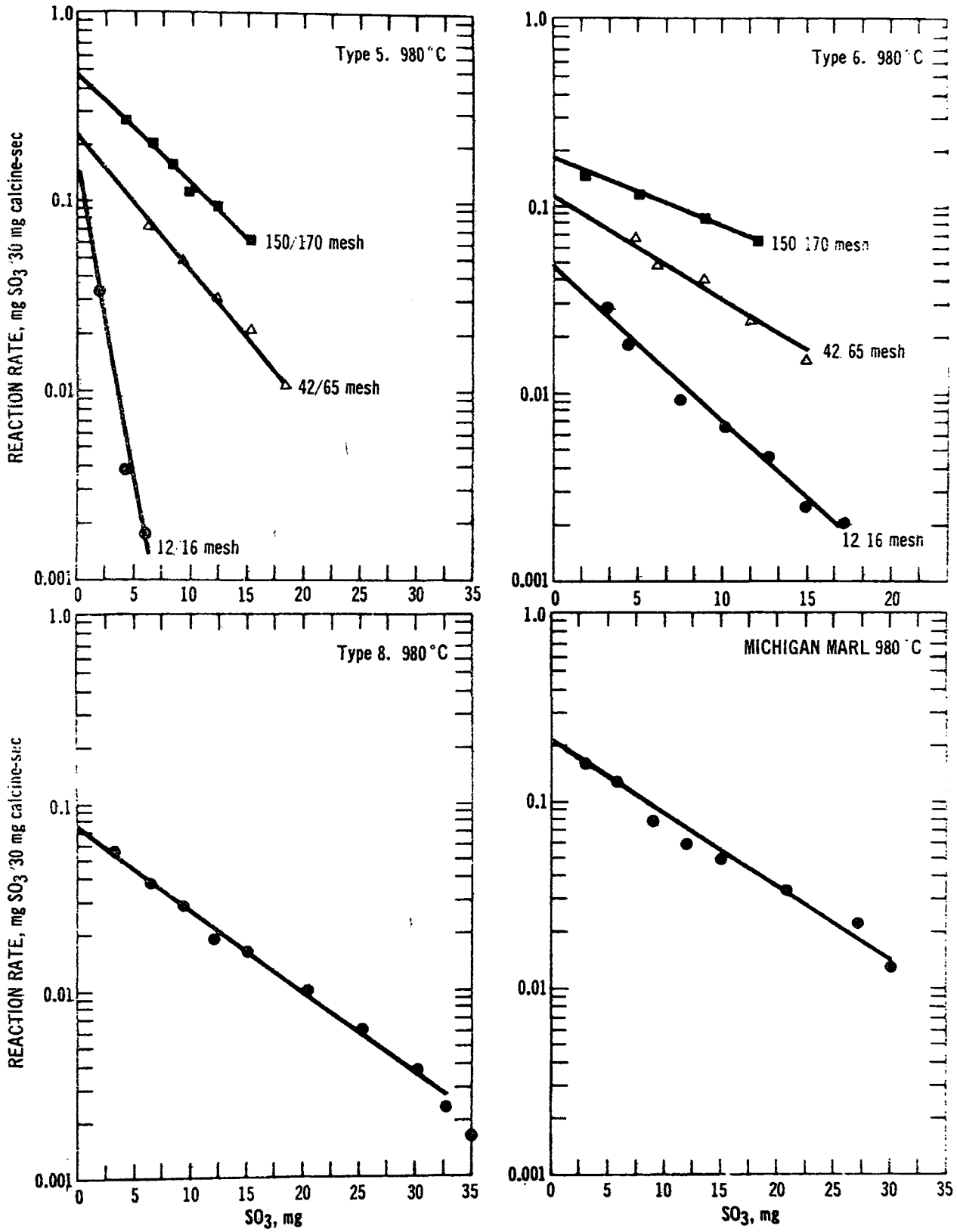
Type 5. 980°C
150/170 mesh
42/65 mesh
12/16 mesh
Type 6. 980°C
150/170 mesh
42/65 mesh
12/16 mesh
Type 8. 980°C
MICHIGAN MARL 980°C
REACTION RATE, mg SO3/30 mg calcine-sec
SO3, mg
1.0
0.1
0.01
0.001
0
5
10
15
20
25
30
35

APPENDIX B

B1. PROCEDURE FOR EXPERIMENTAL DETERMINATION OR COMPUTATION OF REPORTED DATA

1. Flue Gas Absorption - Method of R. H. Borgwardt[14]

   a. Thirty milligrams of screened material are placed on a rock wool mat and into a differential reactor.

   b. Exposure is for 120 seconds at 1800°F.

   c. Recovered sample is analyzed for sulfate and results are reported as $MgSO_3$/30 mg.

2. Pure SO_2 Absorption

   a. One gram of screened material is put in a combustion boat and into a horizontal tube furnace with quartz combustion tube. (See Figure B1-1).

   b. Exposure is for 30 minutes at 1800°F with a gas flow of 2 SCFH. The sample is in a complete atmosphere of SO_2.

   c. Results are reported as per cent weight gain.

3. Pure CO_2 Absorption

   a. One gram of screened material is put in a combustion boat and into a horizontal tube furnace with alumina combustion tube.

   b. Exposure is for 60 minutes at 1400°F with a gas flow of 2 SCFH. The sample is in a complete atmosphere of CO_2.

   c. Results are reported as per cent weight gain.

4. Steam Absorption

   a. One gram of screened material is put in a combustion boat and into a horizontal tube furnace.

   b. Steam from a steam generator is fed to a preheat coil and into the stainless steel combustion tube.

   c. Exposure is for 5 minutes at 500°C with results reported as per cent weight gain.

5. Acid Titration

   a. One gram of screened material is put in a 400 ml beaker and pH probes positioned in place.

   b. At time zero, 200 ml of distilled water is added with vigorous agitation.

   c. Titrations to pH 8 at minute intervals with 1N HCl give results of cumulative acid versus time.

6. B.E.T. Surface Area - as reported by AMINCO.

7. Total Pore Volume - as reported by AMINCO.

8. Small Pore Volume - using the mercury penetration porosimetry curve, volume of pores with diameter less than 2 microns is calculated.

9. Mercury Intrusion Density - as reported by AMINCO.

10. Average IR Band Shift - as reported by GTC[20]; using infrared analysis of samples prepared by the KBr pellet technique, the average shift of three bands is calculated.

11. Median Pore Diameter - using the mercury penetration porosimetry curve, the diameter corresponding to intrusion of 50% of the total volume is reported.

12. Air Pycnometer Density - standard technique.

13. Oil Absorption Density - No. 2 fuel oil is displaced in a graduated cylinder.

14. Hydration-Weight Gain

   a. One gram of material is slaked with one milliliter of distilled water for one hour.

   b. The sample is dried for one hour at 260°C.

   c. The percent weight gain is reported.

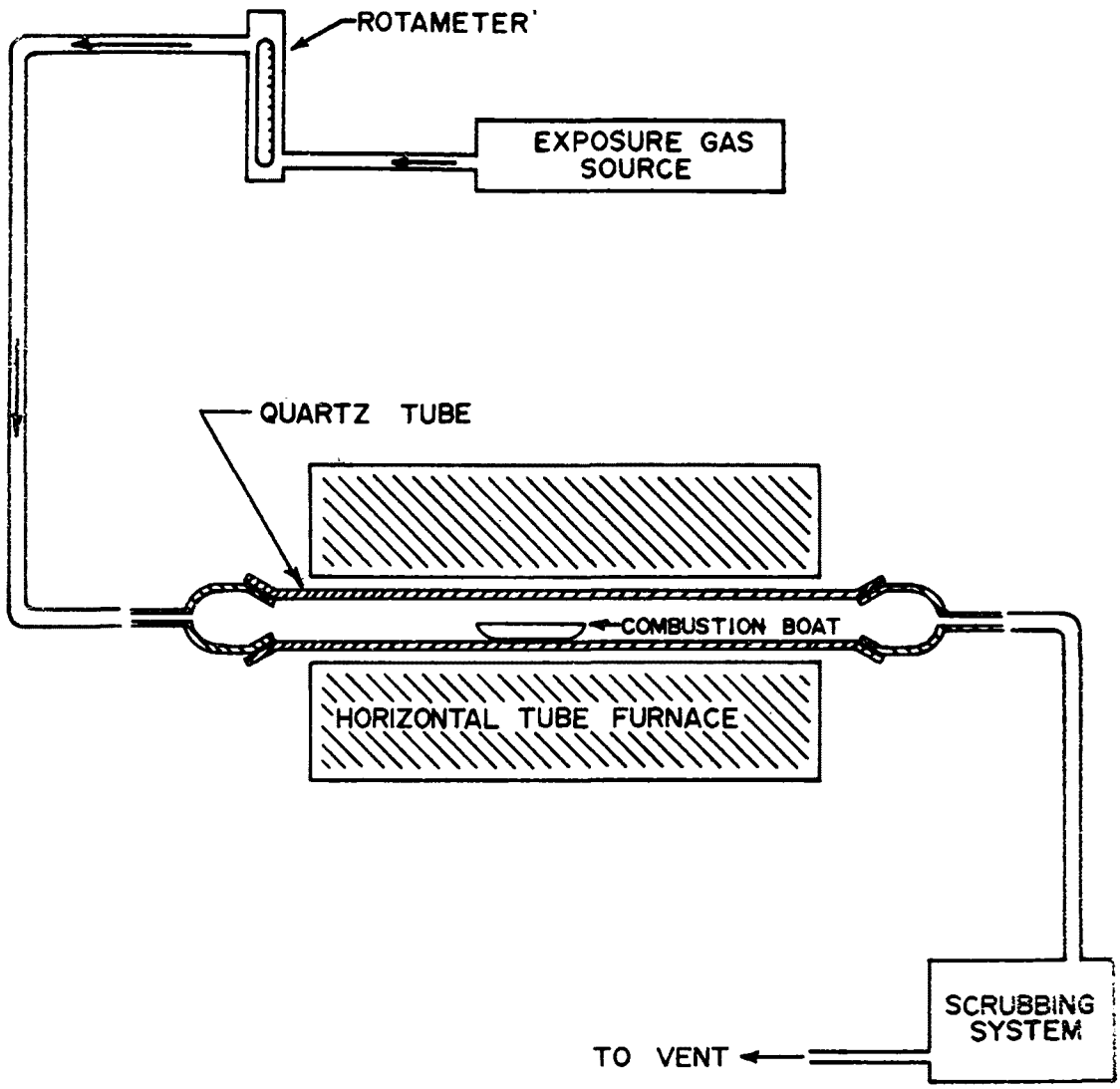

Figure B1-1

COMBUSTION BOAT TEST APPARATUS

B2. SOME STATISTICAL ANALYSES OF "LIMESTONE DEAD-BURNING" DATA

I. SUMMARY

1. Data

As given in Tables B2-1 and B2-2 the data are in two batches on limestones from three sources. A measurement was taken for each source at five preset calcination temperatures. The measurements for Batch II (B2) have eight components besides temperature, and these eight will be termed the "basic set" of variables. The measurements for Batch I (B1) have five additional components. This set of thirteen variables will be called the "extended set" of variables.

2. Purpose

The amount of SO_2 absorbed from the flue gas is a decreasing function of temperature in the range of temperatures for this study. Obviously, a number of other components are also highly correlated to the flue gas measurement and hence they are all controlled by temperature. The purpose of this investigation generally was to search for other, not so obvious, relationships among the variables which may shed light on the dead-burning effect.

TABLE B2-1a

Properties of Fredonia White
Set I, 70/140 mesh

	Calcine Temperature				
	1700	2000	2300	2600	3200
Flue Gas Absorption 1800°F, 2 min, mg/30 mg	8.6	5.9	2.5	1.6	1.0
Pure SO_2 Absorption* 1800°F, 30 min, % gain	66.0	40.7	21.9	10.4	8.0
Pure CO_2 Absorption* 1400°F, 60 min, % gain	37.4	8.7	5.8	2.6	1.7
Steam Absorption 500°C, 5 min, % gain	29.7	22.5	12.5	10.8	7.2
B.E.T. Surface Area m^2/g	3.1	1.6	1.0	0.8	0.3
Total Pore Volume cc/g	.61	.51	.33	.25	.33
Small Pore Volume cc/g	.28	.14	.09	.04	.04
Density by Mercury Intrusion g/cc	2.82	2.44	3.23	3.34	3.30
Average IR Band Shift, %	0	62	80	95	100

* Note: Listed values for 140/200 mesh

TABLE B2-1b: Properties of Cedar Bluff
Set I, 70/140 mesh

	Calcine Temperature				
	1700	2000	2300	2600	3200
Flue Gas Absorption 1800°F, 2 min, mg/30 mg	6.70	3.76	3.81	2.60	2.51
Pure SO_2 Absorption* 1800°F, 30 min, % gain	62.2	27.3	26.7	18.8	13.2
Pure CO_2 Absorption* 1400°F, 60 min, % gain	25.8	8.7	6.6	5.6	3.6
Steam Absorption 500°C, 5 min, % gain	26.6	17.0	15.5	12.3	10.2
B.E.T. Surface Area m^2/g	1.9	1.2	0.9	0.8	0.5
Total Pore Volume cc/g	.70	.37	.49	.49	.37
Small Pore Volume cc/g	.28	.10	.08	.05	.02
Density by Mercury Intrusion, g/cc	2.81	2.95	3.32	3.30	3.19
Average IR Band Shift, %	0	25	44	67	100

*Note: Listed values for 140/200 mesh

TABLE B2-1c: Properties of James River
Set I, 70/140 mesh

	Calcine Temperature				
	1700	2000	2300	2600	3200
Flue Gas Absorption 1800°F, 2 min, mg/30 mg	9.56	9.04	6.60	2.28	1.80
Pure SO_2 Absorption* 1800°F, 30 min, % gain	67.4	62.1	46.2	13.2	7.6
Pure CO_2 Absorption* 1400°F, 60 min, % gain	22.6	12.6	8.3	2.0	1.5
Steam Absorption 500°C, 5 min, % gain	16.8	13.7	10.1	4.6	2.8
B.E.T. Surface Area m^2/g	4.1	2.2	1.5	—	—
Total Pore Volume cc/g	.69	.66	.55	.46	.37
Small Pore Volume cc/g	.35	.31	.21	.01	.01
Density by Mercury Intrusion, g/cc	2.84	2.74	3.39	3.44	3.31
Average IR Band Shift, %	0	26	57	83	100

*Note: Listed values for 140/200 mesh

TABLE B2-2a: Properties of Fredonia White
Set II, 170/270 mesh

	Calcine Temperature				
	1700	2000	2300	2600	3200
Flue Gas Absorption 1800°F, 2 min, mg SO_3/30 mg	7.04	3.52	2.48	2.08	1.92
Flue Gas Absorption 1800°F, 2 hrs, mg SO_3/30 mg	34.3	22.6	13.7	11.2	5.6
Pure SO_2 Absorption 1800°F, 30 min, % gain	90.0	16.8	10.1	6.0	3.2
Pure CO_2 Absorption 1400°F, 60 min, % gain	54.0	9.8	2.5	3.9	0.7
B.E.T. Surface Area m^2/g	2.2	1.1	0.9	1.3	0.7
Total Pore Volume cc/g	.77	.37	.30	.31	.22
Small Pore Volume cc/g	.31	.07	.05	.08	.02
Density by Mercury Intrusion g/cc	3.47	2.91	3.11	2.92	3.09
Extent of Slaking 1 ml, 1 hour, % gain	33.6	28.1	23.1	20.2	11.7

TABLE B2-2b: Properties of Cedar Bluff
Set II, 170/270 mesh

	Calcine Temperature				
	1700	2000	2300	2600	3200
Flue Gas Absorption 1800°F, 2 min, mg/30 mg	4.72	6.04	3.88	3.36	2.64
Pure SO_2 Abosrption 1800°F, 30 min, % gain	31.0	39.4	25.5	21.5	9.8
Pure CO_2 Absorption 1400°F, 30 min, % gain	11.0	6.7	5.4	6.0	2.9
B.E.T. Surface Area m^2/g	1.4	1.2	0.9	1.1	0.5
Total Pore Volume cc/g	.59	.48	.36	.34	.33
Small Pore Volume cc/g	.09	.05	.05	.06	.02
Density by Mercury Intrusion, g/cc	3.27	3.15	3.17	3.16	3.21
Extent of Slaking 1 ml, 1 hour, % gain	32.1	30.4	26.9	27.0	10.4

TABLE B2-2c: Properties of James River
Set II, 120/270 mesh

	Calcine Temperature				
	1700	2000	2300	2600	3200
Flue Gas Absorption 1800°F, 2 min, mg/30 mg	8.92	4.92	4.72	2.92	1.80
Pure SO_2 Absorption 1800°F, 30 min, % gain	69.9	49.4	34.4	10.3	8.0
Pure CO_2 Absorption 1400°F, 30 min, % gain	12.5	6.7	4.3	2.8	1.7
B.E.T. Surface Area m^2/g	2.4	1.3	1.0	1.0	0.7
Total Pore Volume cc/g	.62	.37	.37	.35	.26
Small Pore Volume cc/g	.30	.15	.11	.07	.05
Density by Mercury Intrusion, g/cc	3.09	3.16	3.16	3.25	3.24
Extent of Slaking 1 ml, 1 hour, % gain	17.3	10.4	13.2	2.6	5.2

3. Analyses

Two computational methods of inspecting the data were tried: 1) principal components, and 2) regression with the flue gas measurement as the dependent variable.

II. GRAPHS AND CORRELATIONS

Correlation coefficient matrices are given for the measurements in B1 and B2 on the computer printout as marked by the tabs. The most notable difference between B1 and B2 is that mercury intrusion density (MERDEN) in B1 is negatively correlated with the temperature related variables whereas in B2 it is positively correlated. An inspection of the graphs of MERDEN vs. temperature indicated this pictorially. The B2 measurement from source 1, Fredonia, at 2000°F is a major contributor, but even without it the slope would be negative.

Some anomalies are evident in the ACID measurement, B1, where the three high temperature measurements for source 3, James River, are much lower than the others.

III. PRINCIPAL COMPONENTS

Temperature is a controlled variable, and variables in both the basic set and the additional set are dependent upon temperature,

hence correlational techniques such as principal components analyses must be used and interpreted with appropriate caution. The magnitude of any "correlation" cited in this report is not meaningful itself, since its size is controlled by the selection of temperatures, but it may be meaningful relative to another such correlation from other variables, batches, etc.

For this situation we expect one large temperature component with heavy loadings on those variables most related to temperature. The size of this component is not of itself meaningful for reasons mentioned above. The second and higher components, since they are orthogonal to this first major temperature component, hopefully will exhibit factors perhaps not controlled by temperature and yield useful information on the variable relationships.

1. Batch I, Basic Set of Variables

In the computer printouts as marked by tabs are the results of the principal components computation on the B1 data for the basic set of variables. The first component accounts for 86% of the total variation and all variables are weighted more or less equally with MERDEN, here coded as (MIDEN), and median pore diameter (MDPDIA). MDPDIA have negative weights as expected because of their negative correlation with the other variables. An inspection of case ranking by that component in Table B2-3 shows this to be a good, but not perfect temperature component.

Table B2-3

Batch No. I

Variables: 8 BASIC SET

Component No. 1

Rank	Source			Temperature				
	1	2	3	17	20	23	26	32
1			x	x				
2	x			x				
3			x		x			
4		x		x				
5	x				x			
6			x			x		
7		x			x			
8		x				x		
9	x					x		
10		x					x	
11		x						x
12			x				x	
13	x						x	
14			x					x
15	x							x

Component No. 2

Rank	Source			Temperature				
	1	2	3	17	20	23	26	32
1	x				x			
2		x			x			
3		x						x
4			x		x			
5	x						x	
6	x							x
7	x					x		
8			x					x
9		x		x				
10	x			x				
11			x	x				
12		x					x	
13		x				x		
14			x				x	
15			x			x		

Component No. 3

Rank	Source			Temperature				
	1	2	3	17	20	23	26	32
1	x			x				
2	x						x	
3	x					x		
4		x			x			
5	x							x
6			x	x				
7		x						x
8		x		x				
9			x					x
10		x					x	
11		x				x		
12			x				x	
13			x			x		
14	x				x			
15			x		x			

Component No. 4

Rank	Source			Temperature				
	1	2	3	17	20	23	26	32
1		x		x				
2	x			x				
3			x				x	
4		x					x	
5			x					x
6		x				x		
7	x				x			
8		x						x
9	x							x
10		x			x			
11			x		x			
12	x					x		
13			x			x		
14	x						x	
15			x	x				

The second component shows heavy weight, (-), for MERDEN with some weight, (-), for mercury pore volume (MERPVO). There is no clear linear relationship to temperature or source.

Component three is largely a source component with CO_2 and BET carrying positive weight and MERPVO a negative weight. It is doubtful whether the fourth component is meaningful.

2. Batch II, Basic Set of Variables

The first component for the B2 data is similar to that for the B1 data except that MERDEN enters with the same sign as the temperature related variables instead of the reversed sign as for B1. This is expected because of the change in sign of the correlation for MERDEN from B1 to B2. This component is a strong temperature component (Table B2-4). Note that the direction of the eigenvector is reversed from that of B1, hence temperatures are ordered from high to low.

The second component again has MERDEN as the major contributor but MERPVO is no longer important. Instead the MDPDIA seems to be the contributor in its place in both the 2nd and 3rd component. The third component is clearly the source component.

3. Batch I, Extended Set of Variables

The same computation was done on B1 with the extended set of variables less flue gas. The first component is a pretty good

Batch No. II

Variables: 8 BASIC SET

Component No. 1

Rank	Source			Temperature				
	1	2	3	17	20	23	26	32
1	x							x
2			x					x
3		x						x
4	x					x		
5	x						x	
6			x				x	
7	x				x			
8		x					x	
9		x				x		
10			x			x		
11		x			x			
12			x		x			
13		x		x				
14			x	x				
15	x			x				

Component No. 2

Rank	Source			Temperature				
	1	2	3	17	20	23	26	32
1			x	x				
2	x						x	
3	x				x			
4		x			x			
5			x		x			
6			x			x		
7		x					x	
8		x				x		
9	x					x		
10		x		x				
11			x				x	
12	x							x
13			x					x
14		x						x
15	x			x				

Component No. 3

Rank	Source			Temperature				
	1	2	3	17	20	23	26	32
1		x			x			
2		x				x		
3		x		x				
4		x					x	
5			x			x		
6			x				x	
7			x		x			
8		x						x
9			x					x
10	x				x			
11	x						x	
12	x					x		
13	x			x				
14			x	x				
15	x							x

Component No. 4

Rank	Source			Temperature				
	1	2	3	17	20	23	26	32
1			x	x				
2	x							x
3		x			x			
4			x		x			
5			x			x		
6		x						x
7			x					x
8			x				x	
9	x					x		
10		x		x				
11		x				x		
12		x					x	
13	x			x				
14	x				x			
15	x						x	

temperature component as it was for the basic set, but the additional variables change the later components. In Table B2-5 the strong source difference for ACID shows itself in component two where ACID has the heaviest weight and easily separates James River from Fredonia and Cedar Bluff. Notice the large gap in component values between case no. 1 and case no. 11. The generally low values for AIRPY for James River influence this also. OILAB in component three does for Cedar Bluff what ACID did for James River in component 2. MERDEN (MINT) here tries to influence the components as it did for the basic set, but the source effect on the additional variables dilutes its efforts.

4. Summary of Principal Components Analysis

The temperature component appeared as expected in the first component. Source, another controlled variable just as temperature, appeared strongly in the second or third component, and may have obscured some of the variable relationships. The one variable that does seem to operate somewhat independently of the temperature component is MERDEN. MERPVO does this also for B1, but not for B2 where MDPDIA appears in a similar role.

Table B2-3

Batch No. I

Variables: 12 EXTENDED SET

Component No. 1

Rank	Source			Temperature				
	1	2	3	17	20	23	26	32
1	x			x				
2			x	x				
3		x		x				
4			x		x			
5	x				x			
6			x			x		
7		x			x			
8		x				x		
9		x					x	
10	x					x		
11		x						x
12	x						x	
13	x							x
14			x				x	
15			x					x

Component No.

Rank	Source			Temperature				
	1	2	3	17	20	23	26	32
1		x			x			
2	x				x			
3		x				x		
4	x						x	
5	x					x		
6		x					x	
7		x						x
8	x							x
9		x		x				
10	x			x				
11			x	x				
12			x		x			
13			x				x	
14			x					x
15			x			x		

Component No. 3

Rank	Source			Temperature				
	1	2	3	17	20	23	26	32
1		x				x		
2		x		x				
3		x					x	
4		x						x
5		x			x			
6			x				x	
7			x			x		
8			x	x				
9	x							x
10			x					x
11	x						x	
12	x			x				
13	x					x		
14			x		x			
15	x				x			

Component No. 4

Rank	Source			Temperature				
	1	2	3	17	20	23	26	32
1			x				x	
2	x				x			
3			x		x			
4		x			x			
5		x				x		
6			x					x
7		x		x				
8		x					x	
9			x	x				
10			x			x		
11		x						x
12	x					x		
13	x							x
14	x						x	
15	x			x				

IV. REGRESSION

Linear least square regressions were run on each batch with flue gas as the dependent variable. Only constant and first degree terms were used in the model. Batch I was analyzed first using the basic set of variables (seven independent), and then using the extended set (eleven independent). The stepwise regression program in the UCLA Biomedical Series, BMD02R, and the Linear Least Squares program of Wood and Toman were used. Printouts are marked by tabs with comments below.

1. Stepwise Progress Tables

Tables B2-6, B2-7, B2-8 trace the progress of the stepwise regressions for B1 basic set, for B2 basic set, and for B1 extended set respectively. In these tables the independent variables are listed in the leftmost column. Across the top are the step numbers and underneath them the estimated root mean square for error at that step. In the table for each step the independent variables are ranked by their importance as predictor variables as indicated by their F values.(F to enter for variables not in the equation and F to remove for variables already in. Variables already in the equation are ranked ahead of those not yet in, and they have their ranks underlined.)

Generally the relative predictive value of an independent variable as given by its rank is lowered at a particular step if the

TABLE B2-6

Trace of Stepwise Regression

Batch I, Basic Set

	Step							
	0	1	2	3	4	5	6	7
SO_2	1	1	1	1	1	1	1	1
CO_2	2	2	2	2	2	2	2	2
BET	3	3	3	3	3	3	3	3
MINT	7	7	-	-	7	6	6	6
MPVOL	5	6	-	6	6	5	7	7
SPVOL	2	5	-	4	4	4	4	4
MDPV	3	4	4	5	5	-	5	5
$\hat{\sigma}$		.61	.56	.53	.52	.51	.47	.50

TABLE B2-7

Trace of Stepwise Regression

Batch II, Basic Set

	0	1	2	3	4	5	6	7
SO_2	1	1	1	1	1	1	1	
CO_2	6	2	2	2	2	2	2	
BET	2	4	4	5	-	7	7	
MINT	7	3	5	4	4	4	4	
MPVOL	3	6	3	3	3	3	3	
SPVOL	4	-	-	-	-	6	6	
MDPD	5	5	-	-	5	5	5	
$\hat{\sigma}$		.82	.63	.43	.38	.38	.38	

TABLE B2-8

Trace of Stepwise Regression

Batch I, Extended Set

	Step												
	0	1	2	3	4	5	6	7	8	9	10	11	12
SO_2	1	1	1	1	1	1	1	1	1	1	1	1	3
CO_2	7	3	9	-	-	8	11	-	10	10	10	10	5
STEAM	9	2	2	2	2	2	2	2	2	2	3	3	-
ACID	12	6	12	-	7	7	7	7	6	6	8	7	9
BET	4	7	5	5	5	4	4	4	4	4	4	4	2
AIRPY	10	11	6	7	-	9	9	8	8	8	7	6	4
OILAB	11	4	7	6	9	-	8	-	-	-	11	11	7
MINT	8	12	3	3	3	5	5	5	5	5	5	5	10
MPVOL	5	10	11	8	6	6	6	6	7	7	6	8	-
SMPV	2	9	4	4	4	3	3	3	3	3	2	2	1
MDPV	3	8	8	-	8	-	10	9	-	-	12	12	8
I.R.	6	5	10	-	-	10	-	-	9	9	9	9	6
$\hat{\sigma}$		.61	.53	.50	.48	.35	.34	.33	.29	.30	.32	.35	.11

reduction in the error sum of squares due to that variable (or potential reduction for a variable not yet entered) is made much smaller or "stolen" by the variable just entered, i.e., the two variables yield redundant information. The value will be raised if this (potential) reduction is not lowered very much while the error sum of square is considerably reduced by the entering variable, i.e., the information for the two variables is not very redundant. If two independent variables are completely uncorrelated the reduction due to one variable will not be lowered at all by the other one's entry, hence its rank will probably rise.

2. Residual Error

In B1 the additional variables in the extended step contribute significantly to the regression equation as indicated by the lowering of $\hat{\sigma}$, the root mean square for error, from about .50 to .30. The drastic reduction of $\hat{\sigma}$ to .11 in the 12th step of the B1, extended set, regression is probably specious due to the very low degree of freedom for error.

3. Action of the Independent Variables

Several things should be noticed from this regression.

a. SO_2 enters first and is consistently the most important predictor even though its importance is reduced little by little as correlated variables

enter the equation. It is not as important in B2 as in B1; CO_2 and MPVOL seem to contribute more in B2 to compensate.

b. CO_2 is worth more (relatively, compared to the other variables) in the presence of SO_2 than it is by itself. In all of the regressions it comes from a low ranking to second or third with the entry of SO_2. Its information is apparently less redundant and more complementary to SO_2, than others such as SMPV, MINT, MPVOL, MDDIAM.

c. SMPV is largely redundant with SO_2 since it loses heavily with the introduction of SO_2. For B1, extended set, it finally works up to have first ranking at the last step. The drastic shuffling of rankings at this last step, just as the lowering of o, are suspect because of the very low degrees of freedom for error.

d. BET's influence is reasonably stable in B1. It is probably a good predictor variable, but of secondary importance to SO_2. In B2 it yields to the mercury penetration variables.

e. MINT and to a lesser extent SMPVOL have an interesting action in B1. With the basic set of variables they have little importance after SO_2 and CO_2 are introduced. However, with the extended set, wherein

STEAM enters at the second step in place of CO_2, we see that MINT assumes a high rank. This suggests that the MINT, STEAM variables must be used together as a somewhat equivalent to, but better predictor than CO_2.

f. MPVOL apparently works with CO_2 in B2, but no such action is seen in B1 where it is constantly low in rank.

4. Other Notes

a. In B1 the Cedar Bluff 2300°F measurement shows a rather large residual, but when it was eliminated there was no significant change in the regression results.

b. In B2 the Fredonia 1700° measurement has a large WSSD (Wood-Toman) indicating that the location of the independent variable is far removed from the other 14 measurements. Elimination of this measurement has little effect on the regression equation indicating that the high value of FLUE GAS at that point is well predicated by the high values of the other variable.

5. Conclusions from the Regression Analysis

It appears obvious that the capacity measurements are the strongest predictors. There are at least two useful degrees of freedom

among them which here seem to be given by either the SO_2 and STEAM combination or the SO_2 and CO_2 combination.

After that the mercury penetration measurements add some additional information with probably two or more degrees of freedom. MERDEN AND SMPVOL (together with STEAM) or MPVOL seem most promising.

BET stands as a useful variable in B1 somewhat independent of the rest, but in B2 it is redundant to the mercury penetration measurements.

V. COMPARISON OF REGRESSION AND PRINCIPAL COMPONENTS ANALYSES

Generally, those variables which appeared with some force in the non-temperature components proved to be rather poor predictors in the regression equations. For example, in B1, basic set, MERDEN and MERPVO were strong in the second component but low in predictor value. Similarly in B2, basic set, MERDEN and MDPDIAM act similarly whereas MERPVO does not appear in the second component, but it is instead a good predictor variable for flue gas. This suggests that such variables have a variance component in this process which is unrelated to the basic capacity measurements.

In B1 extended set, the additional variables AIRPY, OILAB, and ACID displayed the same characteristic by carrying heavy weight

in later components but having little predictor value. These variance components seem to be caused by source differences.

B3. CROSSPLOTS OF DATA FROM THE DEAD-BURNING STUDY

As outlined in Section C4, three limestones numbered 2061, 2062, and 2069 were calcined at a range of temperatures and tested for chemical and physical properties. The response for each of these properties to calcination temperature is given in the following crossplots.

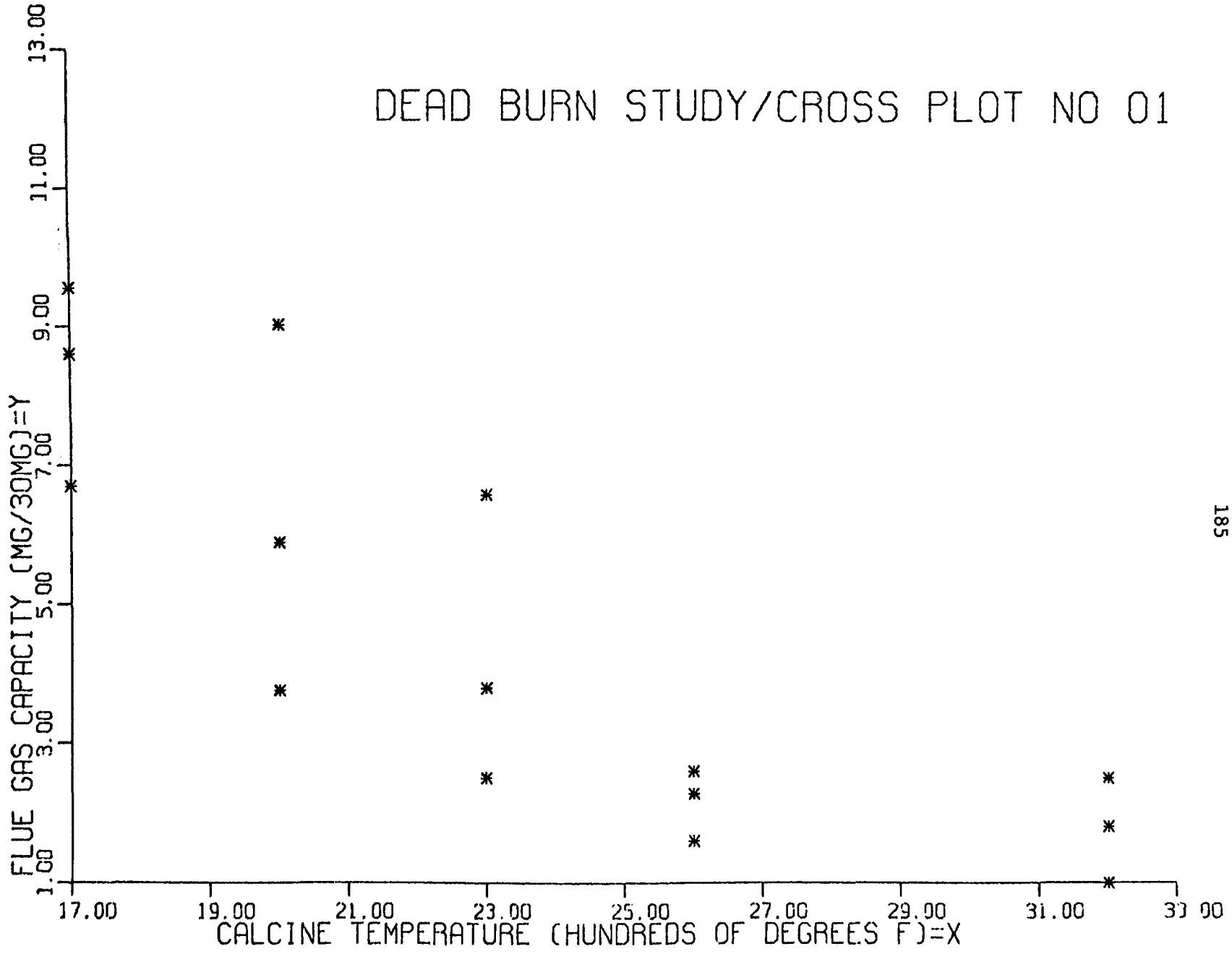
DEAD BURN STUDY/CROSS PLOT NO 01
FLUE GAS CAPACITY (MG/30MG)=Y
1.00
3.00
5.00
7.00
9.00
11.00
13.00
17.00
19.00
21.00
23.00
25.00
27.00
29.00
31.00
33.00
CALCINE TEMPERATURE (HUNDREDS OF DEGREES F)=X

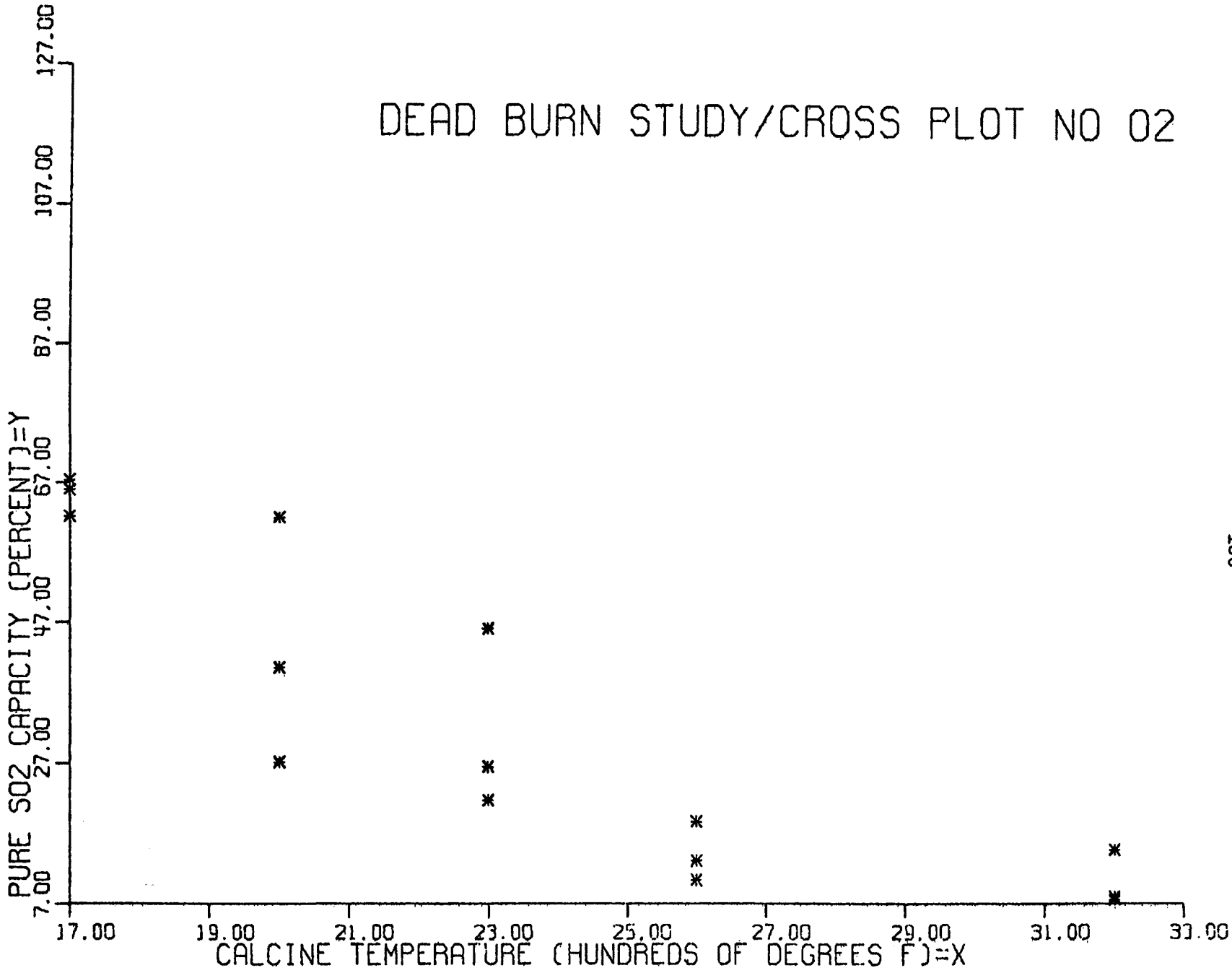
DEAD BURN STUDY/CROSS PLOT NO 02
PURE SO2 CAPACITY (PERCENT)=Y
7.00
27.00
47.00
67.00
87.00
107.00
127.00
17.00
19.00
21.00
23.00
25.00
27.00
29.00
31.00
33.00
CALCINE TEMPERATURE (HUNDREDS OF DEGREES F)=X

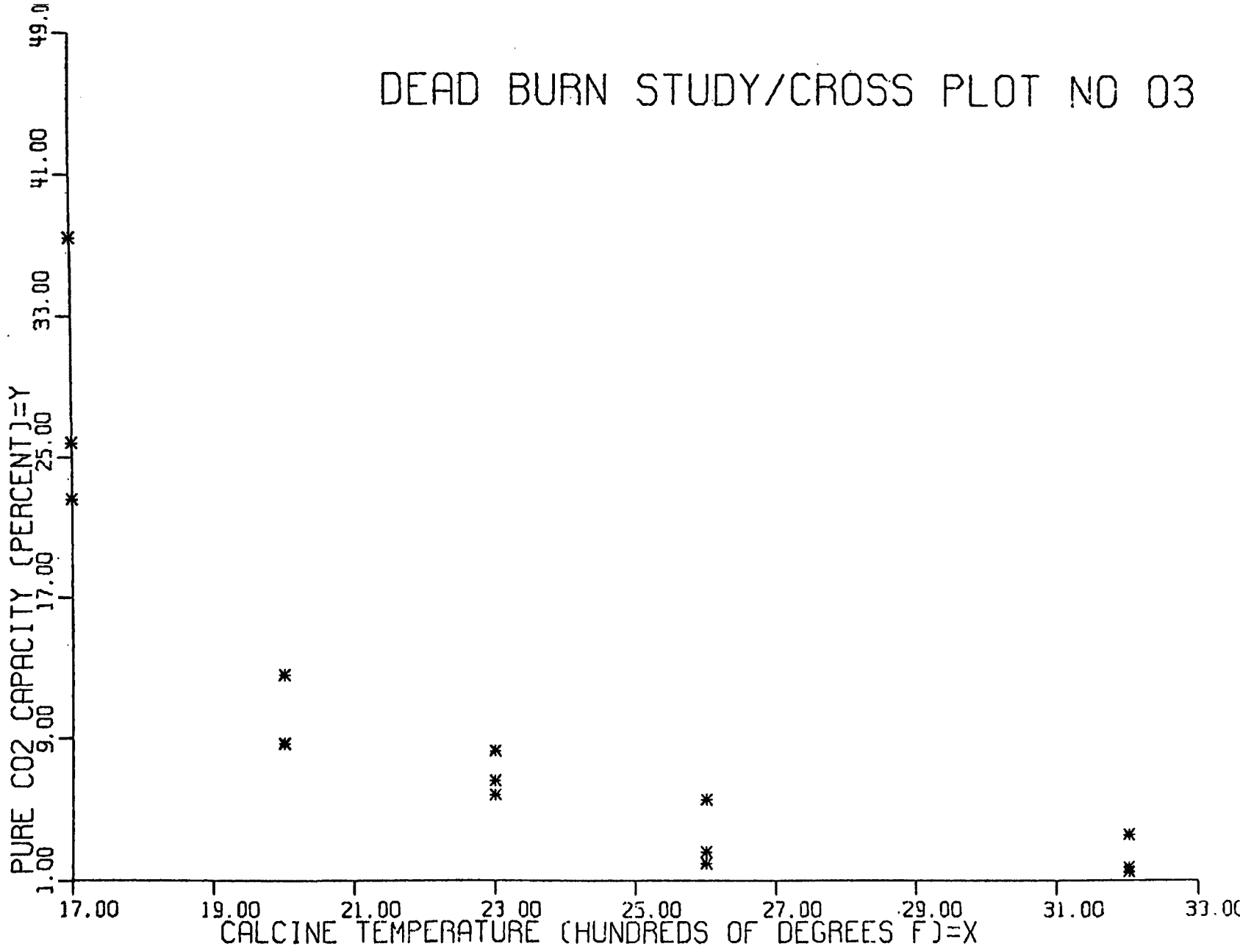
DEAD BURN STUDY/CROSS PLOT NO 03
PURE CO2 CAPACITY (PERCENT)=Y
1.00
9.00
17.00
25.00
33.00
41.00
49.0
17.00
19.00
21.00
23.00
25.00
27.00
29.00
31.00
33.00
CALCINE TEMPERATURE (HUNDREDS OF DEGREES F)=X

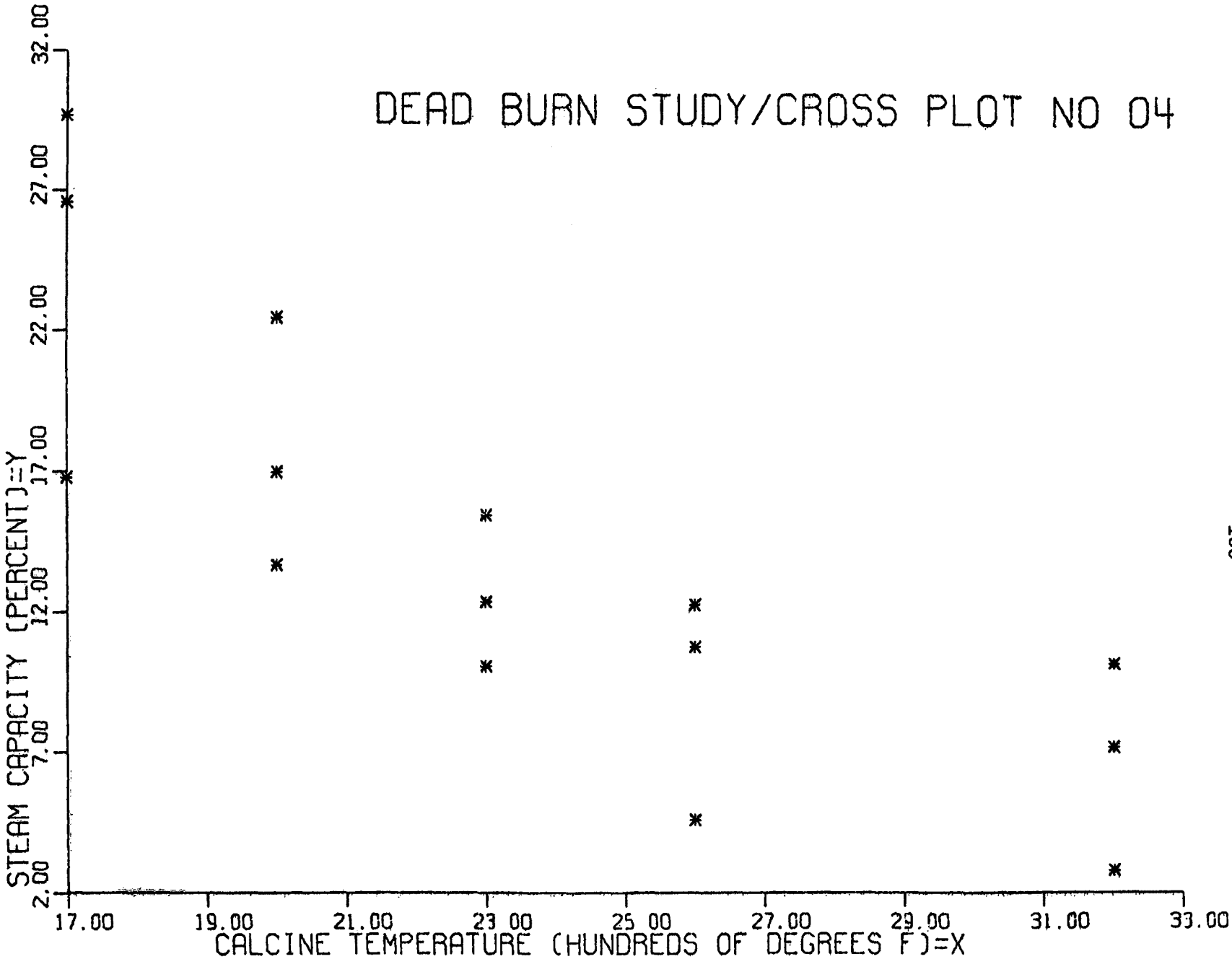
DEAD BURN STUDY/CROSS PLOT NO 04
STEAM CAPACITY (PERCENT)=Y
2.00
7.00
12.00
17.00
22.00
27.00
32.00
17.00
19.00
21.00
23.00
25.00
27.00
29.00
31.00
33.00
CALCINE TEMPERATURE (HUNDREDS OF DEGREES F)=X

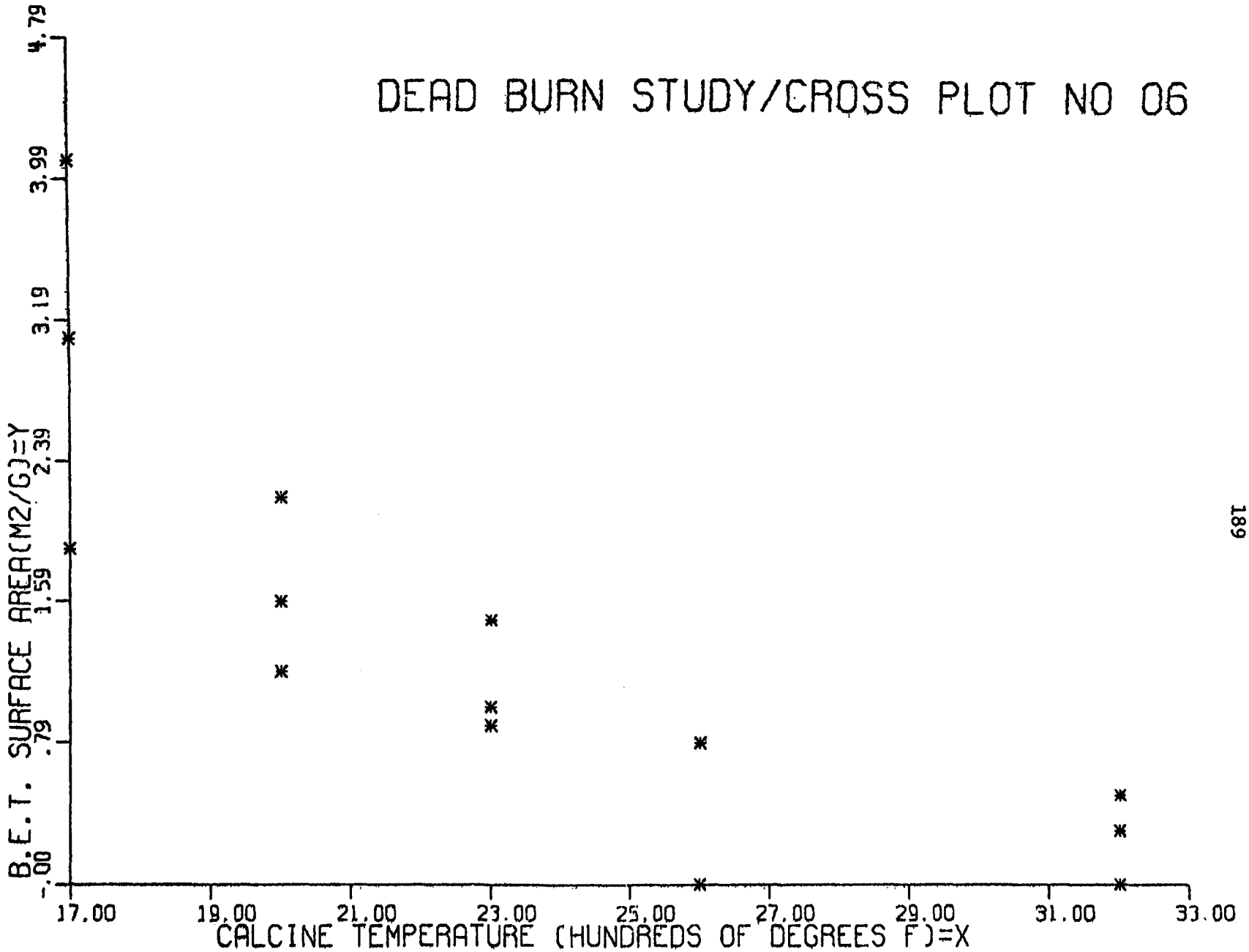
DEAD BURN STUDY/CROSS PLOT NO 06
B.E.T. SURFACE AREA(M2/G)=Y
-.00
.79
1.59
2.39
3.19
3.99
4.79
17.00
19.00
21.00
23.00
25.00
27.00
29.00
31.00
33.00
CALCINE TEMPERATURE (HUNDREDS OF DEGREES F)=X

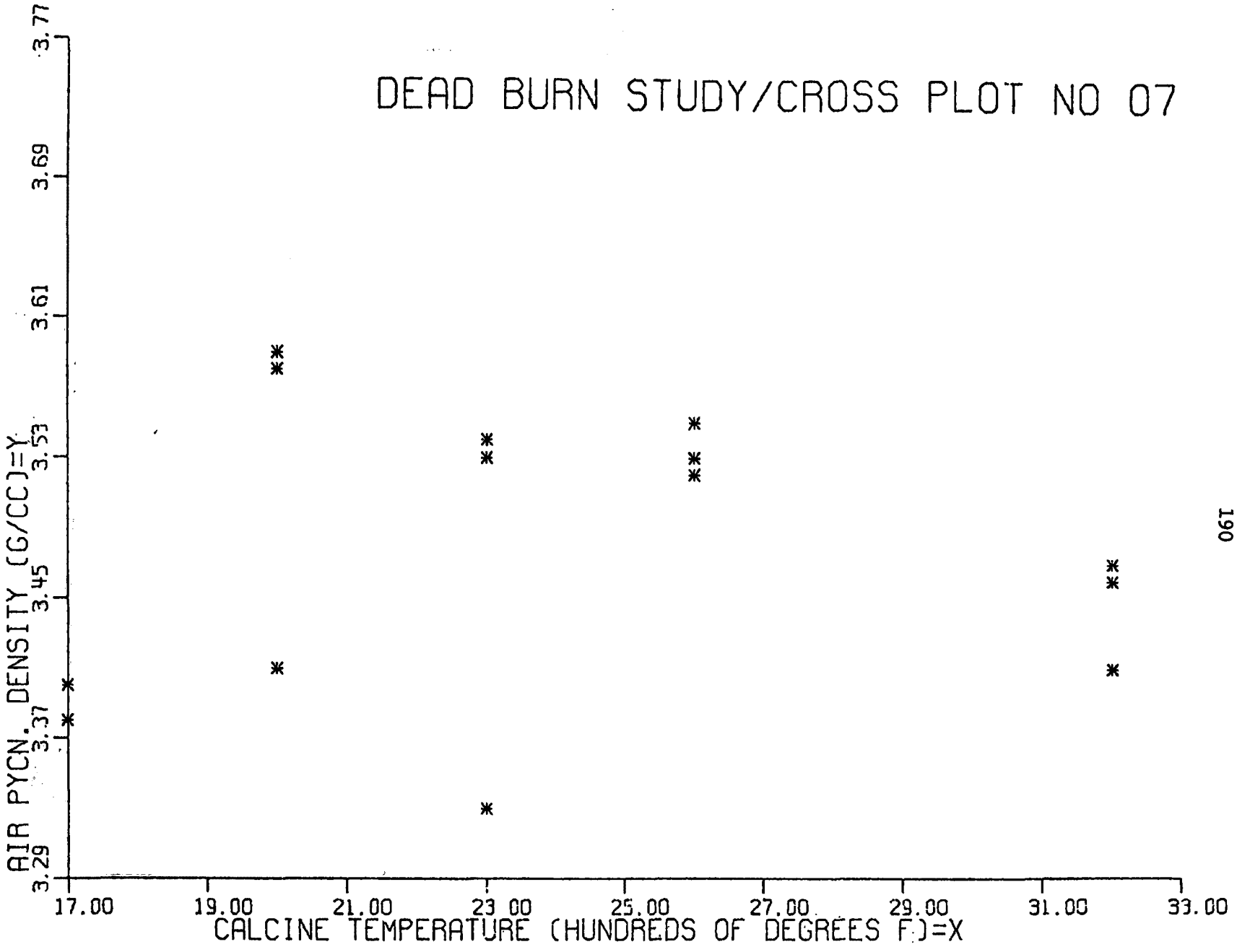
DEAD BURN STUDY/CROSS PLOT NO 07
AIR PYCN. DENSITY (G/CC)=Y
3.77
3.69
3.61
3.53
3.45
3.37
3.29
17.00
19.00
21.00
23.00
25.00
27.00
29.00
31.00
33.00
CALCINE TEMPERATURE (HUNDREDS OF DEGREES F.)=X

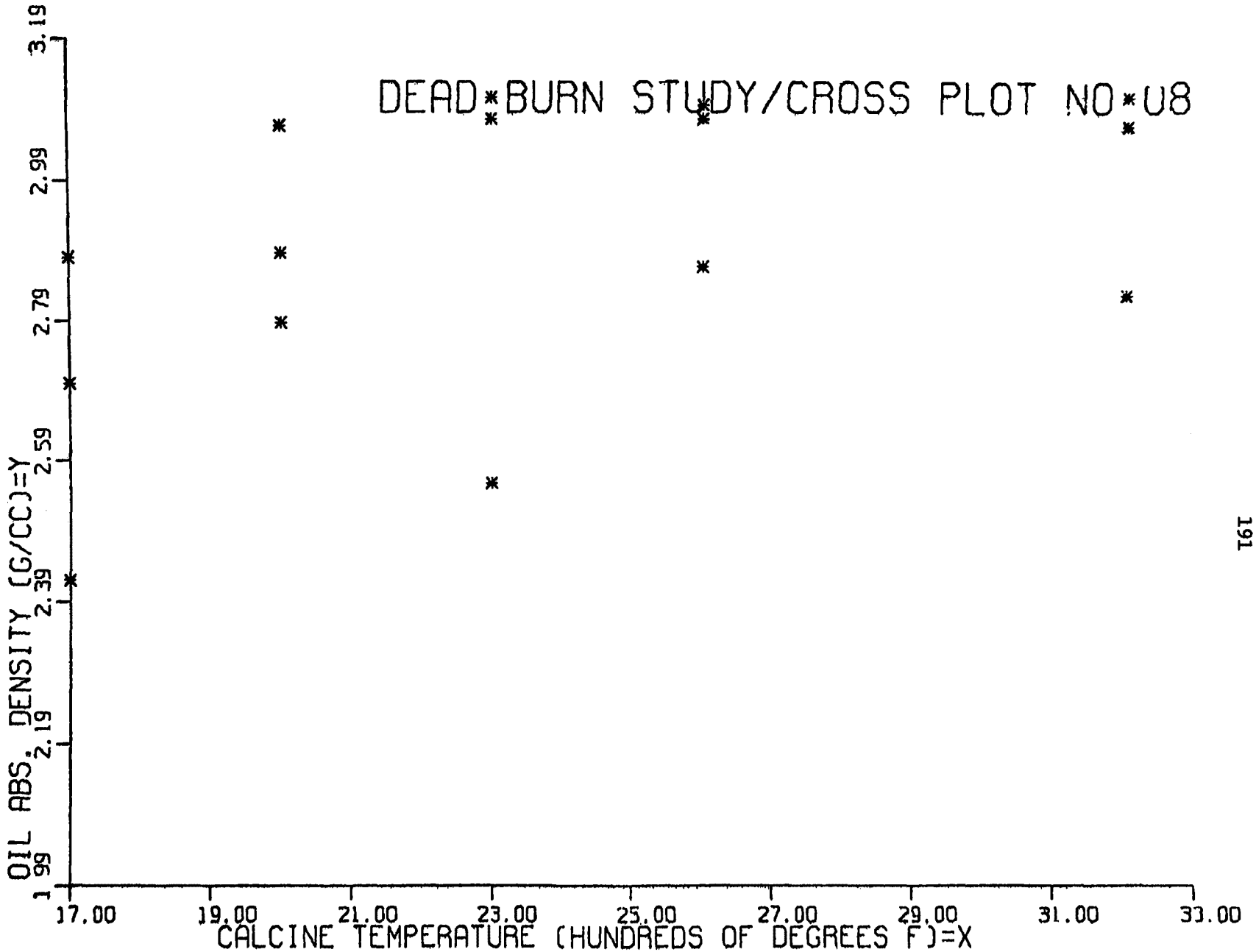
DEAD*BURN STUDY/CROSS PLOT NO*08
OIL ABS. DENSITY (G/CC)=Y
3.19
2.99
2.79
2.59
2.39
2.19
1.99
17.00
19.00
21.00
23.00
25.00
27.00
29.00
31.00
33.00
CALCINE TEMPERATURE (HUNDREDS OF DEGREES F)=X

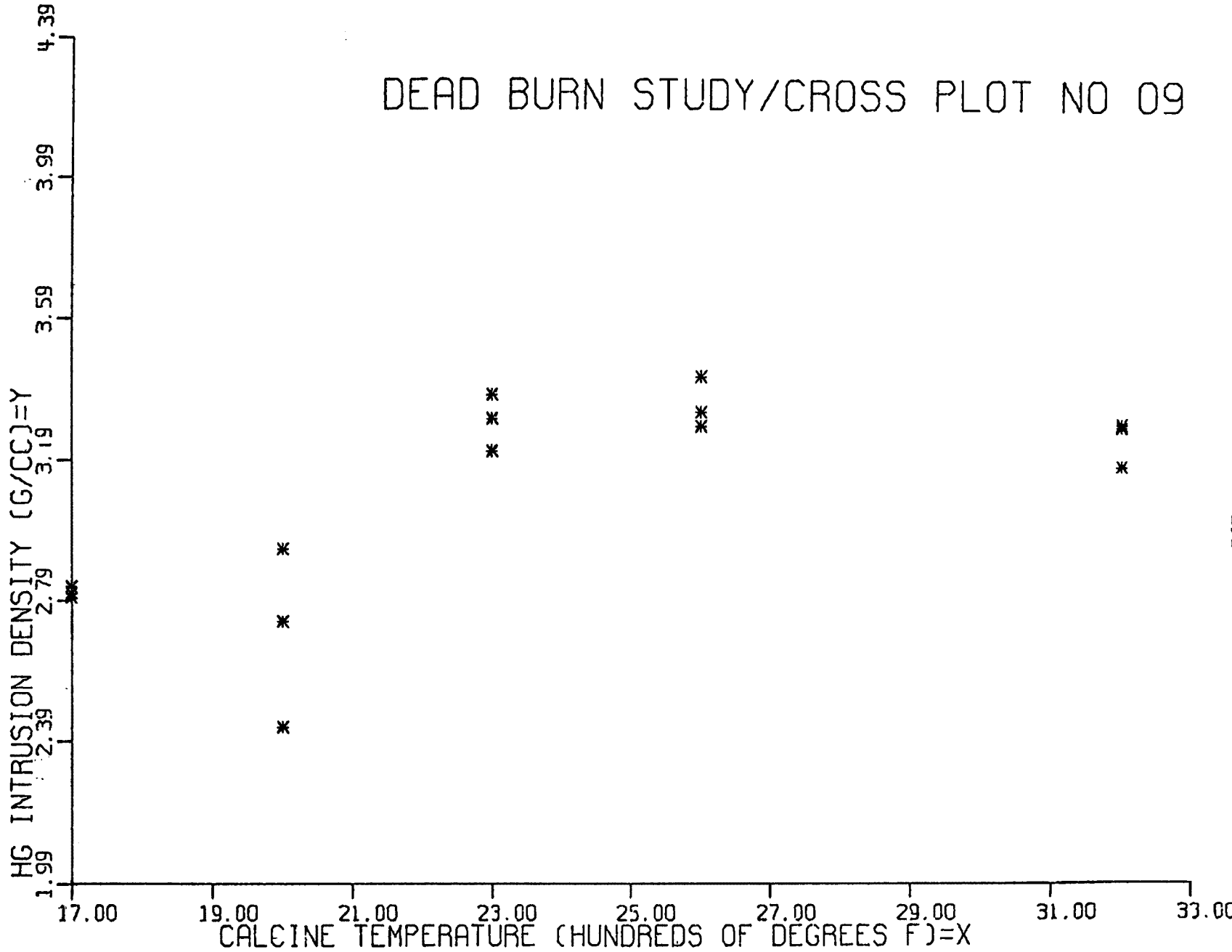
DEAD BURN STUDY/CROSS PLOT NO 09
HG INTRUSION DENSITY (G/CC)=Y
1.99
2.39
2.79
3.19
3.59
3.99
4.39
17.00
19.00
21.00
23.00
25.00
27.00
29.00
31.00
33.00
CALCINE TEMPERATURE (HUNDREDS OF DEGREES F)=X

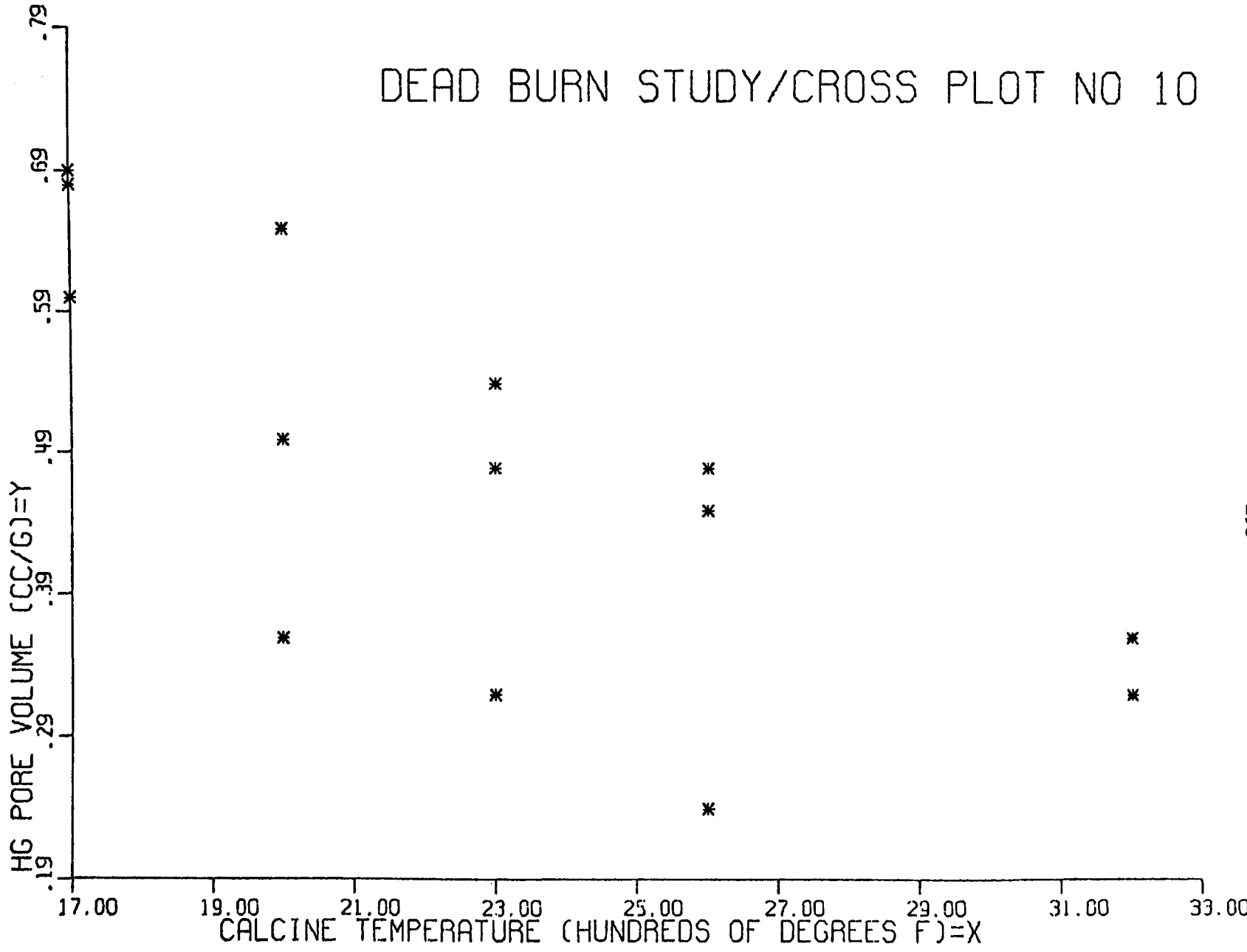
DEAD BURN STUDY/CROSS PLOT NO 10
HG PORE VOLUME (CC/G)=Y
.79
.69
.59
.49
.39
.29
.19
17.00
19.00
21.00
23.00
25.00
27.00
29.00
31.00
33.00
CALCINE TEMPERATURE (HUNDREDS OF DEGREES F)=X

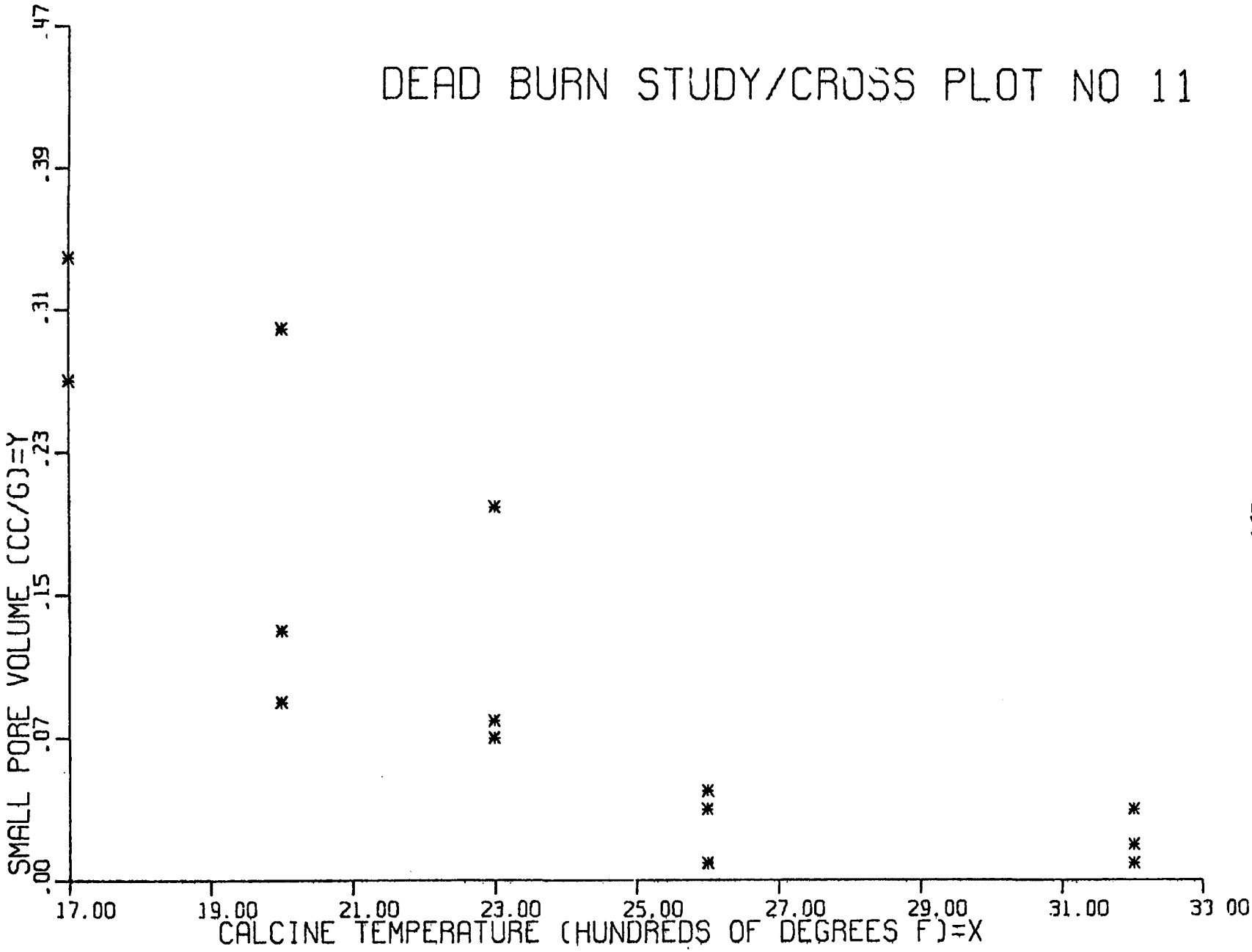
DEAD BURN STUDY/CROSS PLOT NO 11
SMALL PORE VOLUME (CC/G)=Y
.00
.07
.15
.23
.31
.39
.47
17.00
19.00
21.00
23.00
25.00
27.00
29.00
31.00
33.00
CALCINE TEMPERATURE (HUNDREDS OF DEGREES F)=X

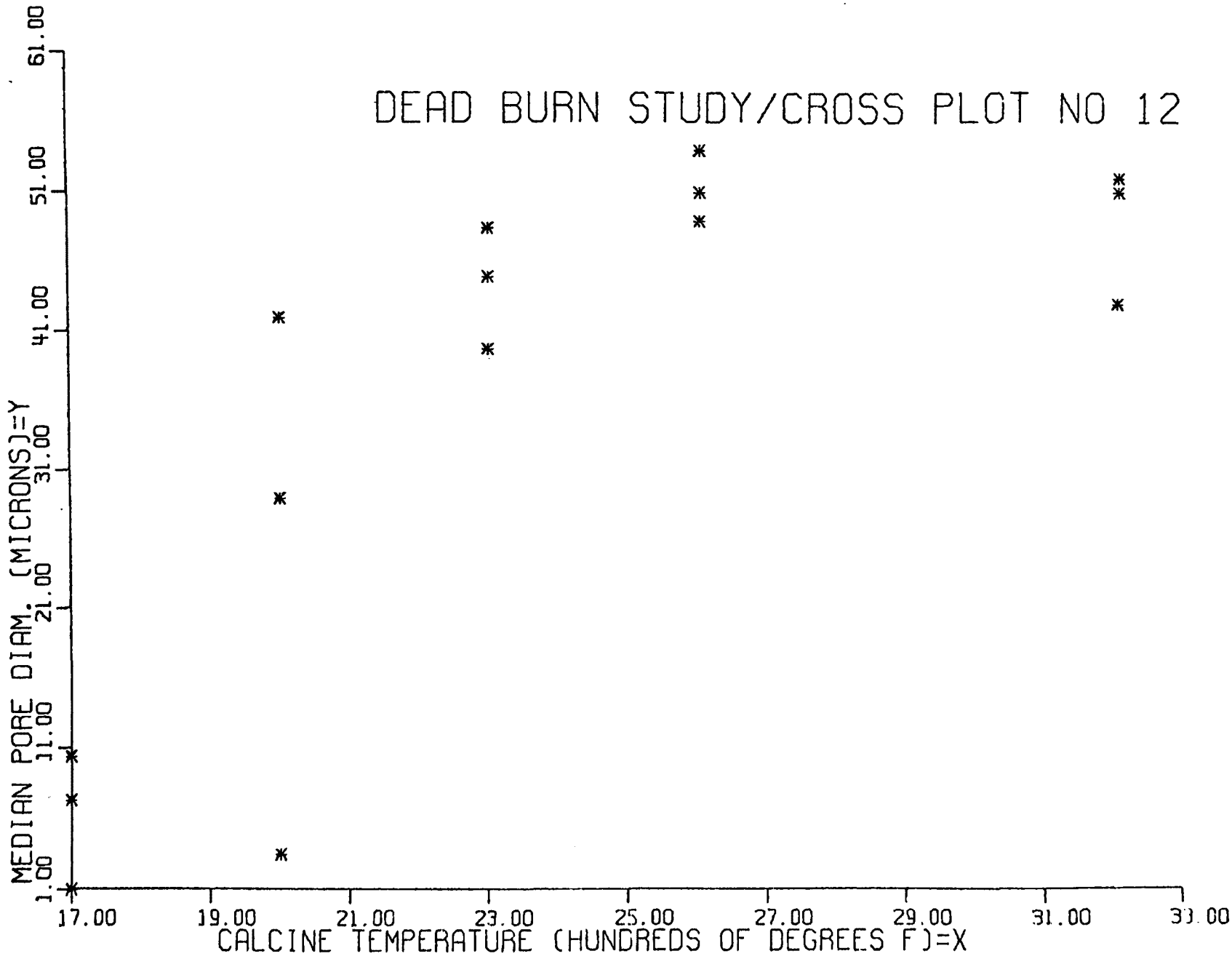
DEAD BURN STUDY/CROSS PLOT NO 12
MEDIAN PORE DIAM. (MICRONS)=Y
1.00
11.00
21.00
31.00
41.00
51.00
61.00
17.00
19.00
21.00
23.00
25.00
27.00
29.00
31.00
33.00
CALCINE TEMPERATURE (HUNDREDS OF DEGREES F)=X

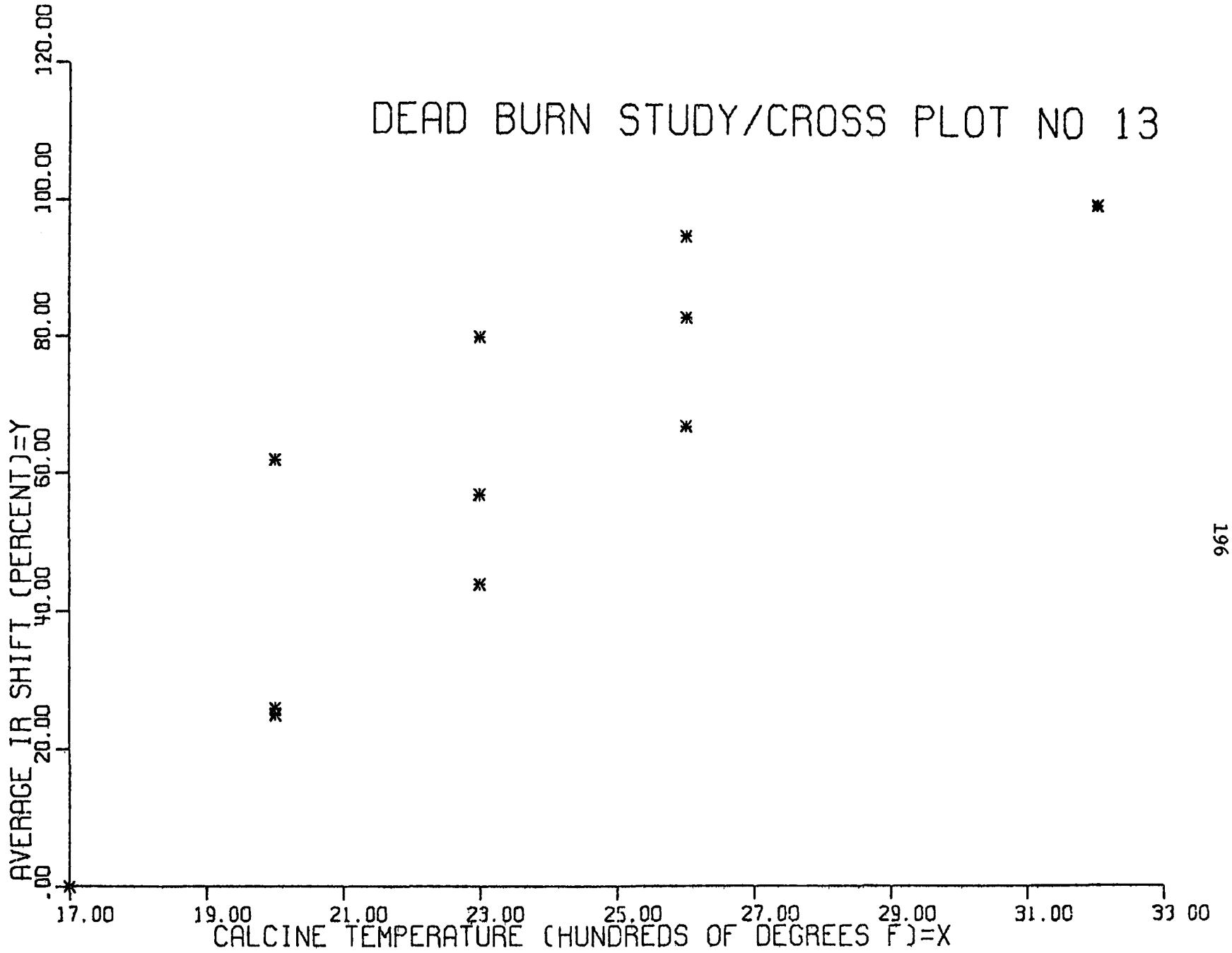
DEAD BURN STUDY/CROSS PLOT NO 13
AVERAGE IR SHIFT (PERCENT)=Y
.00
20.00
40.00
60.00
80.00
100.00
120.00
17.00
19.00
21.00
23.00
25.00
27.00
29.00
31.00
33.00
CALCINE TEMPERATURE (HUNDREDS OF DEGREES F)=X

APPENDIX C

C1. Calcined and Uncalcined Limestones Ranked According to Bed Weight Gain

C2. EPA-APCO Limestone Inventory

C1. Calcined and Uncalcined Limestones Ranked According to Bed Weight Gain

The following limestones were tested in a fixed-bed reactor to determine their capacity to react with flue gas containing sulfur dioxide. The equipment and experimental procedure has been documented by Potter [29] and is also described in Section C5 earlier in this report. Essentially, a fixed bed of 20 grams of calcine is exposed to flue gas at 980°C for 3 1/2 hours. The flue gas, having an average composition of 10.5% CO_2, 3.4% O_2, 9.9% H_2O, 0.27% SO_2, 0.003% SO_3, and 75.9% N_2, flows through the bed at a rate of 425 standard liters per hour.

The bed weight gain of a 20 gram, -18 +20 U.S. mesh, calcined sample (expressed as g SO_3/100 g of calcined stone) was selected as the index of sulfur oxide capacity. For uncalcined samples a weight equivalent to 20 g of calcined stone was used. The bed weight gain, also referred to as "loading" or "capacity", is the weight of SO_3 removed from the flue gas. Data for samples pre-calcined at 980°C for 4 hours are presented in Table C1-1. Data for uncalcined stones are shown in Table C1-2.

The time to 20% breakthrough is the time required for the SO_2 concentration of the gas effluent from the fixed bed of limestone to reach 20% of the inlet SO_2 concentration.

CaO utilization is the percent CaO which reacted based upon the bed weight gain and percent CaO in the limestone sample.

Spectrochemical analyses were provided by Bituminous Coal Research, Inc. (BCR). The limestone numbers in this table were originally assigned by BCR and limestones were referenced by a "BCR Number". However, all limestones in the EPA-APCO limestone inventory are now referenced by a "Limestone Number".

TABLE C1-1. CALCINED LIMESTONES RANKED ACCORDING TO BED WEIGHT GAIN

Limestone Number	Composition, weight %						CaO Utilization %	Time to 20%[1] B. T., min.	Bed Wt. Gain,[2] grams
	CaO	MgO	Fe_2O_3	Al_2O_3	SiO_2	CaO+MgO			
1371	55.00	11.80	1.65	4.65	21.20	66.80	00.00	00.00	00.00
1376	13.90	80.00	1.63	0.86	3.20	93.90	4.92	15.00	1.37
1336	95.00	2.55	0.26	0.36	1.49	97.55	6.60	5.75	1.82
1682	96.00	0.50	0.13	0.20	1.40	96.50	9.40	15.00	2.52
1341	56.00	42.00	0.46	0.12	0.91	98.00	17.00	7.50	2.71
1381	88.00	7.80	0.58	0.46	2.35	95.80	13.60	36.00	3.41
1379	83.00	3.80	0.66	1.27	6.60	86.80	17.10	12.00	4.08
1375	29.50	60.00	1.65	1.12	4.55	89.50	48.65	27.00	4.11
1382	95.00	1.61	0.23	0.20	1.12	96.61	15.20	21.00	4.17
1340	57.00	37.00	2.63	0.27	1.95	94.00	27.20	30.00	4.41
1677	42.50	1.50	0.95	1.35	53.00	44.00	36.60	32.00	4.44
1353	55.00	42.00	1.00	0.19	0.96	97.00	30.70	26.00	4.85
1354	57.00	37.00	0.71	0.43	5.30	94.00	31.70	25.00	5.12
1699	96.00	1.10	0.20	0.30	1.26	97.10	18.60	41.00	5.14
134	57.00	37.00	2.63	0.27	9.5	89.00	30.00	17.00	5.34
1342	63.00	26.00	0.23	0.30	9.50	89.00	29.80	33.00	5.35
1684	57.00	39.00	0.84	0.30	2.53	96.00	32.80	30.00	5.39
1696	57.00	35.50	1.22	0.60	2.00	92.50	33.30	40.00	5.47
1695	58.00	31.50	0.93	1.32	4.50	89.50	33.50	28.00	5.55
1343	94.00	0.85	0.66	0.73	2.98	94.85	21.60	54.00	5.79
1384	97.00	1.10	0.20	0.20	1.00	98.10	21.10	28.00	5.84
1694	56.00	25.00	1.10	1.40	13.30	81.00	37.50	30.00	6.01
1369	96.00	1.40	0.20	0.30	1.16	97.40	22.70	49.00	6.30
1363	66.00	1.42	2.50	6.60	21.00	67.42	32.20	60.00	6.38
1697	92.00	3.70	0.45	0.66	2.40	95.70	24.90	47.00	6.55

[1] Breakthrough time is time in minutes required for SO_2 concentration of effluent gas to reach 20% of inlet SO_2 concentration.

[2] Gain in weight of bed having initial weight equivalent to 20 grams of calcined stone.

TABLE C1-1. CALCINED LIMESTONES RANKED ACCORDING TO BED WEIGHT GAIN (continued)

Limestone Number	Composition, weight %						CaO Utilization %	Time to 20%[1] B. T., min.	Bed Wt. Gain,[2] grams
	CaO	MgO	Fe_2O_3	Al_2O_3	SiO_2	CaO+MgO			
1702	60.00	32.50	1.35	0.79	4.10	92.50	45.80	35.00	7.08
1362	56.00	3.50	18.90	3.65	15.50	59.50	44.50	68.00	7.12
1358	59.00	10.00	4.00	4.20	20.40	69.00	43.70	58.00	7.42
1352	56.00	31.00	1.75	2.48	7.40	87.00	46.70	60.00	7.49
1368	82.00	2.17	1.54	2.20	9.70	84.17	32.80	60.00	7.76
1383	76.00	1.29	3.65	3.10	13.10	77.29	30.40	68.00	8.02
1364	57.00	3.50	2.90	8.50	25.60	60.50	49.80	57.00	8.08
1678	28.50	21.00	1.90	3.15	41.00	49.50	107.00	67.50	8.66
1356	53.00	36.00	7.50	0.42	1.50	89.00	56.80	62.00	8.66
1380	57.00	41.00	0.56	0.30	1.53	98.00	53.50	60.00	8.70
1382	95.00	1.61	0.23	0.20	1.12	96.61	32.00	80.00	8.70
1691	77.00	2.77	0.86	2.03	15.30	79.77	39.70	66.00	8.74
1690	34.00	23.50	1.59	2.30	34.60	57.50	90.00	67.00	8.75
1355	62.00	1.82	2.36	5.60	26.70	63.82	50.80	68.00	8.97
1686	56.50	41.50	0.41	0.30	1.32	98.00	57.50	52.00	9.21
1361	75.00	7.25	5.10	2.37	8.20	82.15	43.80	82.00	9.39
1357	77.00	3.35	1.85	2.80	14.00	80.35	42.80	72.00	9.41
1346	46.00	28.00	2.55	3.40	17.60	74.00	75.50	96.00	9.99
1367	58.00	28.20	9.30	0.35	3.85	86.20	61.00	82.50	10.14
1373	85.00	5.30	1.06	0.95	4.20	90.30	40.50	107.00	10.16
1680	49.00	33.50	1.48	0.94	13.20	82.50	76.90	95.00	10.76
1693	93.00	0.96	0.40	0.82	4.00	93.96	40.60	75.00	10.82
1348	56.00	42.00	0.38	0.22	0.89	98.00	69.50	104.00	11.17
1345	63.00	17.00	1.54	2.48	13.60	80.00	62.90	79.00	11.29
1688	55.00	42.00	0.86	0.30	1.00	97.00	71.50	87.00	11.35

TABLE C1-1. CALCINED LIMESTONES RANKED ACCORDING TO BED WEIGHT GAIN (continued)

Limestone Number	Composition, weight %						CaO Utilization %	Time to 20%[1] B. T., min.	Bed Wt. Gain,[2] grams
	CaO	MgO	Fe_2O_3	Al_2O_3	SiO_2	CaO+MgO			
1374	65.00	18.50	1.70	1.28	12.20	89.50	60.10	107.00	11.47
1378	56.00	41.00	0.37	0.23	2.42	97.00	74.30	87.00	11.90
1930	55.00	43.00	0.36	0.14	0.78	98.00	75.90	132.00	12.14
1698	72.00	19.50	2.35	0.39	5.85	91.50	58.40	110.00	12.59
1365	52.50	22.00	15.50	1.81	7.25	74.50	84.20	114.00	12.63
1370	53.00	36.30	0.79	1.21	7.50	89.30	84.80	100.00	12.72
1366	66.00	16.50	7.10	1.27	7.50	82.50	68.60	115.00	12.92
1351	54.00	28.50	7.00	1.55	8.20	82.50	86.00	117.00	13.07
1685	86.00	8.20	0.69	0.25	2.72	94.50	55.00	138.50	13.51
1679	91.00	2.40	0.59	1.00	4.10	93.40	53.20	118.00	13.84
1701	60.00	23.50	7.40	0.73	6.80	83.50	81.00	112.00	13.93

TABLE C1-2. UNCALCINED LIMESTONES RANKED ACCORDING TO BED WEIGHT GAIN

Limestone Number	Composition, weight %						CaO Utilization %	Time to 20%[1] B. T., min.	Bed Wt. Gain,[2] grams
	CaO	MgO	Fe_2O_3	Al_2O_3	SiO_2	CaO+MgO			
1371	55.00	11.80	1.65	4.65	21.20	66.80	0.67	00.00	00.00
1376	13.90	80.00	1.63	0.86	3.20	93.90	67.20	21.00	2.67
1341	56.00	42.00	0.46	0.12	0.91	98.00	18.00	7.50	2.89
1368	82.00	2.17	1.54	2.20	9.70	84.17	14.30	19.00	3.36
1355	62.00	1.82	2.36	5.60	26.70	63.82	19.00	52.00	3.41
1375	29.50	60.00	1.65	1.12	4.55	89.50	41.00	16.00	3.47
1379	83.00	3.80	0.66	1.27	6.60	86.80	14.30	19.00	3.54
1336	95.00	2.55	0.26	0.36	1.49	97.55	15.33	23.30	4.18
1369	96.00	1.40	0.20	0.30	1.16	97.40	16.20	35.00	4.49
1699	96.00	1.10	0.20	0.30	1.26	97.10	17.20	31.00	5.00
1695	58.00	31.50	0.93	1.32	4.50	89.50	32.20	21.00	5.35
1694	56.00	25.00	1.10	1.40	13.30	81.00	33.70	34.00	5.40
1697	92.00	3.70	0.45	0.66	2.40	95.70	20.80	32.00	5.47
1363	66.00	1.42	2.50	6.60	21.00	67.42	29.20	31.00	5.49
1702	60.00	32.50	1.35	0.79	4.10	92.50	42.90	27.00	6.03
1354	57.00	37.00	0.71	0.43	5.30	94.00	37.20	36.00	6.03
1686	56.50	41.50	0.41	0.30	1.32	98.00	40.60	67.00	6.05
1343	94.00	0.85	0.66	0.73	2.98	94.85	22.70	41.00	6.09
1362	56.00	3.50	18.90	3.65	15.50	59.50	39.80	45.00	6.37
1696	57.00	35.50	1.22	0.60	2.00	92.50	39.20	12.00	6.39
1358	59.00	10.00	4.00	4.20	20.40	69.00	39.20	45.00	6.68
1684	57.00	39.00	0.84	0.30	2.53	96.00	41.20	35.00	6.73
1381	88.00	7.80	0.58	0.46	2.35	95.80	27.40	45.00	6.92
1688	55.00	42.00	0.86	0.30	1.00	97.00	44.00	40.00	6.96
1352	56.00	31.00	1.75	2.48	7.40	87.00	43.96	26.00	7.03

TABLE C1-2. UNCALCINED LIMESTONES RANKED ACCORDING TO BED WEIGHT GAIN (continued)

Limestone Number	Composition, weight %						CaO Utilization %	Time to 20%[1] B. T., min.	Bed Wt. Gain,[2] grams
	CaO	MgO	Fe_2O_3	Al_2O_3	SiO_2	CaO+MgO			
1342	63.00	26.00	0.23	0.30	9.50	89.00	39.80	70.00	7.17
1373	85.00	5.30	1.06	0.95	4.20	90.30	29.20	64.00	7.32
1353	55.00	42.00	1.00	0.19	0.96	97.00	47.20	31.00	7.45
1677	42.50	1.50	0.95	1.35	53.00	44.00	62.00	45.00	7.55
1693	93.00	0.96	0.40	0.82	4.00	93.96	28.40	64.00	7.58
1680	49.00	33.50	1.48	0.94	13.20	82.50	55.50	48.00	7.80
1357	77.00	3.35	1.85	2.80	14.00	80.35	35.80	42.00	7.91
1678	28.50	21.00	1.90	3.15	41.00	49.50	100.00	45.00	8.12
1681	72.00	3.45	0.96	1.20	16.90	75.45	39.60	62.00	8.14
1380	57.00	41.00	0.56	0.30	1.53	98.00	51.20	49.00	8.27
1356	53.00	36.00	7.50	0.42	1.50	89.00	54.90	137.00	8.32
1361	75.00	7.25	5.10	2.37	8.20	82.15	40.00	75.00	8.59
1682	96.00	0.50	0.13	0.20	1.40	96.50	32.40	62.00	8.96
1384	97.00	1.10	0.20	0.20	1.00	98.10	32.70	43.00	9.08
1691	77.00	2.77	0.86	2.03	15.30	79.77	43.80	87.00	9.63
1690	34.00	23.50	1.59	2.30	34.60	57.50	101.80	52.00	10.04
1930	55 00	43.00	0.36	0.14	0.78	98.00	66.30	99.50	10.46
1345	63.00	17.00	1.54	2.48	13.60	80.00	58.30	79.00	10.49
1346	46.00	28.00	2.55	3.40	17.60	74.00	81.50	112.00	10.78
1366	66.00	16.50	7.10	1.27	7.50	82.50	58.20	113.00	11.00
1701	60.00	23.50	7.40	0.73	6.80	83.50	60.80	105.00	11.34
1367	58.00	28.20	9.30	0.35	3.85	86.20	70.00	82.00	11.60
1698	72.00	19.50	2.35	0.39	5.85	91.50	55.20	102.00	11.85
1364	57.00	3.50	2.90	8.50	25.60	60.50	85.30	62.00	13.90
1365	52.50	22.00	15.50	1.81	7.25	74.50	90.20	165.00	13.93
1351	54.00	28.50	7.00	1.55	8.20	82.50	93.60	150.00	14.22
1679	91.00	2.40	0.59	1.00	4.10	93.40	55.00	167.00	14.42
1374	65.00	18.50	1.70	1.28	12.20	89.50	80.20	115.00	15.04

C2. EPA-APCO Limestone Inventory

The following is a listing of the current limestone inventory maintained by EPA-APCO. These samples are located in Cincinnati, Ohio, at two main locations: (1) Research Laboratory Branch, Fairfax Facility, 3914 Virginia Avenue, and (2) U.S. Post Office, Main Building, Room 37C.

The limestone samples are listed according to limestone number, source, identification of material, and the amount of material on hand as of August 1970.

EPA-APCO LIMESTONE INVENTORY - August, 1970

Limestone Number	Source	Identification of Material	Amount of Material on Hand, (lbs.)
1335	Hills Material Co. Rapid City, South Dakota Supt. of Quarry - John Holmes	Limestone Dust	3
1336	Georgia Marble Co. Tate, Georgia Mr. Hall	#2 White crushed marble	132
1337 (reordered as 1930)	Min., Pigm., & Metals, Chas. Pfizer Co. Gibsonburg, Ohio Mr. Plantz	#10 glass house stone	38
1338	Number Not Used (changed to 1693)	----	-
1339	Number Not Used	----	-
1340	Nantahala Talc & Limestone Lexington, Kentucky Mr. Ferebee	Aglime	83
1341	New England Lime Co. Div. of Chas. Pfizer & Co., Inc. Canaan, Connecticut Mr. Ingram	Limestone	59
1342	Conklin Limestone Co. Lincoln, Rhode Island C. E. Conklin	Lime	67
1343 (reordered as 1700)	Hooper Bros. Quarries Weeping Water, Nebraska Mr. Hooper	1/8" down aglime	101
1344	Number Not Used	----	-
1345	New Point Stone Company Batesville, Indiana Norman A. Wanstrath		258
1346	Mankato Aglime & Rock Co. Mankota, Minnesota		137

EPA-APCO LIMESTONE INVENTORY - August, 1970

Limestone Number	Source	Identification of Material	Amount of Material on Hand, (lbs.)
1347	Number Not Used	----	-
1348	J. E. Baker Co. Millersville, Ohio	Ground Raw Stone	205
1349	TVA Paradise Steam Plant Drakesboro, Kentucky Owen C. Janow	Greenville Quarry I	244
1350	Batesville White Lime Batesville, Arkansas General Manager - Mr. Cobb		147
1351 (reordered as 1701)	Jeffrey Limestone Co. Parma, Michigan John C. Jeffrey	Ground Stone	130
1352 (reordered as 1702)	Millard Limestone Co. Annville, Pennsylvania	Dolomite stone	210
1353	J. E. Baker Co. York, Pennsylvania Mr. Paul	Ag Lime	8
1354	Montevallo Limestone Co. Montevallo, Alabama	Granular limestone	67
1355	Elkins Limestone Co. P. O. Box 1228 Elkins, West Virginia Darrel Hankey	8 mesh sand	232
1356	Valley Dolomite Bonne Terre, Missouri Louis Huber	Ag Lime	83
1357	TVA Paradise Steam Plant Drakesboro, Kentucky Owen C. Janow	Greenville Quarry II, Limestone gravel	176
1358	Hanna Coal Company Adena, Ohio	Ag Lime	133

EPA-APCO LIMESTONE INVENTORY - August, 1970

Limestone Number	Source	Identification of Material	Amount of Material on Hand, (lbs.)
1359 (reordered as 1699)	Grove Lime Company Stephens City, Virginia	Ag Lime	140
1360 (reordered as 1698)	Monmouth Stone Co. Monmouth, Illinois Dan Kistler		29
1372	L. F. Rooney Dept. of Geology Indiana University Bloomington, Indiana	Sample B Rockford, Indiana	72
1373	L. F. Rooney Dept. of Geology Indiana University Bloomington, Indiana	Sample C North Vernon, Indiana	84
1374	L. F. Rooney Dept. of Geology Indiana University Bloomington, Indiana	Sample D Position 8	180
1375	Basic Chemicals Cleveland, Ohio	B	119
1376	Basic Chemicals Cleveland, Ohio	D	108
1377	TVA Russfield Nashville, Tennessee		78
1378	Verplanks Coal & Dock Fettysburg, Michigan	Fluxing Fines	136
1379	Limestone Products of Amer. P. O. Box 490 Newtown, New Jersey 07860 Mr. Thompson	Crestite #3	190
1380	Rockwell Lime Co. Manitowac, Wisconsin Pres. - Michael Brisch	Dolomitic Lime-stone 1/4" to 1/8"	148

EPA-APCO LIMESTONE INVENTORY - August, 1970

Limestone Number	Source	Identification of Material	Amount of Material on Hand, (lbs.)
1381	Teeter Stone, Inc. Gettysburg, Pennsylvania		158
1382	Hemphill Bros., Inc. Seattle, Washington		116
1383	Colarusso & Sons Hudson, New York		120
1384	Southern Materials P. O. Box 218 Ocala, Florida V. Pres. - H. B. Roberts, Jr.	Coarse Granular $CaCO_3$	200
1677	Lone Star Materials P. O. Box 918 Austin, Texas Noble W. Prentice	Limestone Screenings	201
1678 (reordered as 1931)	Dolomite Products Buffalo & Howard Road Rochester, New York		114
1679	Indus Limestone Immokalee, Florida		88
1680	John S. Lane & Son, Inc. Meriden, Connecticut		172
1681	Countyline Stone Co. County Line Road Akron, New York 14001 Pres. - John W. Buyers	Crushed Limestone 5/32" + #35	249
1682	California Rock & Gravel 1800 Hobart Building 582 Market Street San Francisco, California Pres. - F. N. Woods III	3/4" limestone	127
1683	Union Carbide Corp. New York, New York		12
1684	G. & W. H. Corson, Inc. Plymouth Meeting, Pa. 19462 Wm. Webster		170

EPA-APCO LIMESTONE INVENTORY - August, 1970

Limestone Number	Source	Identification of Material	Amount of Material on Hand, (lbs.)
1685	Raid Quarries, Inc. F. & M. Bank Building Budington, Iowa Paul R. Orr	Aglime	155
1686	Mayville White Limeworks Mayville, Wisconsin 53050 James O. Smith	Fertilizer Grit	234
1687	$CaCO_3$ Company Frount & 8th Sts. Quincy, Illinois 62301 Dir. of R&D - Vernon R. Heaton	Quincy Granular Limestone	217
1688	Marblehead Lime Co. 300 W. Washington St. Chicago, Illinois 60606 John F. Romanyak	Dolomitic lime-	185
1689 (reorder of 1361)	Tennessee Valley Authority Paradise Steam Plant Drakesboro, Kentucky Gene Farmer		158
1690	McConville, Inc. Ogdensburg, New York		210
1691	Warren Brothers Roads Co. Syracuse, New York		260
1692	Partin Limestone Products San Bernadino, California	Very Fine Ground Pool Covering	234
1693	Pete Lien & Sons Rapid City, South Dakota	Gravel	76
1694	Willingham - Little Ga. Marble Co., Stone Div. Lohitestone, Georgia	Georgia White Grandlux	214
1695	Willingham - Little Ga. Marble Co. Stone Div. Jasper, Georgia	Willingham White Size #10	166

EPA-APCO LIMESTONE INVENTORY - August, 1970

Limestone Number	Source	Identification of Material	Amount of Material on Hand, (lbs.)
1696	James River Hydrate Supply Co. Buchanah, Virginia	#3	196
1697	Marble Cliff Quarries Co. Carntown, Kentucky		249
1698 (reorder of 1360)	Monmouth Stone Co. Monmouth, Illinois		40
1699 (reorder of 1359)	Grove Lime Co. Stephens City, Virginia	Aglime	158
1700 (reorder of 1343)	Hooper Bros. Quarries Weeping Water, Nebraska	Aglime	205
1701 (reorder of 1351)	Jeffrey Limestone Parma, Michigan John C. Jeffrey		138
1702 (reorder of 1352)	A. E. Millard Limestone Co. Annville, Pa. 17003 Mr. Schredder	#2 Dolomite Limestone	139
1921	Chas. Pfizer & Co., Inc. 260 Columbia Street Adams, Massachusetts	Calcite crystals 95 brand	98
1930 (reorder of 1337)	Chas. Pfizer & Co., Inc. Gibsonburg, Ohio		53
1931 (reorder of 1678)	Dolomite Products Buffalo & Howard Road Rochester, New York		138
2057	TVA Prototype Sample Kentucky Stone Irvington, Kentucky	Limestone	16
2058	TVA Prototype Sample Kentucky Stone Russellville, Kentucky	Limestone	16

EPA-APCO LIMESTONE INVENTORY - August, 1970

Limestone Number	Source	Identification of Material	Amount of Material on Hand, (lbs.)
2059	TVA Prototype Sample Road Material, Inc.	Limestone	16
2060	TVA Prototype Sample Fredonia Valley	Blue Limestone	16
2061	TVA Prototype Sample Fredonia Valley	White Limestone	50
2062	TVA Prototype Sample Cedar Bluff Limestone		16
2063	TVA Prototype Sample National Gypsum	Limestone	16
2064	TVA Prototype Sample Alabaster Limestone		16
2065	TVA Prototype Sample Longview Limestone		20
2066	TVA Prototype Sample Hoover Limestone		9
2067	TVA Prototype Sample Rigsby and Bernard Limestone		15
2068	TVA Prototype Sample Williams Limestone		5
2069	TVA Prototype Sample James River Limestone	Sample 1696 from James River Hydrate	16
2070	TVA Prototype Sample Greenville Limestone		5
2071	TVA Prototype Sample Marble Cliff Limestone	Sample 1697 from Marble Cliff, Carntown, Kentucky	16
2072	TVA Prototype Sample Lambert & Lambert Limestone		21

EPA-APCO LIMESTONE INVENTORY - August, 1970

Limestone Number	Source	Identification of Material	Amount of Material on Hand, (lbs.)
2073	TVA		
2074	TVA		
2075	TVA		
2076	TVA		
2077	Longhorn Portland Cement Div. Kaiser Cement and Gypsum San Antonio, Texas 78218 Mr. Art Knutson	Austin Chalk	83
2078	Indiana Limestone Co. P. O. Box 72 Bedford, Indiana Mr. Gary (G. W.) Gaiser	Standard Bluff	58
2079	Indiana Limestone Co. P. O. Box 72 Bedford, Indiana Mr. Gaiser	Rustic Gram	70
2080	Ohio Geological Survey Columbus, Ohio Mr. Horace Collins	Marl (Tufa) Northeastern Ohio	98
2081	State Geological of Kansas Lamerence, Kansas 66045 Mr. R. G. Hardy	Kansas Chalk	55
2082	Ward's Natural Science Establishment Rochester, New York	Iceland spar Second grade	4
2083	Ward's Rochester, New York	Iceland spar First grade	3
2084	Ward's	Dolomite Selasvann, Norway	5
2085	Ward's	White Chalk Dover Cliffs England	2

EPA-APCO LIMESTONE INVENTORY - August, 1970

Limestone Number	Source	Identification of Material	Amount of Material on Hand, (lbs.)
2086	TVA Spring Valley Limestone	Colbert County Limestone	100
2087	Lone Star Cement P. O. Box 839 Demopolis, Alabama Mr. Mike Ried	Selma Chalk	94
2105	Ward's	Sharp pseudo-hexagonal aragonite crystals from Spain	20 pieces
2106	Ward's	New York marl	1
2107	Filer's P. O. Box 995 Loma Linda, Calif. 92354	California, tan banded aragonite	
2108	Eckert Educational Mineral Research Co. 1244 East Colfax Denver, Colorado 80218 Lois Hurianek (303) 272-8943	Massive Colorado Aragonite	12
2109	Soil Conservation Service U.S. Dept. of Agriculture Midtown Plaza Syracuse, N. Y. Mr. Bernard Ellis	Marl, Canastota, Madison Co., N.Y.	10
2110	Soil Conservation Service U.S.D.A.	Marl, Canastota Madison Co., N.Y.	35
2111	Soil Conservation Service U.S.D.A.	Marl, Prattsburg, Stuben Co., N.Y.	36
2112	Soil Conservation Service U.S.D.A.	Marl, Gorham, Ontario Co., N.Y.	27
2113	Missouri Lead Operating Co. Boss, Missouri 65440 Mr. J. H. Davis	Lead doped Dolomite, 5/8"	40

EPA-APCO LIMESTONE INVENTORY - August, 1970

Limestone Number	Source	Identification of Material	Amount of Material on Hand, (lbs.)
2114	Ward's	English Oolitic Limestone	
2115	Ward's	Indiana, Bull, Oolitic limestone	
2116	Ward's	Pennsylvania, dark gray, oolitic limestone	
2117	Ward's	Chocolate, Tennessee, Marble	1
2118	Ward's	Black, Vermont, Marble	2
2119	Ward's	Gray-White Mississippi Chalk	
2120	Ward's	Fine crystalline White Vermont Marble	3
2121	Ward's	Coarse crystalline White, Georgia Marble	5
2122	Ward's	Coarse crystalline Pink, Georgia	2
2123	Ward's	Coarse, White dolomitic, New York Marble	2
2124	Ward's	Fine white dolomitic Mass. Marble	1
2125	Ward's	Travertine, Tivoli, Italy	
2126	Ward's	Calcareous, Tufa Mumford, N. Y.	2
2127	Ward's	Cherty Limestone Leroy, New York	2
2128	Ward's	Oolitic Limestone Bedford, Indiana	

EPA-APCO LIMESTONE INVENTORY - August, 1970

Limestone Number	Source	Identification of Material	Amount of Material on Hand, (lbs.)
2129	Babcock & Wilcox (from S. K. Vorres R. R. #2 Fremont, Michigan 47912)	Newaygo County Michigan marl	20
2201	Ecjunga, Durango, Mexico Supplier: Filer's Redlands, California (1)	Calcite, Iceland spar, IGS Type 1 (2)	1
2202	Hillside Mine Dump Rosiclare, Illinois (1)	Calcite, IGS Type 2	20
2203	Columbia Quarry Company Mine Valmeyer, Illinois (1)	Limestone, coarse-grained, high purity, ISG Type 3	30
2204	Allied Stone Co. Quarry Milan, Illinois (1)	Limestone, fine-grained, high purity, IGS Type 4	30
2205	Midway Stone Quarry Osborne, Illinois (1)	Dolomite, Reef type, high purity, IGS Type 5	30
2206	Abandoned Quarry Bourbonnais, Illinois (1)	Dolomite, IGS Type 6	30
2207	Red Mountain District Santa Clara County, California (1)	Magnesite, fine-grained, high purity, IGS Type 7	10
2208	North Cat Cay, Bahama Islands Supplier: Ocean Industries, Ft. Lauderdale, Florida (1)	Aragonite, IGS Type 8	18
(1351)	Jeffery Limestone Company Quarry Parma, Michigan (1)	Dolomite, IGS Type 9	Same as Limestone 1351

(1) Supplier: R. D. Harvey, Illinois State Geological Survey
(2) ISG - Illinois State Geological Survey

EPA-APCO LIMESTONE INVENTORY - August, 1970

Limestone Number	Source	Identification of Material	Amount of Material on Hand, (lbs.)
2210	Chrzanow, Poland Supplier: Power Metrology Research Organization Energopomiar, R. T. Chrusciel, Glivice, Poland	Dolomite for Nova Huta Iron & Steel Plant, uncalcined	1
2211	Nova Huta Plant Krakow, Poland Supplier: Power Metrology Research Organization Energopomiar, R. T. Chrusciel, Glivice, Poland	Limestone No. 2210 Calcined in Nova Huta Plant, iron and steel process	1

APPENDIX D

Sorption of SO_2 by Waste Kiln Dust from Portland Cement Manufacturing Operations

Sorption of SO_2 by Waste Kiln Dust from Portland Cement Manufacturing Operations

In addition to limestone as a material for sorbing SO_2 from power plant flue gases by dry-injection processes, other materials have also been considered. Some interest has been shown in kiln dust as a SO_2 sorbent. Kiln dust consists of the fines and condensed volatiles blown from the raw mix as it passes through a rotary kiln in portland cement manufacturing processes. This dust is collected from kiln exhaust systems in cyclones and baghouses. In order to maintain an acceptable low alkali content in the cement product, the kiln dust cannot be recombined with the product.

Table D-1 lists chemical analyses for three kiln dust samples. Table D-2 lists the reactivity of these kiln dust samples to flue gas in a differential reactor. Details of the design and operation of this reactor are given in the paper, "Kinetics of the Reaction of SO_2 with Limestone"[1]. Results for a 100 second exposure to flue gas are reported in milligrams SO_3 per 30 milligrams calcined. When as-received or uncalcined material is tested, the charge weight used is equivalent to 30 milligrams calcined. Absorptivity of the kiln dust is comparable to but no better than Stone No. 2061, an oolitic calcite. Moreover, the Na_2O content of kiln dust may be as high as 2.5%,[2] whereas, it is only a trace quantity (<0.02%)

---

[1] Environmental Science & Technology, Jan. 1970, p. 59-63.

[2] Nebgen, J. W., et al., Midwest Research Institute Prospectus, No. RC-199, May 5, 1970, p. 2

Table D-1

Analysis of Kiln Dust[1]

	North Western States[2]	Medusa[3]	American[4]
% Loss on Ignition @ 1800°F	23.6	17.3	27.2
% Silica (SiO_2)	15.5	15.1	15.9
% Iron Oxide (Fe_2O_3)	2.6	3.1	3.0
% Aluminum Oxide (Al_2O_3)	6.6	7.3	4.0
% Calcium Oxide (CaO)	49.5	52.9	47.5
% Magnesium Oxide (MgO)	0.9	3.1	2.2

(1) Analysis by Gilbert Associates, Inc., 2249 Fairview St., Reading, Pennsylvania 19606. Analyses for alkali content not requested.

(2) Sample provided by North Western States Portland Cement Co., Mason City, Iowa.

(3) Sample provided by Medusa Portland Cement Co., Box 5668, Cleveland, Ohio 44101.

(4) Sample provided by American Cement Corp.

Table D-2

Reactivity of Kiln Dust in a Differential Reactor[1]

Temperature °F	Stone No.[2] 2061	mg SO_3/30 mg calcine Samples from Cement Companies (uncalcined) North Western States	Medusa	American
800	(1.5)*	2.3	3.7	--
1000	(3.1)*	2.1	3.1	0.5
1200	4.6	2.9	4.4	1.8
1400	6.4	6.2	6.2	3.0
1600	8.0	6.5	6.4	2.7
1800	9.4	7.2	5.9	4.8

* extrapolated

Note: 1. 100 second exposure to flue gas of following composition:

Component	Volume %
CO_2	10.5
O_2	3.4
H_2O	9.9
SO_2	0.27
SO_3	0.003
N_2	75.9

2. Sample supplied by Fredonia Valley Quarries, Kentucky (White limestone).

in most limes. Unfortunately, the presence of sodium in fly ash decreases fusion temperature of fly ash which leads to increased quantity and strength of deposits encountered around the superheater and reheater tubes in a power boiler. Thus, injection of kiln dust to remove SO_2 before these tubes would likely lead to unacceptable periods of "downtime" for tube cleaning and loss of heat transfer efficiency.

Table D-3 indicates the reactivity of several kiln dust samples in an aqueous batch scrubber. A description of this apparatus is given by Potter[1]. The procedure is to bubble flue gas through a stirred slurry of the tested material and to monitor the pH of the solution and the SO_2 content of the scrubbed gas. An important datum is the breakthrough time, i.e., the length of time during which the slurry successfully removes all of the sulfur oxides. The pH of the solution at breakthrough as well as the breakthrough time in minutes is given. Reactivity of the kiln dust is comparable to finely ground uncalcined limestone.

---

1 International Symposium for Lime and Limestone Scrubbing, Pensacola, Florida, March 16-20, 1970.

Table D-3

Reactivity of Kiln Dust in an Aqueous Scrubber

North Western States Kiln Dust	Breakthrough Time, min.	pH at Breakthrough
Uncalcined	44	4.3
Calcined	41	4.5
Medusa Kiln Dust		
Uncalcined	41	4.4
Calcined	39	4.3
Stone No. 1700[1]		
Uncalcined	45	5.3
Calcined	61	5.5

(1) A calcitic aglime supplied by Hooper Brothers Quarries, Weeping Water, Nebraska.

APPENDIX E

Copper Oxide Sorption of SO_2

Sorption of SO_2 by Copper Oxides

The Air Preheater Company and the Owens-Corning Fiberglas Corporation have established the fabric filterhouse to be an effective chemical contactor for removal of sulfur dioxide from flue gas streams. It has been suggested that one potential application for the filterhouse would be to remove SO_2 from the flue gases from the reverbatory furnace in the copper smelting industry. The idea would be to inject either cupric oxide or the solid effluent from the roaster or reverberatory furnace into a filterhouse along with the effluent gases from the reverberatory furnace. After sorbing SO_2 the solid reaction products would then be fed back into the roaster feed stream where the sorbed SO_2 would be driven off in the roaster to enrich the roaster effluent gases which contain five to ten percent SO_2 by volume. The roaster effluent gases containing SO_2 are normally sent to a sulfuric acid manufacturing process.

An exploratory investigation was made to show the reactivity of cupric oxide to sulfur dioxide. Chemical grade cupric oxide (Baker A.C.S. grade) was exposed to pure SO_2 in a thermogravimetric analyzer (an Aminco Modular Thermo-Grav). In the thermogravimetric analysis (TGA) mode it automatically records sample weight change as a function of sample temperature at

pre-selected heating rates. In this case the TGA was performed with 100 milligrams of cupric oxide exposed to a 100 cc/min SO_2 purge and heated at a rate of 6°C/min. Figure E-1 shows the reactivity of cupric oxide with SO_2.

As shown in Figure E-1 the cupric oxide reached a maximum weight gain of 50% at a temperature of about 720°C, after which the reacted sample underwent decomposition. The significance of the break in the graph between 560 - 695°C is not known.

The significant information to be obtained from Figure E-1 is that at 315°C (600°F) there is only a 2-3 percent weight gain by the cupric oxide. Since commercially available fabric filters have a maximum operating temperature of 600°F, cupric oxide would not be an effective sorbent for a fabric filterhouse application unless fabric filters with higher operating temperatures can be developed.

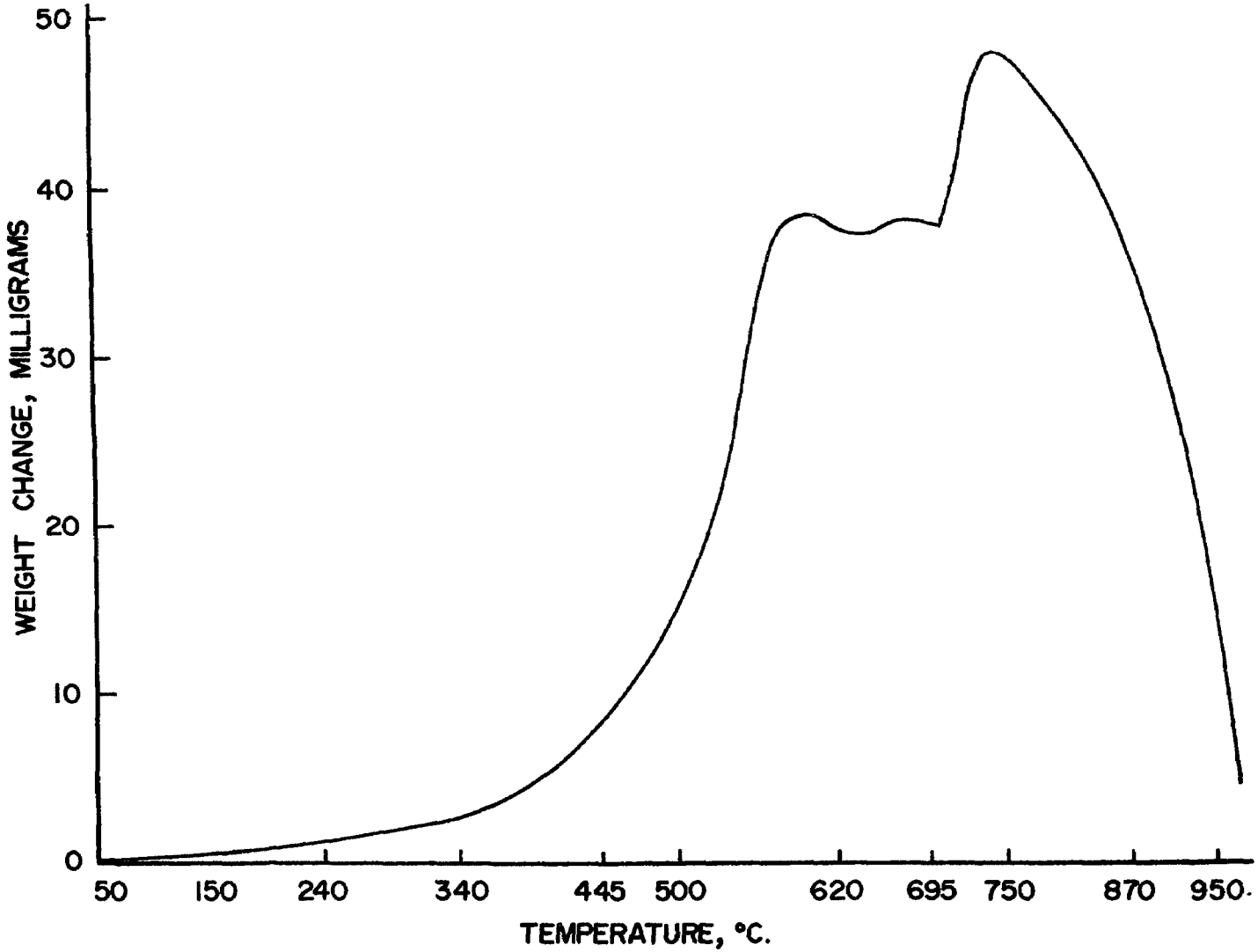

Figure E-1. Thermogravimetric Analysis of Reactivity of Cupric Oxide to SO_2

APPENDIX F

Char Sorption of SO_2 and Regeneration

CHAR SORPTION OF SO_2 AND REGENERATION

A number of processes under development for the control of sulfur oxides employ the catalytic properties of activated carbon to oxidize sulfur dioxide to sulfur trioxide on the carbon surface and to retain the sulfuric acid formed from the sulfur trioxide in the pores of the activated carbon. Thermal regeneration of the carbon results in significant consumption of the rather expensive activated carbon. In order to avoid this problem associated with the regeneration of the spent carbon, the West Virginia Pulp and Paper Company (Westvaco) has suggested a reductive type regeneration in which hydrogen sulfide is used. The hydrogen sulfide is reacted first with a portion of the sulfuric acid to yield elemental sulfur. A part of the sulfur then reacts with the remainder of the sulfuric acid, presumably preventing reaction of the sulfuric acid with the carbon and thereby averting consumption of the carbon.

Several experiments to check the char sorption-regeneration scheme proposed by Westvaco were run. The following aspects of this scheme were tested: (1) SO_2 sorption capacity of the char at 250°F, (2) the reduction of H_2SO_4-loaded char by H_2S at 300°F, (3) the reduction of H_2SO_4 with sulfur at 600°F.

The attached data summarize the results obtained in these experiments. The following additional comments are offered:

SO_2 Sorption

A fixed bed containing 9.38 grams (15 cm^3) of char (supplied by Westvaco) was exposed to flue gas containing 2800 ppm SO_2 (dry basis) at 250°F. The gas flow was 505 ml. per minute (21°C) through the bed, for a space velocity of 2000 $hr.^{-1}$. Figure F-1 gives the breakthrough curve for the run, as measured with an infrared analyzer continuously recording the SO_2 concentration in the reactor effluent gas stream. SO_2 concentration in the effluent gas stream reached 10 per cent of the inlet concentration (10% breakthrough) in 6.65 hours, at which time the char loading was 15.8 wt. percent SO_2. Exposure to flue gas was ended at 8.75 hours. The weight gained by the char during the total exposure period was 2.80 grams. Integration of the IR curve indicated an SO_2 sorption equivalent to 2.83 grams H_2SO_4.

H_2SO/H_2S Reduction

Three samples of char from the experiment described above were exposed to pure H_2S at 300 °F using the apparatus shown in Figure F-2. The gas volumes were measured in 100 ml burettes using saturated salt solution (acidified with HCl) as the displacement fluid. Different volumes of H_2S were fed to each char sample, equivalent to 33%, 88% and 100% stoichiometric to H_2SO_4 based on the assumed reaction

$$H_2SO_4 + 3H_2S \rightarrow 4S + 4H_2O$$

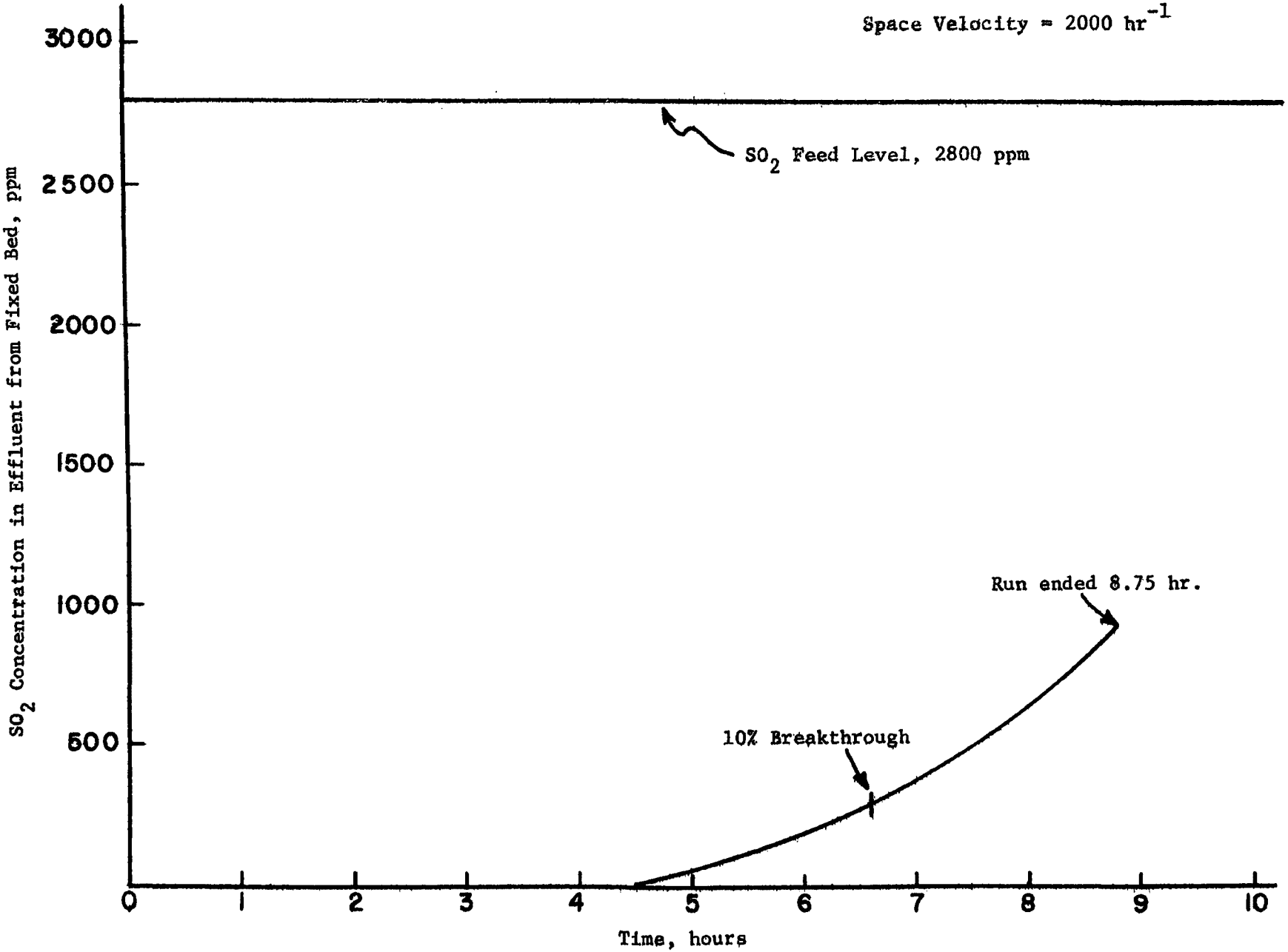

Figure F-1. Breakthrough Curve: SO_2 Sorption from Flue Gas at 250°F with Wesvaco Char

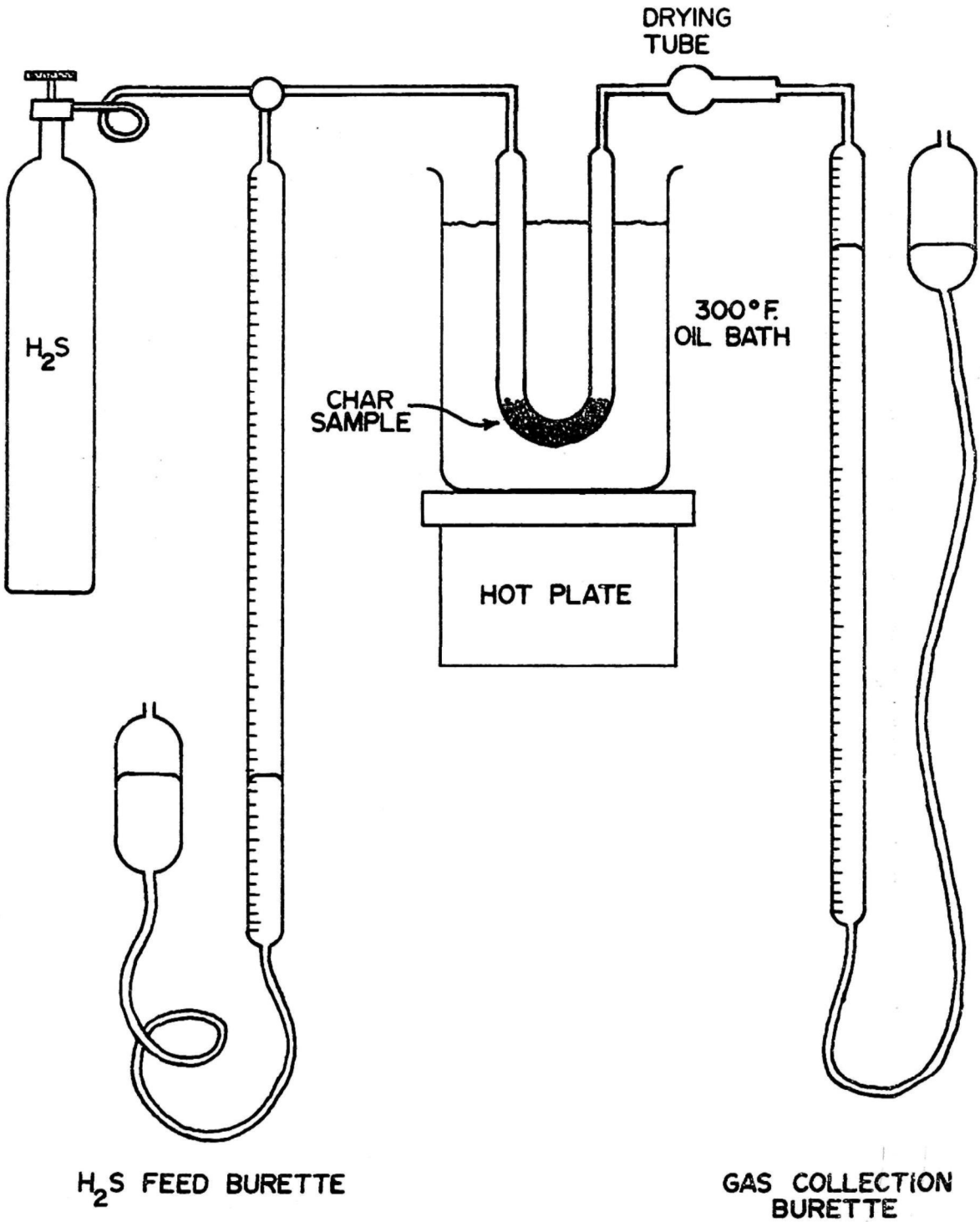

Figure F-2. Apparatus used for H_2SO_4/H_2S Reduction Experiments

The data obtained are summarized in Table F-1, along with three additional runs made with as-received char which had not been exposed to flue gas. Figures F-3, 4 and 5 show the relationship between the amount of H_2S fed to the char (at constant rate) and the amount of gas which passed through the char bed. The gas collected includes the air displaced from the reactor tube which had a volume of 28 ml.

H_2SO_4/S Reaction

The char samples obtained from the above H_2S treatment were each heated to 600°F under flowing nitrogen using the apparatus shown in Figure F-6. The presumed reaction for this stage is

$$H_2SO_4 + 1/2\ S \rightarrow 3/2\ SO_2 + H_2O$$

The sulfur dioxide collected in the peroxide absorbers was analyzed to determine the total SO_2 evolved. When SO_2 evolution was completed, the char was removed and extracted in a Soxlet apparatus with carbon disulfide to recover elemental sulfur. Results of these tests are listed in Tables F-2 and 3. Finally, the three samples of as-received char which were exposed to H_2S (runs A, B, C), were composited and extracted with carbon disulfide. Sulfur recovery was 0.288 grams for the composite of nine grams of unloaded char for a baseline loading of 0.032 grams of sulfur per gram of unloaded char. This may be compared with the results for runs 1, 2, and 3 in Table F-3 where the maximum sulfur recovery was 1.52 grams of sulfur on 3.56 grams of loaded char or 0.745 grams of sulfur per gram of unloaded char (i.e.,

Table F-1: H_2SO_4/H_2S Reaction Stage at 300°F

Weight H_2SO_4-loaded char put in reactor tube = 3.82 grams each run

Feed rate of H_2S to char during reaction = 1.6 ml/min (20°C, 1 atm)

Run (Stoich.)	Total H_2S added, ml. (20°C, 1 atm.)	Total gas passed thru char, ml. (20°C, 1 atm.)	Wt. gain by char, gm.	Wt. gain by drying tube, gm.
1 (33%)	219	28	0.187	0.107
2 (88%)	575	34	0.576	0.042
3 (100%)	655	76	0.713	0.035

Weight as-received char put in reactor tube = 2.92 grams

Feed rate of H_2S to char during reaction = 1.6 ml/min.

A	219	80	0.052	0.035
B	575	262	0.069	0.058
C	655	381	0.046	0.052

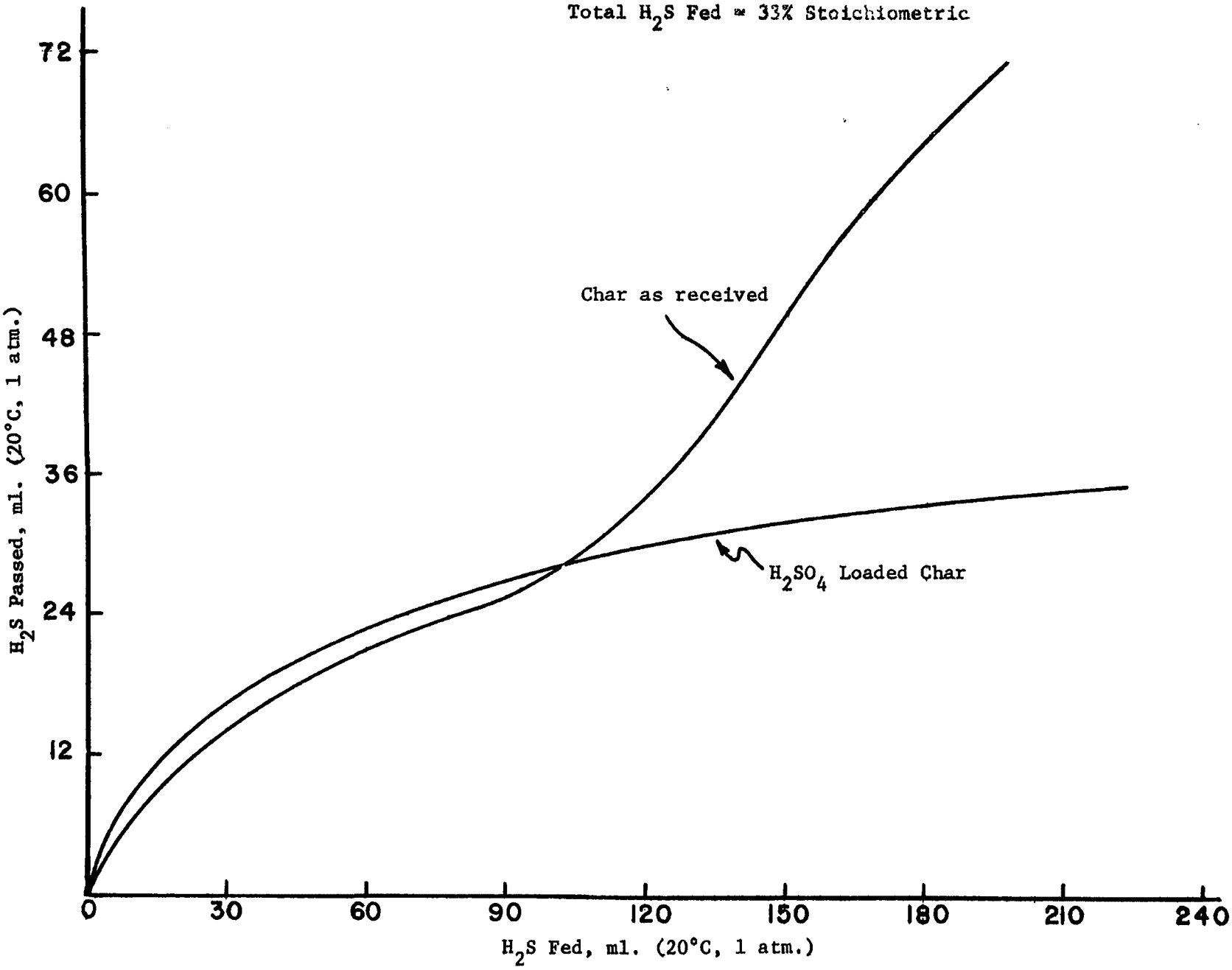

Figure F-3. 300°F H_2S Reduction

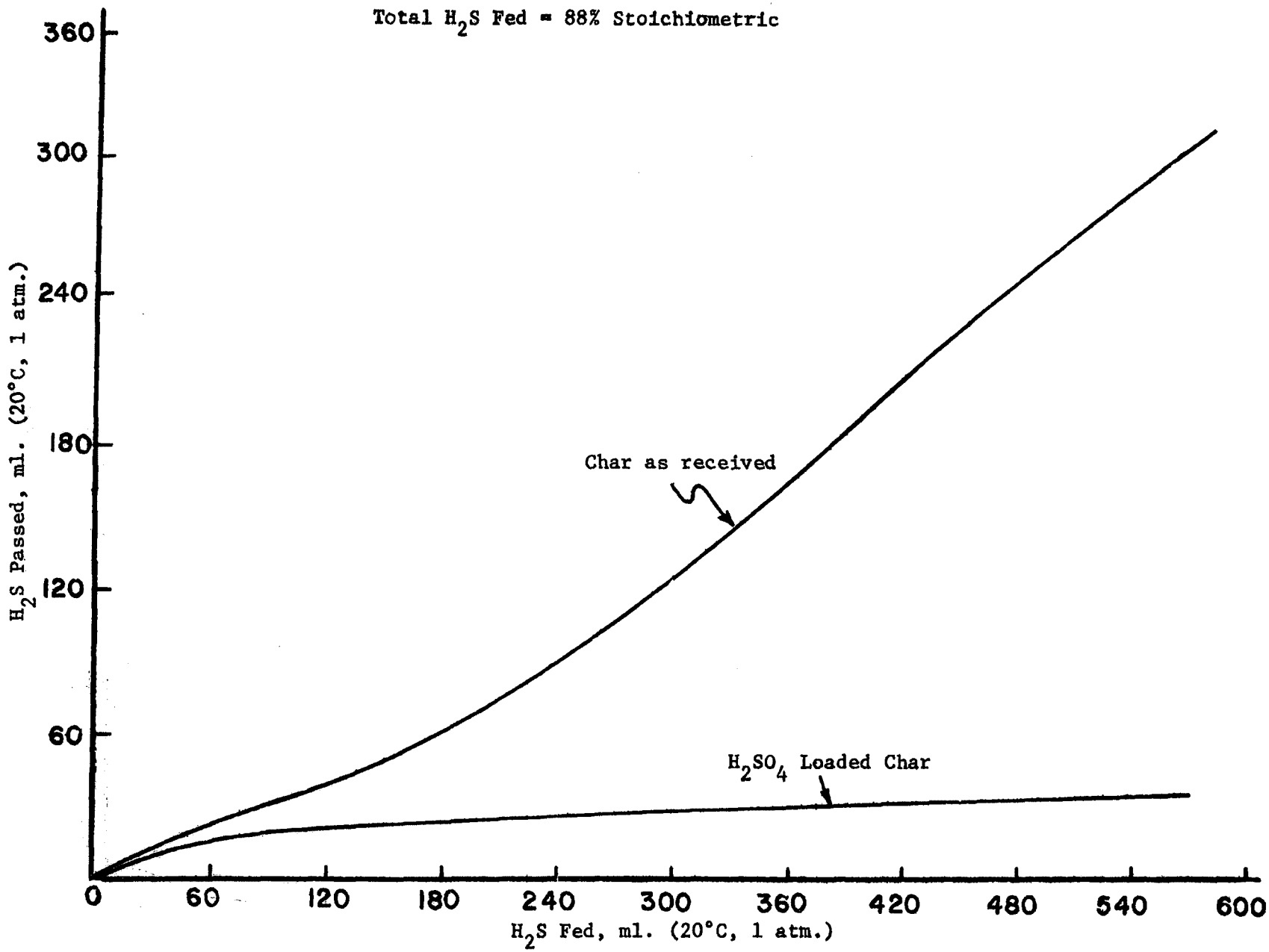

Figure F-4. 300°F H_2S Reduction

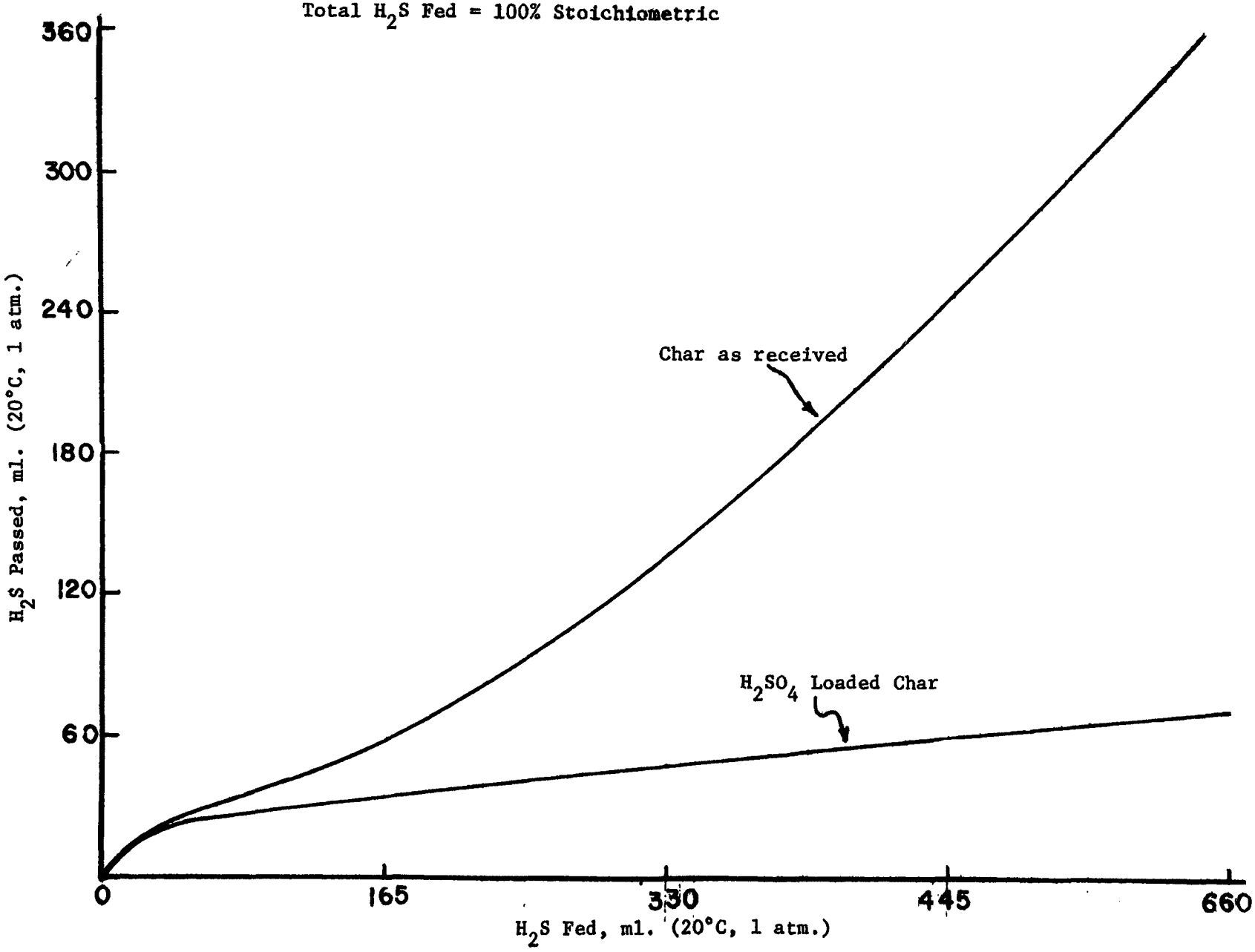

Figure F-5. 300°F H_2S Reduction

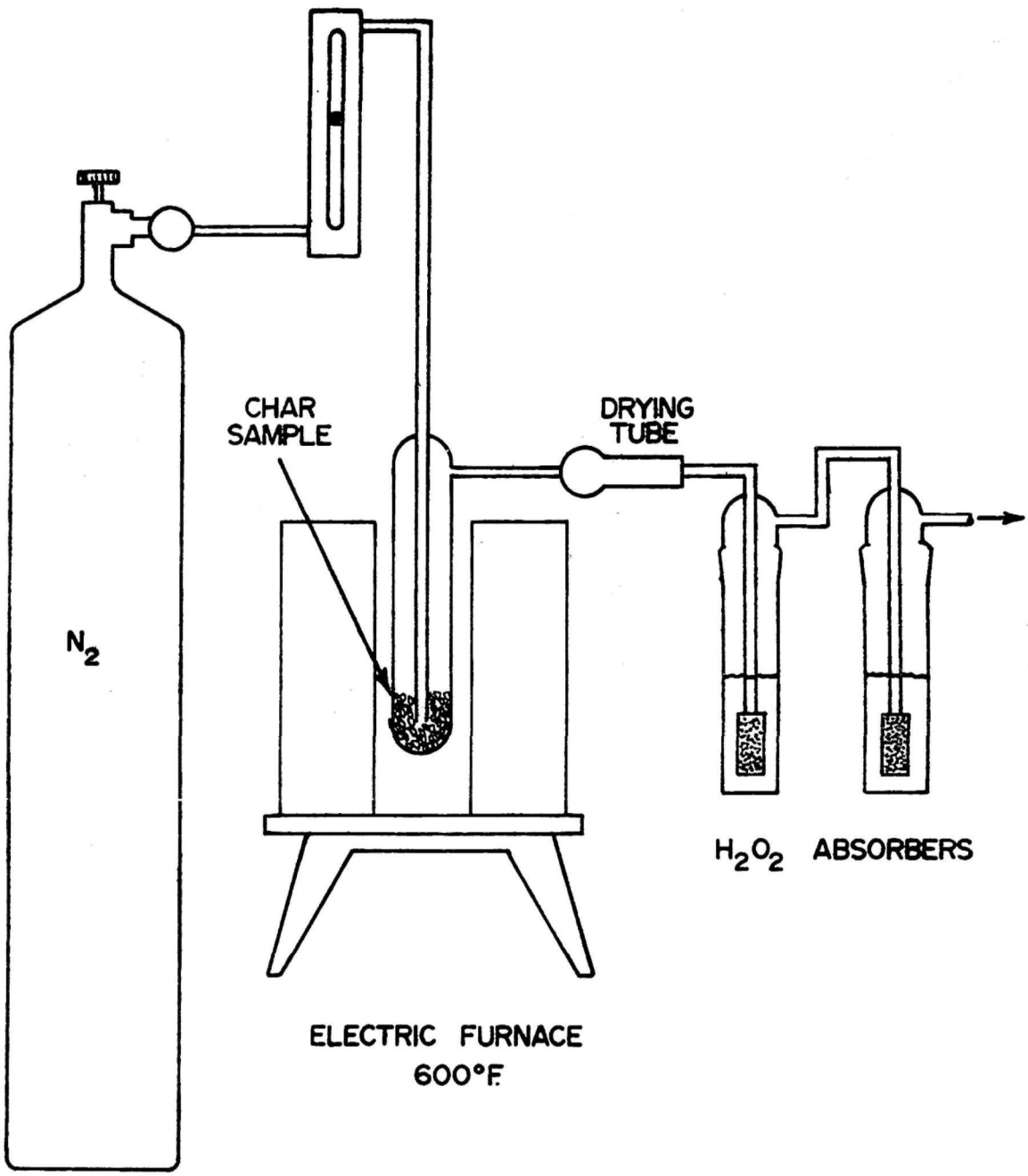

Figure F-6. Apparatus used for H_2SO_4 Reaction Experiments

Table F-2: H_2SO_4/S Reaction Stage at 600°F

Char from Run No.	Wt. char to reactor, gm.	SO_2 recovered, gm.	Wt. loss of char during reaction, gm.
1 (33%)	3.85	0.568	0.900
2 (88%)	4.21	0.227	0.789
3 (100%)	4.30	0.169	0.769

Table F-3: Sulfur Extraction

Char from Run No. (Table 2)	Wt. char to Extractor, gm.	Sulfur recovered, gm.
1 (33%)	2.96	0.183
2 (88%)	3.42	0.449
3 (100%)	3.56	1.52

23 times the baseline loading). The work showed conclusively that H_2SO_4 can be reduced to elemental sulfur in yields exceeding 80 percent at a constant temperature of 300°F, and that the product of that reduction can be recovered by solvent extraction methods.